ASD-TR-69-15
PART I

PROPELLER STATIC PERFORMANCE TESTS FOR V/STOL AIRCRAFT

PART I. SUMMARY REPORT

MATTHEW H. CHOPIN

TECHNICAL REPORT ASD-TR-69-15, PART I

JANUARY 1970

DEPUTY FOR ENGINEERING
AERONAUTICAL SYSTEMS DIVISION
AIR FORCE SYSTEMS COMMAND
WRIGHT-PATTERSON AIR FORCE BASE, OHIO

NOTICE

When Government drawings, specifications, or other data are used for any purpose other than in connection with a definitely related Government procurement operation, the United States Government thereby incurs no responsibility nor any obligation whatsoever; and the fact that the government may have formulated, furnished, or in any way supplied the said drawings, specifications, or other data, is not to be regarded by implication or otherwise as in any manner licensing the holder or any other person or corporation, or conveying any rights or permission to manufacture, use, or sell any patented invention that may in any way be related thereto.

This document has been approved for public release and sale; its distribution is unlimited.

Copies of this report should not be returned unless return is required by security considerations, contractual obligations, or notice on a specific document.

200 - June 1970 - CO455 - 121-2660

ASD-TR-69-15
PART I

PROPELLER STATIC PERFORMANCE TESTS FOR V/STOL AIRCRAFT

PART I. SUMMARY REPORT

MATTHEW H. CHOPIN

FOREWORD

In-house technical support for the test program and report preparation was provided by members of the V/STOL Propulsion Branch, Directorate of Propulsion and Power Subsystems Engineering of the Deputy for Engineering, under System 478A. The test report was prepared by Mr. Matthew Chopin, and the data presentation was prepared by Mr. Gerald Cafarelli. Test facilities were under the direction of Mr. Harold Schuetz of the Propulsion Branch of the Air Force Aero Propulsion Laboratory. This report covers work accomplished from July 1965 to November 1967. This report was submitted by the author 17 July 1969.

For ease of handling and convenience for the reader, information on the test program is presented in two physical documents, ASD-TR-69-15, Part I, identified by the subtitle, "Summary," and ASD-TR-69-15, Part II, "Test Data (Appendix III)."

The author wishes to express appreciation to the following persons: Major Alan Gay of the Directorate of Computation Services, Deputy for Engineering, for developing the computer program used for data reduction; Mr. Charles Mitchell of the Aerodynamics Branch, Directorate of Airframe Subsystems Engineering, Deputy for Engineering, for his consultation and review of the draft report; and Dr. Henry Velkoff, The Ohio State University Mechanical Engineering Department, for his consultation in support of this test program.

Contractor technical support was provided by the XC-142A airframe manufacturer, Ling-Temco Vought Inc., and propeller manufacturers, Hamilton Standard Division of United Aircraft Corporation, and Curtiss-Wright Corporation. Appreciation is also extended to Canadair Limited, Montreal, Quebec, for permission to include information and data on the CL-84 propeller.

This technical report has been reviewed and is approved.

James L Barrett

JAMES BARRETT
Technical Director
Directorate of Propulsion and Power
Subsystems Engineering

ABSTRACT

Part I of ASD-TR-69-15 presents the test results obtained from an extensive series of propeller static performance tests conducted on Electric Whirl Rig No. 4, located at Wright-Patterson Air Force Base. The tests were made because of a static performance thrust deficiency encountered during flight tests of the XC-142A V/STOL Cargo Aircraft.

Twenty-eight versions of propellers were tested. Parameters studied during the tests included blade cuff (on or off), tip shape, twist, activity factor, camber, and airfoil section. Reduced data is presented in the form of performance coefficients and various tip Mach numbers for each configuration tested. Data on several other VTOL static thrust propellers is presented for additional information although they were not a part of this test series.

Complete blade characteristic charts describing the physical characteristics of each blade tested provide a means of comparing the distribution of twist, thickness, chord, and camber against blade radial location for any given blade.

A drawing of the 30,000-horsepower Propeller Mount Configuration (Rig No. 4) shows dimensions of the test stand. Its operation and effects of the protective walls on the measured static performance are discussed. Data reduction was performed in-house on the ASD IBM-7094 computer and details of a special program used for the reduction, originally published as ASD-TR-69-19, "Computer Program for Reducing Static Propeller Test Data," are included.

The performance of the original XC-142A propeller was verified to be approximately 10% below the predicted value. As a result of these tests, the "induced inflow velocity" effect, due to the proximity of the protective walls surrounding the test rig, was dismissed as a contributing factor to the low performance of the original XC-142A propeller. Approximately 90% of the thrust deficiency was eliminated by a redesigned propeller utilizing performance information obtained from these tests.

Perhaps the most significant finding was that for every degree of increased blade twist, the figure of merit was increased approximately one-half point.

The tests and their results represent the state-of-the-art and point the way for improving propeller static performance for V/STOL aircraft applications. The information obtained can be used to predict more accurately the static thrust for future propeller driven V/STOL

aircraft. The vast amount of test data presented involves the inter-relationships of many propeller design parameters from which the researcher should be able to derive significant aspects of propeller static thrust related specifically to V/STOL applications.

Test results show that follow-on test programs should include investigations of the effects of radial twist and camber distribution on performance and the significance of total blade twist.

TABLE OF CONTENTS
PART I

TABLE OF CONTENTS (CONTD)
PART I

ILLUSTRATIONS

ILLUSTRATIONS (CONTD)

ILLUSTRATIONS (CONTD)

ILLUSTRATIONS (CONTD)

ILLUSTRATIONS (CONTD)

ILLUSTRATIONS (CONTD)

ILLUSTRATIONS (CONTD)

ILLUSTRATIONS (CONTD)

LIST OF SYMBOLS, DEFINITIONS, AND COEFFICIENTS

D	propeller diameter, feet
R	total blade radius, feet
r	radius along blade, feet
N	propeller speed RPM (revolutions/minute)
B	number of blades
b	blade width, feet
h	blade section maximum thickness, feet
AF	activity factor $= \frac{100{,}000}{16} \int_{0.2}^{1.0} \frac{b}{D} \left(\frac{r}{R}\right)^3 d\left(\frac{r}{R}\right)$ (The activity factor is a measure of a blade's capacity for power absorption)
TAF	total activity factor, (B X AF/blade)
C_{l_i}	blade section design lift coefficient (amount of camber of the blade section)
C_{L_i}	integrated design lift coefficient $= 4 \int_{0.2}^{1.0} C_{l_i} \left(\frac{r}{R}\right)^3 d\left(\frac{r}{R}\right)$
β	blade angle at % R, degrees
J	advance ratio $= \frac{88\, V_{mph}}{ND}$
V_{mph}	aircraft forward velocity or propeller inflow velocity = mph
$\frac{\pi ND}{60}$	rotational tip speed, feet/second or ft/sec
a	speed of sound, ft/sec $= 49.04 \sqrt{^\circ \text{Rankine}}$
$^\circ$Rankine	absolute temperature, 1.8 ($^\circ$C + 273.16)
M	tip Mach No. $= \frac{\pi ND}{60a}$
σ	density ratio, $\frac{\rho}{\rho_o}$

LIST OF SYMBOLS, DEFINITIONS, AND COEFFICIENTS (CONTD)

ρ	local density, $lb-sec^2/ft^4$
ρ_0	sea level standard density, $lb-sec^2/ft^4$
Hp	corrected rig horsepower = $\frac{\text{test horsepower}}{\sigma}$
C_P	power coefficient = $\frac{0.5\left(\frac{Hp}{1000}\right)}{\sigma\left(\frac{N}{1000}\right)^3\left(\frac{D}{10}\right)^5}$
Th	corrected rig thrust, pounds = $\frac{\text{test thrust}}{\sigma}$
C_T	thrust coefficient = $\frac{0.1515\left(\frac{Th}{1000}\right)}{\sigma\left(\frac{N}{1000}\right)^2\left(\frac{D}{10}\right)^4}$
F.M.	figure of merit = $0.798\ \frac{C_T^{(1.5)}}{C_P}$ (a measure of static efficiency)
η	propeller efficiency = $\frac{C_T}{C_P}\ J$ (forward flight)
$\Delta\beta$	blade twist = $(\beta_r = 0.25 - \beta_r = 1.0)$

COMPUTER PRINTOUT FOR FIGURE 3

Line 3

Beta - Test blade angle at 75% R (reference only)

AF - Blade activity factor (reference only)

DIA - Propeller diameter in feet

NBL - Number of blades in Hub (reference only)

TEMPC - Ambient temperature in degrees Centigrade

TEMPR - Absolute ambient temperature in degrees Rankine

SIGMA - Density ratio (reference only)

RAW DATA POINTS * * * * *

RPM - Propeller rpm

HP - Corrected horsepower

TH - Corrected thrust

TMACH - Propeller tip Mach number

RCT - Raw thrust coefficient

RCP - Raw power coefficient

RCT/CP - Ratio of raw thrust coefficient to power coefficient

RFM - Raw figure of merit

RTH/HP - Ratio of raw thrust to horsepower

FITTED CURVE DATA FOR CONSTANT MACH NUMBER INCREMENTS * * * * *

MACH - Selected Mach number increment

HP - Horsepower at Mach increment

TH - Thrust at Mach increment

TIPS - Propeller tip speed in ft/sec corresponding to Mach increment

RPM - Propeller rpm at Mach increment

CT - Thrust coefficient at Mach increment

CP - Power coefficient at Mach increment

CT/CP - Ratio of thrust coefficient to power coefficient at Mach increment

FM - Figure of merit at Mach increment

TH/HP - Ratio of thrust to horsepower at Mach increment

SECTION I
INTRODUCTION

This report presents the results of an extensive propeller test program conducted in support of the XC-142A System Program Office. The basic purpose of the testing was to obtain data necessary to improve propeller static performance of the XC-142A V/STOL cargo transport.

The XC-142A is a prototype tilt-wing vertical takeoff cargo aircraft with four wing-mounted turbo-prop power plants which provide thrust for both vertical and forward propulsion. The XC-142A in vertical takeoff and transition is illustrated in Figure 1. A static thrust of approximately 10,000 pounds per propeller was required for the design takeoff gross weight of 37,470 pounds (plus control power) at sea level standard (S. L. S) day contitions. This thrust corresponds to a propeller disc loading of approximately 50 pounds per square foot. (Static thrust provided by a propeller is developed while the propeller is stationary with respect to a fixed reference, i.e., while operating at zero forward velocity.)

Initial flight testing of the XC-142A indicated a need for additional propeller static thrust to provide the desired vertical takeoff capability for the aircraft. A program was initiated by the XC-42A System Program Office to increase the static thrust performance of the propeller system. A major portion of this performance improvement program consisted of static propeller whirl testing conducted on the propeller electric whirl test facility at Wright-Patterson Air Force Base (WPAFB), Ohio.

The objectives of this performance improvement program were the following:

a. Determine the efficiency of the existing propeller design

b. Determine the adequacy of the contractor's performance prediction method

c. Provide empirical performance data so the design could be improved

d. Determine the efficiency of a redesigned propeller for the XC-142A

The bulk of this report covers Objective c. Data covering several other propellers of interest, including the X-19 and CL-84 aircraft, are presented also.

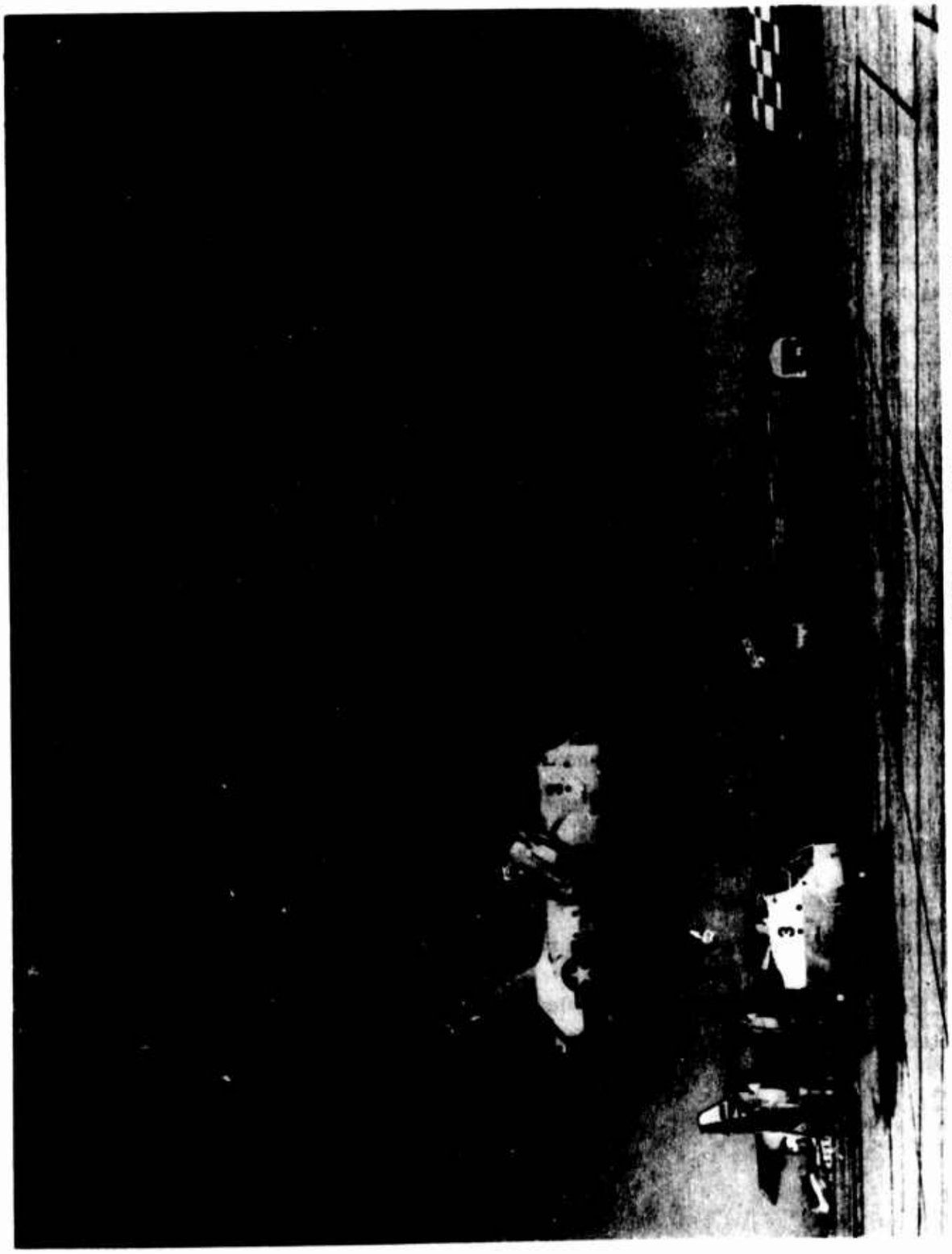

Figure 1. XC-142A V/STOL Aircraft in Conversion Flight

The XC-142A aircraft operational requirements that dictated the specific propeller design were the following:

a. V_{max} - 37,474 lbs gross weight (G.W.) on a standard day at sea level, at military rated shaft power* (not less than) --- 355 kts (409 mph)

b. Vertical thrust to weight ratio — 37,474 lbs G.W. on a standard day at sea level, out of ground effect, at takeoff rated shaft power*, not less than 1.15 lbs thrust/lb gross weight.

The range of each parameter studied during these tests was limited, therefore, primarily to that necessary to satisfy the above conditions. The parameters studied during these tests included the effects of blade cuff, tip shape, twist, activity factor, camber, and airfoil section.

The conventional propeller is an efficient device for converting power to thrust. Propellers have demonstrated high figures of merit at the static or hover condition, and well designed propellers, in the past, have demonstrated efficiencies above 90% at cruise speeds in the range of 200 to 400 kts. Thus, the propeller is a very suitable device for providing lift in the hover mode or thrust at cruise speeds in this speed range. Unfortunately, a compromise must be made between hover efficiency and cruise efficiency in the design of the optimum propeller for V/STOL applications.

In general, the hover performance of V/STOL aircraft has been below expectation, due in part to the lack of an accurate propeller-performance prediction theory at zero airspeed. Developing a theory for calculating static performance requires good experimental data to check the accuracy of the theory. Very little experimental test data is available for propellers intended for high static thrust. Data which are available have been obtained on various commercial and government test devices, and results obtained from different devices make direct comparison difficult. Data in this report was obtained under controlled conditions from the same test facilities. Although limited in the range of parameters covered, the test program was designed to obtain data primarily for V/STOL applications and to obtain data that would be as accurate as possible under existing conditions.

A special computer program was used during these tests for reducing the data. Details of this computer program may be found in technical report ASD-TR-68-19, "Computer Program for Reducing Static Propeller Test Data."

*Rated takeoff propeller speed of 1232 rpm (1008 ft/sec tip speed, M = 0.903 at standard day conditions)

The reduced data accumulated during the tests is not reported herein; it is presented in Part II (ASD-TR-69-15, Part II, subtitled "Test Data (Appendix III)."

In the absence of accurate theoretical performance prediction methods, the empirical findings contained in this report are believed to be of vital significance to the performance of advanced propellers and to the early development of successful V/STOL aircraft. It is hoped that these tests will contribute to a better understanding of the factors affecting static thrust of propellers and may aid in the development of an accurate method of predicting the static performance of propellers for V/STOL aircraft application.

SECTION II

TEST AND FACILITIES

1. TESTS

The tests described in this report consist basically of static whirl tests of various propeller configurations and the measuring and recording of pertinent performance data.

The original purposes of the propeller electric whirl rigs at W-PAFB were for verifying structural integrity and obtaining a reasonable measurement of performance. Very accurate performance measurements for V/STOL applications were not considered in the design of these rigs, so they were not optimized in configuration and instrumentation for this purpose.

Rig No. 4, installed in the mid 1950's at an approximate cost of $8 million, is the only equipment of this type and power range in the free world. It is the most accurate of the four whirl rigs at W-PAFB.

The effect of rig blockage or the effect of the flat rig face on the indicated performance has often been questioned. For a smaller diameter propeller operating in proximity to the rig face, the effect is essentially that of operating in ground effect. This produces an increase in indicated thrust over that which would be produced in a free stream condition. A comprehensive investigation of the blockage effect on a half-scale model of Rig No. 4 was performed by the NACA in 1952. Results of this investigation are contained in Reference 2. Figures 61 and 62 of Appendix II have been reproduced from Reference 2 and include least square curve fits for the calibrator propeller tested on Rig. No. 4 with the 12-foot extension gearbox and with the walls in their original (Phase I) location. It was concluded in Reference 2 that any blockage effect upon the propeller performance was less pronounced for a tractor configuration when the 12-foot gearbox extension was used. Therefore, all tests on Rig No. 4 for this series utilized the 12-foot gearbox extension.

Surrounding the front of the whirl rigs are massive wood and steel bomb-proof wall structures whose purposes is to contain particles of any propeller which might fail during testing. Questions recently presented due to the XC-142A thrust deficiency were the following: "Do the bomb-proof walls affect the airflow into the plane of the propeller and thus its indicated performance and if the airflow is affected, how much is the performance affected?" If there is, in fact, an induced inflow (of V_{mph}) created by the walls, there would be an effective advance ratio (where $J \neq 0$), and the test results would not be truly static.

The conventional method for presenting cruise efficiency becomes meaningless (where $\eta = C_T/C_P J$, and J = O) when the forward speed of the propeller is zero. The parameter chosen to represent the efficiency at static conditions is defined as the figure of merit (F. M.). Figure of merit can be thought of as the relationship of the thrust-to-power ratio of the propeller to that which would be obtained with an ideal actuator disk operating at the same disk loading.

During Phase I (with the bomb-proof walls in their original location), the original XC-142A (2FE16A3-4A) propeller and two others were tested. The performance of the 2FE16A3-4A (as shown by Figures 10 a/b) was found to be approximately 10% below that predicted at the design takeoff point of $C_P = 0.085$. The prediction method used for the 2FE16A3-4A was based on forward flight performance theory which was then standard in the industry, since propeller static thrust was not of primary interest prior to that time.

Both the 2J17G3-26R and the SK59868-0 (a specially built fiberglass test propeller) demonstrated relatively good static performance compared to the 2FE16A3-4A. A comparison of the performances of these three blades is provided in Figure 13 a/b. The camber distribution and outboard thickness ratio for the 2FF16A-4A and the 2J17G3-26R are very similar, however, the 2J17G3-26R has a significantly greater activity factor of 122. The SK59868-0 thickness, camber, and twist distribution are essentially the same as that of the 2FE16A3-4A; however, the activity factor of 98 is between 122 for the 2J17G3-26R and 86 for the 2FE16A3-4A. Exact details of the differences between these blades can be found from Blade Characteristic Sheets Numbers 2, 7, and 8 in Appendix I.

One explanation for the thrust deficiency of the 2FE16A3-4A propeller was that an inflow velocity was caused by the proximity of the walls. In an effort to resolve the concept of "induced inflow velocity," the bomb-proof walls were completely removed for Phase II of the tests*. During the early part of Phase II, both the 2J17G3-26R and SK59868-0 propellers were again tested. The 10% performance deficiency was still evident for the 2FE16A3-4A propeller (see Figures 15 a/b).

Sufficient data was obtained during Phase II to verify that there was, in fact, a slight difference between performances with the walls up (Phase I) and walls down (Phase II), generally at low power coefficients. Figures 18 through 21 present the test data for the

*To the author's knowledge, this was the first time in the history of propeller testing at Wright-Patterson Air Force Base that test data had been obtained with the bomb-proof walls removed.

preceding three propellers and provide a comparison of performance with the walls both up and down. In the case of the 2FE16A-4A blade, the effect did not extend into the XC-142A takeoff power range of C_p = 0.085. Therefore, the "induced inflow velocity" concept was dismissed as a contributing factor for the low performance of the 2FE16A3-4A propeller.

Additional propellers were tested during Phase II so that various parameters, such as tip shape, number of blades, and twist, could be studied.

A redesigned XC-142A propeller, designated 2FF16A1-4A, was fabricated and tested with the walls down in the later part of Phase II. The basic difference between the two propellers was that the redesigned 2FF16A1-4A had a round tip and a substantial increase in activity factor. It also had a higher integrated lift coefficient with the peak camber distribution located further outboard. The loading in the tip region of the 2FF16A1-4A was substantially below that of the 2FE16A3-4A. The tip twist distribution of the 2FE16A3-4A (identical to that of the 2J17G3-26R) was reduced for the 2FF16A1-4A. A detail comparison of the two blades can be obtained from Blade Characteristic Sheet No. 2 in Appendix I.

The 2FF16A1-4A performance was very close to that predicted and resulted in gaining back approximately 90% of the original 10% thrust deficiency of the 2FE16A3-4A propeller (see Figures 22 a/b). The performance prediction method used for the 2FF16A1-4A was based on a modified performance theory using data obtained from Phases I and II of these tests. Figures 23 a/b show the significant improvement in performance of the redesigned 2FF16A1-4A over the original 2FE16A3-4A. Not only did the 2FF16A1-4A produce more thrust per power, but it did this in a more efficient manner as shown by Figure 23b. This figure shows a substantial F.M. increase and also a shift of peak F.M. to the XC-142A takeoff power of C_p = 0.085.

The walls were <u>permanently</u> relocated against the building outer walls for Phase III in order to minimize any induced velocity effects which might still exist. This greatly enlarged the total flow area into the propeller test chamber and still provided protection to the surrounding area. Several of the same peopellers run during Phase II were again tested to study wall effects in the relocated position. No significant wall effects were found. Figures 27 a/b show correlation of the redesigned 2FF16A1-4A propeller for walls down, walls relocated and aircraft flight tests. The illustration shows there is essentially no difference between the 2FF16A-4A performance with the walls down (Phase II) or relocated (Phase III). Flight test correlation was adequate, but not as good as that for the 2FE16A3-4A shown in Figures 19 a/b.

It is the author's opinion that the walls in their relocated (Phase III) position do not noticeably affect propeller test static performance compared to test results which would be obtained in a true free air test situation.

A series of 13-foot diameter propellers was manufactured and tested to study additional parameters not covered in Phase II. These solid-dural blades allowed studying such parameters as blade twist, camber, activity factor, and airfoil section. These 0.832-scale blades were actually parametric variations of the full-scale XC-142A 2FF16A1-4A propeller.

The ranges of rpm and blade angle (β) used during the tests were determined by test objectives or by limitations of the test hardware or test equipment.

2. FACILITIES

All testing covered in this report (with the exception of X65SEJDR and 13166A10P3 propeller tests, which were run on Rig No. 1) were conducted on the 30,000-hp Electric Whirl Rig No. 4.

For all these tests, the auxiliary jack shaft mount (gearbox extension) was installed on the high speed shaft which places the plane of the propeller approximately 12 feet ahead of the flat face of the rig. Exact dimensions, plus a general view of the test rig, are provided in Appendix II by Figure 60, Propeller Mount Configuration, Rig No. 4.

The following paragraphs give a brief description of the torque, thrust, and rpm measuring systems used for these tests.

a. Torque

The torque shaft is located between the propeller mount and the drive motor. A constant voltage source (66.6 volts) was routed through torque shaft mounted slip rings to the differential transformer or transducer in the torque shaft. The transducer produces an electrical output signal that is proportional in amplitude to the applied torque. The transducer output signal was applied to a torque signal preamplifier and then to a ring demodulator. The signal from the ring demodulator then went to a digital voltmeter where the read-out voltage units were proportional to the torque applied.

The torque system was calibrated statically by applying a series of known torques to the torque shaft by use of a static mount and hydraulic load cells. (These load cells and their read-out equipment have been calibrated by the National Bureau of Standards.) The torque

shaft output voltage, which was a function of the known torque, was then adjusted to a suitable 20 x 1 or 40 x 1 multiple between read-out voltage and applied torque. Torque shaft static calibrating plots are presented in Figure 64.

b. Thrust

The thrust measuring system incorporated on Rig No. 4 is of the "NULL" type. Propeller thrust is transmitted to the speed-increaser gearbox which is mounted upon vertical flexure supports thus allowing the gearbox to move freely in an axial direction. The entire unit is maintained in its axial position by hydraulic thrust measuring and jacking cells. The hydraulic jacking cells are used to force the gearbox axially back to its null position when it becomes displaced due to propeller thrust. The amount of jacking necessary to return the gearbox to its null position is measured and indicated on a linear displacement gage system thus providing a readout of thrust produced by the propeller.

The thrust measuring system consists of A. H. Emery Company hydraulic cells, a Differential Tate-Emery Indicator which measures thrust load, and a General Electric Linear Disp acement Gage system for indication null position of the gearbox. A device can also be attached for applying a known thrust while running which is used for calibrating the readout equipment.

c. RPM

Accurate shaft rpm was provided by a magnetic pickup which receives impulses from a 60-tooth gear. These impulses are then presented on a digital display meter as propeller rpm.

SECTION III

PROPELLER CONFIGURATIONS TESTED

Table I, List of Propeller Configurations Tested, provides pertinent information for the 28 blade variations which were tested, including designation, parametric data, type construction, and appropriate comments. This table, in combination with the individual charts showing blade characteristics (Appendix I), provides complete blade design data for each version of the propellers tested.

The symbol chart shown in Table II, identifies each propeller designation with a specific symbol. The symbols are linked in three categories corresponding to the position of the bombproof walls, i.e., Phase I — walls up, Phase II — walls down, or Phase III — walls relocated. Note that propellers tested in more than one category retain the same basic symbol throughout this report. Corresponding blade characteristic sheet numbers are provided for rapid comparison of any given blade.

Two types of static performance curves are presented in this report — Thrust Coefficient/Power Coefficient vs Power Coefficient (C_T/C_P vs C_P) and figure of merit vs Power Coefficient (F.M. vs C_P). An attempt was made to compare all data at Mach =0.9; however, if this data was not available, other Mach number data, ranging from Mach = 0.750 to 0.950, was used. Likewise, an attempt was made to assign the same symbol to a specific Mach number increment throughout the report.

The blades in series 47 x 91 through 47 x 138 were control test blades manufactured specifically for these tests. The 0.832-scale solid dural blades are actually parametric variations of the full-scale fiber-glass (2FF16A1-4A) XC-142A propeller. Existing tooling for this size-scale blade provided for obtaining the desired study parameters in an economical and timely manner.

TABLE I

LIST OF PROPELLER CONFIGURATIONS TESTED

Test Categories	Diameter (Feet)	Number Blades	Activity Factor	Integrated Lift Coeff. C_{L_i}	NACA Airfoil Section	Twist 25% R-Tip	Blade Construction Details	Comments
Rig #4 - Phase I, Walls Up								
Calibrator (Curtiss 836-14C2-18R1) (15,000 ft-lb Shaft)	13.0	4	98	0.50		32.0°	Hollow Steel	Standard Rig Calibrator
2FE16A3-4A	15.625	4	86	0.475	16,64	29.0°	Fiberglass*	Original XC-142A Prop
2J17G3-26R	14.88	4	122	0.459	16,64	35.2°	Steel Core & Shell	C-119 Production Prop
SK59868-0	16.643	4	98	0.407	16,64	35.0°	Fiberglass*	Basic SK59868-0 Blade
156109A2P3	16.50	4	109	0.482		37.0°	Fiberglass	Designed for XC-142A
Rig #4 - Phase II, Walls Down								
Calibrator (15,000 ft-lb Shaft)	13.0	4	98	0.50		32.0°	Hollow Steel	Standard Rig Calibrator
2FE16A3-4A	15.625	4	86	0.475	16,64	29.0°	Fiberglass*	Original XC-142A Prop
2FE16A3-4A (with tabs)	15.625	4	86	0.475+	16,64	29.0°	Fiberglass*	(See Note Below)
2FF16A1-4A	15.625	4	105	0.500	16,64	35.5°	Fiberglass*	Redesigned XC-142A Prop
47 x 75	16.643	4	98	0.407	16,64	28.4°	Fiberglass*	Twisted SK59868-0
SK59868-0	16.643	4	98	0.407	16,64	35.0°	Fiberglass*	Basic SK59868-0 Blade
SK59868-0R	16.653	4	89	0.407	16,64	35.0°	Fiberglass*	Round Tip SK59868-0
SK59868-12.22	15.625	4	109	0.476	16,64	30.0°	Fiberglass*	Cut Down SK59868-0
SK59868-12.22R	15.625	4	99	0.476	16,64	30.0°	Fiberglass*	Round Tip SK59868-12.22
SK59868-17.22	15.208	4	115	0.497	16,64	28.3°	Fiberglass*	Cut Down SK59868-12.22
SK59868-17.22R	15.208	4	105	0.497	16,64	28.3°	Fiberglass*	Round Tip SK59868-17.22
6903A-0 in 43E60 Hub (3-Way)	15.2	3	99	0.500	16	33.7°	Solid Dural	Lockheed Constellation (C-121) Production Prop
6903A-0 in 34E60 Hub (4-Way)	15.2	4	99	0.500	16	33.7°	Solid Dural	C-121 Blades in 4-Way Hub
6903A-0T in 34E60 Hub	15.2	4	99	0.500	16	38.5°	Solid Dural	Twisted 6903A Blade
2J17G3-26R	14.88	4	122	0.459	16,64	35.2°	Steel Core - Shell	C-119 Production Prop

*Fiberglass shell over steel core, foam filled.
NOTE: 2FE with Balsa Wedge on Face Side T.E. (78 in. Sta - 12.5°, 1.54 in width; to Tip -120°, 0.815 in width)

TABLE I (CONTD)

Test Categories	Diameter (Feet)	Number Blades	Activity Factor	Integrated Lift Coeff. C_{L_i}	NACA Airfoil Section	Twist 25% R-Tip	Blade Construction Details	Comments
Rig #4 - Phase II, Walls Down (Cont'd)								
1490A2P3	14.0	4	90	0.498	65	39.0°	Fiberglass**	CL-84 Propeller
Calibrator (30,000 ft-lb Shaft)	13.0	4	98	0.50		32.0°	Hollow Steel	Calibrations for 30,000 ft-lb torque shaft
2FF16A1-4A (30,000 ft-lb Shaft)	15.625	4	105	.500	16,64	35.5°	Fiberglass*	
Rig #4 - Phase III, Walls Relocated								
Calibrator (30,000 ft-lb Shaft)	13.0	4	98	0.50		32.0°	Hollow Steel	Standard Rig Calibrator
2FF16A1-4A	15.625	4	105	0.500	16,64	35.5°	Fiberglass*	Redesigned XC-142A Prop
2FF16A1-4A (β Locked at 10.5°)	15.625	4	105	0.500	16,64	33.5°	Fiberglass*	Used as Calibrator Prop
47 x 91	13.0	4	105	0.500	16,64	35.5°	Solid Dural	0.832-Scale 2FF
47 x 92	13.0	4	103	0.500	16	35.5°	Solid Dural	47 x 91 Without Cuff
47 x 93	13.0	4	117	0.500	16,64	35.5°	Solid Dural	117 Activity Factor 2FF
47 x 94	13.0	4	115	0.500	16	35.5°	Solid Dural	47 x 93 Without Cuff
47 x 95	13.0	4	105	0.500	16,64	38.5°	Solid Dural	Twisted 47 x 91 Scale 2FF
47 x 96	13.0	4	103	0.500	16	38.5°	Solid Dural	47 x 95 Without Cuff
47 x 97	13.0	4	115	0.558	16	35.5°	Solid Dural	Recambered 47 x 94
47 x 121	13.0	4	117	0.500	65	35.5°	Solid Dural W/Fiber-glass	47 x 93 with NACA Series 65 Section for full radius
47 x 138	13.0	4	103	0.500	16	30.3°	Solid Dural	Retwisted 47 x 92
Rig #1 - Walls Up								
Calibrator	13.0	4	98	0.50		32.0°	Hollow Steel	Standard Rig Calibrator
X65-SEJDR	12.8	4	106	Approx 0.300	Modi-fied Series 65 w/o Cusp	46.5°	Solid Dural	Experimental Prop
13166A10P3	13.0	3	166	0.055	64	33.5°	Fiberglass**	X-19 Propeller

*Fiberglass shell over steel core, foam filled. **Fiberglass monocoque with steel shank.

TABLE II

PROPELLER PLOTTING SYMBOLS

PROPELLER	RIG FOUR			BLADE CHARACTERISTIC DATA SHEET NUMBER (in Appendix I)
	WALLS UP	WALLS DOWN	WALLS REL.	
2FE16A3-4A				2
2FE16A3-4A (TABS)				2
2J17G3-26R				7
156109A2P3				14
2FF16A1-4A (30,000 Shaft)				2
2FF16A1-4A (15,000 Shaft)				2
SK59868-0				8
SK59868-0R				8
SK59868-12				10
SK59868-12R				10
SK59868-18				11
SK59868-18R				11
6903A-0(34E60)				3
6903A-OT(34E60)				3
6903A-0(43E60)				3
1490A2P3				12
47 x 75				8
47 x 91				4
47 x 92				4
47 x 93				4
47 x 94				5
47 x 95				6
47 x 96				6
47 x 97				5
47 x 121				4
47 x 138				6
Calibrator				1

TABLE II (CONTD)

PROPELLER	RIG ONE			BLADE CHARACTERISTIC DATA SHEET NUMBER (in Appendix I)
	WALLS UP	WALLS DOWN	WALLS REL.	
X65SEJDR	×			15
1366A10P3	⏚			13
Calibrator				1

MACH NO. PLOTTING CODE FOR ALL DATA	
MACH NO.	SYMBOL
0.750	○
0.800	□
0.850	◇
0.900	Particular Prop
0.950	◇
ALTERNATE:	△

SECTION IV
METHOD OF DATA REDUCTION

The measured test data, i.e., rpm, horsepower, thrust, and other parameters from each propeller, were reduced by using a specially written program which was used on the IBM 7094 Digital Computer at WPAFB. This program is entitled, "Computer Program for Reducing Static Propeller Test Data," and is published as ASD-TR-68-19 (Reference 5).

The program accepts static whirl rig test data (i.e., test rpm and corrected horsepower and thrust data) at any given blade angle (β). The computer rapidly reduces the test data into pertinent propeller relationships, such as power coefficient (C_P), thrust coefficient (C_T), C_T/C_P, figure of merit (F.M.), and thrust/horsepower (Th/Hp), and computes the corresponding propeller tip Mach number.

The computer then fits a running second-degree polynomial, using the method of least squares, through six consecutive test data points (thrust or horsepower) that are equally distributed on either side of the desired smoothed (selected Mach number increment) data value. The routine proceeds until smoothed horsepower and thrust curves are created for the entire array of evenly incremented Mach number values. Intermediate horsepower and thrust values are determined from the fitted curves at the selected Mach number increments, and all coefficients are recomputed using these derived intermediate values. The reduced data are then presented in two forms: (1) coefficients computed from the actual test (or raw) data, and (2) coefficients obtained from the fitted curves at specific constant tip Mach number increments.

A tip Mach number increment of 0.025 from M = 0.525 to M = 1.0 (or the last data point) was used. No extrapolation of the data past actual test points was performed although data extrapolation is permitted in the program. It should be emphasized that the procedure used is essentially one of creating equal tabular entries through a smoothing rather than an inpolative procedure.

Figure 2 illustrates a typical test rig data sheet and Figure 3 shows a typical computer print-out of the reduced data for a fixed blade angle of 12.1 degrees.

Hand-faired curves through the test thrust and horsepower points vs rpm are shown in Figures 4 and 6 for a family of blade angles. Figures 5 and 7 show the excellent agreement between the test data and the computer curve fit data at constant Mach number increments. The curve fit technique results in a substantial smoothing of the data.

It should be noted that the raw test data (Hp and Th) shown in Figure 3 has already been corrected to standard day conditions at the time it is recorded on the Rig Data Sheet Shown in Figure 2. Therefore no corrections to standard day conditions are necessary or are performed by the computer program. The value of "Sigma" is provided for reference purposes only.

PROPELLER ELECTRIC MOTOR WHIRL TEST
(OBSERVED DATA - RIG NO. 4)

DATE: 7 Jan 66	MFR:	MOTOR: ☐ HIGH ☒ LOW	ENGINEER: Chopin - Schuetz
TASK NO.: 478A	HUB DWG:	SHAFT: ☒ HIGH ☐ LOW	CREW CHIEF:
BAROMETER: 29.35 / TEMPERATURE: -4.0 °C / AIR FACTOR: 1.05 σ	HUB SERIAL: 2FF16A1-4A	GEAR RATIO: 4 x 1	CONTROLS OPR: Howerton
TORQUE-MULTIPLIER: 20 x 1 (15,000 ft-lb Shaft)	BLADE DWG:	BRUSH TIME:	TORQUE OPR: McCabe
ROTATION: Right Hand	BLADE SERIAL:	RIG TIME:	RIG THRUST OPR: Lee
ADAPTER: Gearbox Extension			DUAL THRUST OPR: Steele
TABLE: 230 / ANGLE: 12.1			BALCONY OPR:

TIME	MOTOR RPM	SHAFT RPM IND	SHAFT RPM X	TORQUE IND	TORQUE FT-LBS	HORSEPOWER TOTAL	HORSEPOWER LOSS	HORSEPOWER NET	THRUST RIG	THRUST DUAL	th/hp	CORRECTED DATA RPM	CORRECTED DATA HP	CORRECTED DATA THRUST
				164		407	17	390			7.428	652	372	2762
				194		519	19	500			6.842	702	476	3257
				221		630	21	609			6.403	749	580	3714
				257		782	23	759			5.967	797	723	4314
				285		920	25	895			5.615	848	853	4790
				329		1125	27	1098			5.308	898	1046	5552
				380		1382	30	1352			4.932	955	1288	6352
				426		1625	32	1583			4.677	1003	1519	7105
				476		1905	34	1871			4.415	1052	1784	7476
				527		2200	36	2164			4.221	1096	2060	8695
				606		2624	39	2585			3.957	1148	2486	9838
				675		3070	41	3029			3.765	1194	2884	10857
				732		3430	43	3387			3.604	1230	3224	11619

Figure 2. Typical Test Rig Data Sheet

STATIC PROP PERFORMANCE

2FF15A1-4A 7JAN66 ROT .0 230 WALLS DOWN 15000 FT-LB

BETA=12.1 AF= -0. DIA=15.625 NBL=4 TEMPC= -4.0 TEMPR= 484.49 SIGMA=1.0500

***** RAW DATA POINTS *****

RPM	HP	TH	TMACH	RCT	RCP	RCT/CP	RFM	RTH/HP
652.	372.	2762.	0.494	0.1655	0.0721	2.2964	0.7454	7.4247
702.	476.	3257.	0.532	0.1683	0.0739	2.2786	0.7460	6.8424
749.	580.	3714.	0.568	0.1686	0.0741	2.2752	0.7455	6.4034
797.	723.	4314.	0.604	0.1730	0.0767	2.2559	0.7487	5.9668
848.	853.	4790.	0.643	0.1696	0.0751	2.2589	0.7425	5.6155
898.	1046.	5552.	0.681	0.1753	0.0775	2.2611	0.7555	5.3078
955.	1283.	6352.	0.724	0.1774	0.0794	2.2342	0.7509	4.9317
1003.	1519.	7105.	0.760	0.1799	0.0808	2.2255	0.7532	4.6774
1052.	1784.	7876.	0.797	0.1812	0.0823	2.2032	0.7485	4.4148
1096.	2060.	8695.	0.831	0.1843	0.0840	2.1945	0.7519	4.2209
1148.	2486.	9838.	0.870	0.1901	0.0882	2.1551	0.7499	3.9574
1194.	2884.	10857.	0.905	0.1940	0.0910	2.1323	0.7494	3.7646
1230.	3224.	11619.	0.932	0.1956	0.0930	2.1028	0.7421	3.6039

***** FITTED CURVE DATA FOR CONSTANT MACH NUMBER INCREMENTS ***** (HP, 6 POINT 2ND ORDER. TH, 6 P

MACH	HP	TH	TIPS	RPM	CT	CP	CT/CP	FM	TH/HP
0.725	1293.	6379.	783.	957.	0.1775	0.0793	2.239	0.753	4.934
0.750	1453.	6892.	810.	990.	0.1793	0.0805	2.227	0.753	4.745
0.775	1615.	7389.	837.	1023.	0.1800	0.0811	2.219	0.751	4.576
0.800	1804.	7956.	864.	1056.	0.1819	0.0823	2.209	0.752	4.411
0.825	2022.	8574.	891.	1088.	0.1843	0.0842	2.190	0.750	4.241
0.850	2262.	9243.	918.	1121.	0.1872	0.0861	2.174	0.750	4.086
0.875	2528.	9934.	944.	1154.	0.1898	0.0882	2.152	0.748	3.930
0.900	2819.	10663.	971.	1187.	0.1926	0.0904	2.131	0.746	3.784
0.925	3134.	11430.	998.	1220.	0.1954	0.0926	2.111	0.745	3.647

Figure 3. Typical Computer Printout

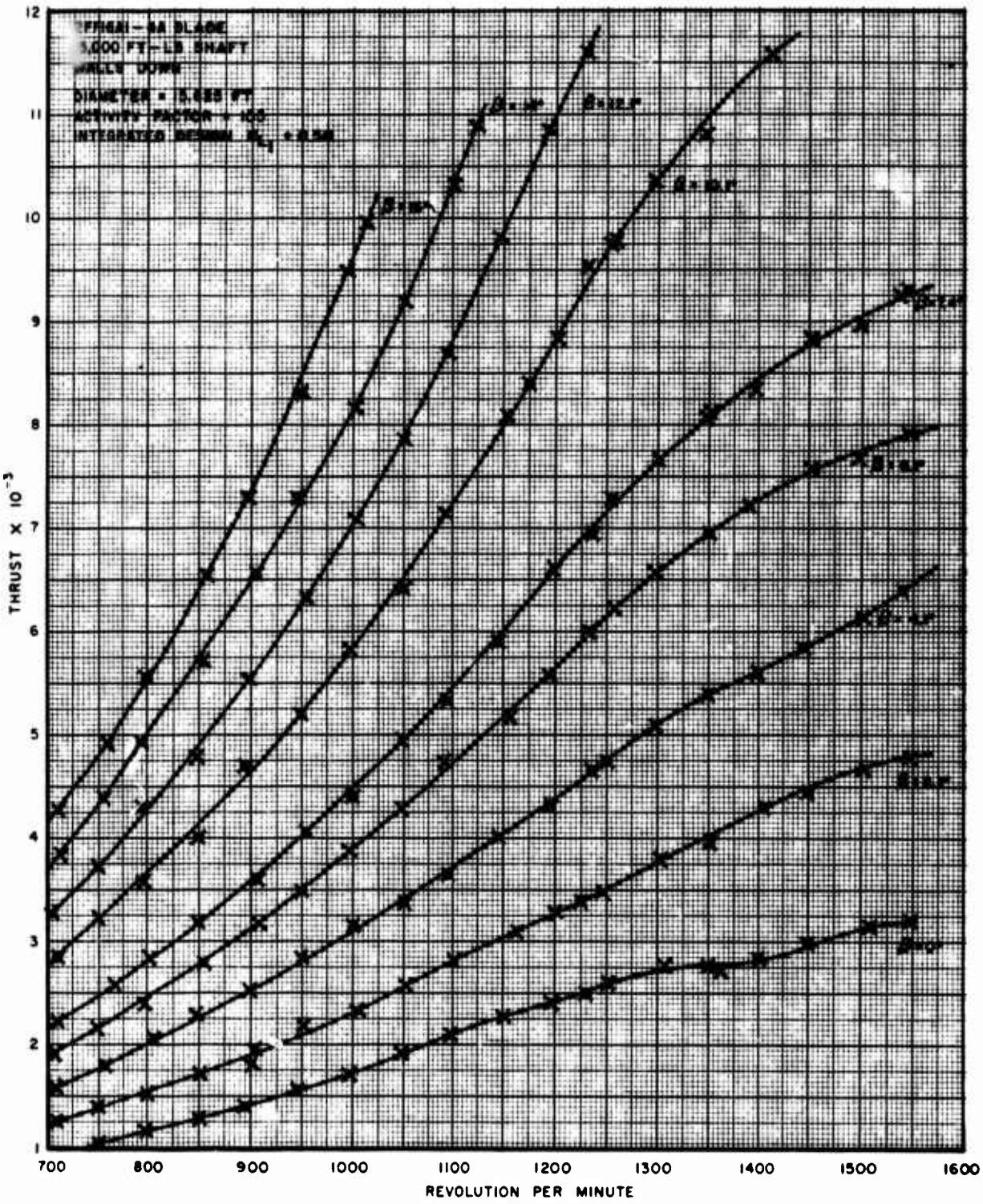

Figure 4. Sample of a Raw Data Plot; Thrust vs RPM

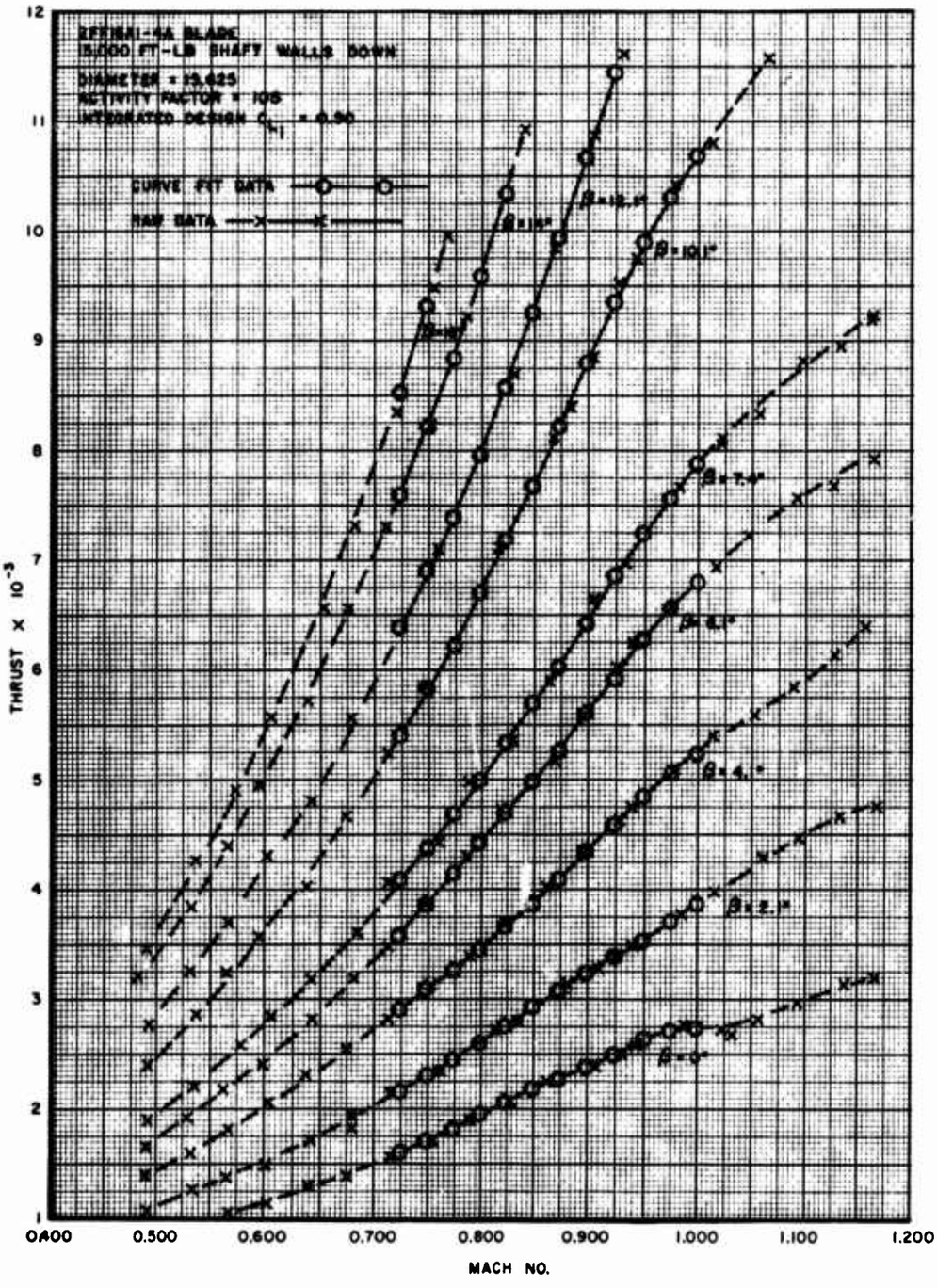

Figure 5. Comparison of Curve Fit Data to Raw Data; Thrust vs Mach Number

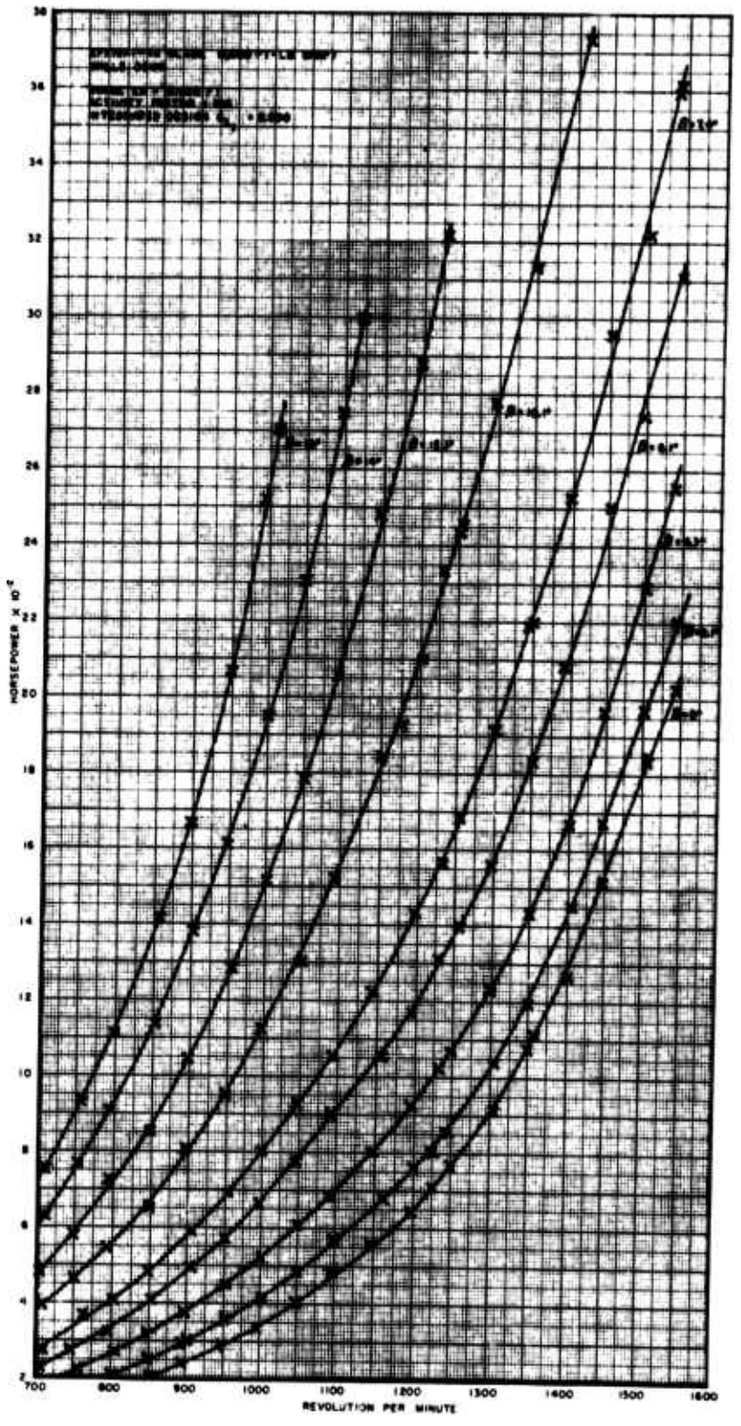

Figure 6. Sample of a Raw Data Plot; Horsepower vs RPM

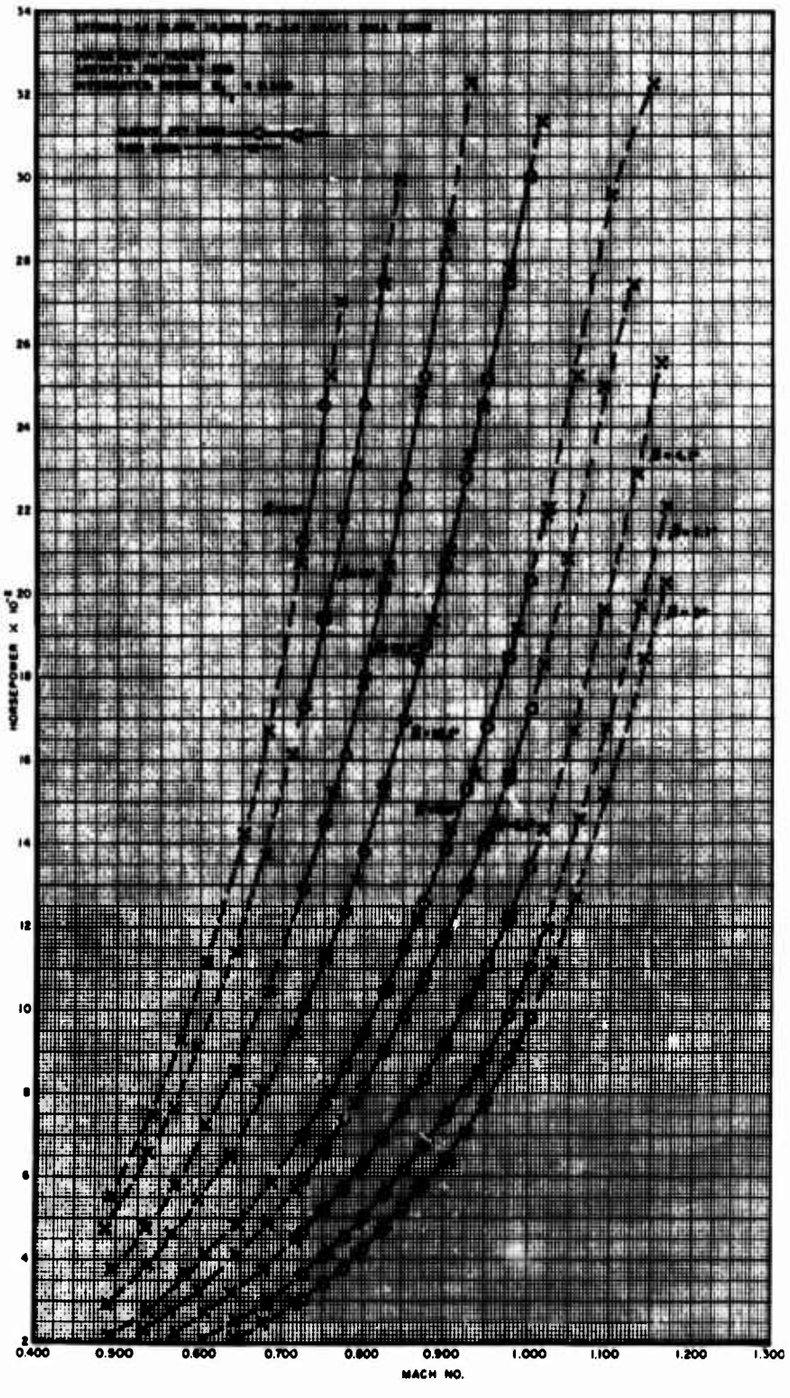

Figure 7. Comparison of Curve Fit Data to Raw Data; Horsepower vs Mach Number

SECTION V

DATA ANALYSIS

1. EFFECT OF PROTECTIVE WALLS

The following tabulated propeller configurations were all tested on Rig No. 4 for the three phases of this test program. Although many other propeller configurations were tested during Phases II and III, the propellers in the tabulation are the only ones which can be directly compared between the protective walls in the Phase I - Up, Phase II - Down, and Phase III - Relocated positions. Examination of the data obtained during test of the listed propellers might present additional insight as to the significance of other data accumulated during these tests.

Propeller	Phase I Walls Up	Phase II Walls Down	Phase III Walls Relocated
Calibrator	X	X	X
2FE16A3-4A	X	X	
2J17G3-26R	X	X	
SK59868-0	X	X	
2FF16A1-4A		X	X

Figure 8 illustrates the difference between the propeller test chamber for the three phases of tests. The increase in inflow area afforded by the Phase III configuration is seen to be considerable. The walls were retained permanently in the Phase III relocated position.

a. Phase I, Walls Up

The following portion of this section contains performance plots for the 2FE16A3-4A, 2J17G3-26R, and SK59868-0 blades tested with the protective walls in their original up position. A view of these protective walls is given in Figure 9.

Figures 10 a/b illustrate the performance of the 2FE16A3-4A (or original XC-142A propeller) as compared to its predicted performance. At the take-off rated power coefficient of $C_P = 0.085$, the tested 2FE16A3-4A propeller was 10% below the predicted C_T/C_P performance curve and was 11.5 points below the predicted figure of merit curve. (1 point = 0.01 F.M.). It should be noted that the sensitivity to tip Mach number is significant.

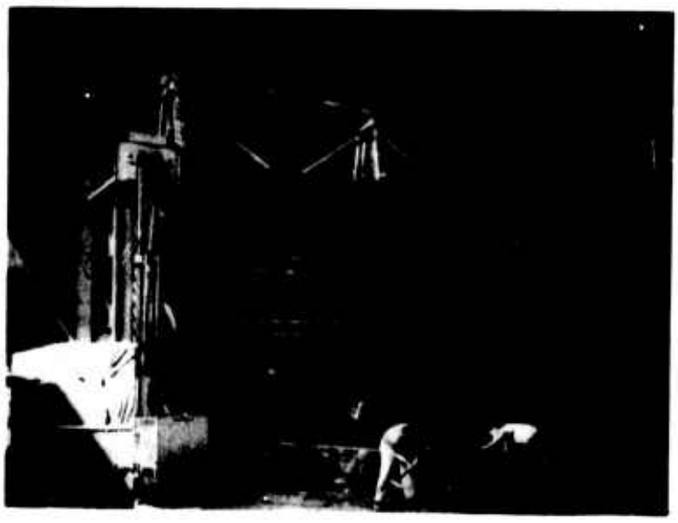

Phase I

Walls Up

Walls are in their original positions (Initial disassembly following Phase I is illustrated)

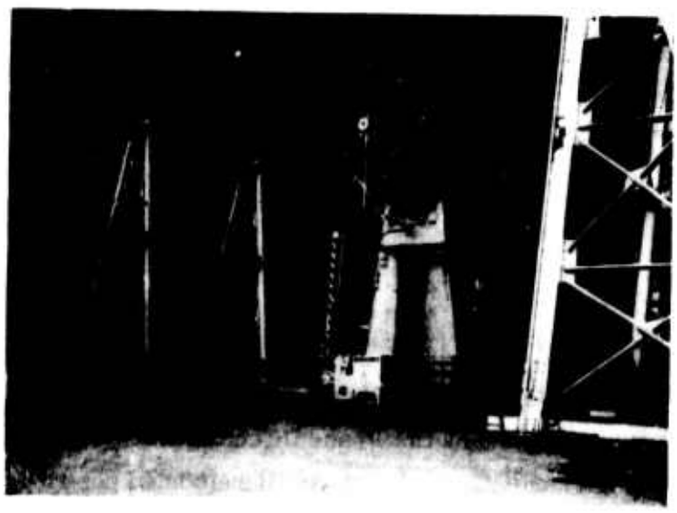

Phase II

Walls Down

Only the steel support structure is in the original position for this phase

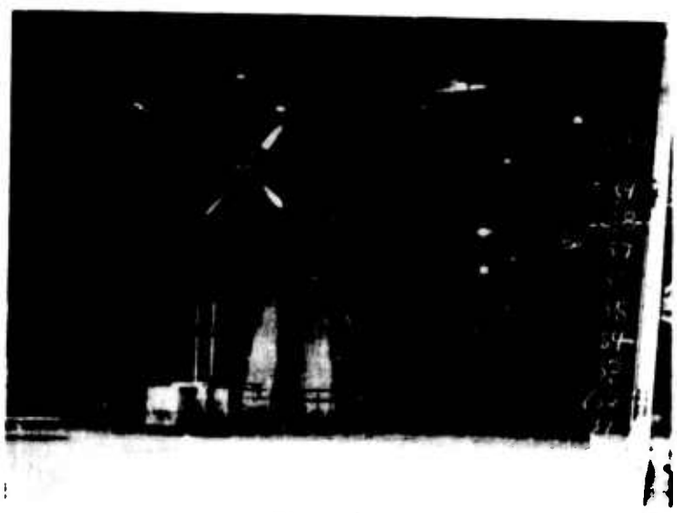

Phase III

Walls Relocated

The steel support structure and walls have been moved outward to the building walls

Figure 8. Position of Protective Walls for Three Test Phases (Whirl Rig No. 4)

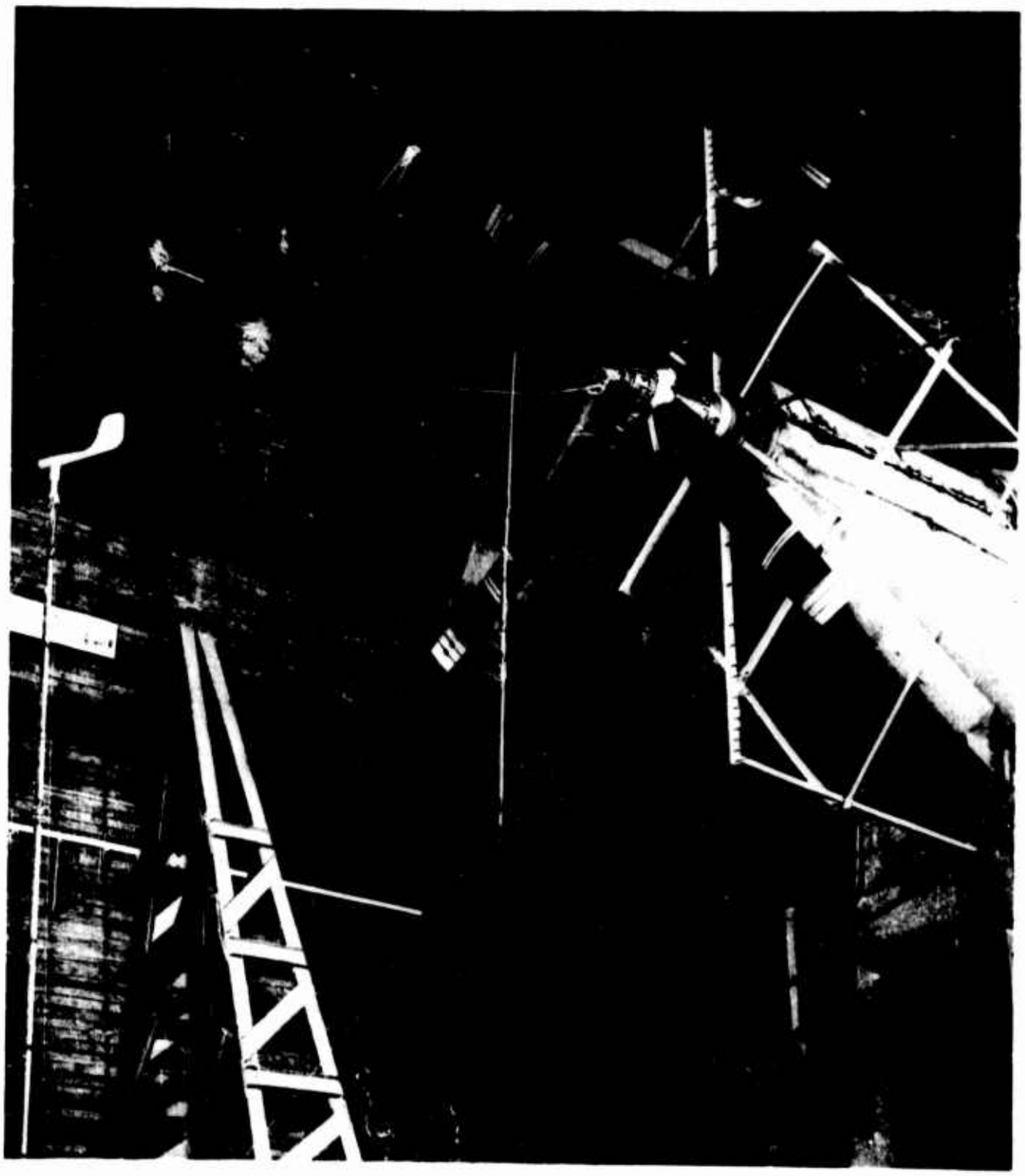

Figure 9. XC-142A Propeller Test Phase I, Front 3/4 View of SK-59868-0, 16 1/2-Foot Diameter Propeller on Whirl Rig No. 4

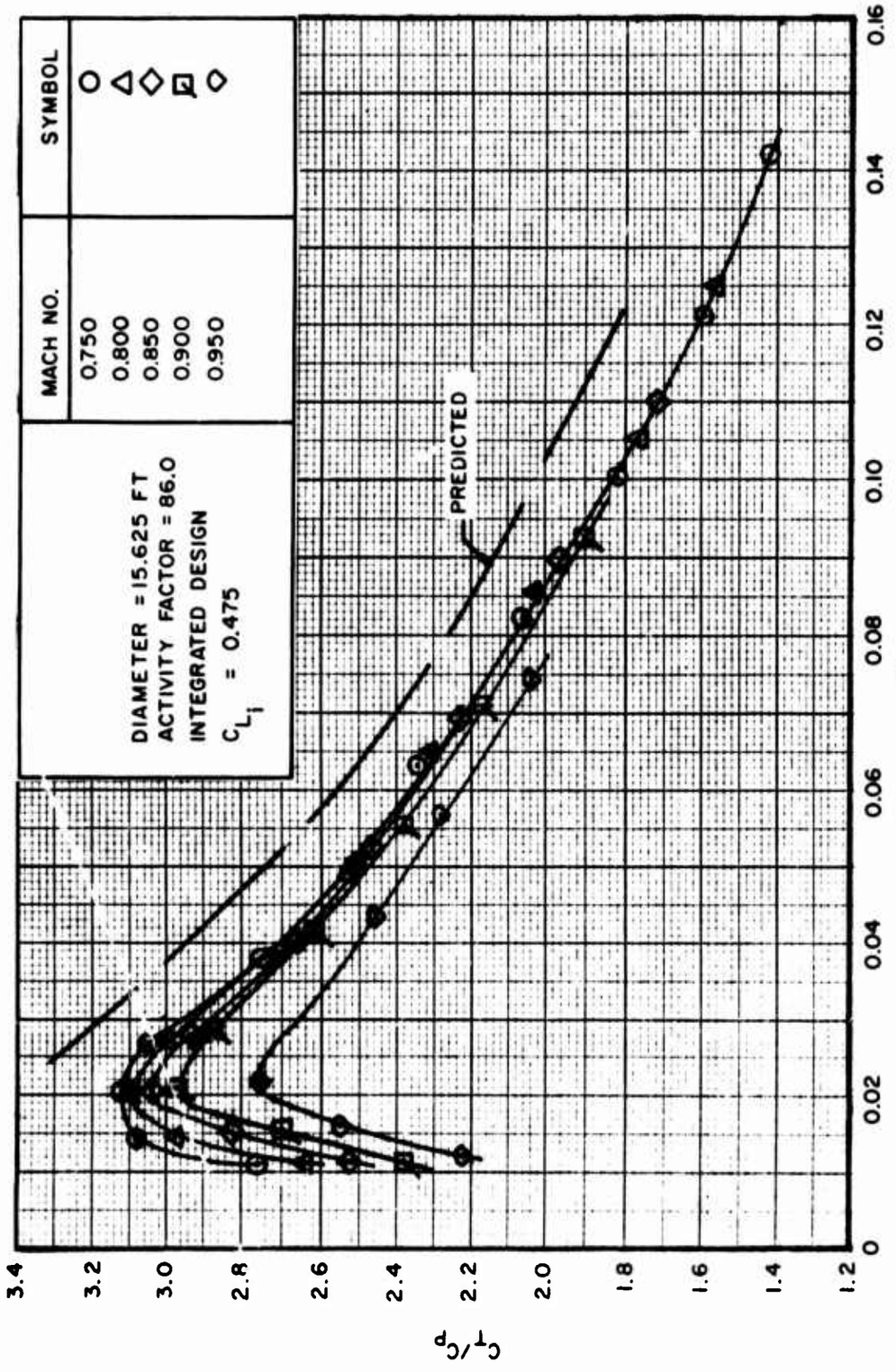

Figure 10. 2FE16A3-4A, Walls Up, Performance at Different Tip Mach Numbers
a. C_T/C_P vs C_P plot

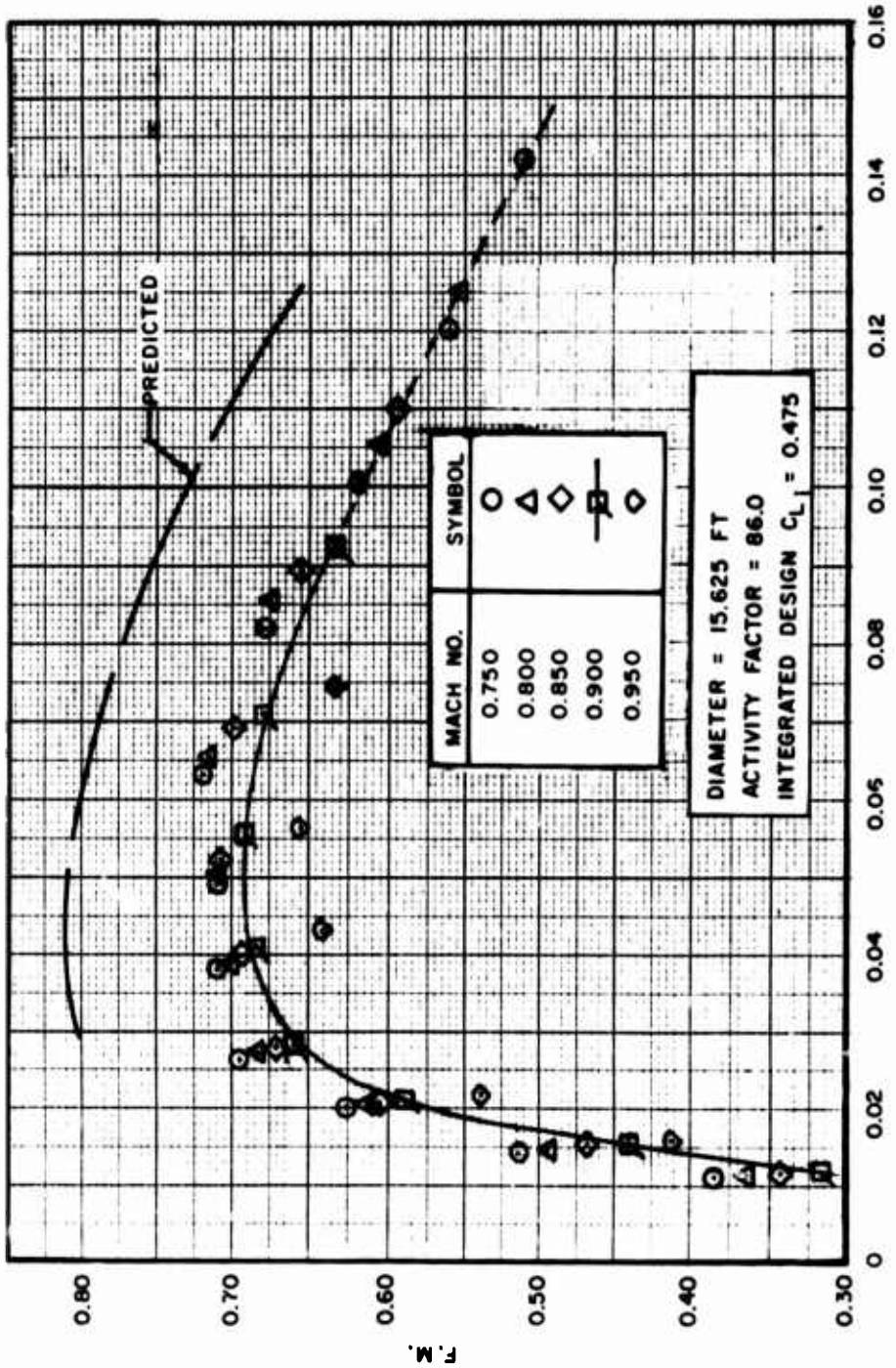

Figure 10. Continued
b. F.M. vs C_p plot

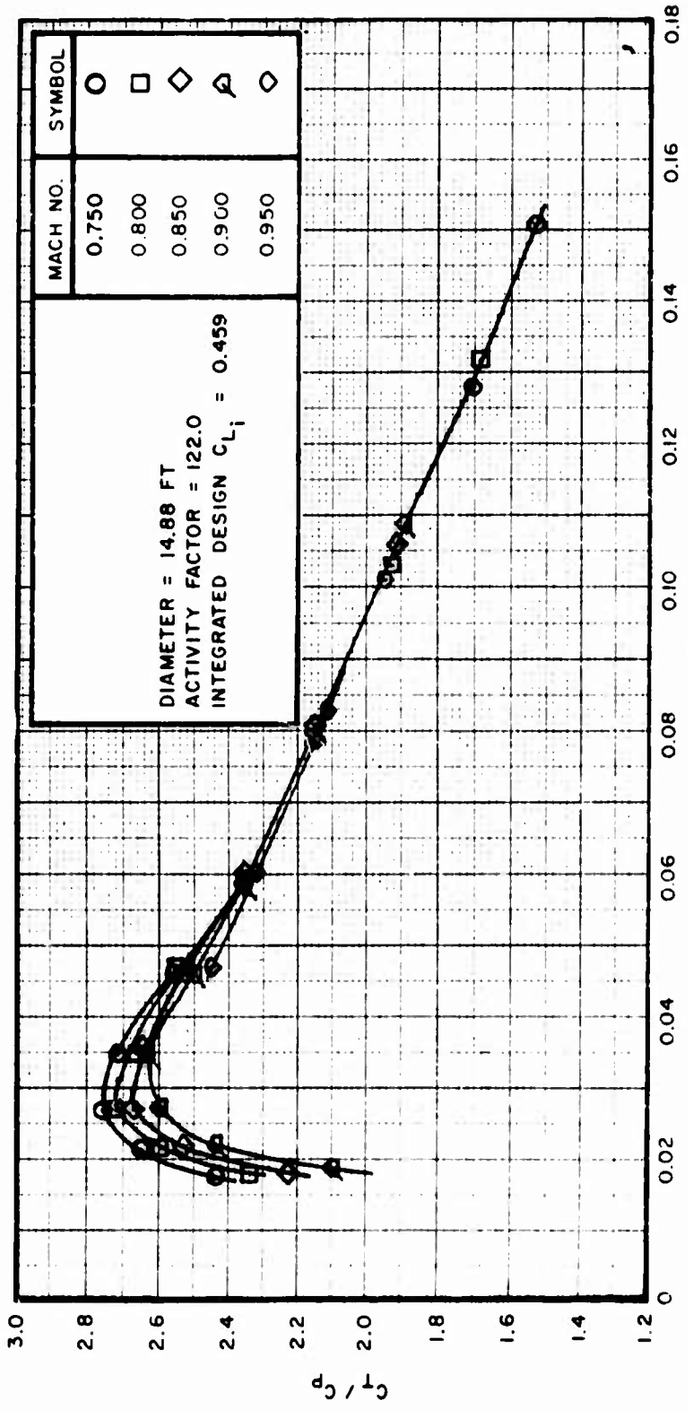

Figure 11. 2J17G3-26R, Walls Up, Performance at Different Tip Mach Numbers

a. C_T/C_P vs C_P plot

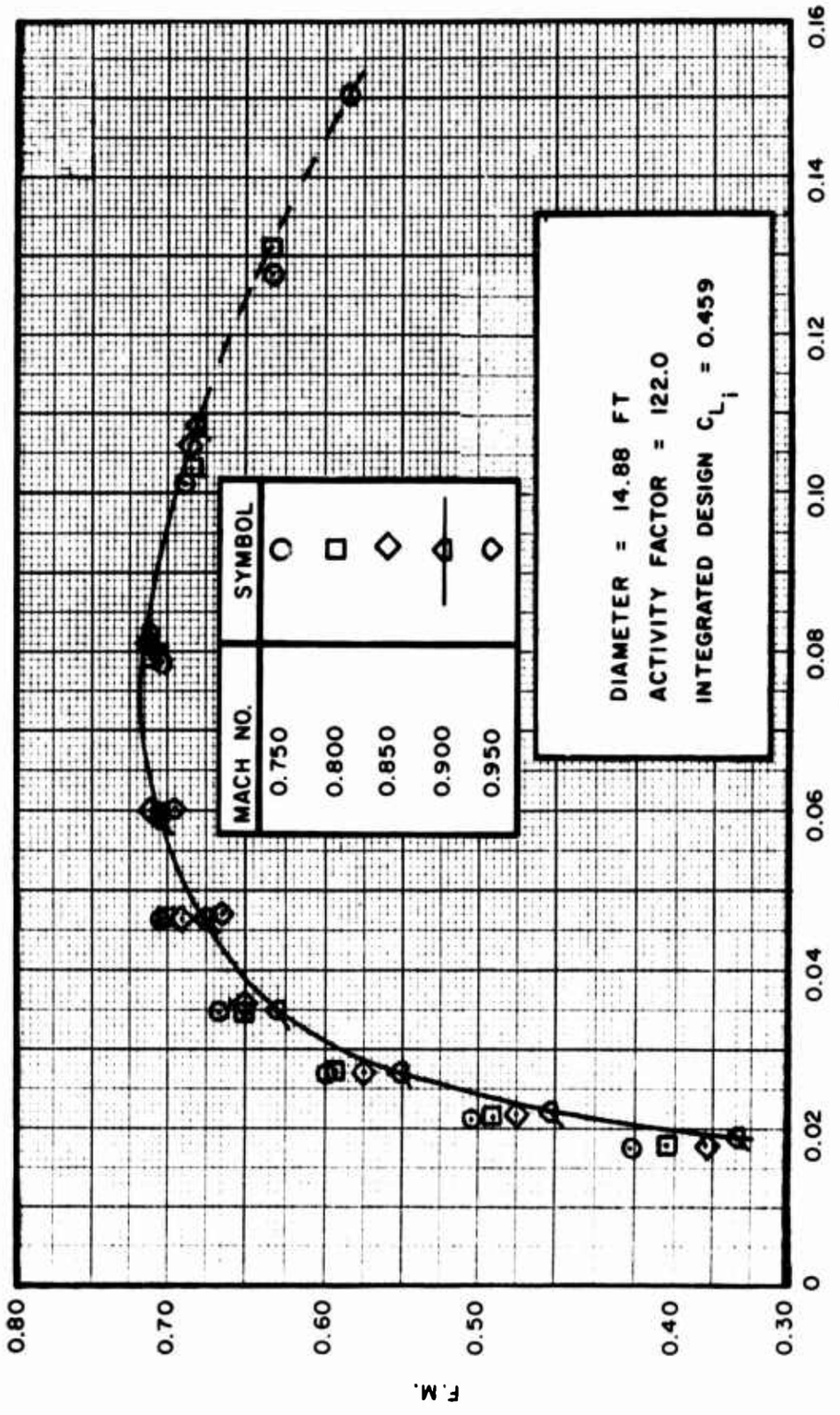

Figure 11. Continued

b. F.M. vs C_P plot

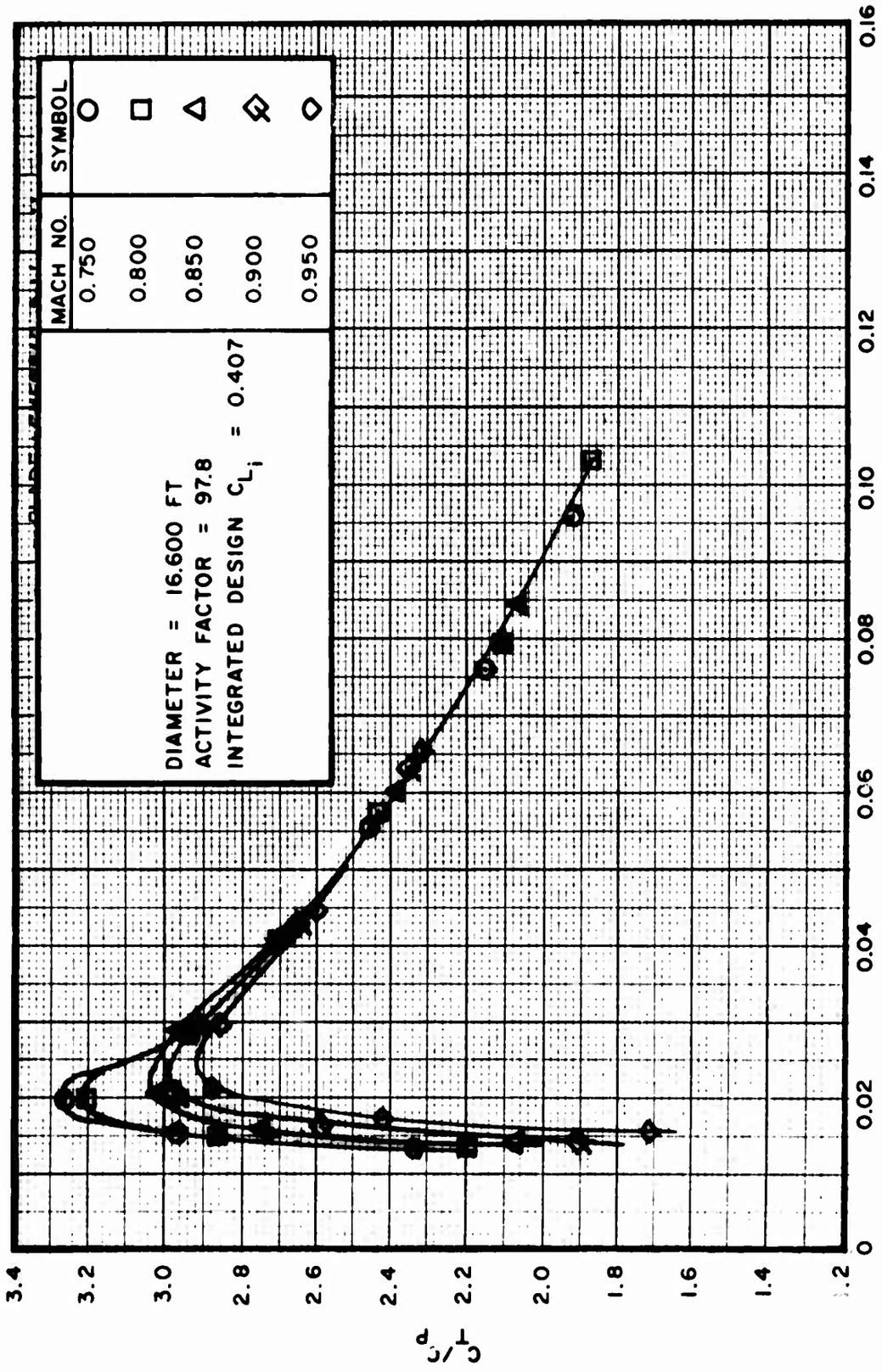

Figure 12. SK59868-0, Walls Up, Performance at Different Tip Mach Numbers
a. C_T/C_P plot

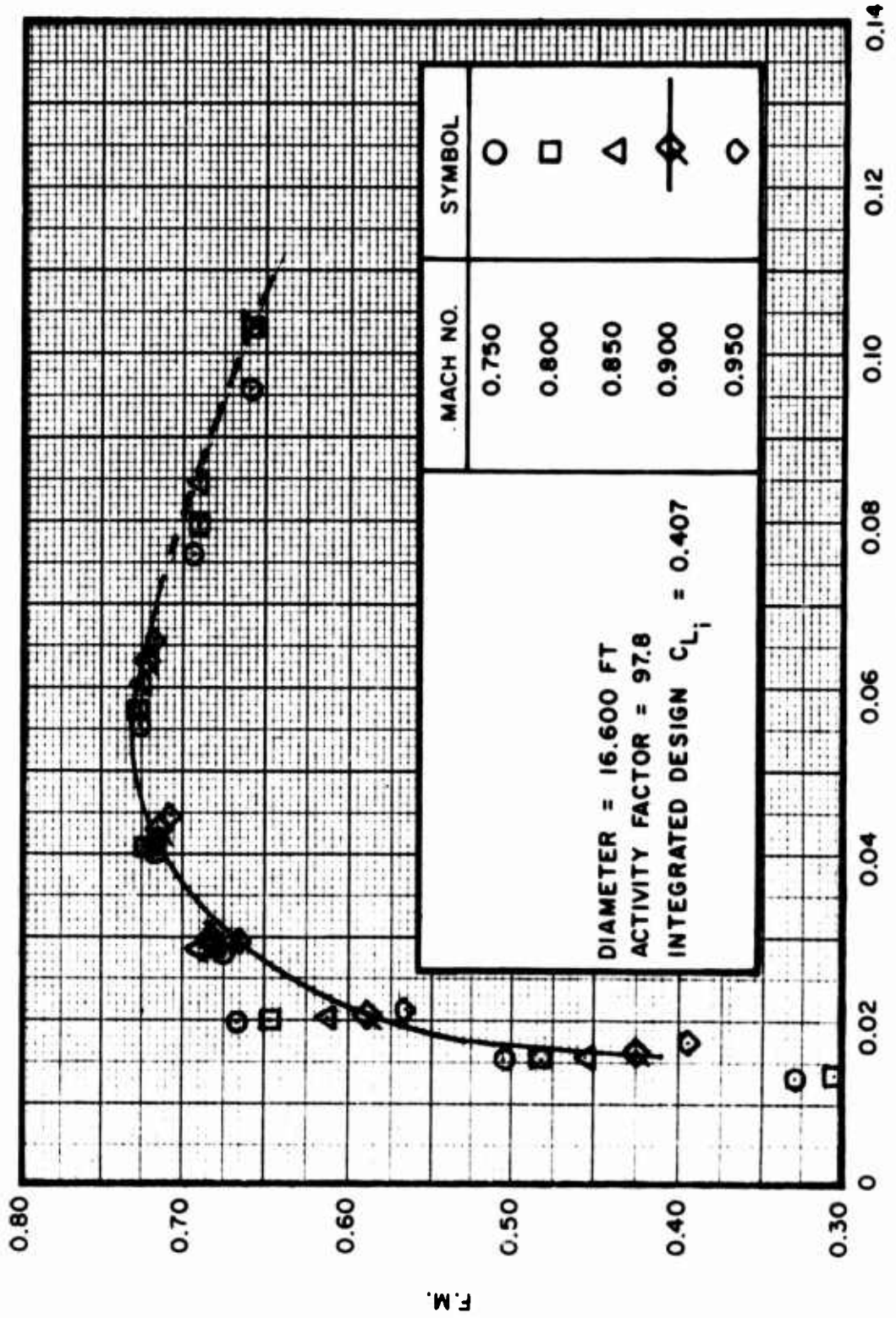

Figure 12. Continued
b. F. M. vs C_P plot

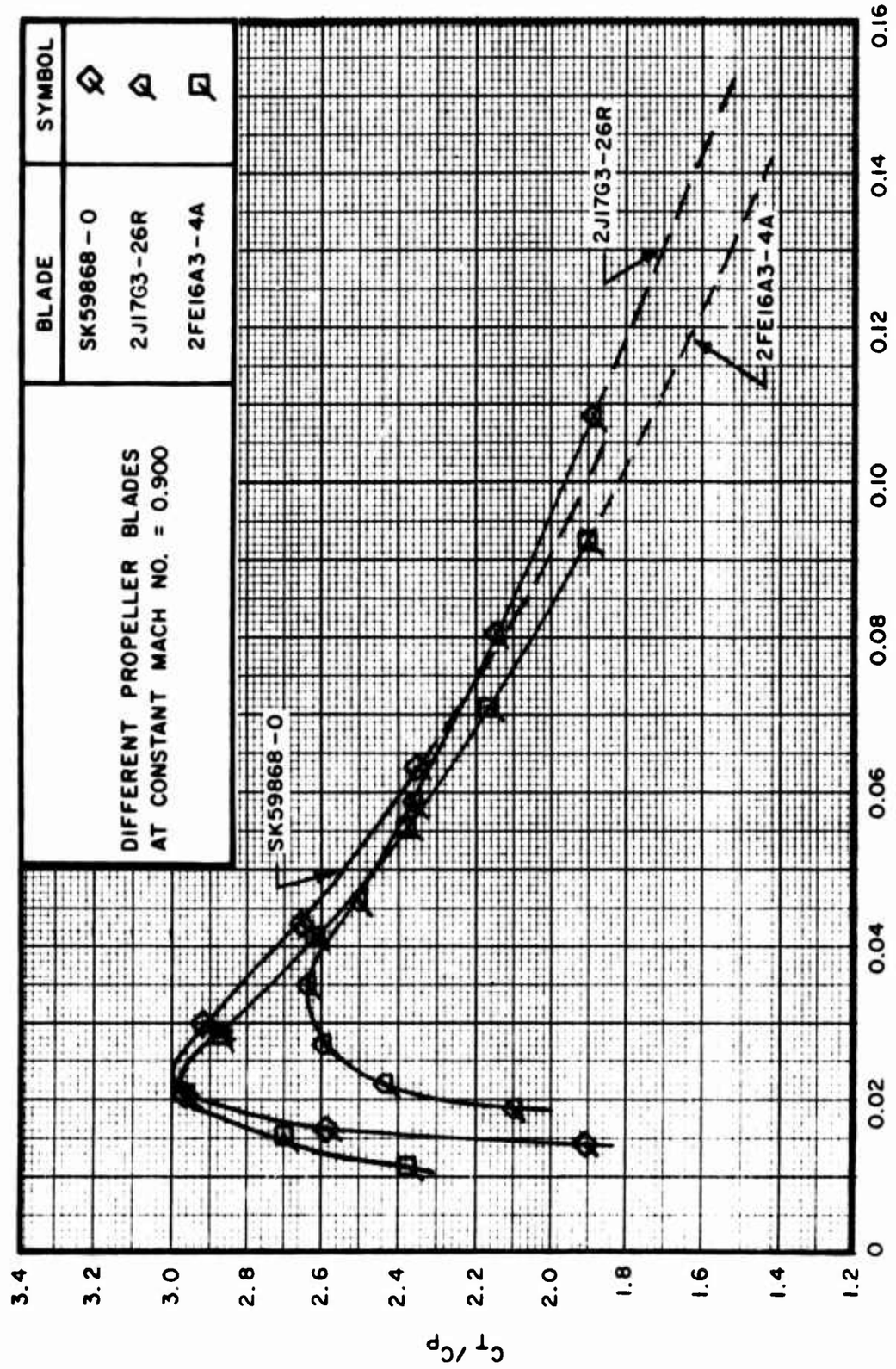

Figure 13. Comparison of SK59868-0, 2J17G3-26R, and 2FE16A3-4A, Walls Up, Performance at Tip Mach Number = 0.900

a. C_T/C_P vs C_P plot

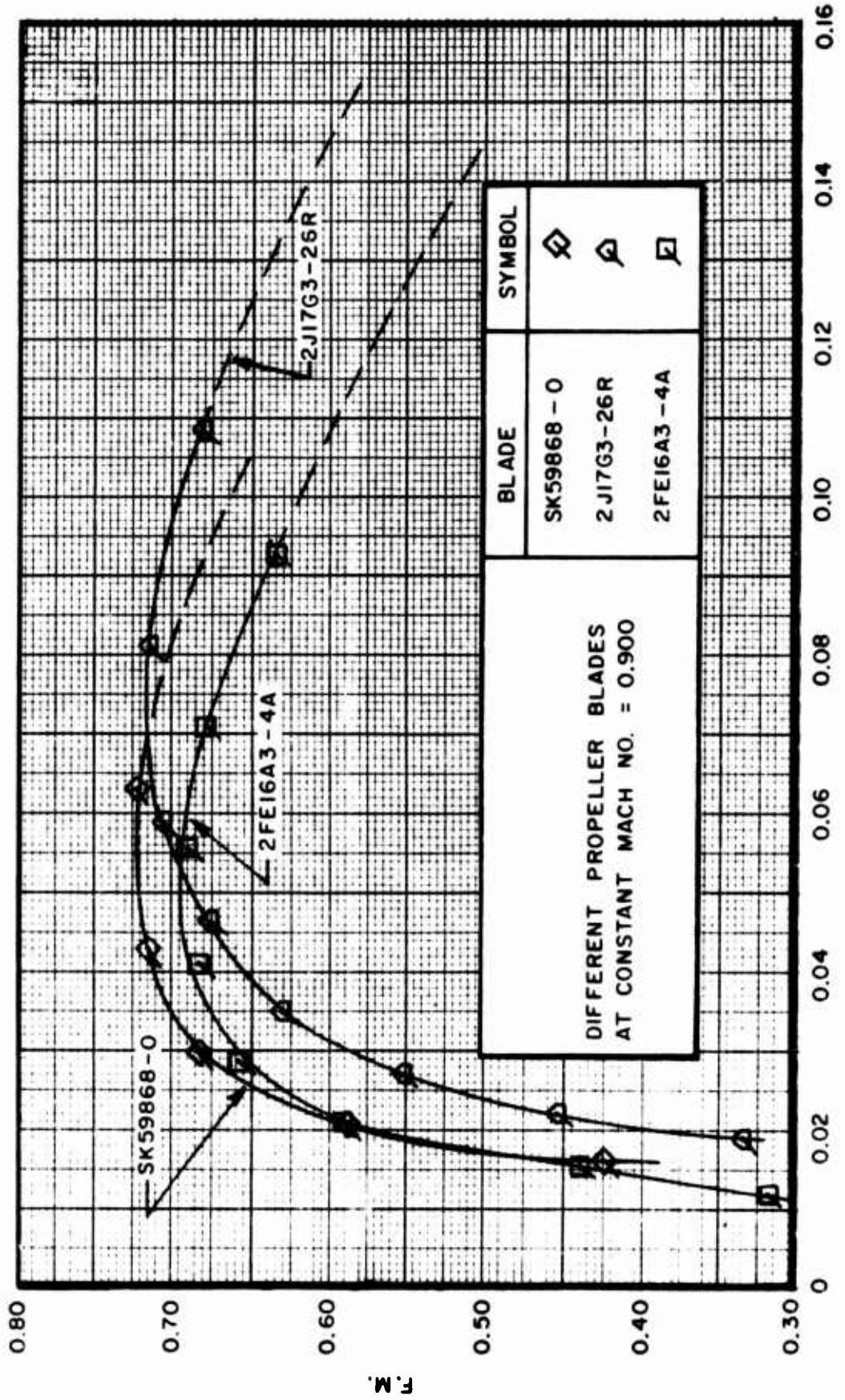

Figure 13. Continued
b. F.M. vs C_P plot

Figures 11 a/b present the results of the 2J17G3-26R solid dural propeller used on the C-119 aircraft. The static thrust and efficiency were relatively insensitive to Mach number.

Figures 12 a/b present the performance results of the SK59868-0 fiberglass propeller that was built specifically as a test item for these tests.

Figures 13 a/b present composite performance plots of the above three propellers. The performance of the 2J17G3-26R was substantially better than the 2FE16A3-4A, both in F. M. and the design power coefficient range. The F. M. peak for the 2FE16A3-4A occurred at C_p = 0.05 whereas the 2J17G3-26R peaked very near the XC-142A design point of C_p = 0.085.

b. Phase II, Walls Down

Following Phase I testing, the concept of "induced velocity" due to the proximity of the protective walls to the propeller was introduced. In an effort to resolve these effects, the protective walls of the test chamber, with the exception of the steel support structures, were removed (Figure 14).

During the initial period of this phase, the same three blades, namely the 2FE16A4A, 2J17G3-26R, and the SK59868-0, were again stested and their performances were compared with their performances from the Phase I tests.

Figures 15 a/b present the walls down performance of the 2FE16A3-4A blades and the same 10% performance deficiency that was observed in Phase I can be noted. The variation of performance with Mach number is still evident, particularly above Mach 0.90.

Figures 16 a/b present the performance of the 2J17G3-26R blades, and Figures 17 a/b provide similar walls down performance for the SK59868-0 blades.

Comparison plots of walls up versus down are presented in Figures 18 a/b and 19 a/b for the 2FE16A3-4A. Figures 19 a/b also provide flight test correlation of the XC-142A aircraft in hover flight with whirl test results at a propeller tip Mach number = 0.85. The correlation is in excellent agreement throughout the entire C_p range (this data was taken from a faired curve through the test results which are contained in Reference 7).

Figures 18a and 19a show that, for the 2FE16A3-4A design point of C_p = 0.085, there was no difference between the tested performance with walls up or down. In both cases (in the lower power coefficient range) the propeller run with the walls down indicated a higher peak figure of merit than with the walls up.

Figures 20 a/b and 21 a/b provide comparison plots of the 2J17G3-26R and SK59868-0, respectively, at the same 0.90 Mach number.

In comparing these three different blades, a substantially higher C_T/C_P for a given C_P at lower power coefficients was noted with the protective walls down. This difference reduced to essentially zero (except for the SK59868-0) at higher power coefficients in the range of C_P = 0.08 to 0.10.

During the latter part of Phase II, the 15,000 ft-lb Rig 4 torque shaft previously used was replaced with a 30,000 ft-lb torque shaft to provide a higher power capability for the subsequent tests of Phase III. Correlation of the two torque shafts is presented in Figures 22 a/b for the 2FF16A1-4A and is seen to be quite good over the entire C_P range.

Figures 23 a/b illustrate the significant increase in performance realized from the redesigned 2FF16A1-4A propeller. At the take-off point of C_P = 0.085, the redesigned 2FF16A1-4A produced approximately 9% increase in thrust/power (C_T/C_P) and gained approximately 9.5 points in figure of merit. Thus, the tested performance of the 2FF16A1-4A came very near to the predicted performance of the original 2FE16A3-4A propeller and a significant increase in the static performance of the XC-142A aircraft was realized.

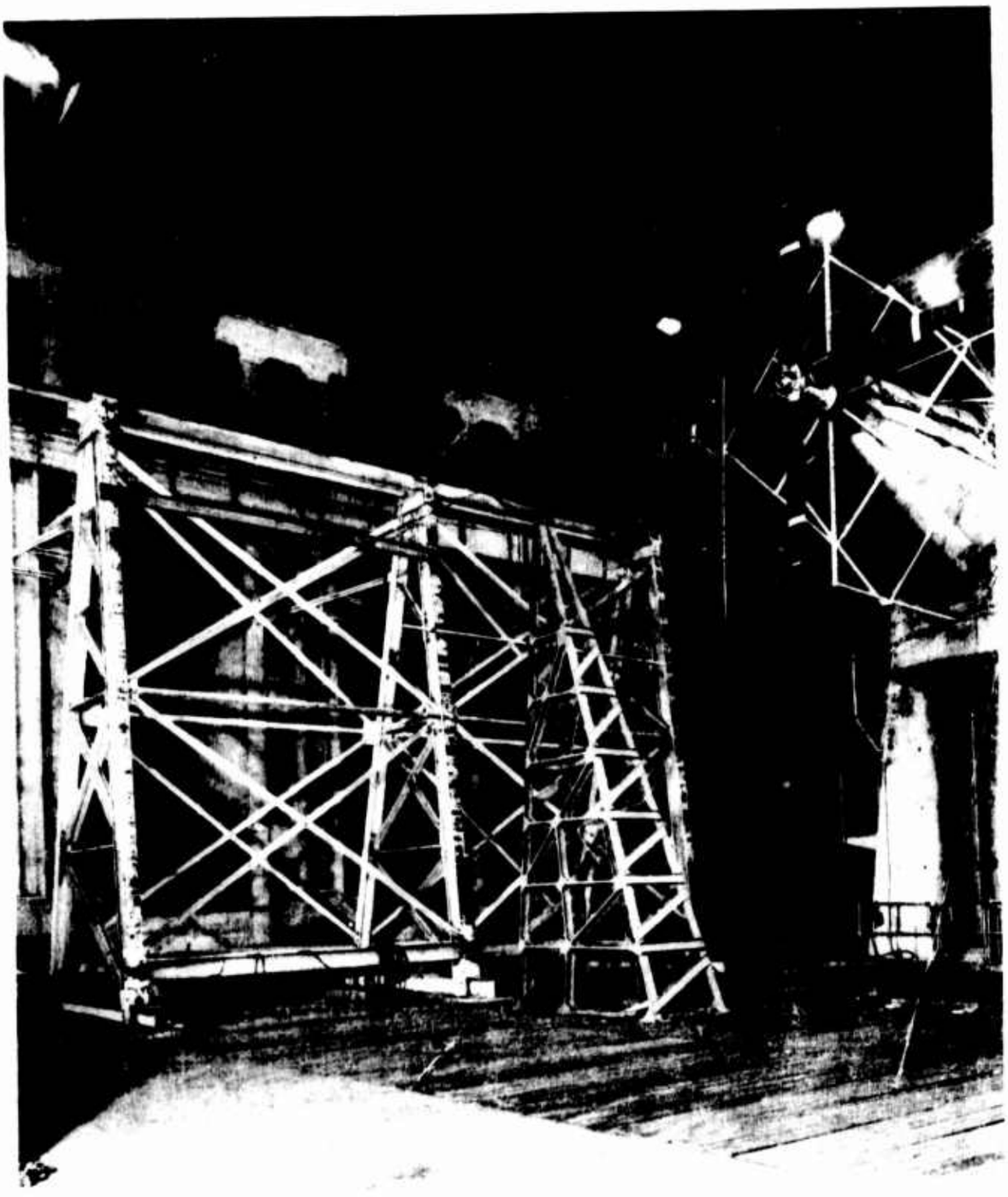

Figure 14. XC-142A Propeller Test - Phase II View of 2FE16A3-4A Propeller on Whirl Rig 4, After Wall Removal

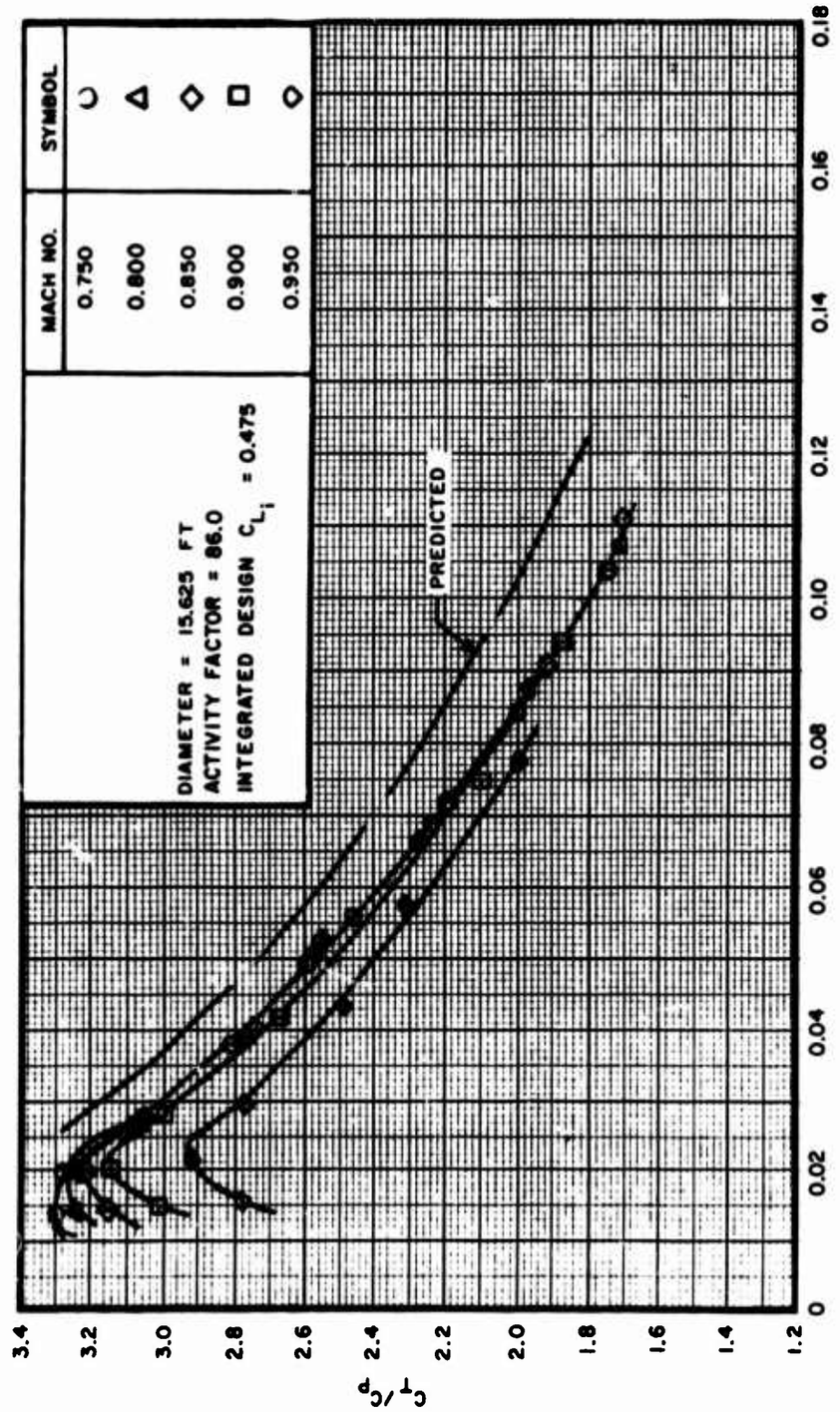

Figure 15. 2FE16A3-4A Walls Down, Performance at Different Tip Mach Numbers

a. C_T/C_P vs C_P plot

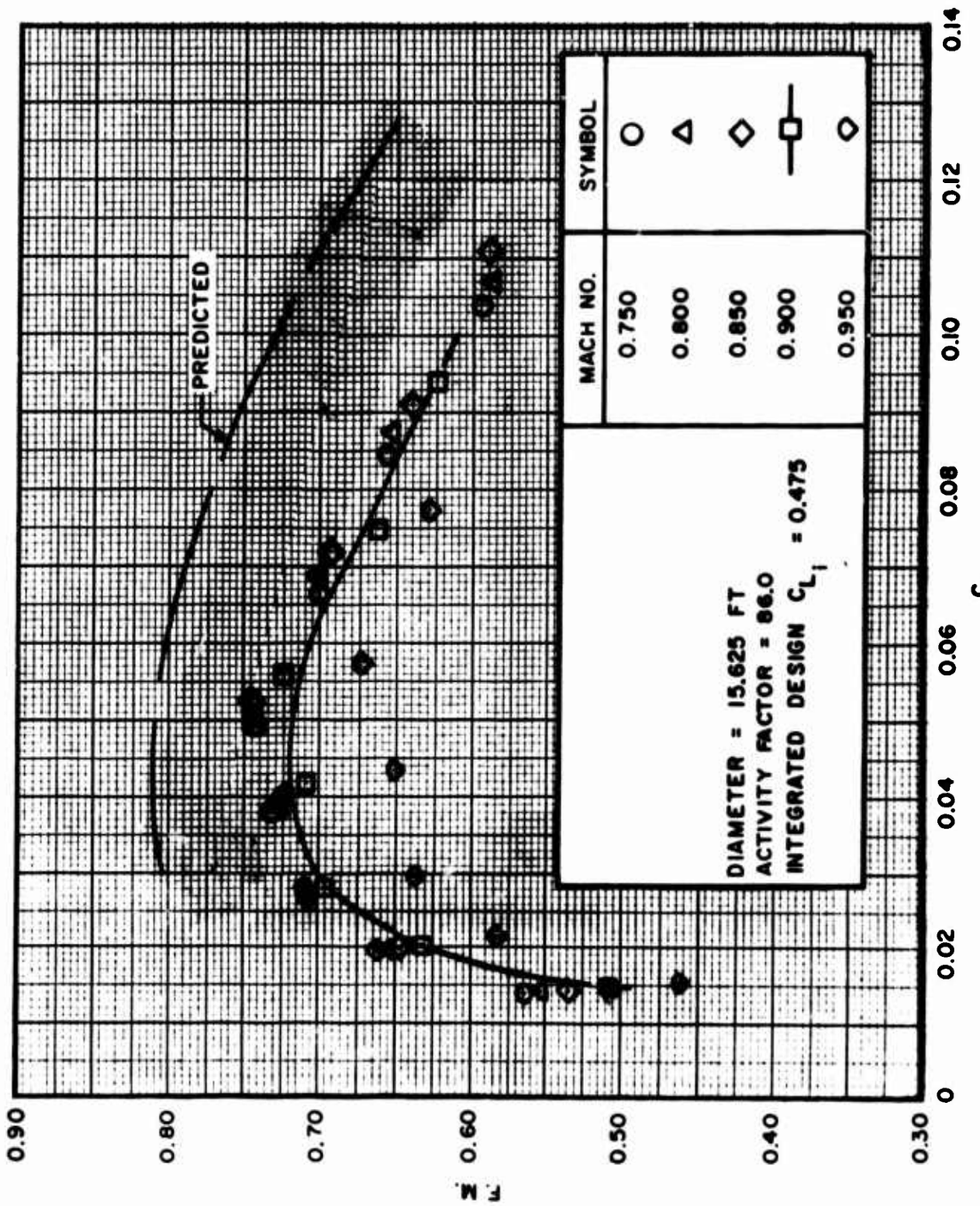

Figure 15. Continued

b. F.M. vs C_P plot

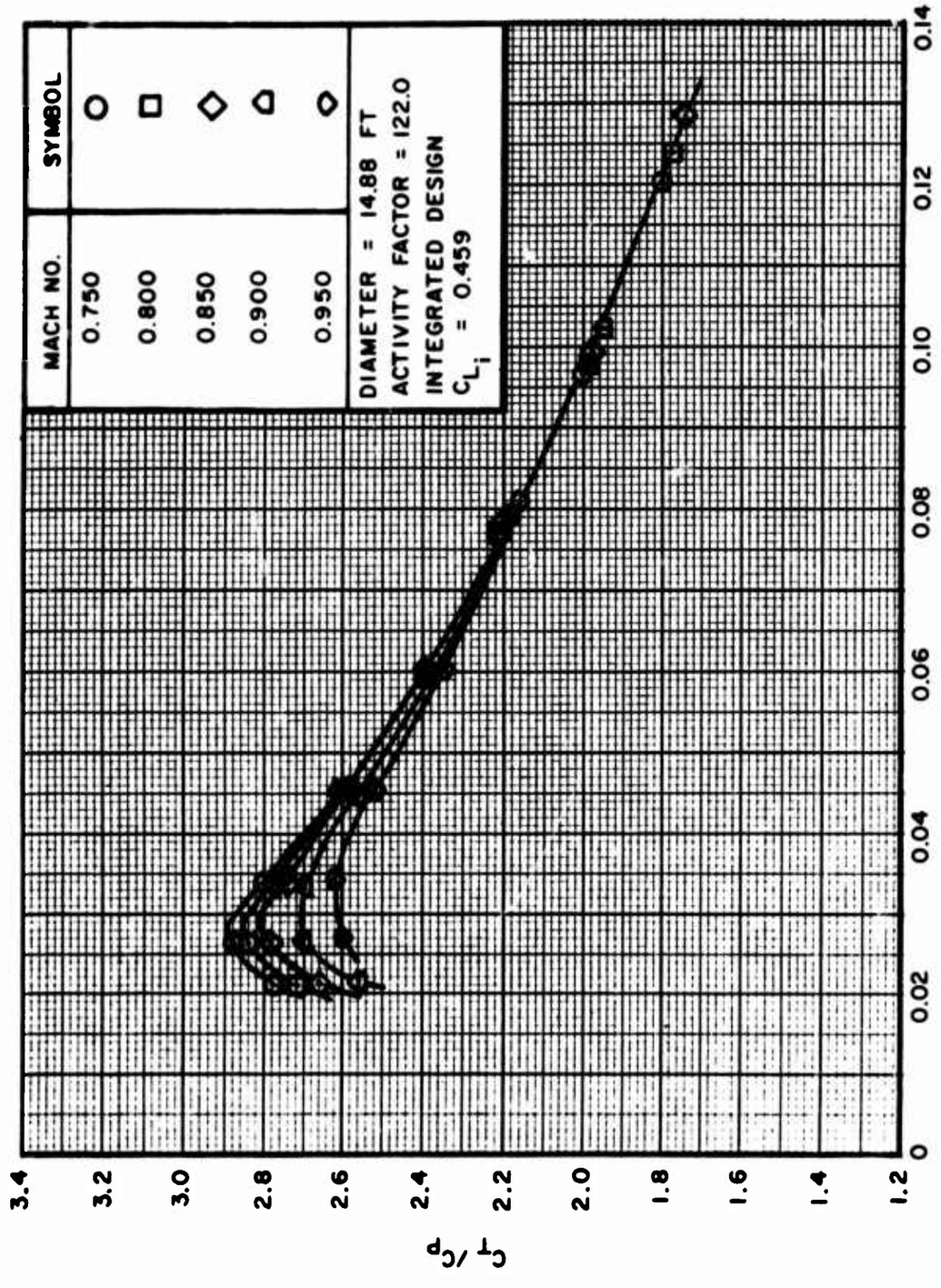

Figure 16. 2J17G3-26R, Walls Down, Performance at Different Tip Mach Numbers

a. C_T/C_D vs C_D plot

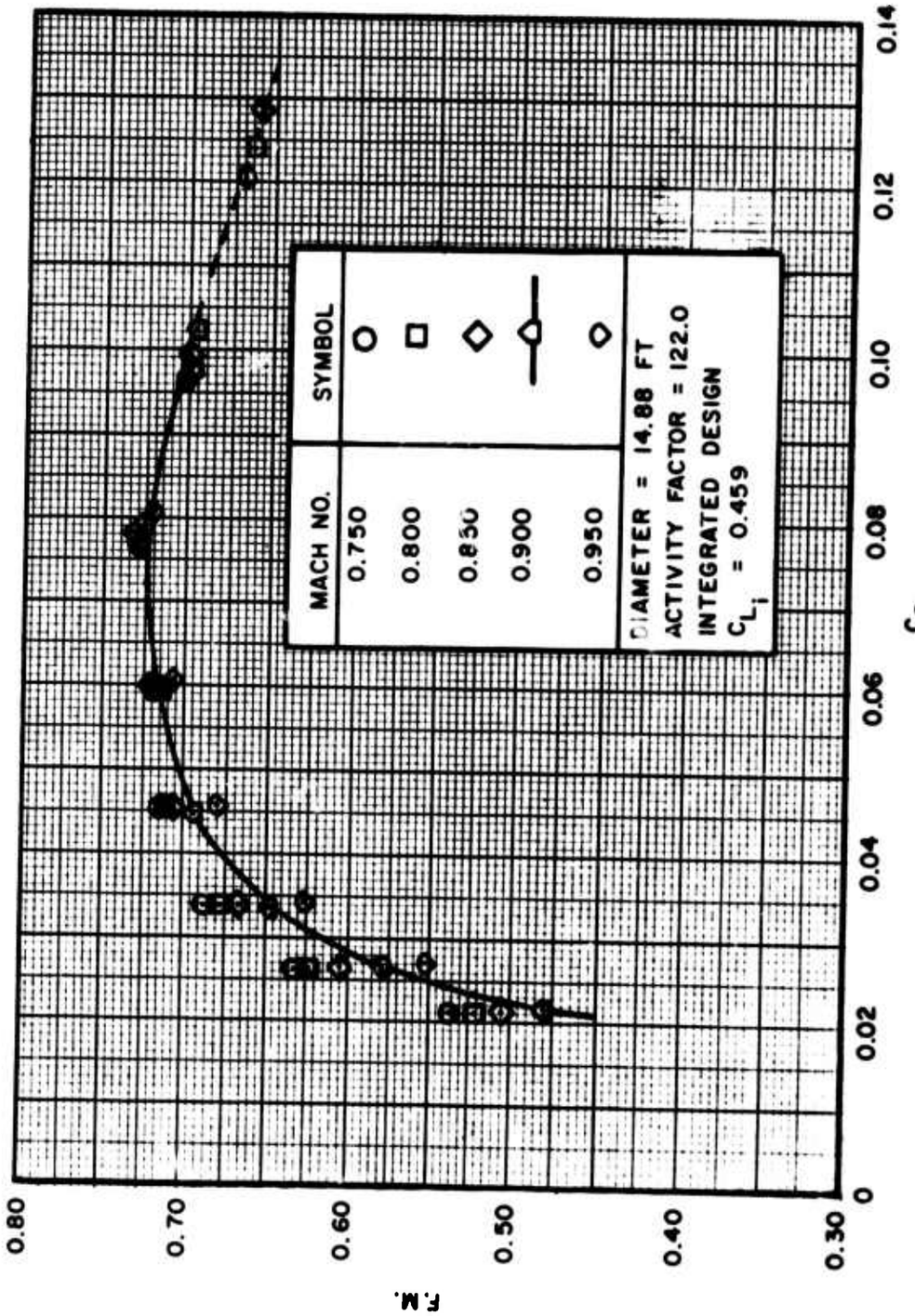

Figure 16. Continued

b. F.M. vs C_p plot

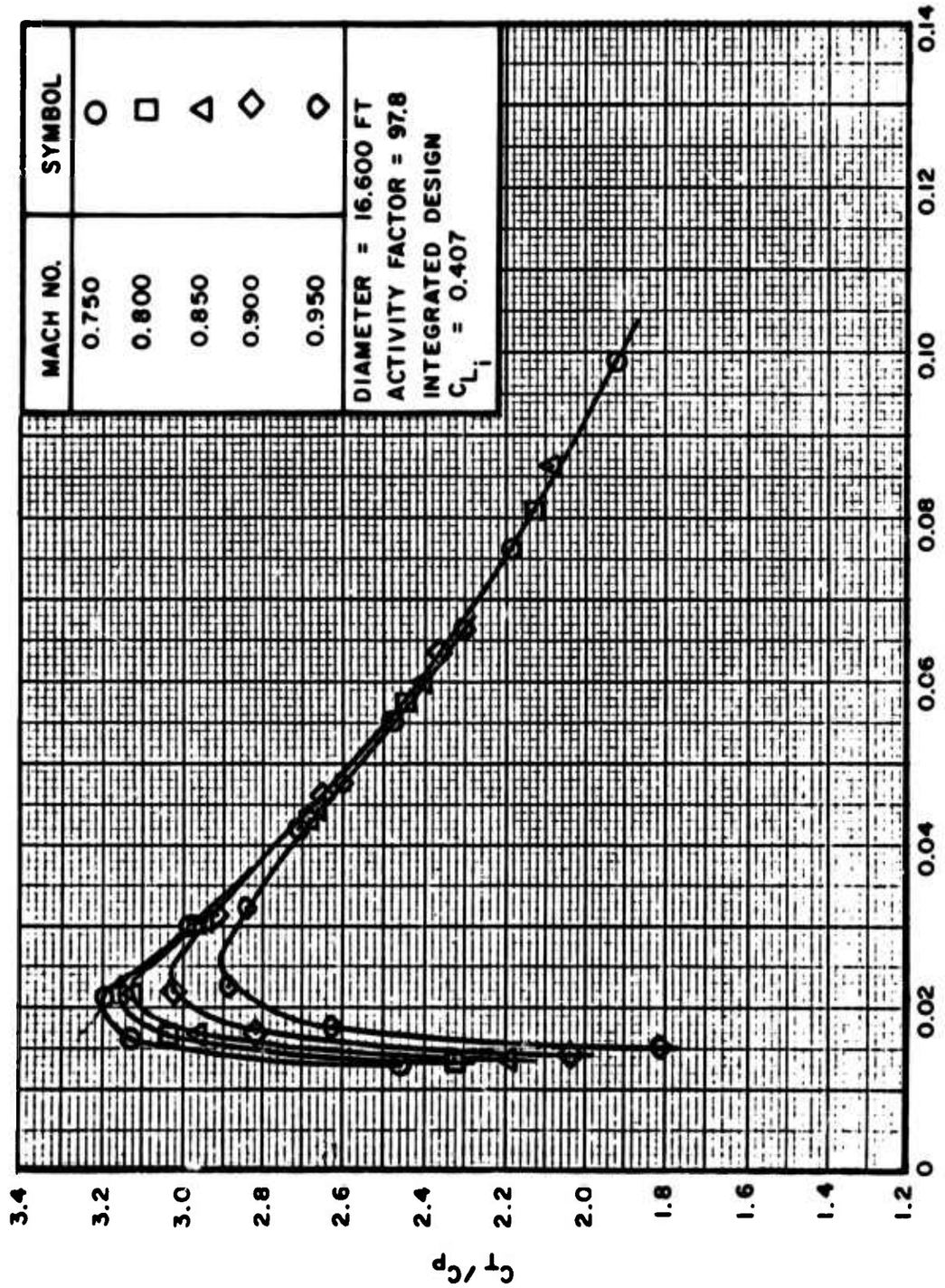

Figure 17. SK59868-0, Walls Down, Performance at Different Tip Mach Numbers

a. C_T/C_P vs C_P plot

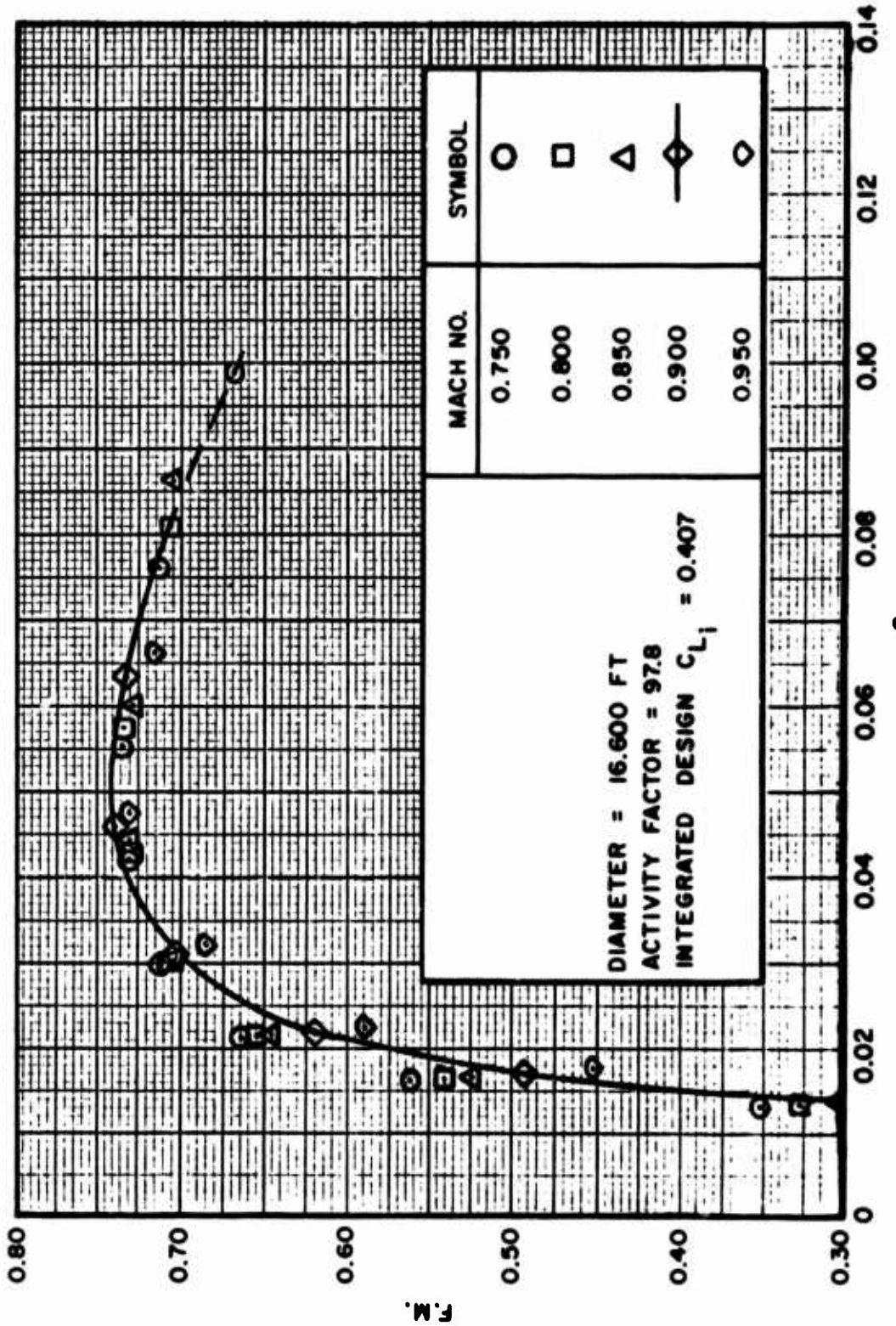

Figure 17. Continued

b. F.M. vs C_p plot

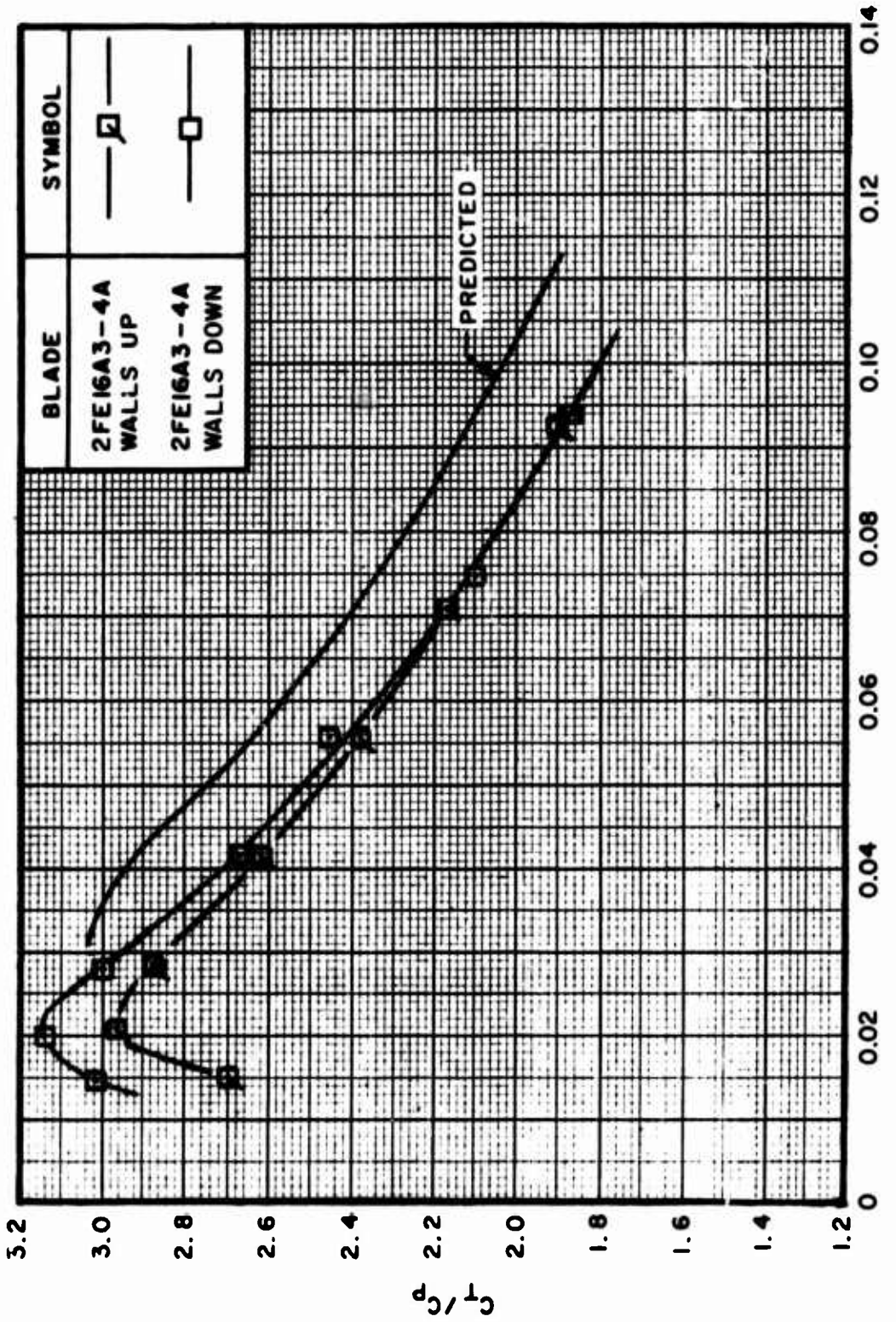

Figure 18. Test Correlation for the 2FE16A3-4A Propeller at Tip Mach Number = 0.900; Walls up and Walls Down Performance a. C_T/C_P vs C_P plot

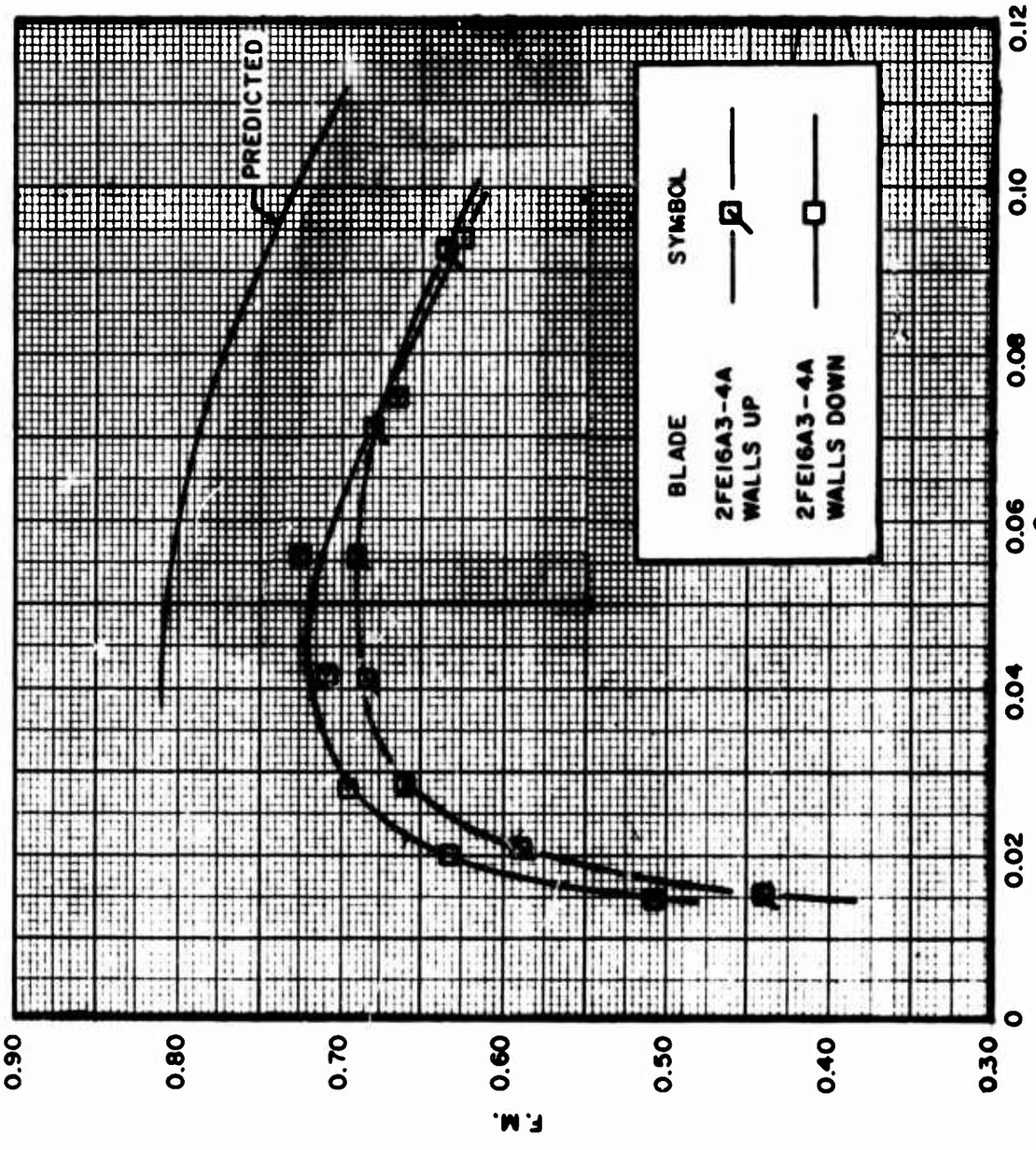

Figure 18. Continued

b. F.M. vs C_P plot

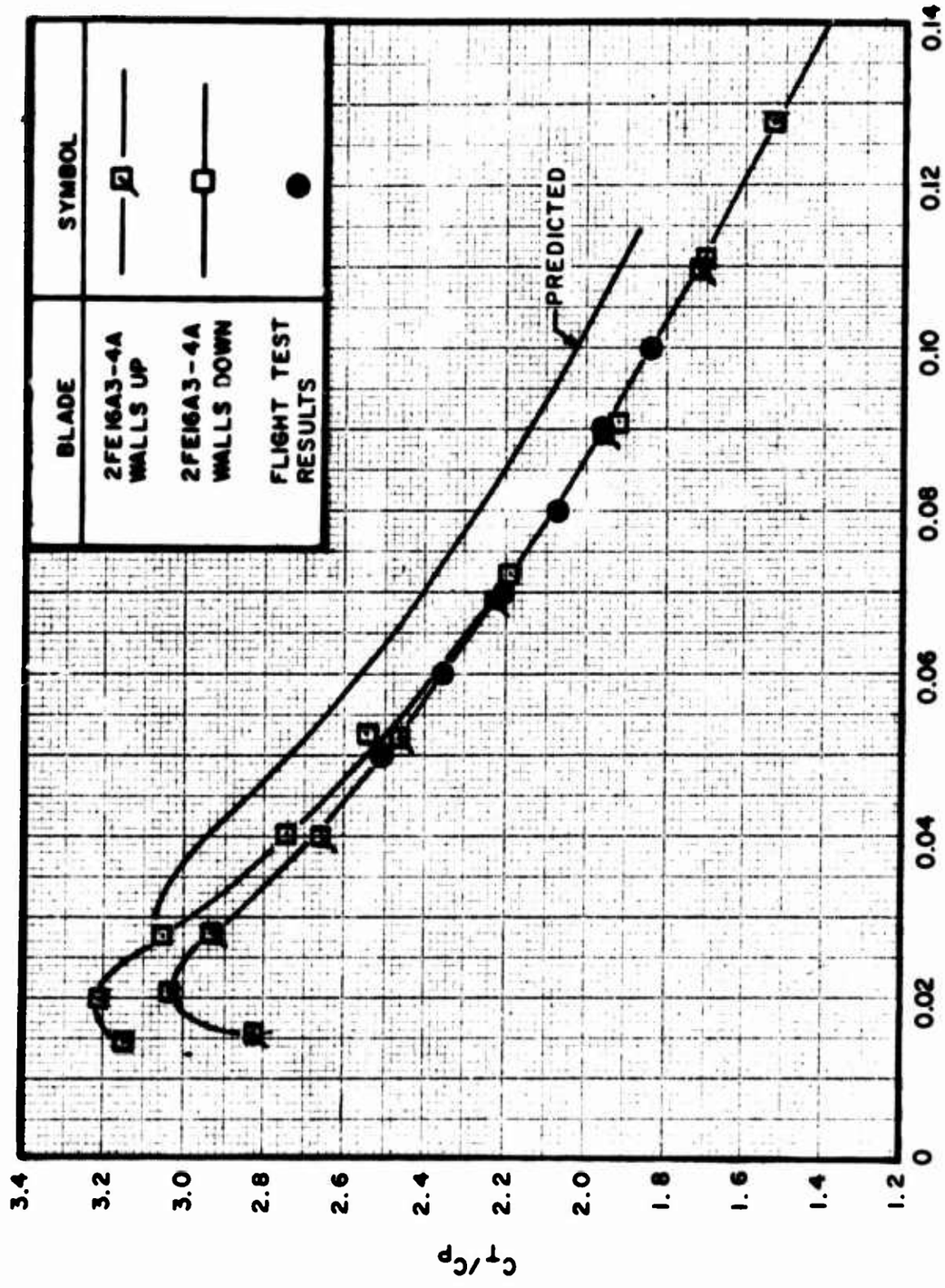

Figure 19. Test Correlation for the 2FE16A3-4A Propeller at Tip Mach Number = 0.850; Walls Up, Walls Down, Predicted and Flight Test Performance

a. C_T/C_P vs C_P plot

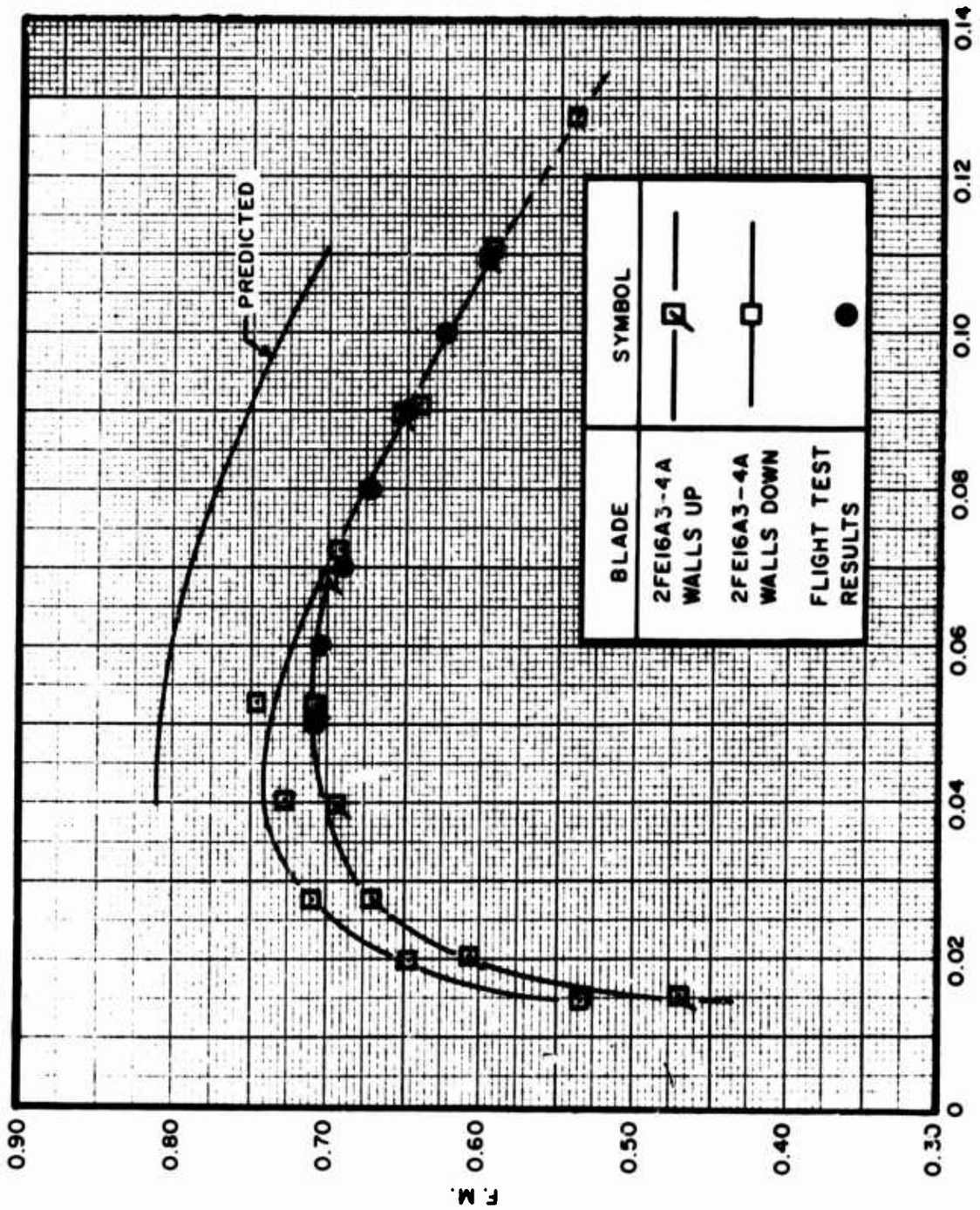

Figure 19. Continued

b. F.M. vs C_P plot

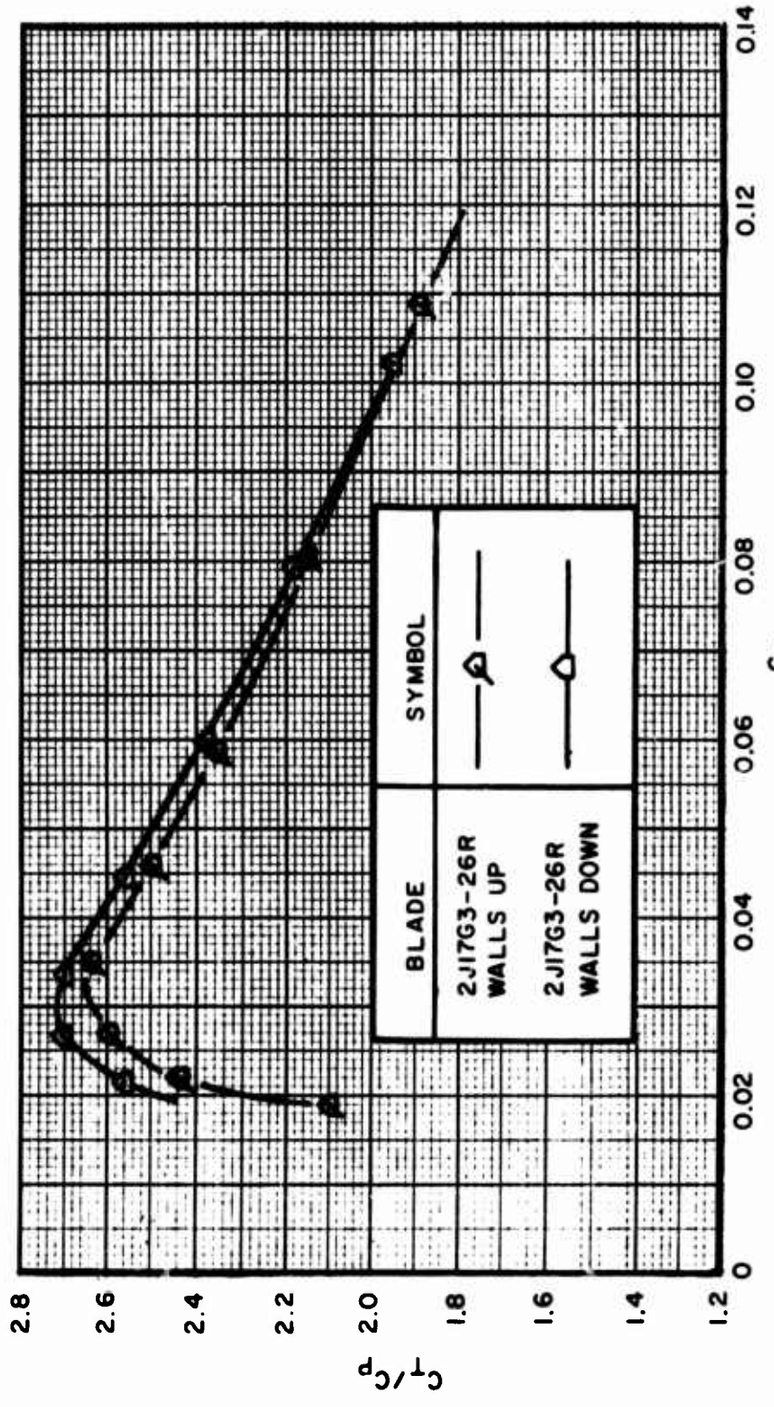

Figure 20. Test Correlation for the 2J17G3-26R Propeller at Tip Mach Number = 0.900, Walls Up and Walls Down Performances

a. C_T/C_P vs C_P plot

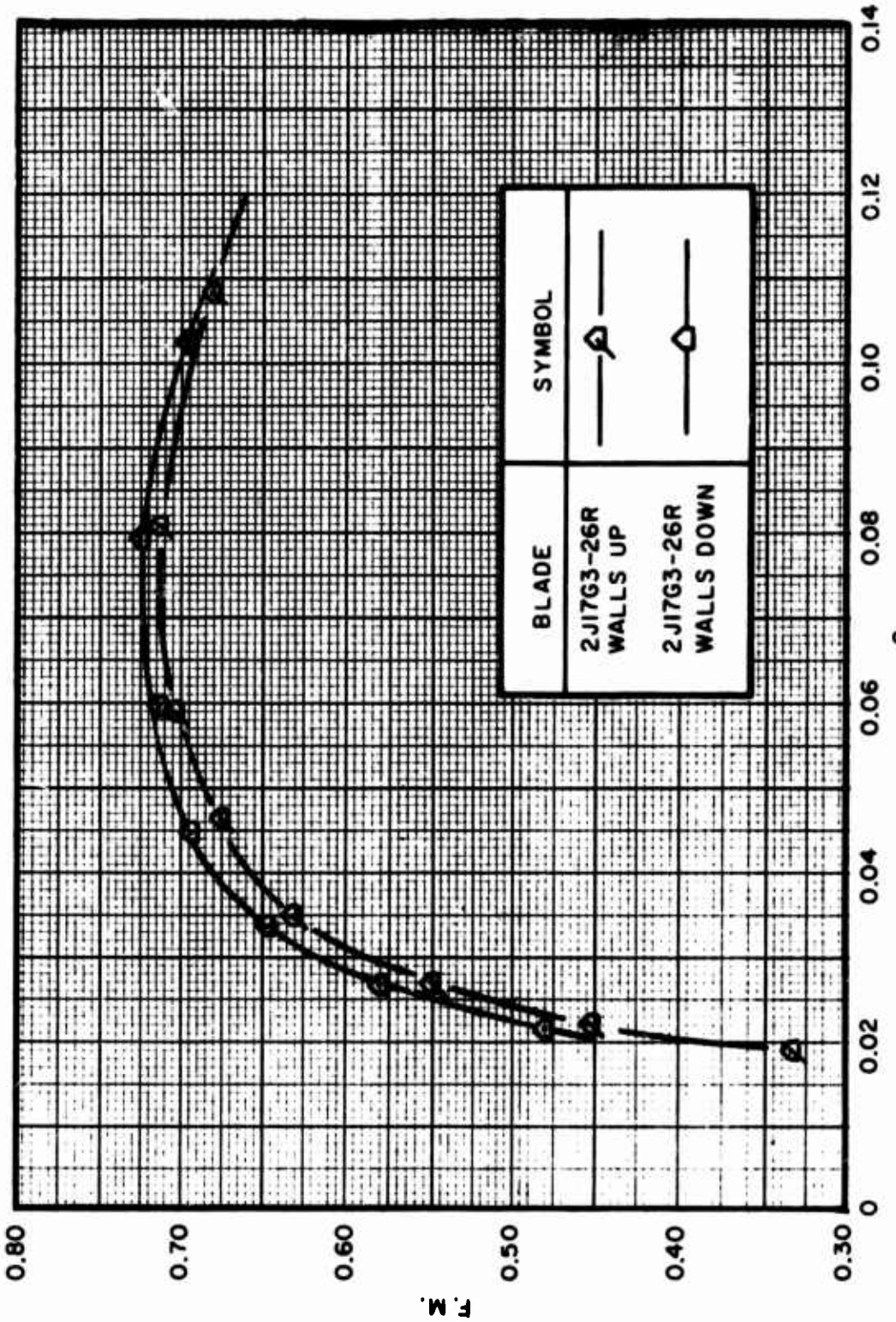

Figure 20. Continued

b. F. M. vs C_P plot

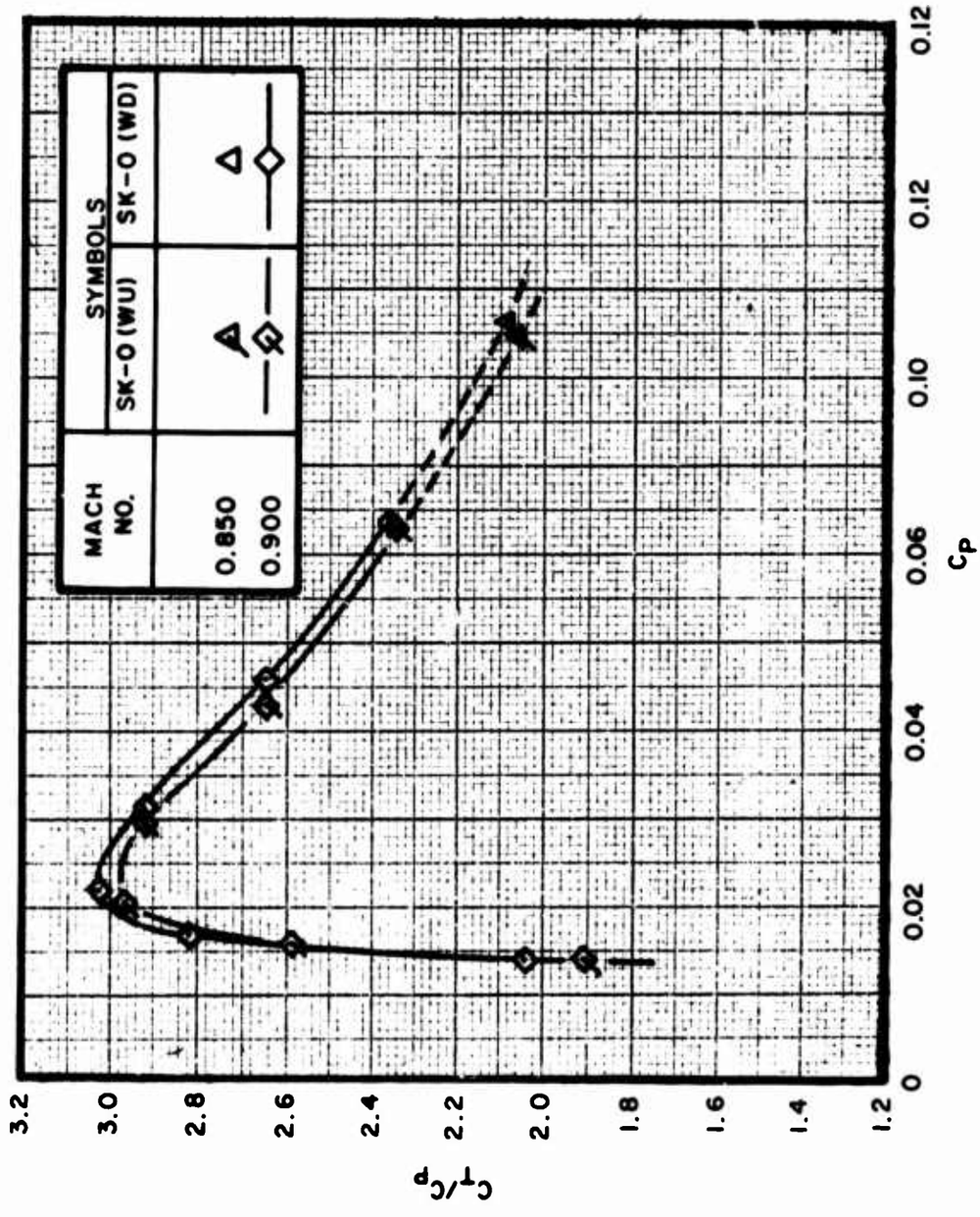

Figure 21. Test Correlation for the SK59868-0 Propeller at Tip Mach Number = 0.900, Walls Up and Walls Down Performances

a. C_T/C_P vs C_P plot

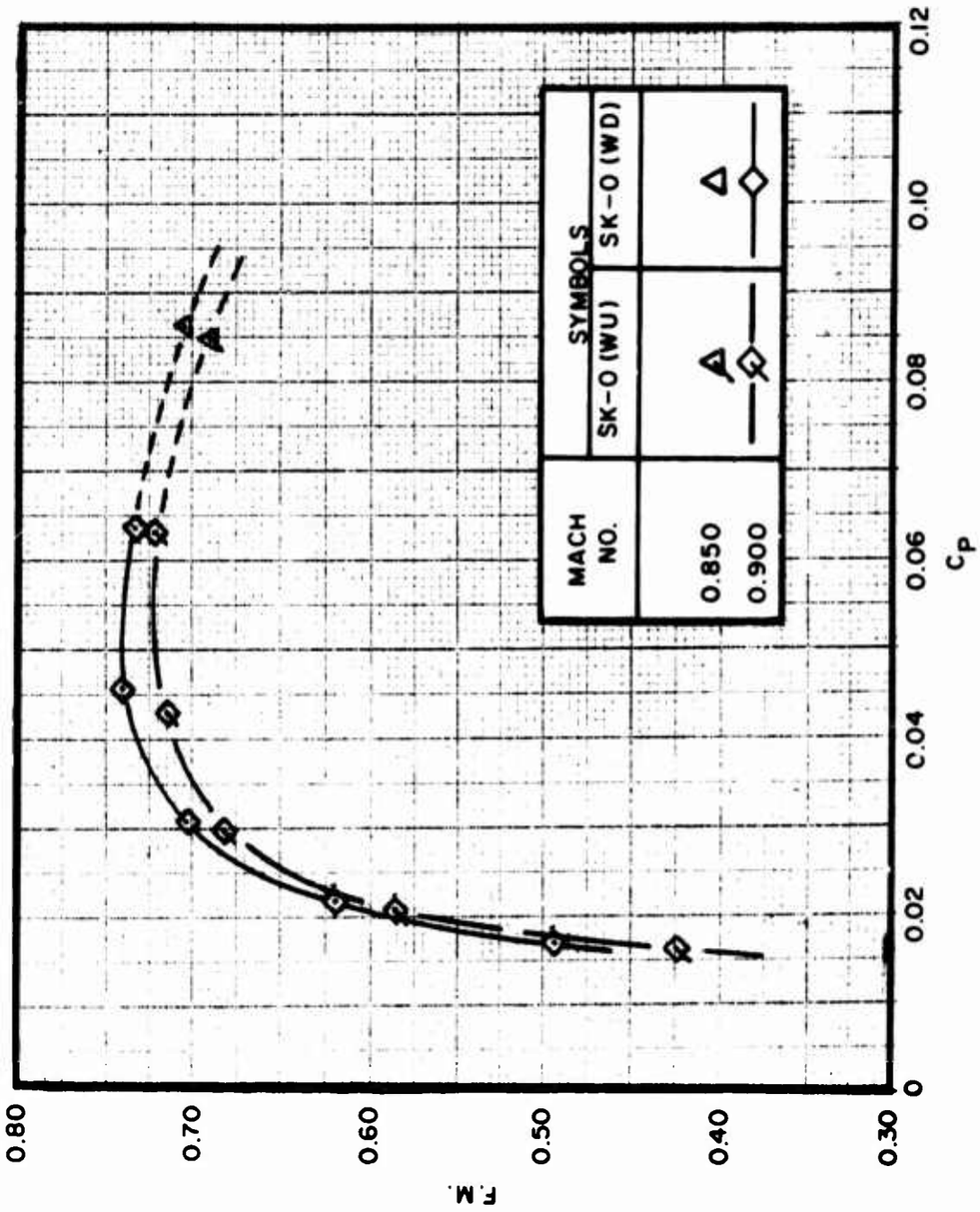

Figure 21. Continued
b. F. M. vs C_P plot

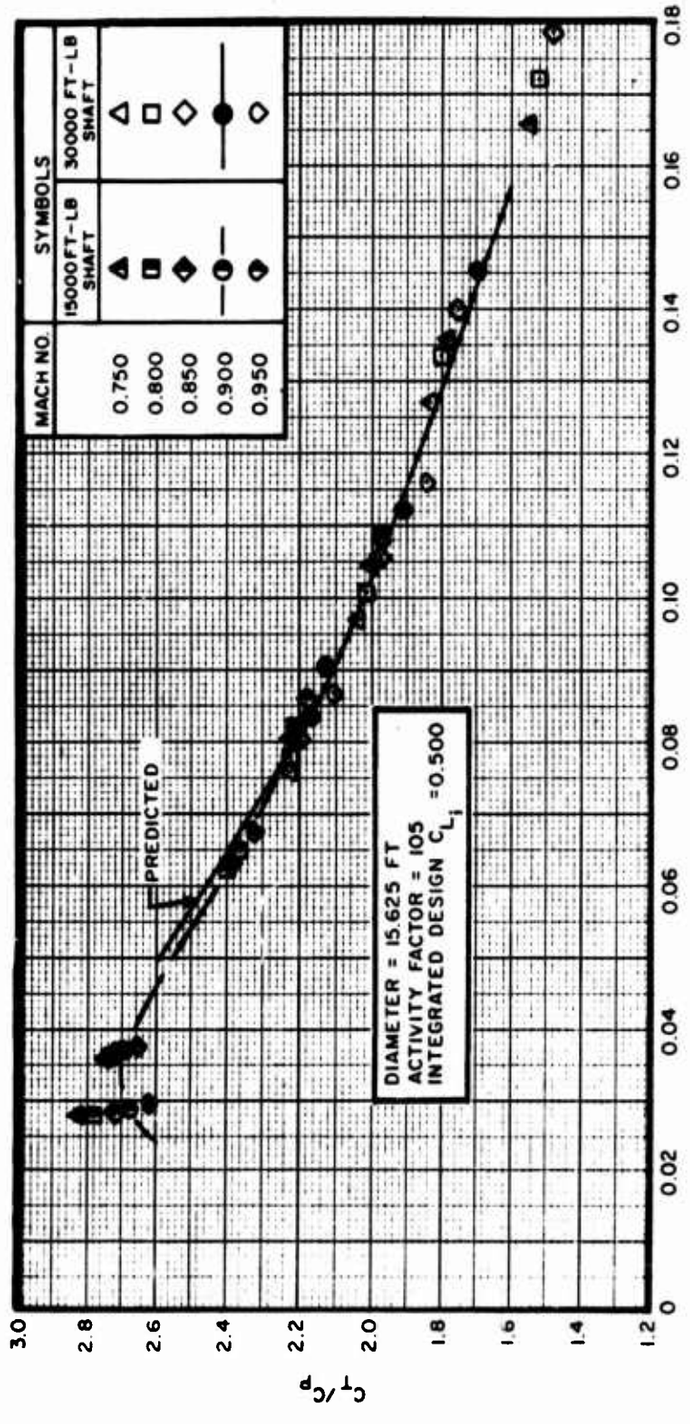

Figure 22. 2FF16A1-4A, Walls Down, Performance at Different Mach Numbers (15,000 ft-lb and 30,000 ft-lb Torque Shaft Comparison)
a. C_T/C_P vs C_P plot

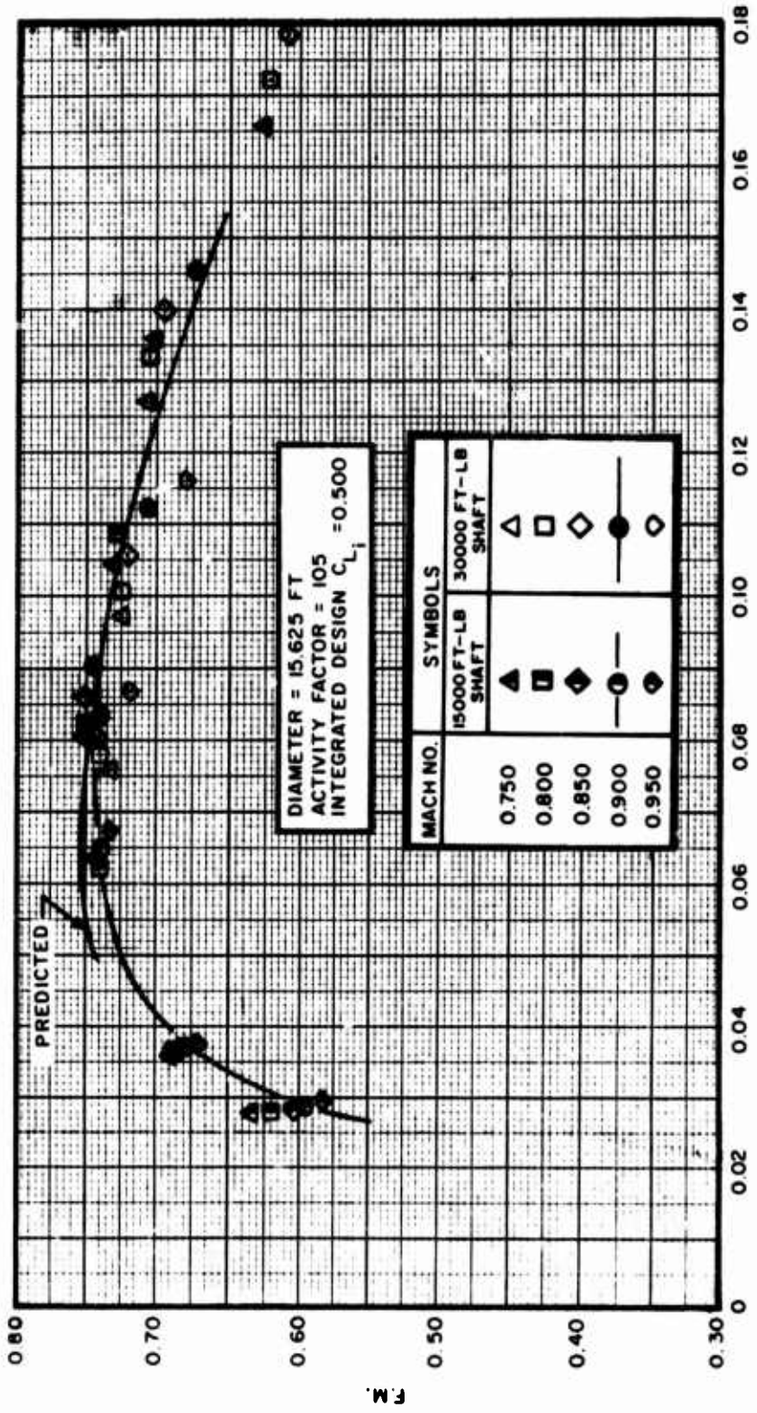

Figure 22. Continued
b. F.M. vs C_P plot

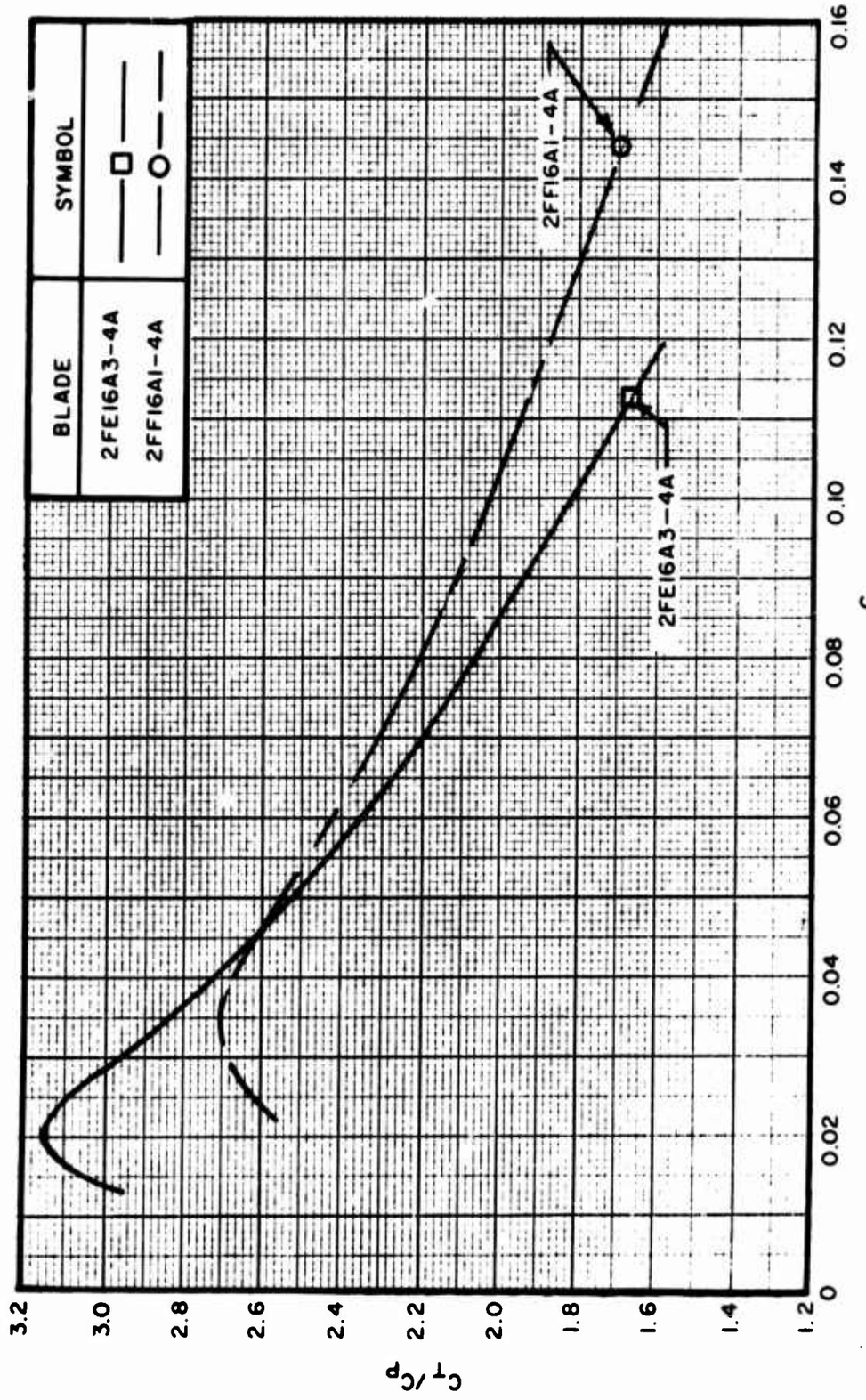

Figure 23. Comparison of 2FE16A3-4A and 2FF16A1-4A Propellers, Walls Down, Performance at Mach Number = 0.900

a. C_T/C_P vs C_P plot

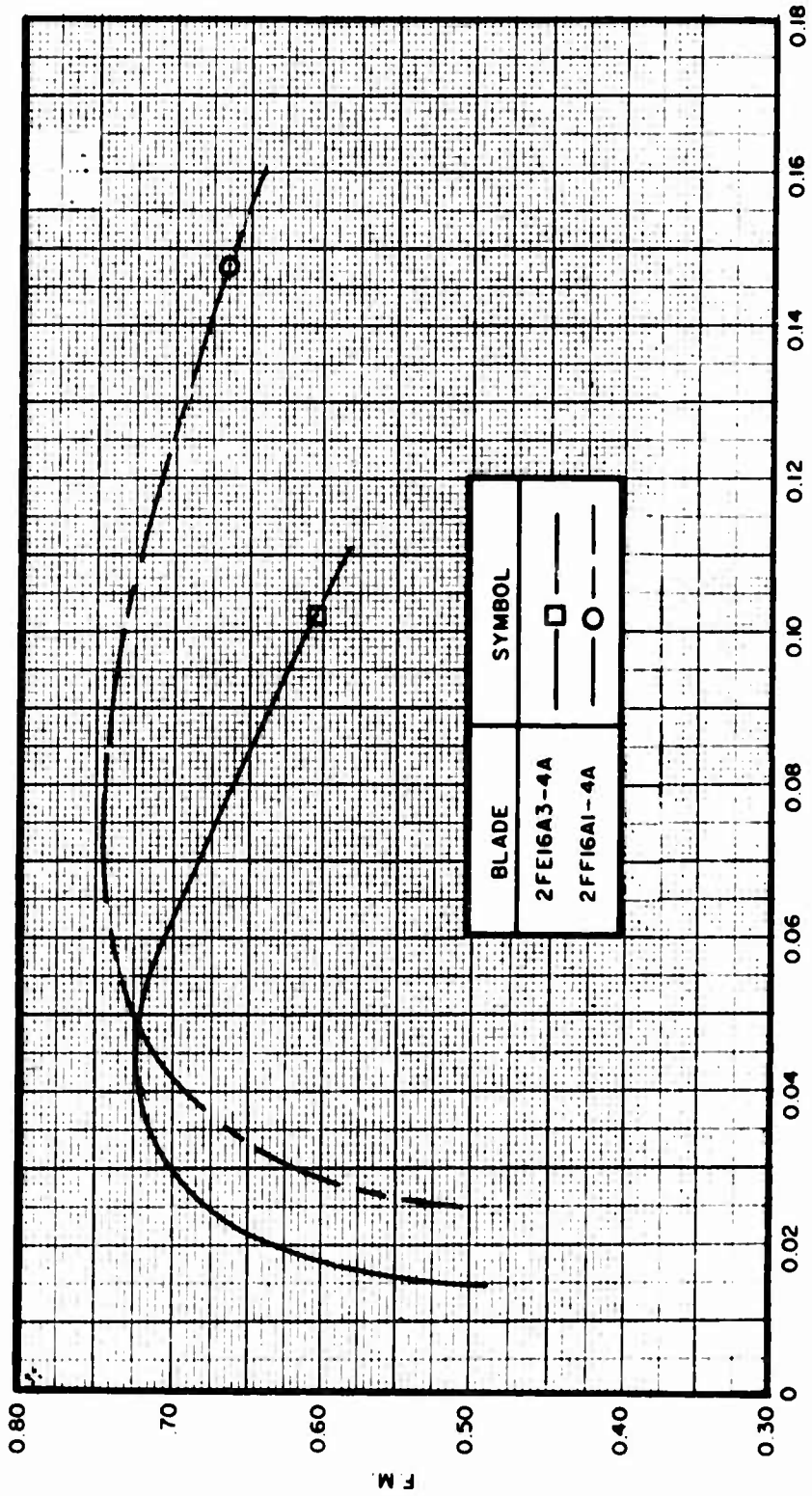

Figure 23. Continued
b. F.M. vs C_P plot

c. Phase III, Walls Relocated

Following completion of Phase II, the protective walls were permanently relocated approximately 16 feet farther away from the rig than their original position, thereby placing them against the exterior walls of the test chamber. This new position is shown for both the north and south walls in Figures 24 and 25.

Figures 26 a/b present the performance of the 2FF16A1-4A tested during this phase in the higher C_p range. The power limit imposed by the 15,000 ft-lb rig torque shaft had previously limited testing to low blade angles and thus low power coefficients.

A comparison plot of the 2FF16A1-4A tested with the walls both up and down and the XC-142A hover flight test data and predicted performance are presented in Figures 27 a/b. The flight test data was calculated based on engine performance at three aircraft gross weights, (heavy - 39,840 lbs, medium - 37,000 lbs, and light - 33,490 lbs) as contained in Reference 6. The flight test data did not correlate as favorably as did that of the 2FE16A3-4A data from Phase II. These test results show that there is essentially no difference between the indicated thrust for the 2FF16A1-4A with the protective walls down or in their relocated position. It can be seen from Figure 27b that the peak F.M. value for the walls relocated was reduced slightly, in the range of 1 point.

Figures 28 a/b provide comparison plots of the 2FF16A1-4A and the entire 47 x XXX series of propellers which were tested during Phase III so that the effects of various parameters can be studied. The 47 x 91, which is a 0.832-scale solid dural version of the 2FF16A1-4A, was used as a baseline propeller for this study. It should be clearly noted from Figure 28a that the performance of the 2FF16A1-4A and the 47 x 91 did not correlate closely, particularly in the higher power coefficient range. This performance difference is even more obvious in the F.M. plot shown in Figure 28b. No acceptable reason for the difference in performance between these two blades has been substatiated to date; however, the two most obvious differences are those of scale and material. If the 47 x 91 blade were to be used as a baseline against which to evaluate the parametric changes, then the relative parametric performance difference should also apply to the 2FF16A1-4A blade.

The 47 x 95 is seen to produce the highest F.M. of the entire series and displays a substantial increase in static performance capability over the 47 x 91. Likewise, the 47 x 93 produced a significant increase in performance over the 47 x 91. By using the 47 x 91 baseline

blade and applying the increased twist of the 47 x 95 and the increased activity factor of the 47 x 93 blades, it appears that an impressive F.M. of 0.79 could be achieved in the range of C_P = 0.09 to 0.11 for a scale dural blade.

It is the author's opinion that much can be learned from this 47 x XXX series and that only the most obvious factors have been presented here. By a close scrutiny of the various blade characteristic sheets, one might glean more information on the factors which affect static thrust.

2. EFFECT OF BLADE CUFF

The effect of a propeller blade cuff on performance is presented in Figures 29 through 31. These figures represent the 47 x 91/92, 47 x 93/94, and 47 x 95/96 groups of blades tested, both with and without blade cuffs. All data presented in this section is based on testing with the walls relocated.

In general, removing the cuff improved propeller performance slightly at power coefficients up to C_P = 0.09 - 0.10. Beyond this point, either no change was noted or a slight performance reduction was observed. For the XC-142A take-off point of C_P - 0.085, the effect of cuffs on the propeller performance would have been negligible.

A properly designed cuff would provide significant improvement in increased engine inlet pressure recovery, resulting in a net thrust increase compared to the same propeller not equipped with a cuff. Incorporation of a cuff should be based upon the particular installation and the engine pressure recovery requirements. If pressure recovery is not a factor, then consideration should be given to a blade without a cuff.

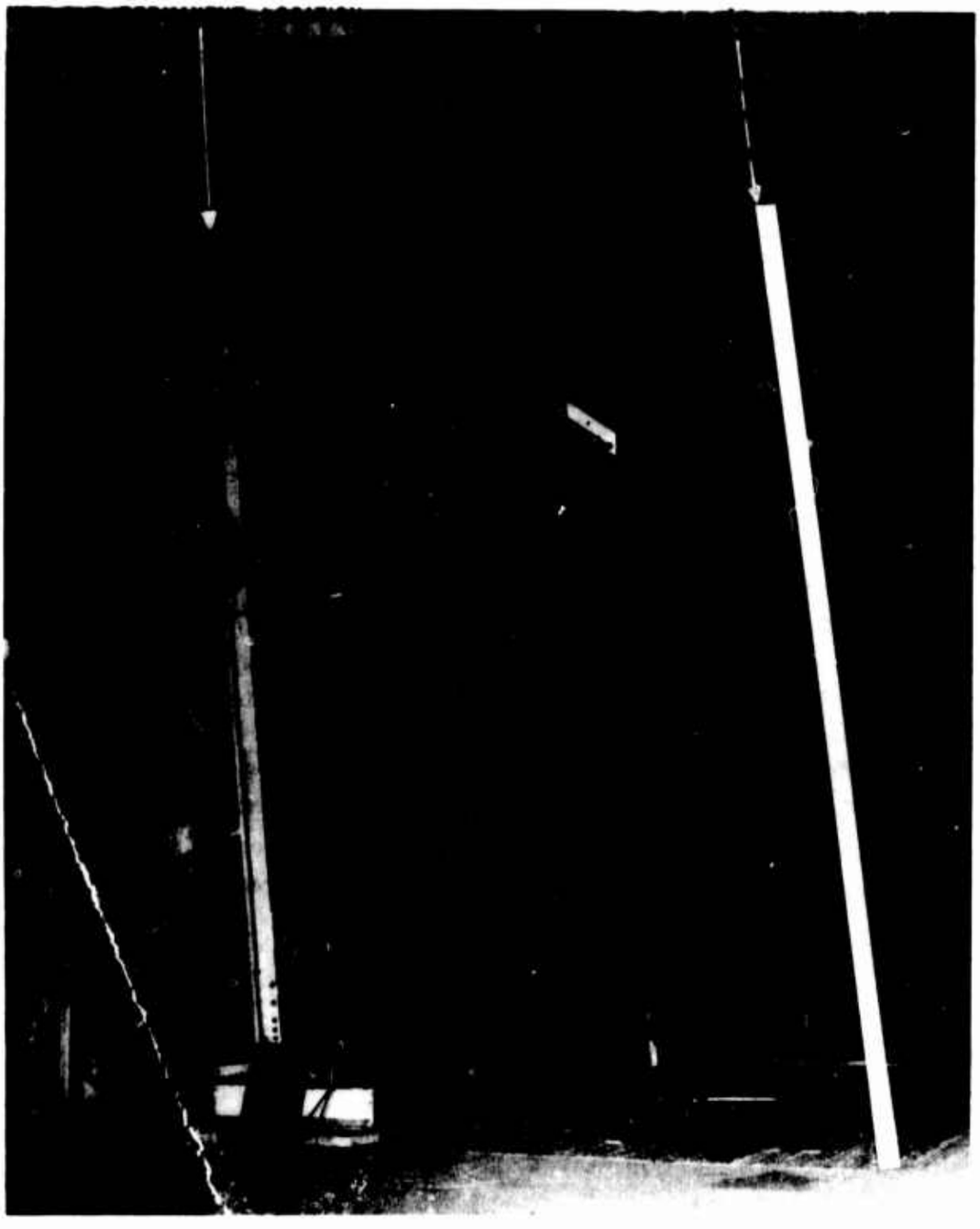

Figure 24. XC-142A Propeller Tests - Phase III, Relocated North Bomb-Proof Wall, Showing Original Position

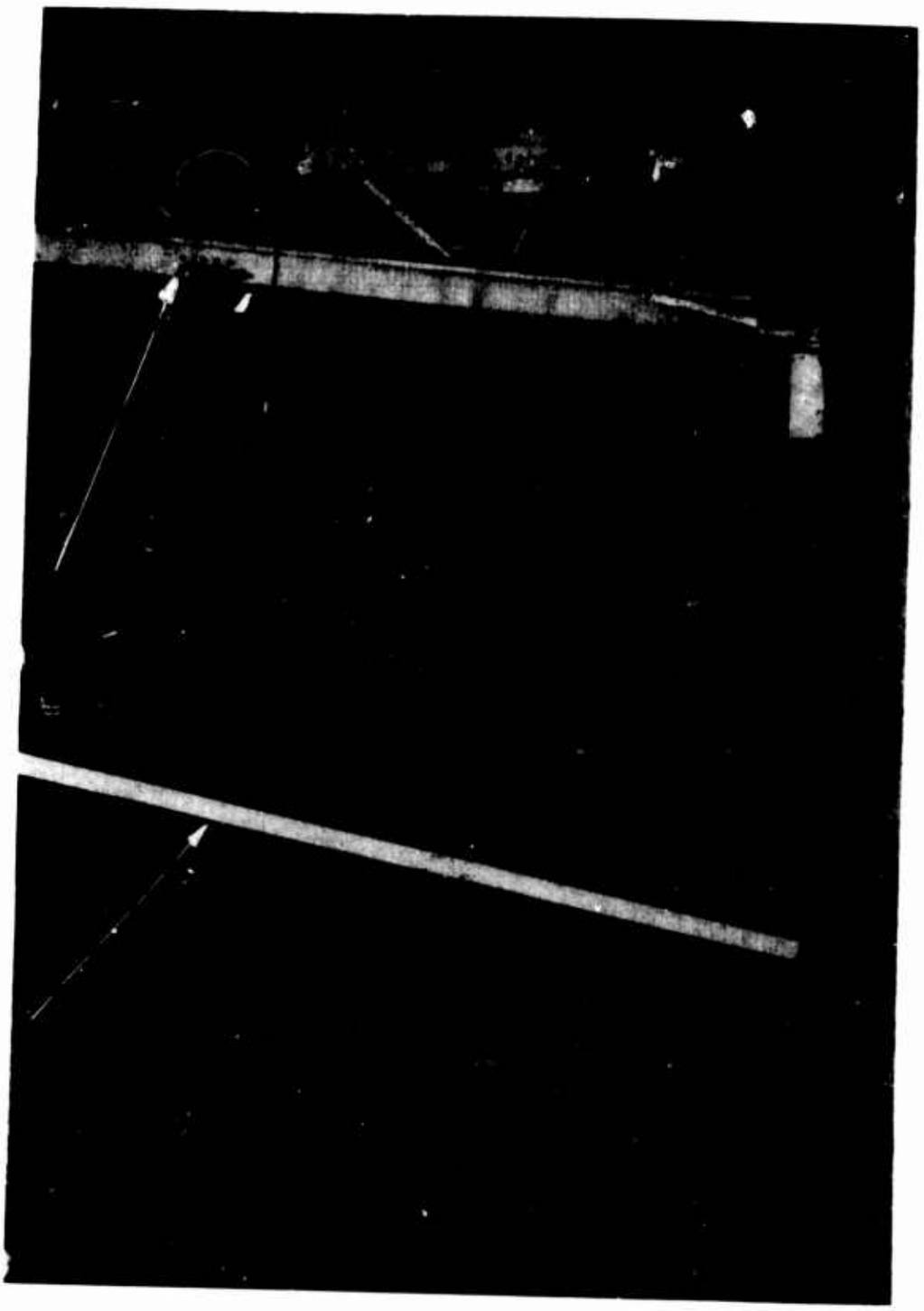

Figure 25. XC-142A Propeller Tests - Phase III, Relocated South Bomb-Proof Wall, Showing Original Position

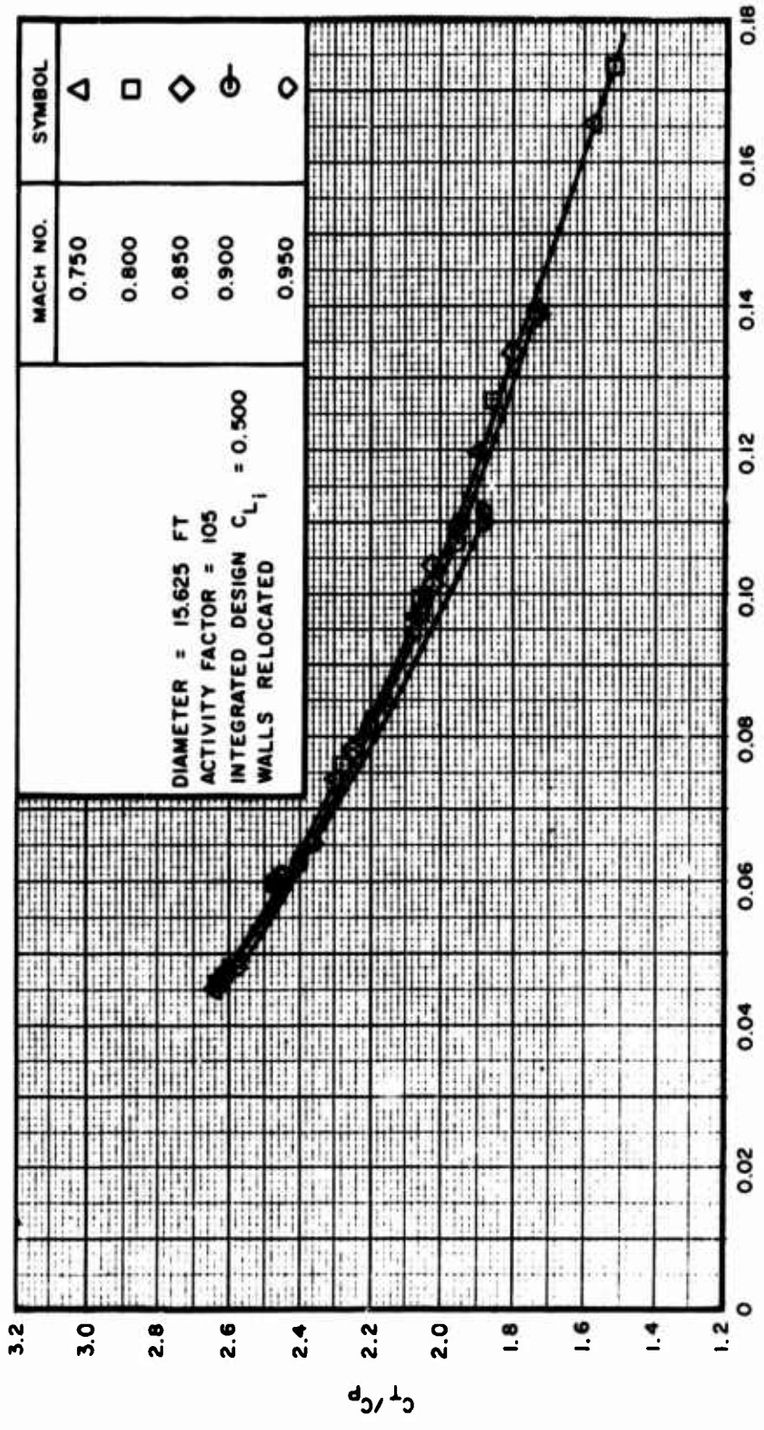

Figure 26. 2FF16A1-4A, Walls Relocated, Performance at Different Tip Mach Numbers
a. C_T/C_P vs C_P plot

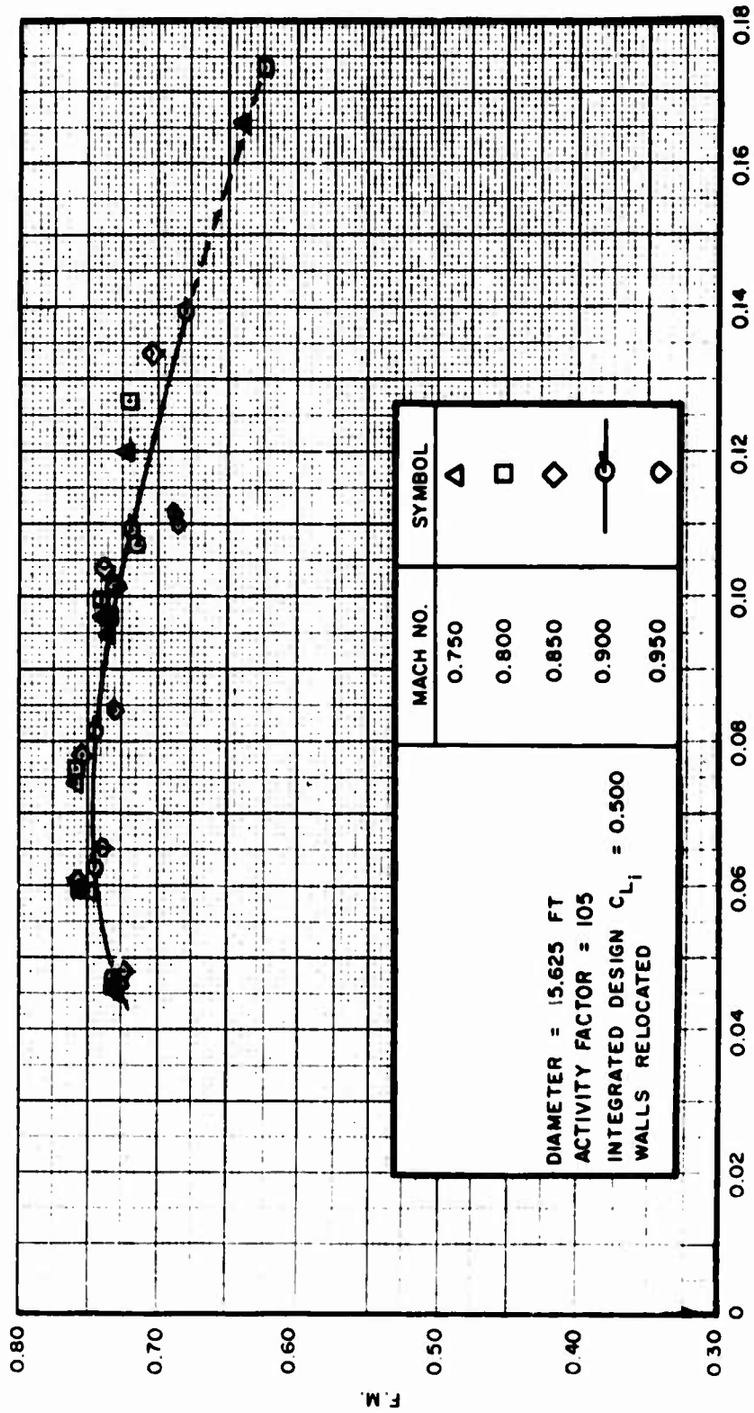

Figure 26. Continued
b. F.M. vs C_P plot

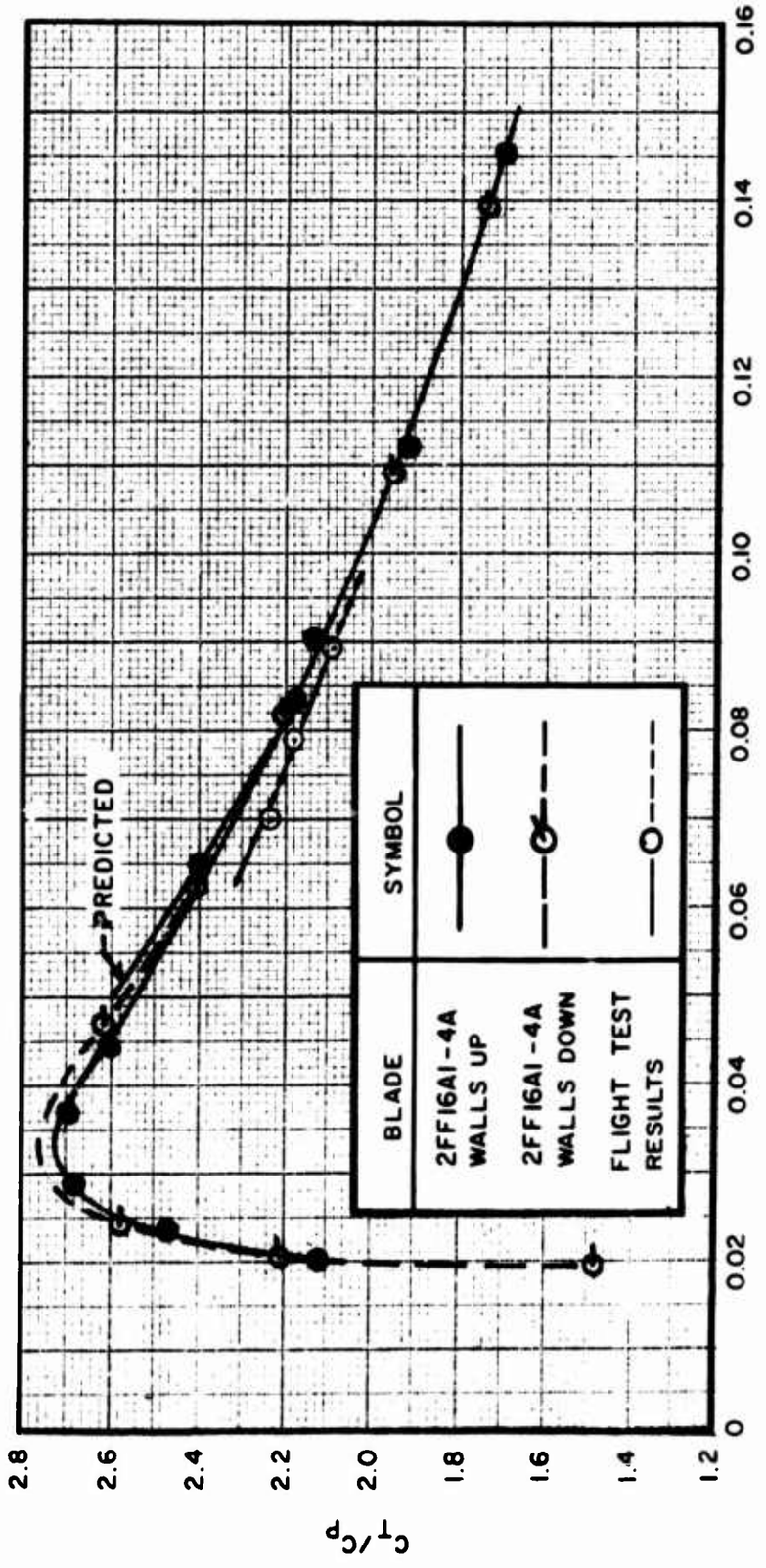

Figure 27. Test Correlation for the 2FF16A-1-4A at Tip Mach Number = 0.900; Walls Down, Walls Relocated, Predicted, and Flight Test Performances

a. C_T/C_P vs C_P plot

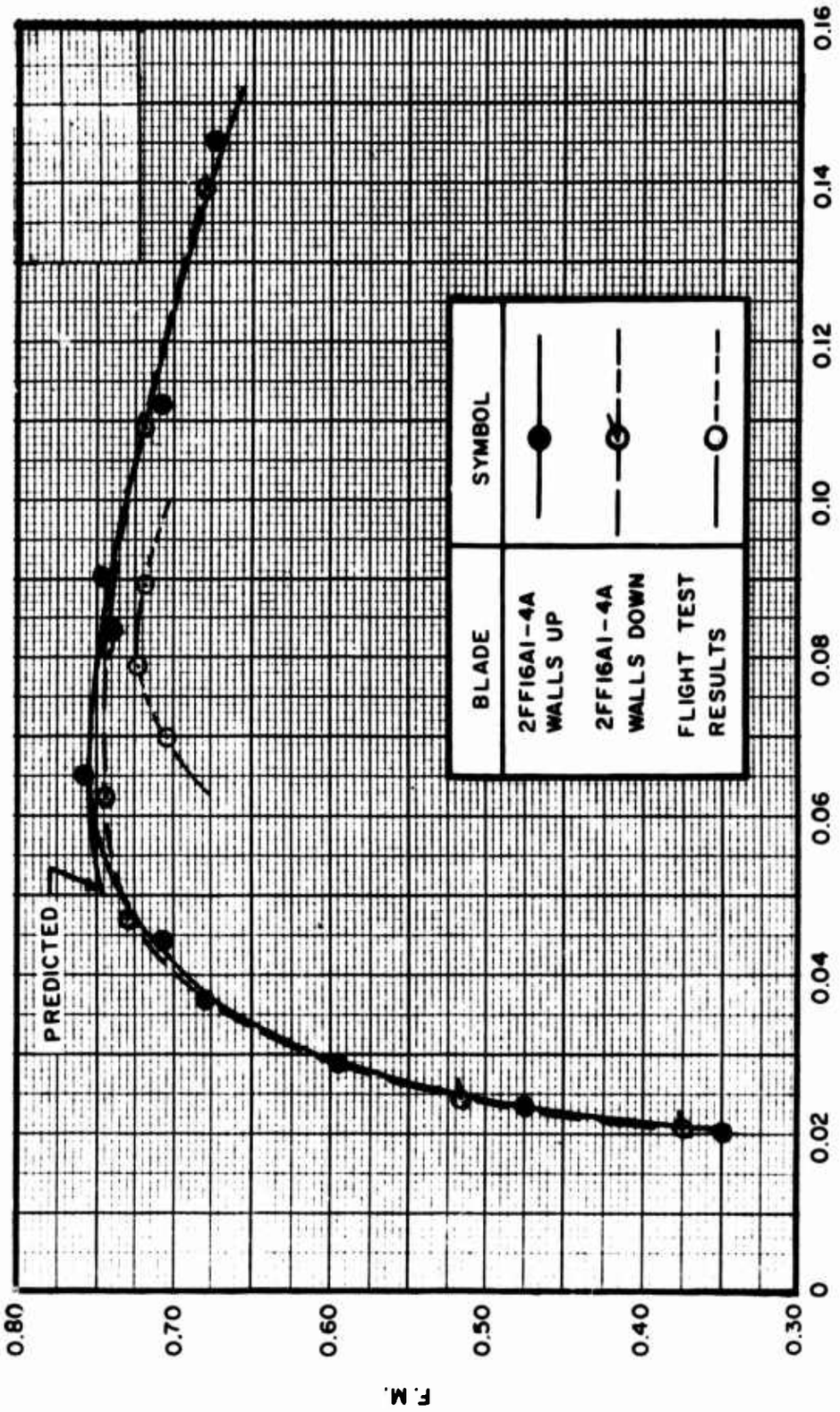

Figure 27. Continued

b. F. M. vs C_P plot

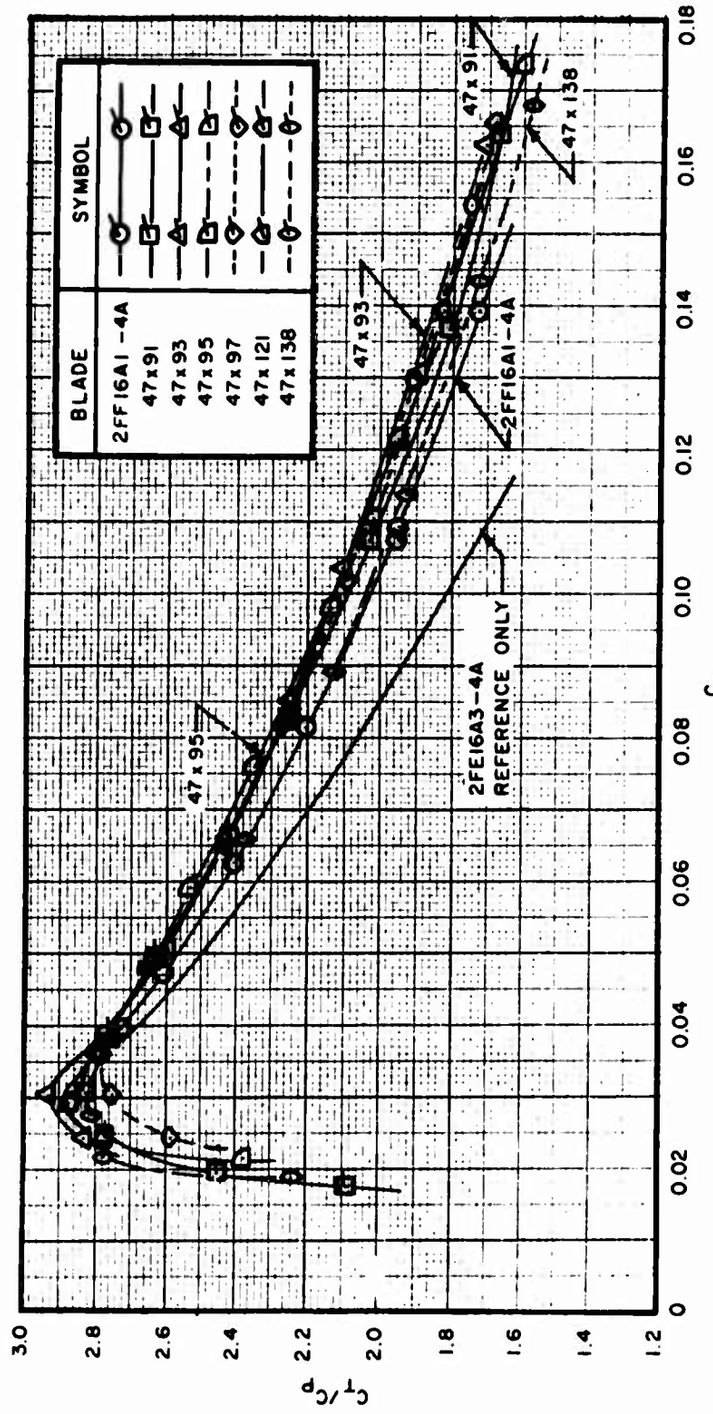

Figure 28. Comparison of 2FF16A1-4A, 47 x 91, 47 x 93, 47 x 95, 47 x 97, 47 x 121, 47 x 138, and 2FE16A3-4A Propellers, Walls Relocated, Performance at Tip Mach Number = 0.900

a. C_T/C_P vs C_P plot

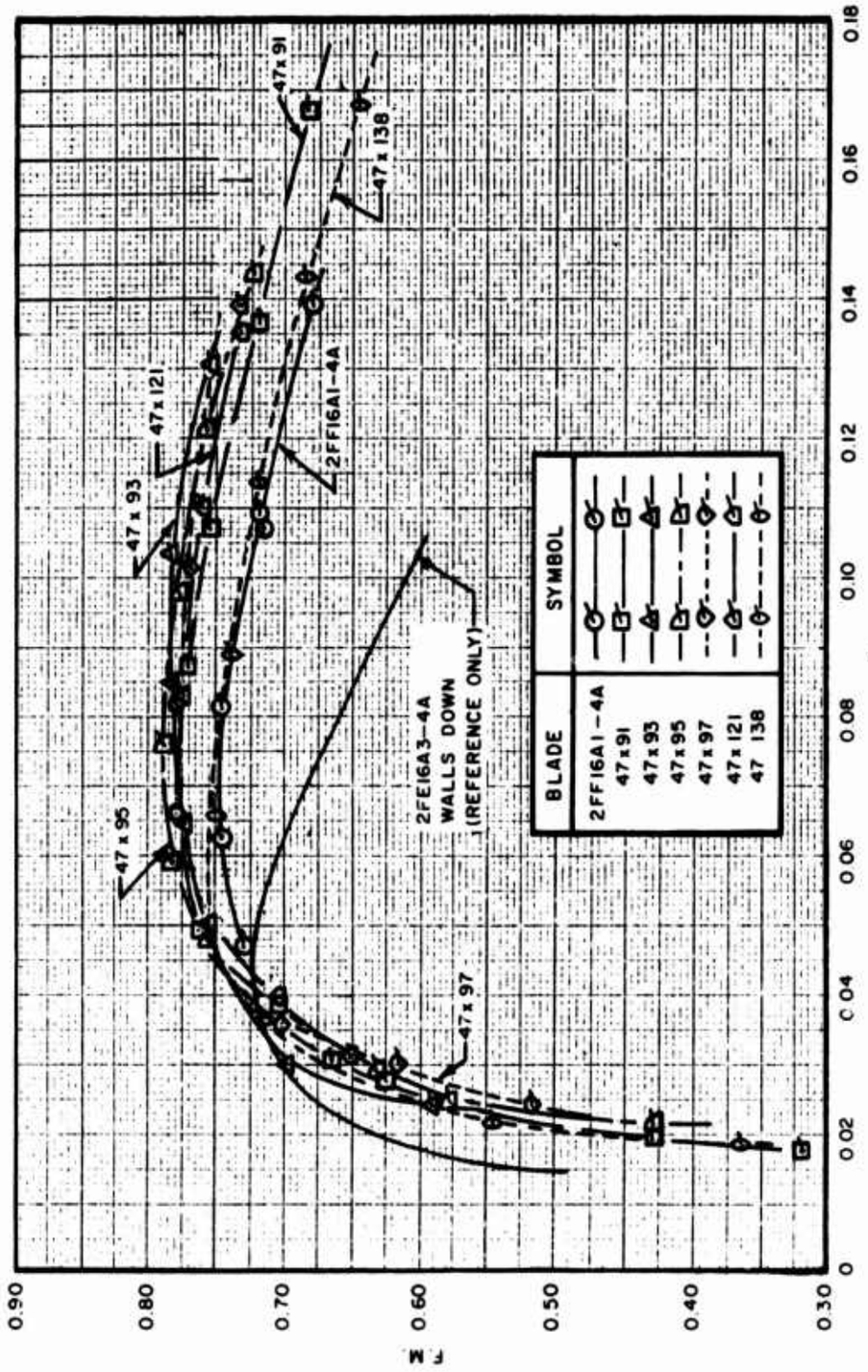

Figure 28. Continued
b. F.M. vs C_p plot

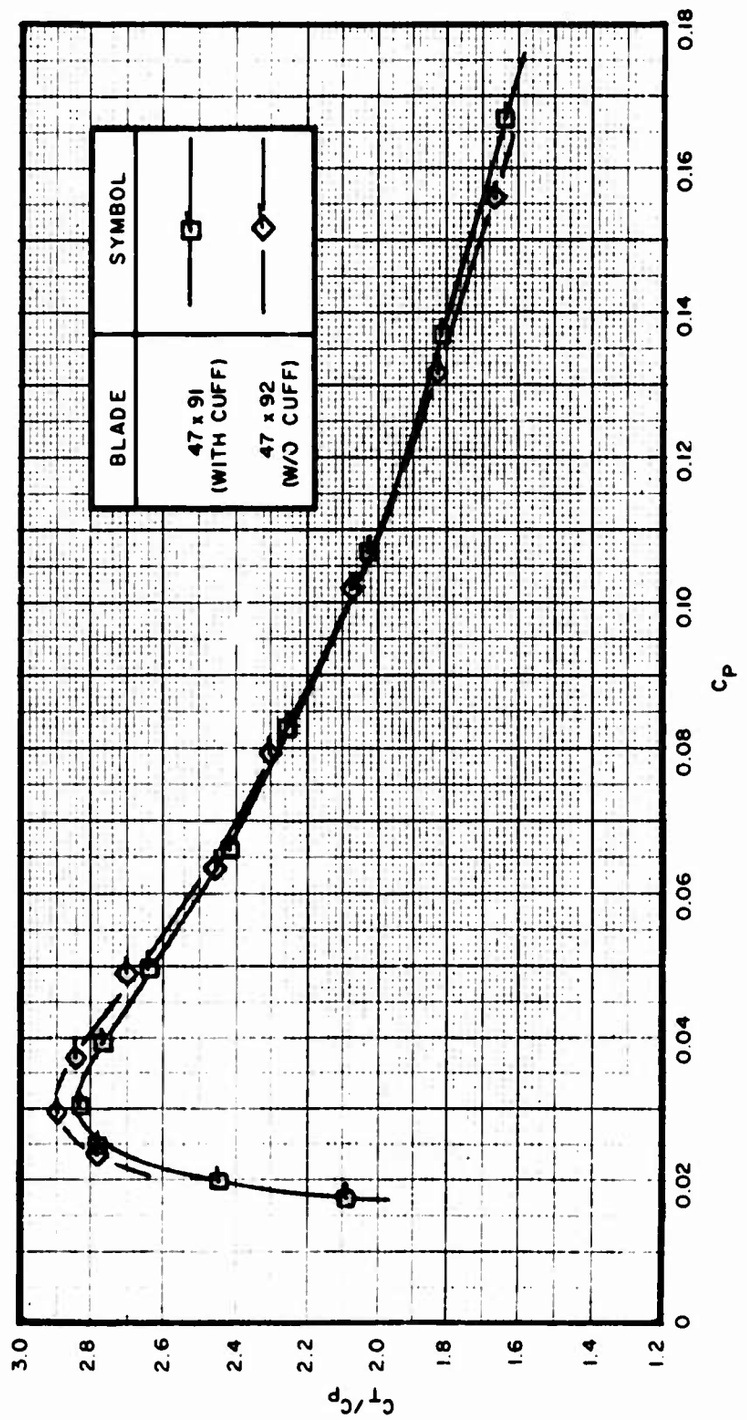

Figure 29. Comparison of 47 x 91 (With Cuffs) and 47 x 92 (Without Cuffs), Walls Relocated, Performance at Tip Mach Number = 0.900

a. C_T/C_P vs C_P plot

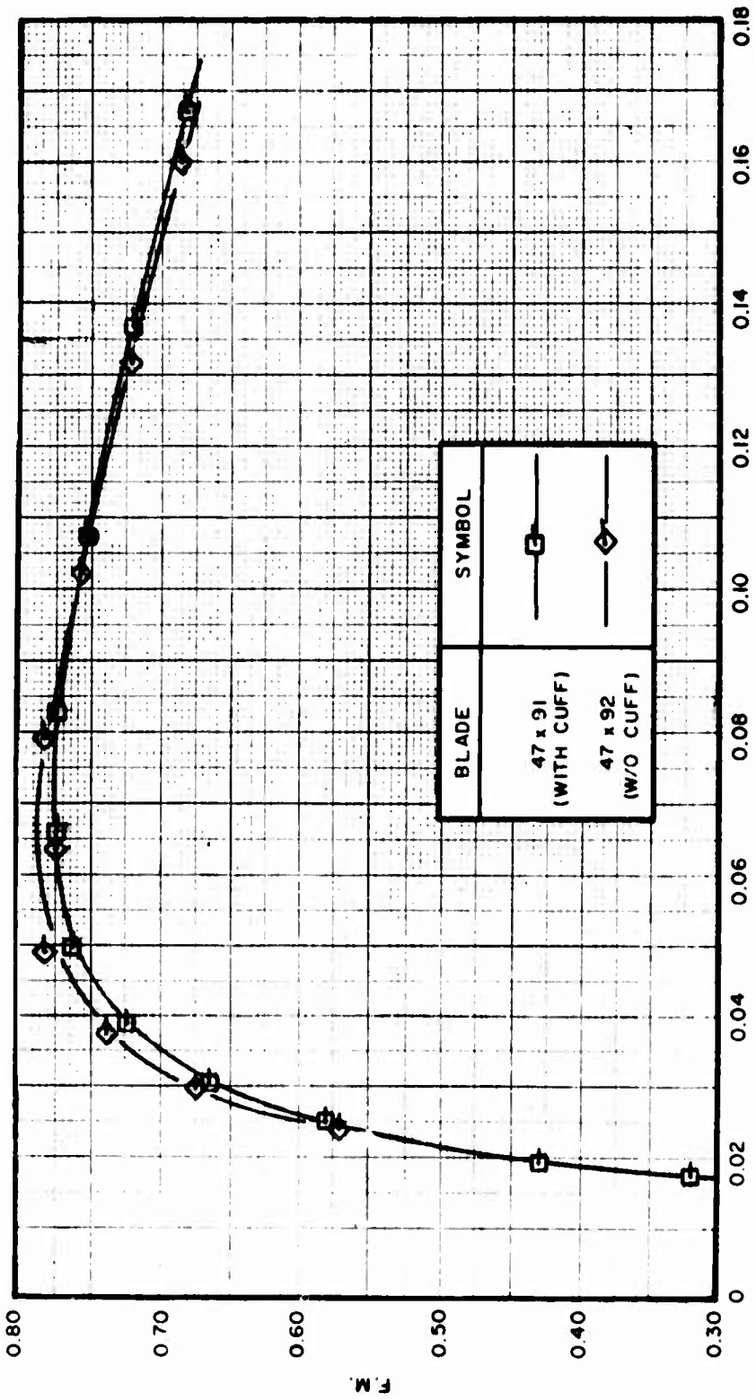

Figure 29. Continued
b. F. M. vs C_p plot

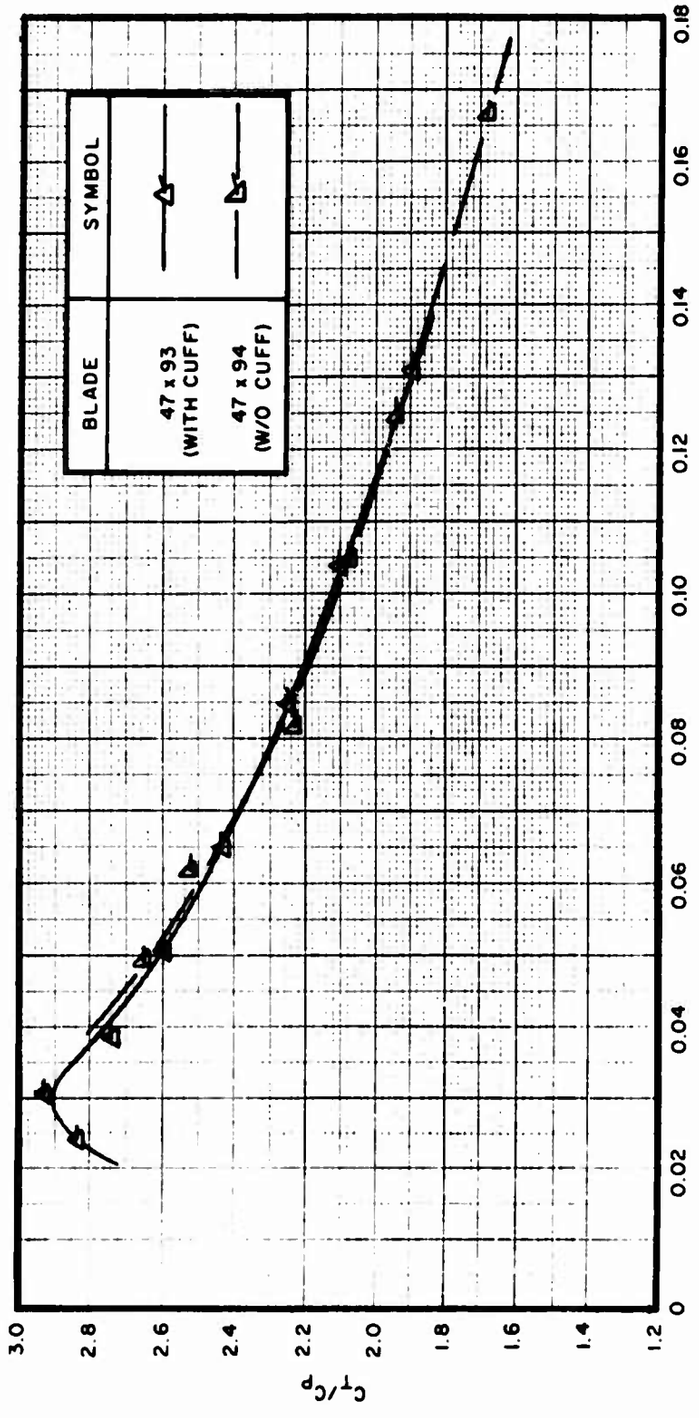

Figure 30. Comparison of 47 x 93 (With Cuffs) and 47 x 94 (Without Cuffs), Walls Relocated, Performance at Tip Mach Number = 0.900

a. C_T/C_P plot

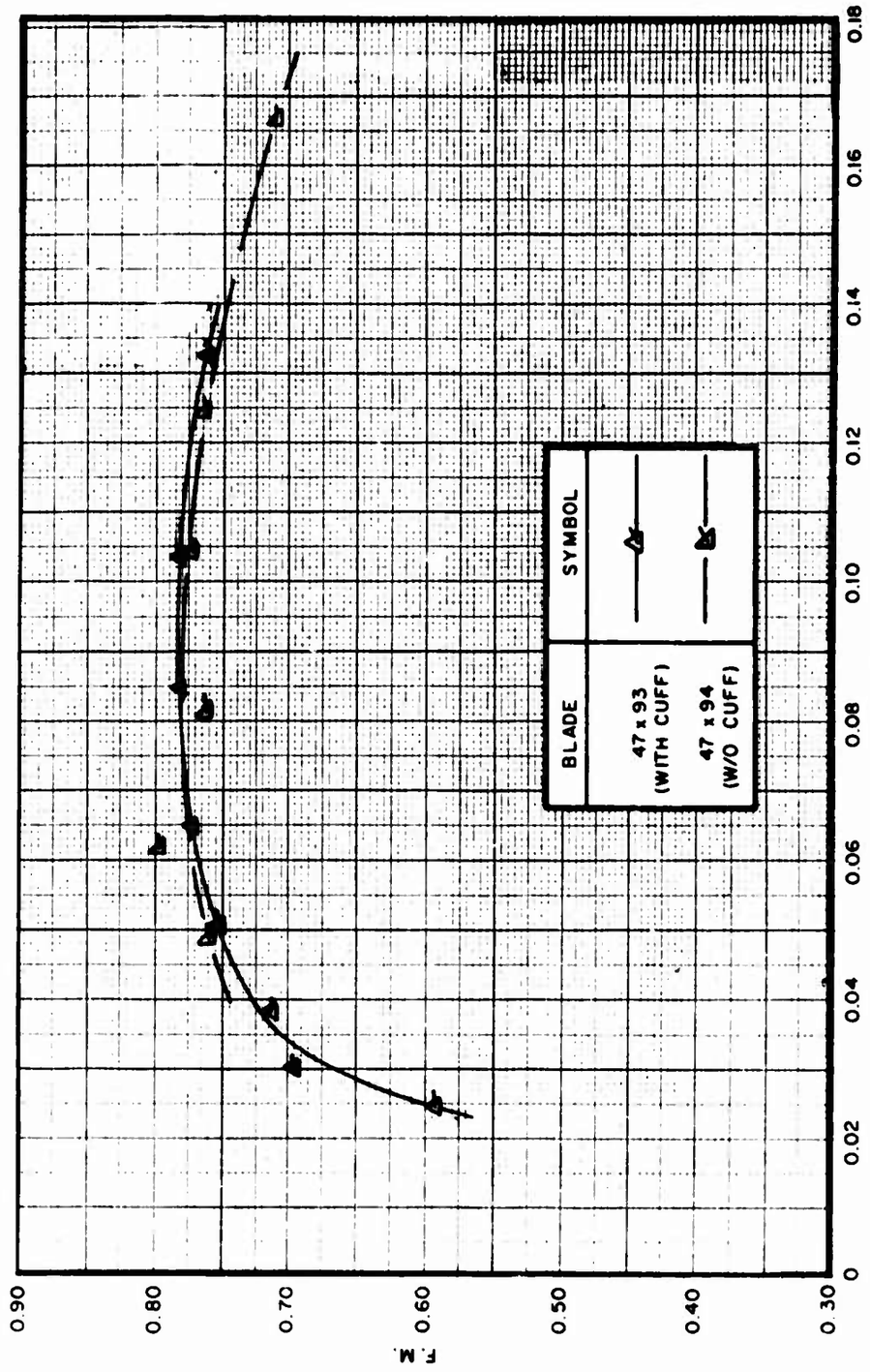

Figure 30. Continued
b. F. M. vs C_P plot

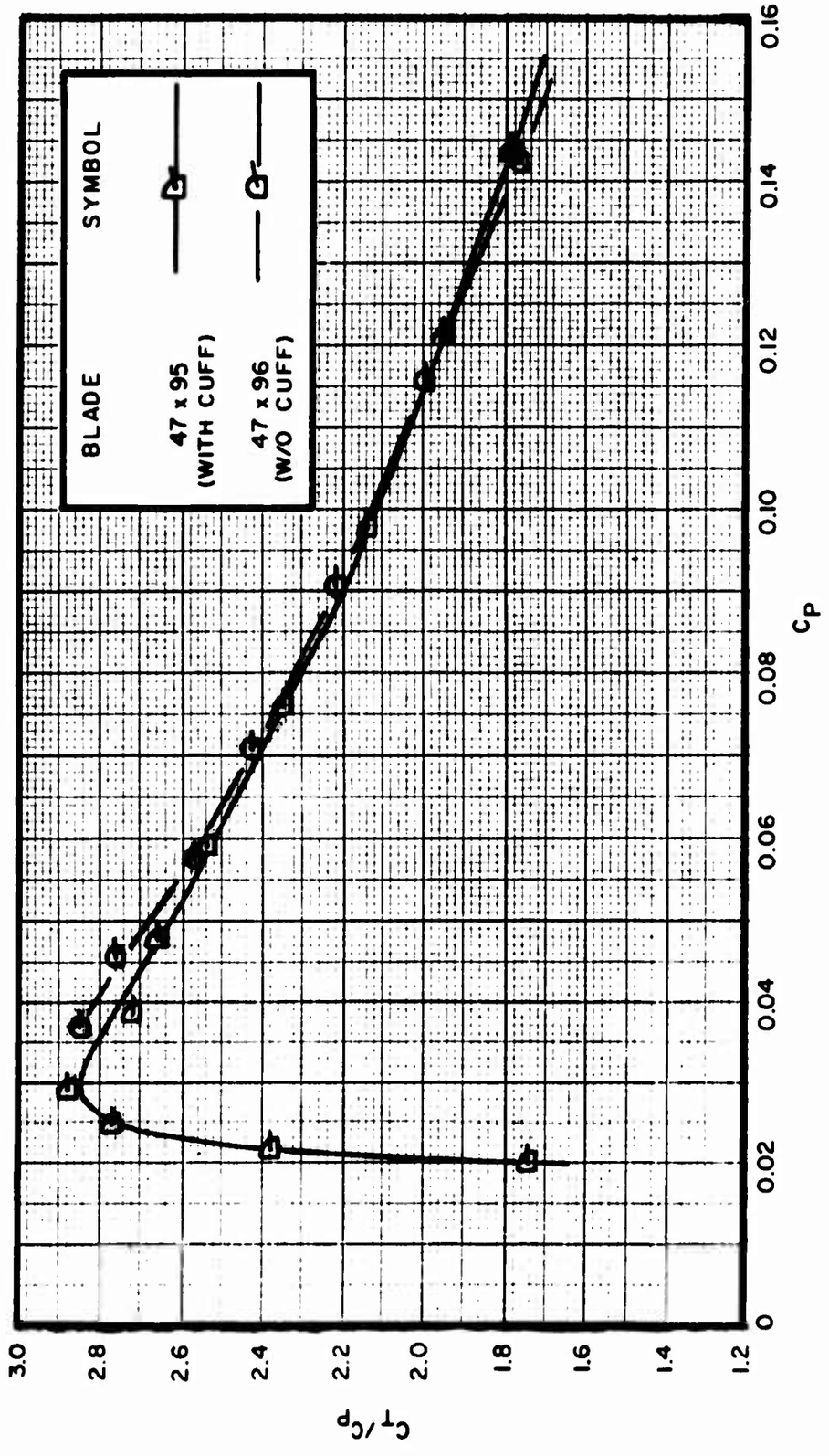

Figure 31. Comparison of 47 x 95 (With Cuffs) and 47 x 96 (Without Cuffs); Walls Relocated, Performance at Tip Mach Number = 0.900

a. C_T/C_P vs C_P plot

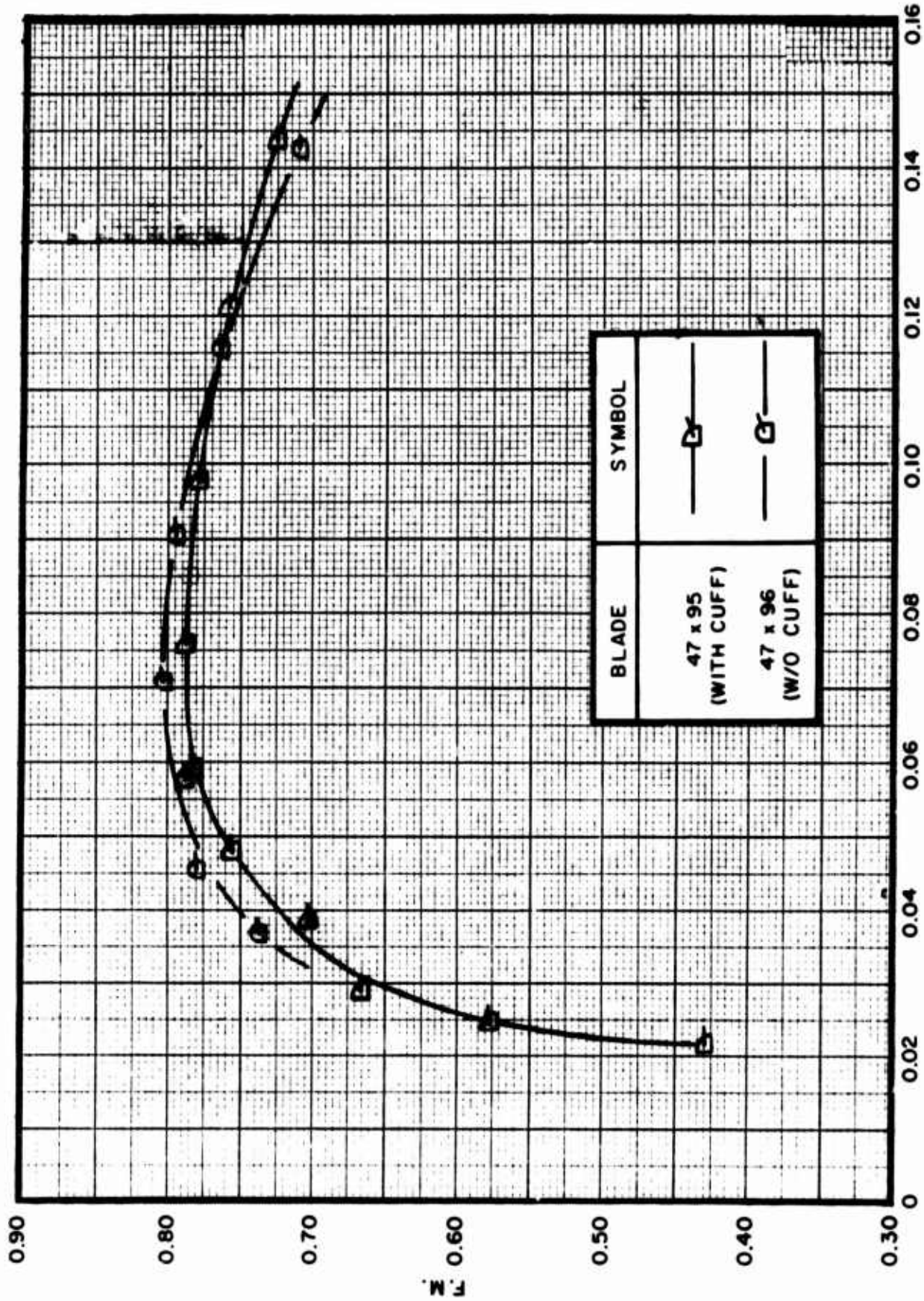

Figure 31. Continued
b. F.M. vs C_P plot

3. EFFECT OF TIP SHAPE

The effect of blade tip shape is shown by Figures 32 through 37 for the SK59868-0/0R, -12.22/12.22R and -17.22/17.22R, respectively. The basic dash number represents a square tip configuration while the suffix R represents the same blade with the tip rounded. Exact differences can be obtained from the particular blade characteristic charts located in Appendix I.

Figures 32 a/b and 33 a/b provide performance plots of the SK59868-0 and -0/0R respectively. Figures 38 a/b are comparison plots of these two propellers. Figures 34 a/b and 35 a/b provide performance plots of the SK59868-12 and -12R, respectively. Figures 39 a/b are comparison plots of these two propellers. Figures 36 a/b and 37 a/b provide performance plots of the SK59868-18 and -18R, respectively. Figures 39 a/b are comparison plots of these two propellers.

An examination of Figures 38a, 39a, and 40a shows that in all cases up to $C_P = 0.08$, thrust coefficient/power coefficient (C_T/C_P vs C_P) was higher for the round tip blades, thus in this range, the round tip blades produced more thrust for a given power than did the square tip blades.

Figures 38b, 39b, and 40b indicate that the round tip blades, produce a higher F.M. (approximately 1.5 point) up to a $C_P = 0.06 - 0.08$ value; beyond this point, there is either no difference, or the square tip blade might have a slight advantage.

It should be noted that in all cases the round tip blade had a slightly lower activity factor than the corresponding square tip blade. The basic square blade tip (at each diameter) was rounded on the leading and trailing edges, thus producing the round tip configuration of reduced acticity factor. (See Blade Characteristic Sheets Numbers 8 through 11).

This increased performance of the lower activity factor blades is in direct opposition to the findings of Section VI, Paragraph 5, Effect of Activity Factor. The increased performance of the round tip blades, therefore, is probably attributed to the combined effects of reducing the thickness ratio, providing a more ideal spanwise blade loading because of the more elliptical tip shape, and producing a tip vortex of lower strength.

It can be concluded that a round tip blade will provide a performance increase over an identical square tip blade in the power coefficient range of $C_P = 0.06-0.08$.

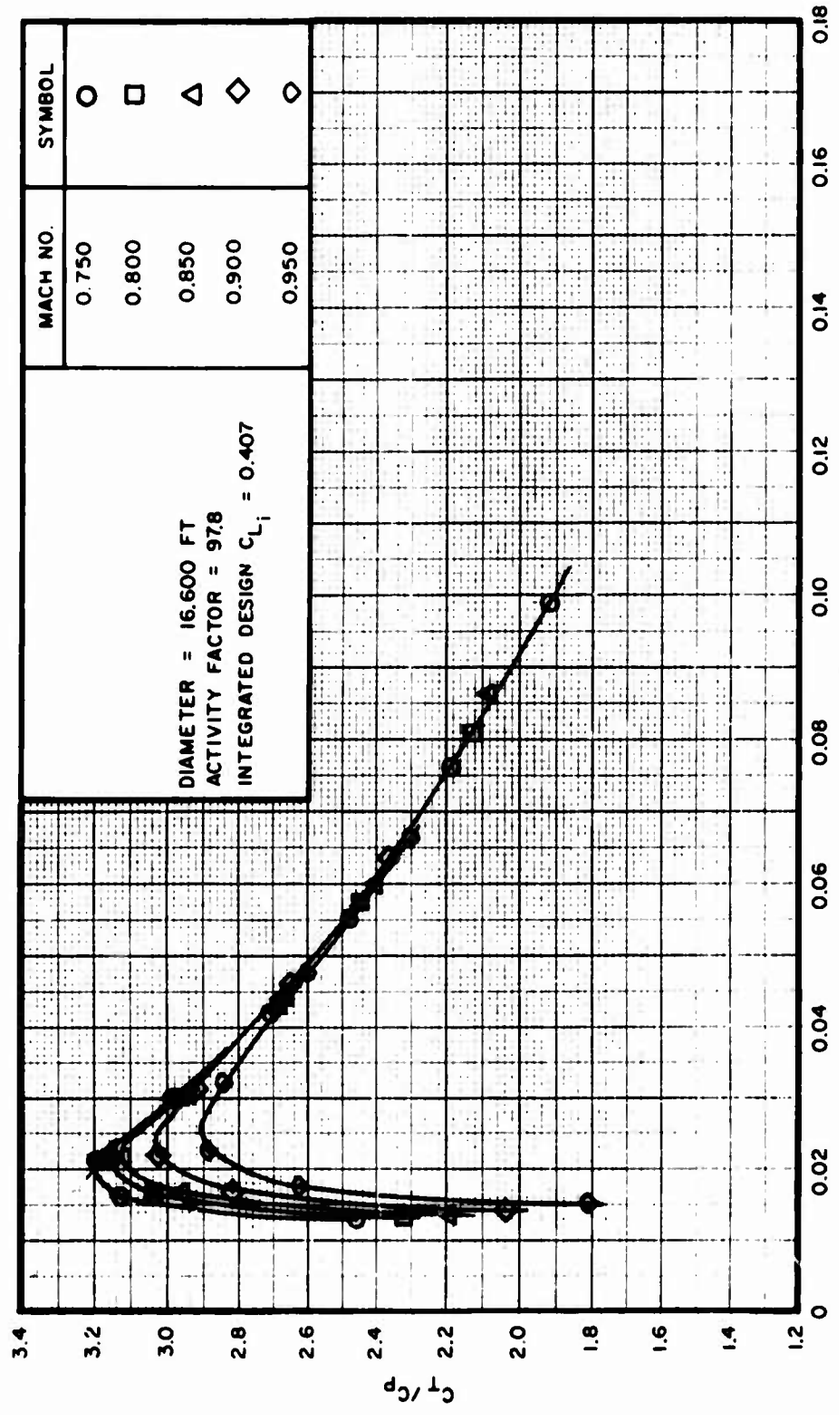

Figure 32. SK59868-0 (Square Tip), Walls Down, Performance at Different Tip Mach Numbers

a. C_T/C_P vs C_P plot

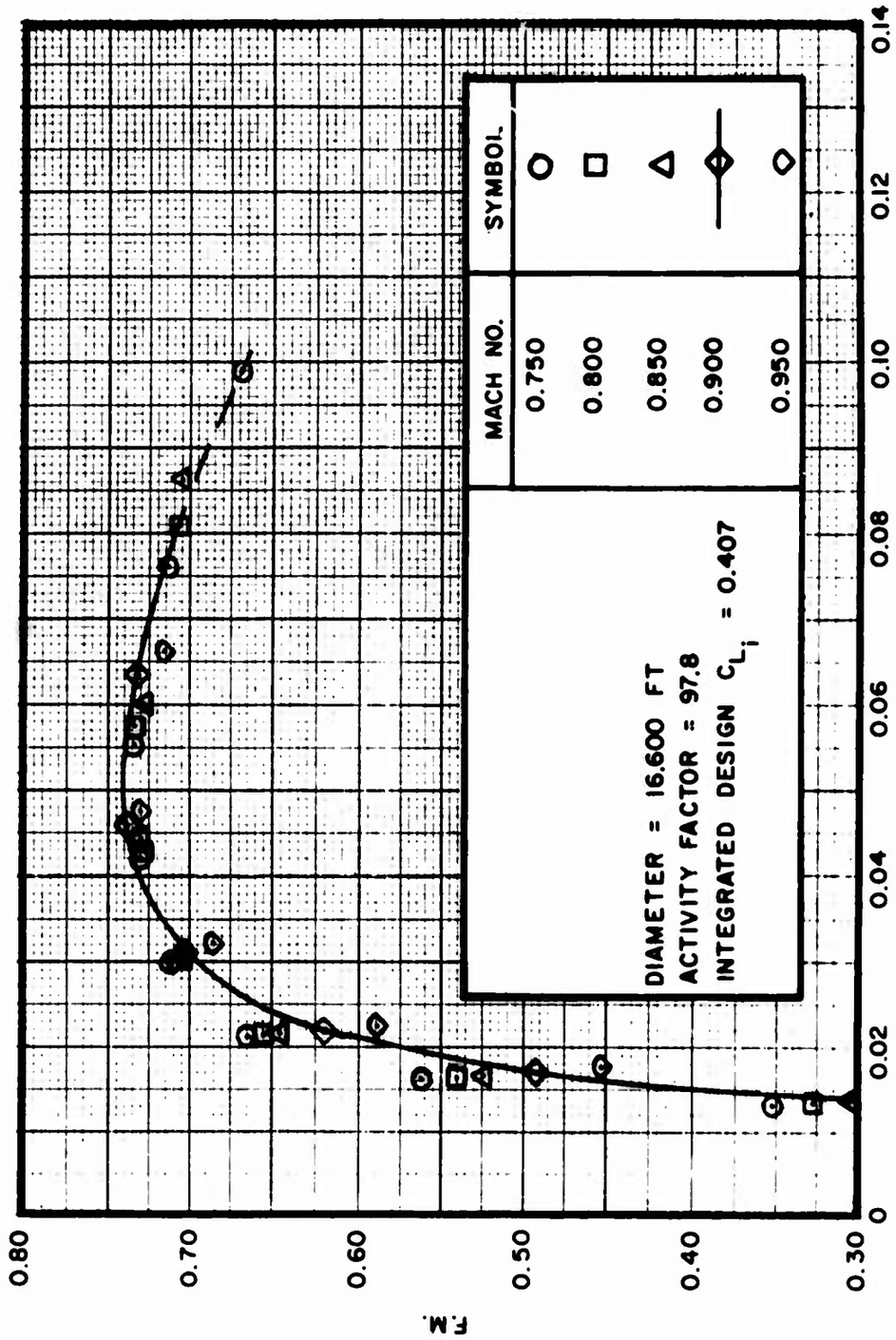

Figure 32. Continued

b. F. M. vs C_P plot

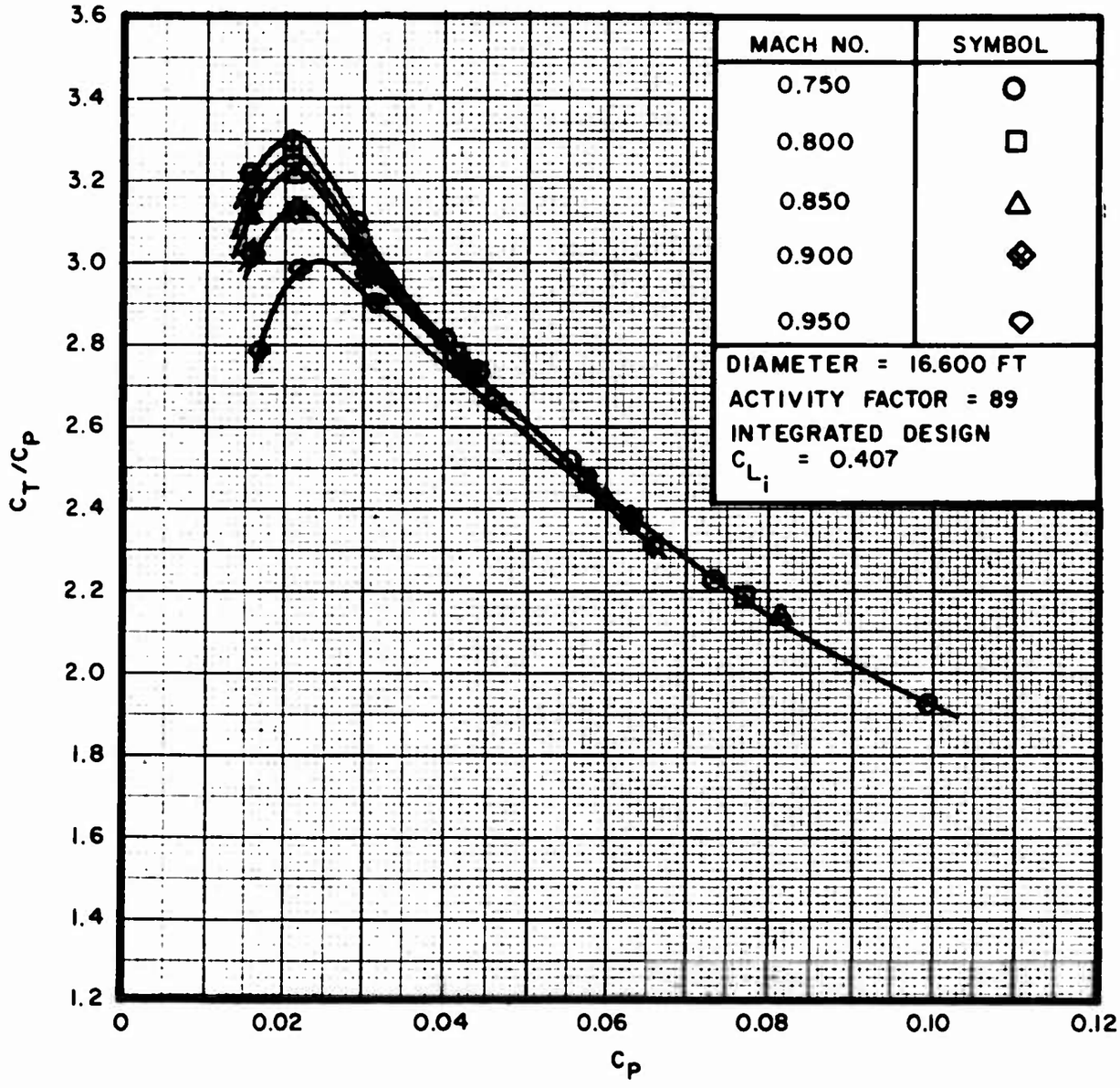

Figure 33. SK59868-0R (Round Tip), Walls Down, Performance at Different Tip Mach Numbers

a. C_T/C_P vs C_P plot

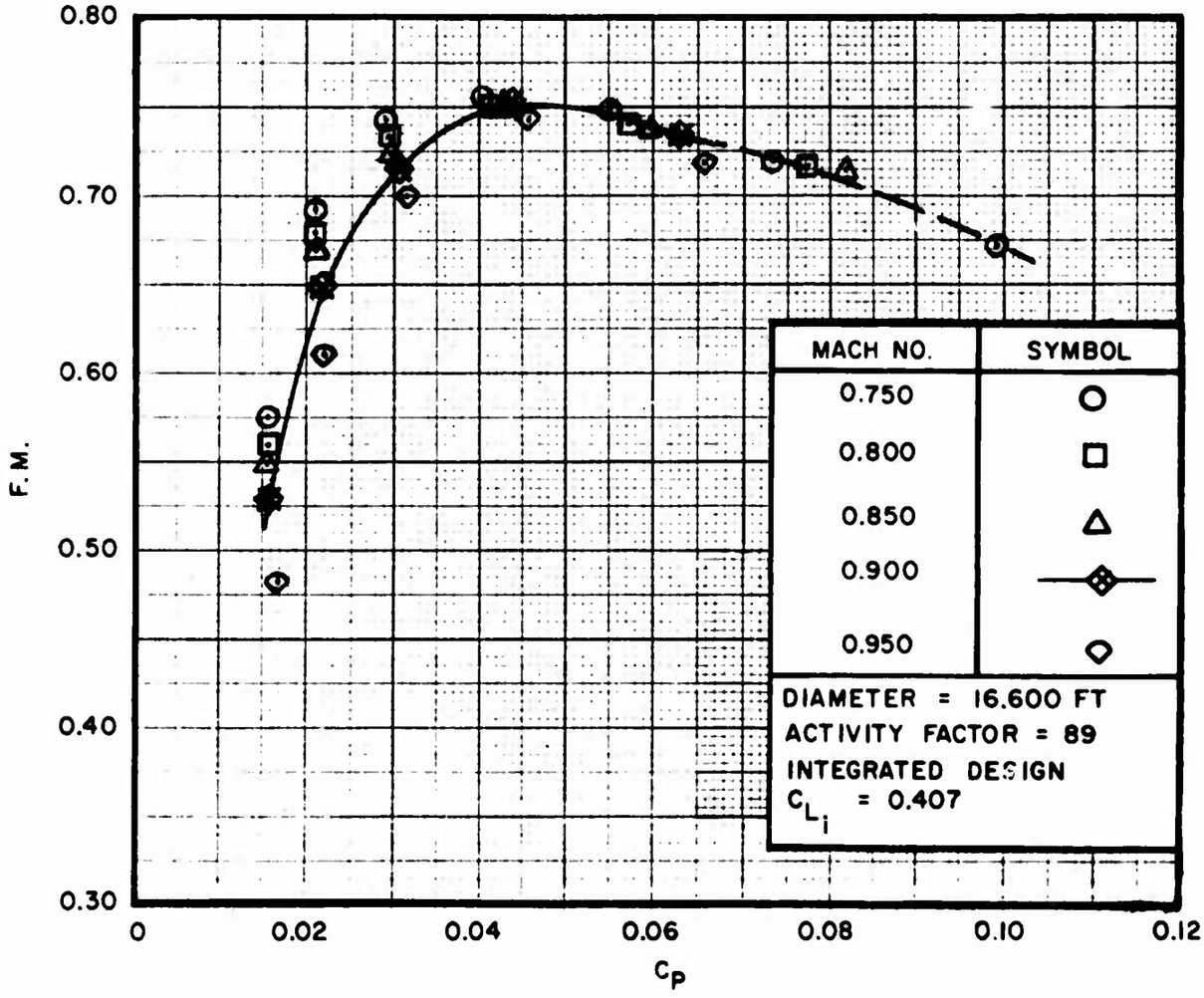

Figure 33. Continued

b. F.M. vs C_P plot

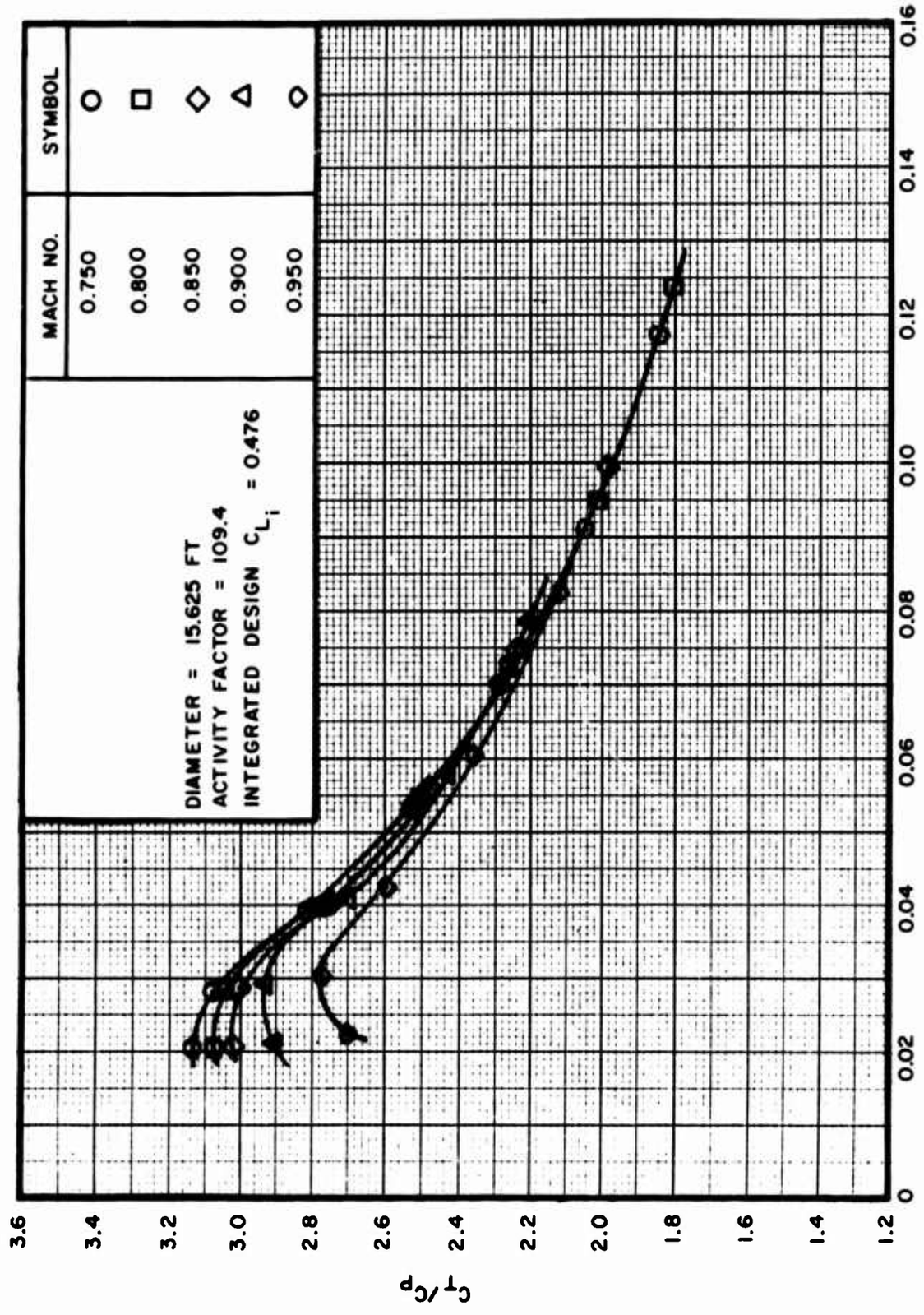

Figure 34. SK59868-12 (Square Tip), Walls Down, Performance at Different Tip Mach Numbers

a. C_T/C_P vs C_P plot

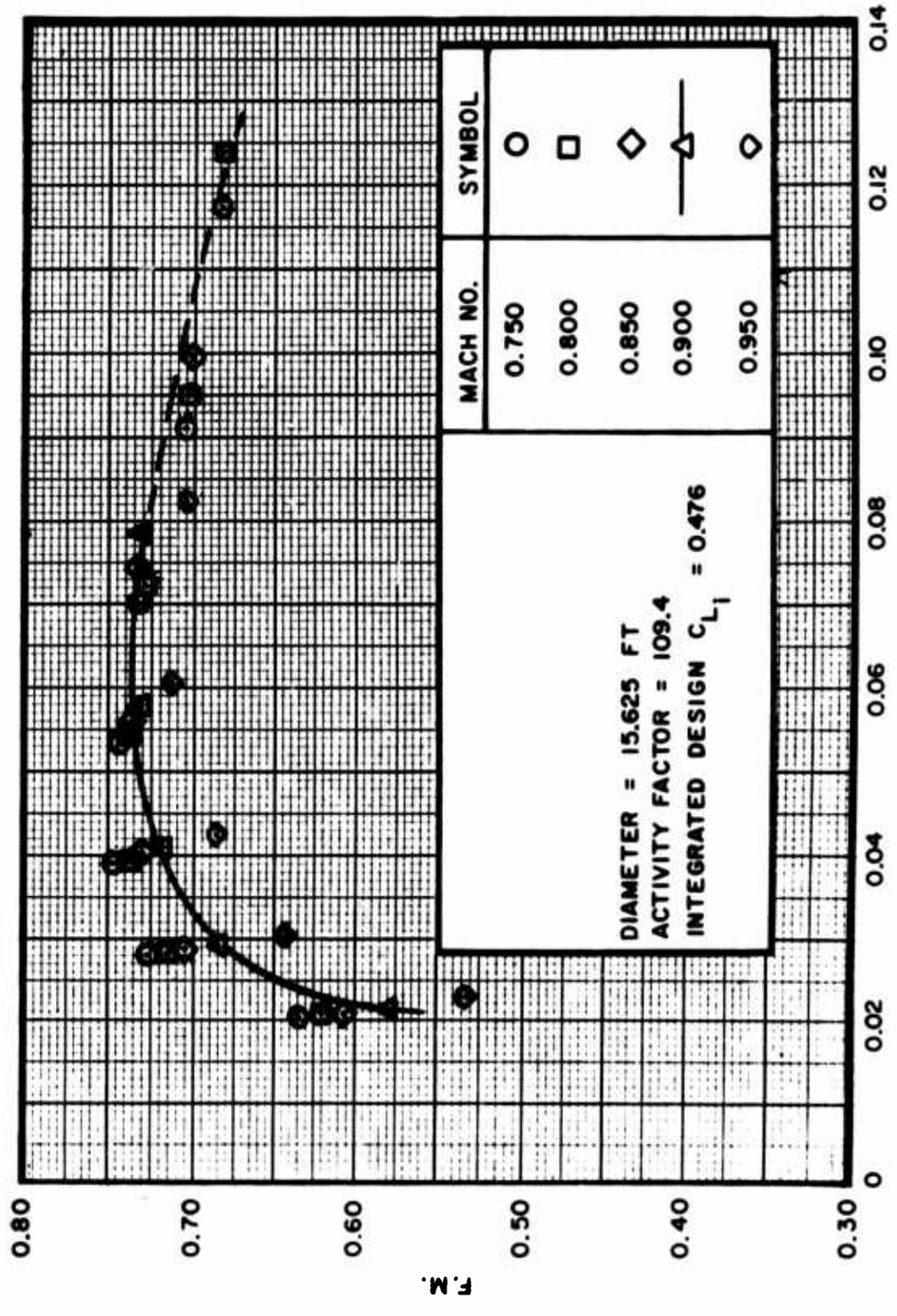

Figure 34. Continued

b. F.M. vs C_P plot

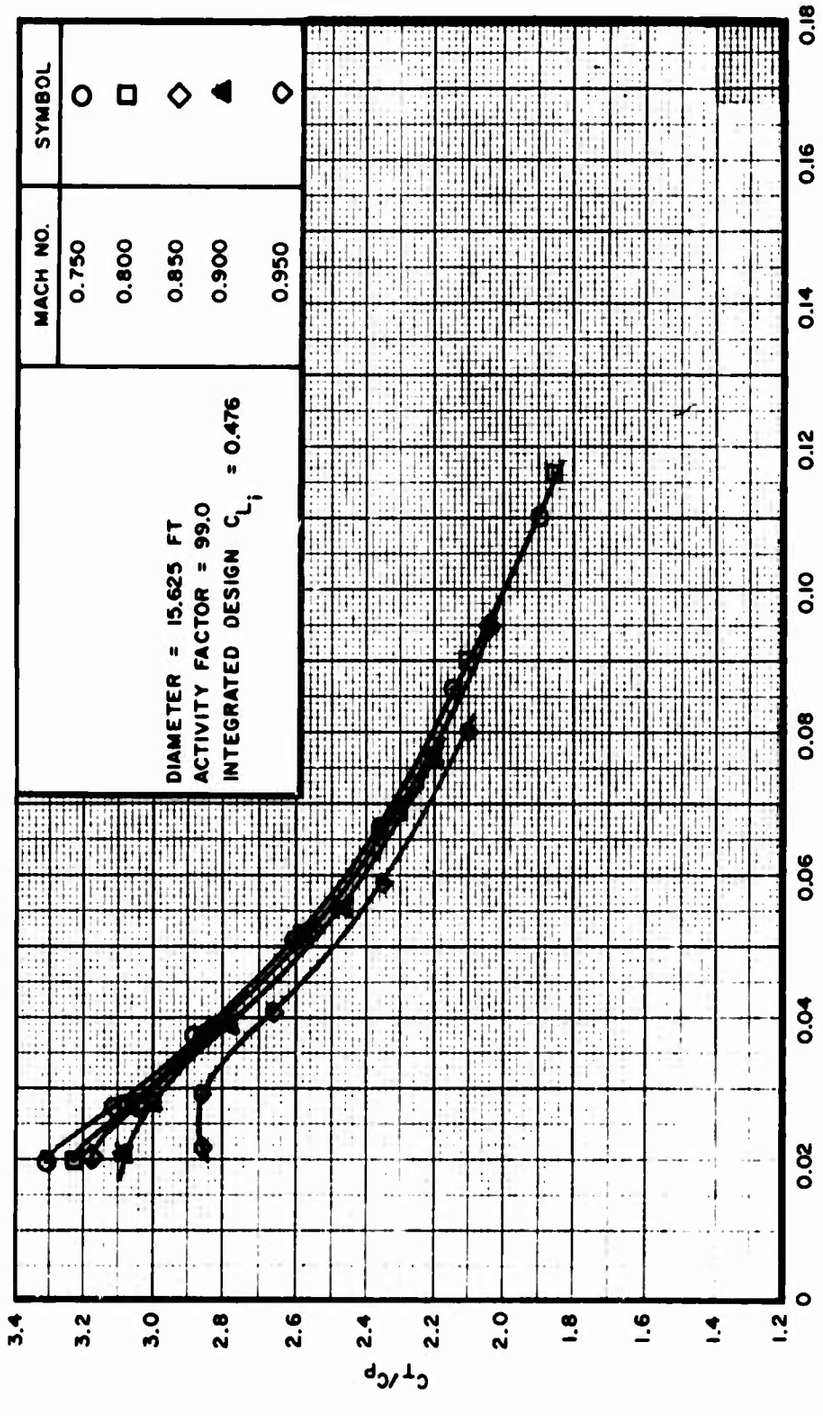

Figure 35. SK59868-12R (Round Tip), Walls Down, Performance at Different Tip Mach Numbers

a. C_T/C_P vs C_P plot

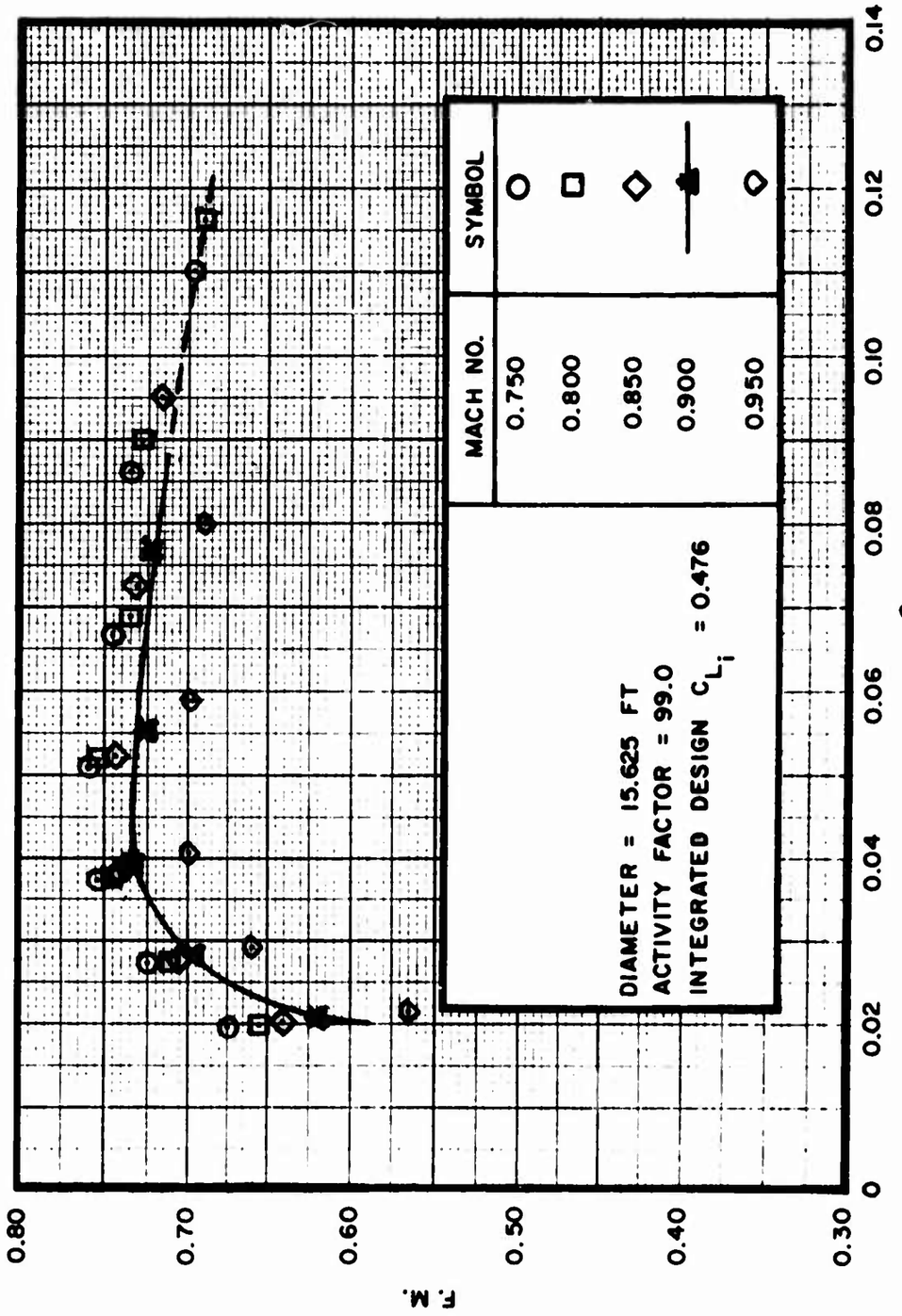

Figure 35. Continued

b. F.M. vs C_P plot

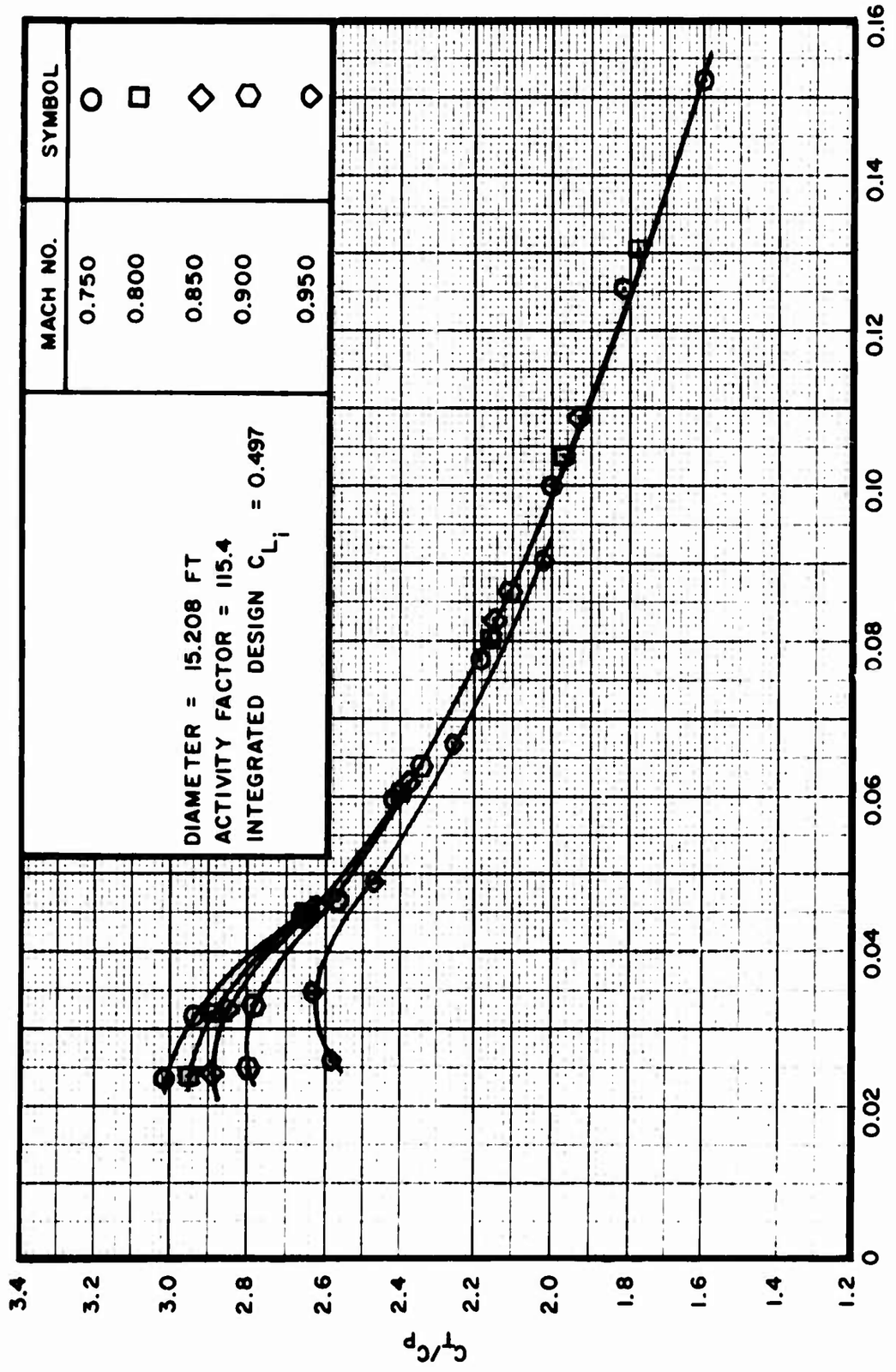

Figure 36. SK59868-18 (Square Tip), Walls Down, Performance at Different Tip Mach Numbers

a. C_T/C_P vs C_P plot

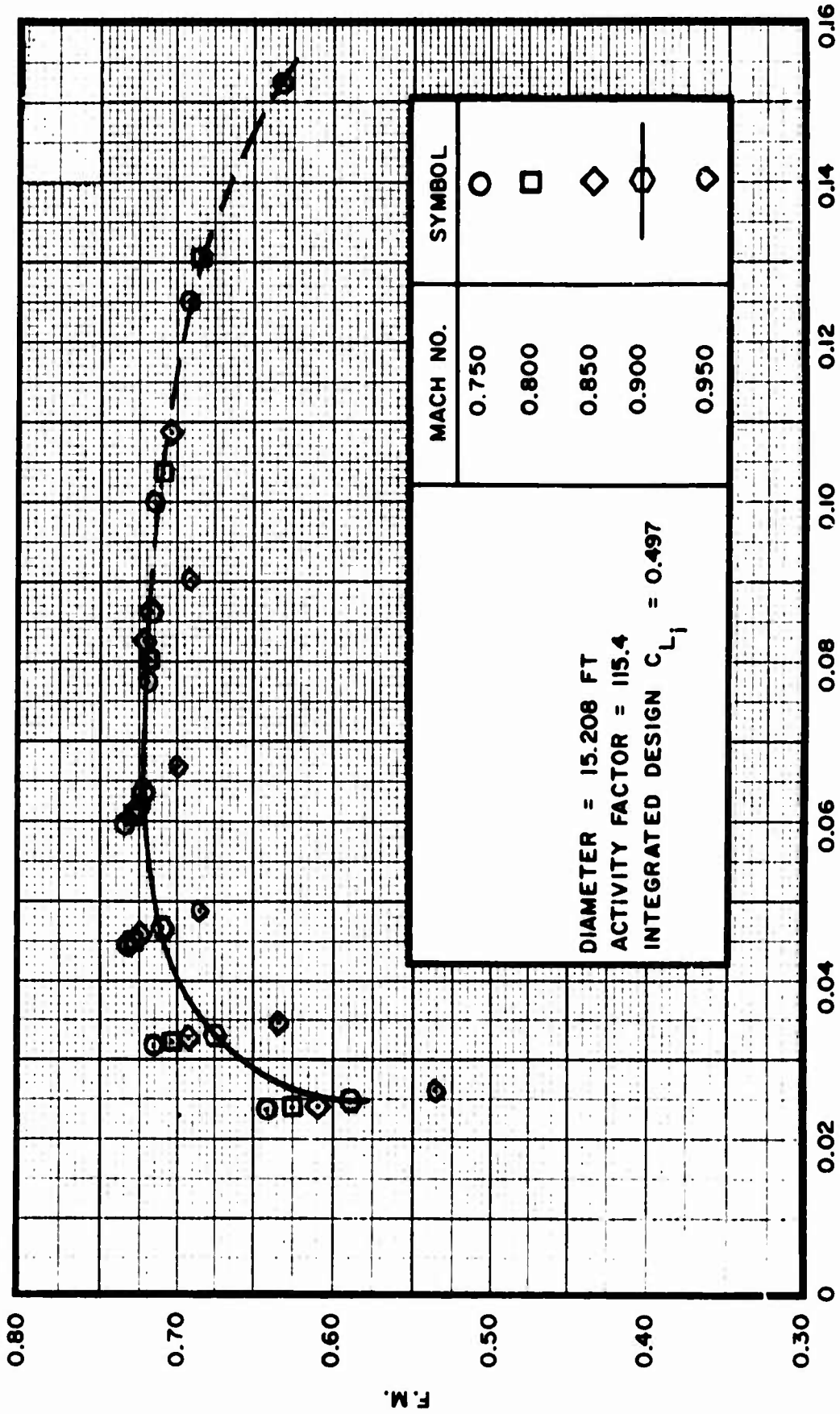

Figure 36. Continued

b. F.M. vs C_p plot

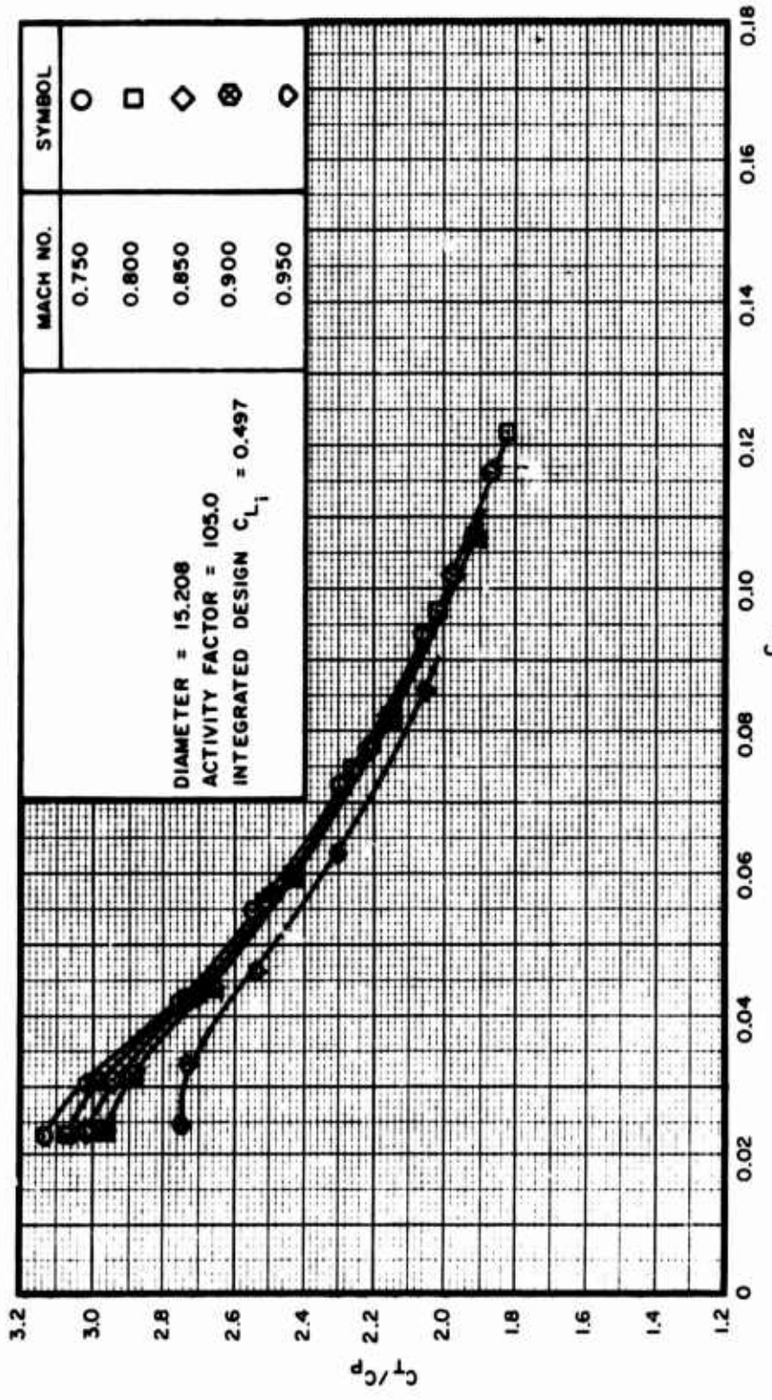

Figure 37. SK59868-18R (Round Tip), Walls Down, Performance at Different Tip Mach Numbers

a. C_T/C_P vs C_P plot

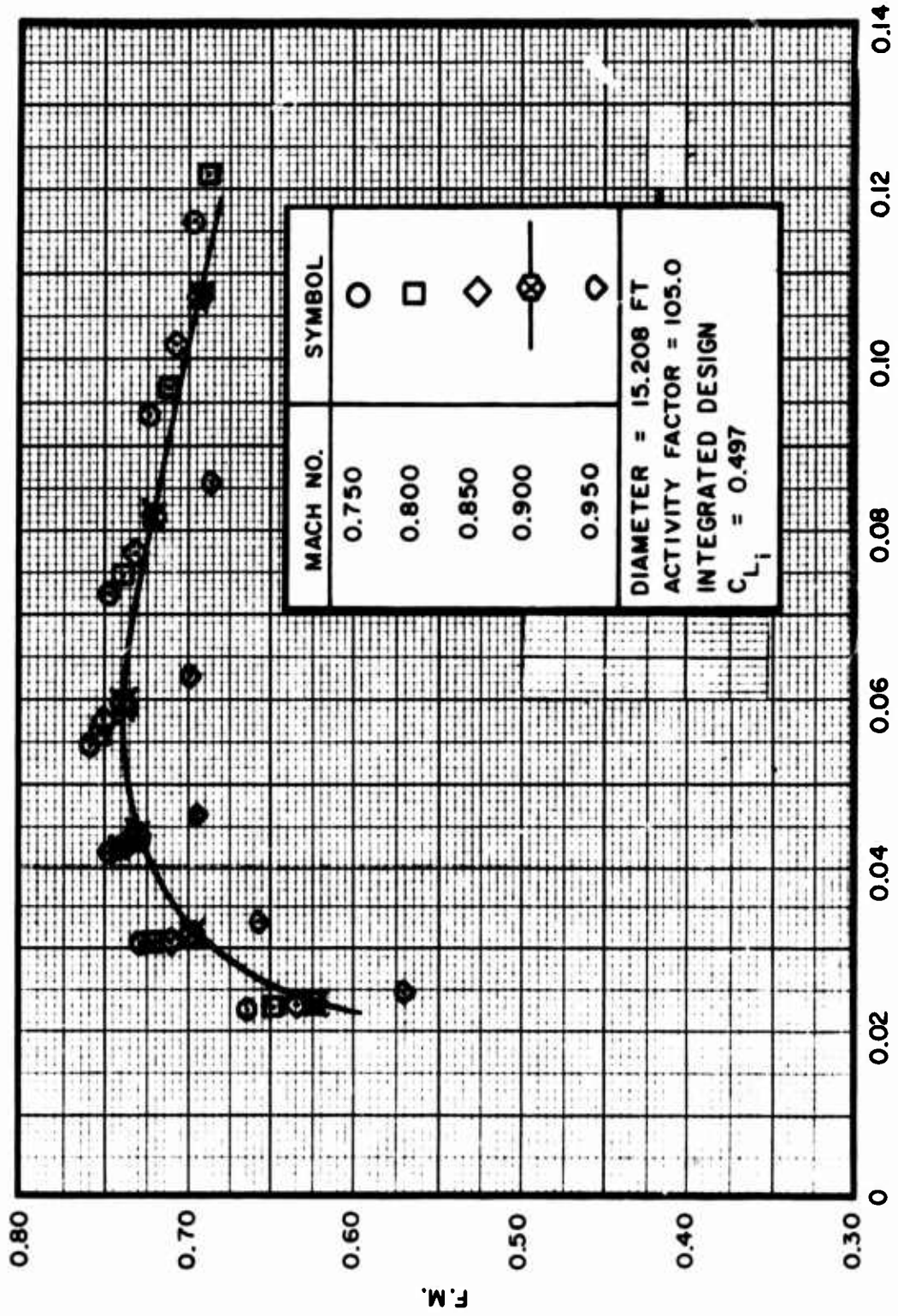

Figure 37. Continued
b. F. M. vs C_P plot

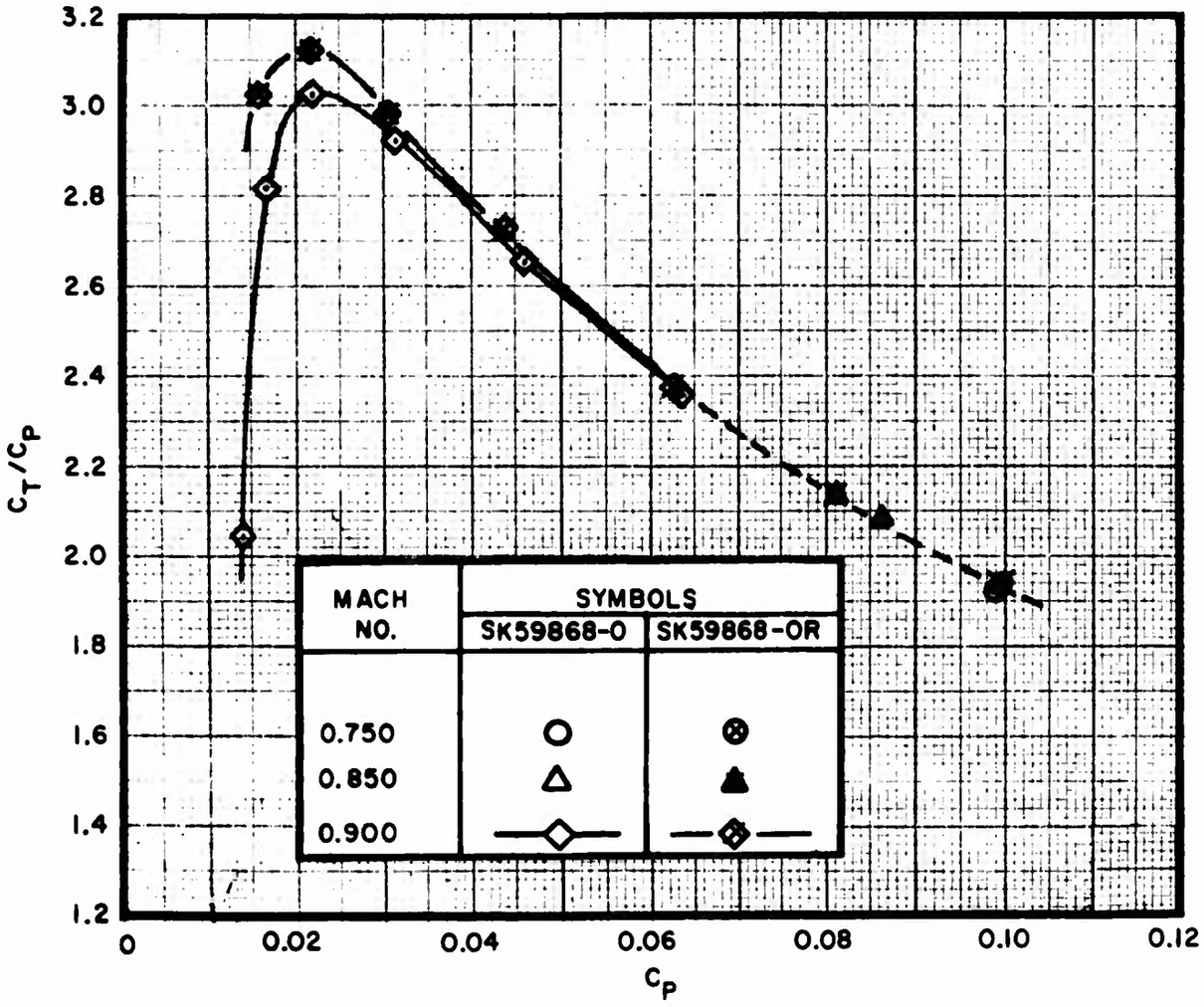

Figure 38. Comparison of SK59868-0 (Square Tip) and SK59868-0R (Round Tip), Walls Down, Performance at Different Tip Mach Numbers

a. C_T/C_P vs C_P plot

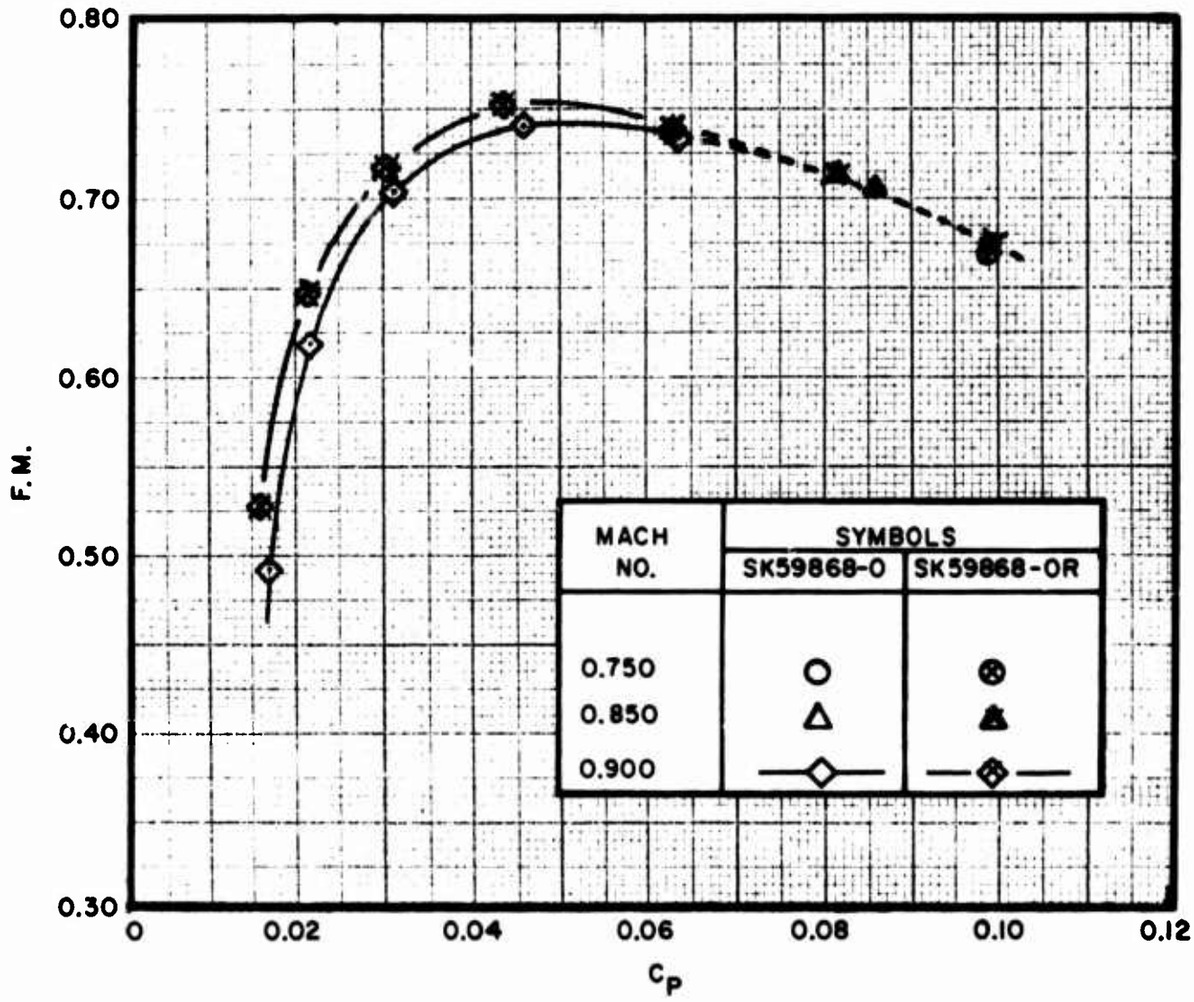

Figure 38. Continued

b. F. M. vs C_P plot

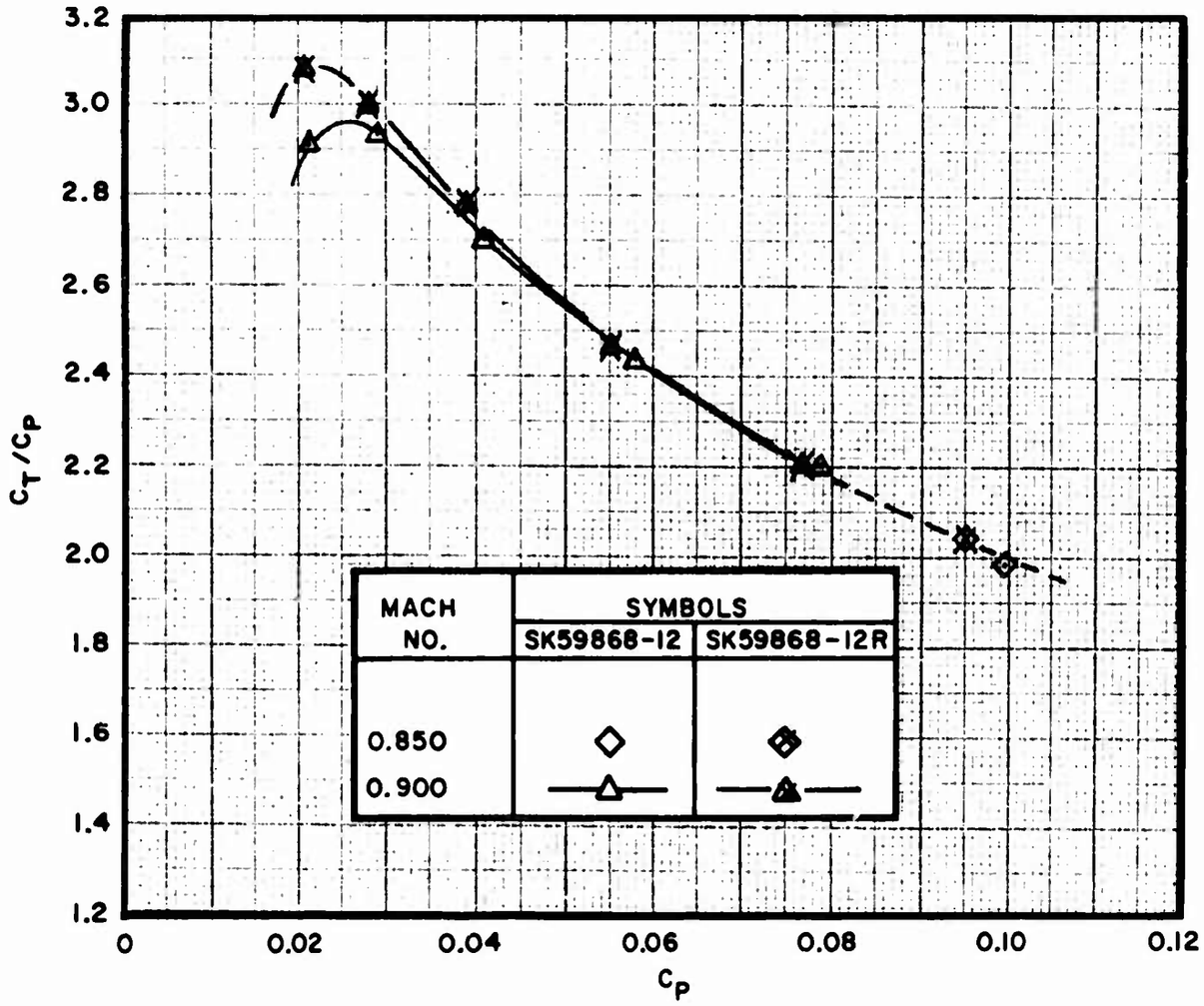

Figure 39. Comparison of SK59868-12 (Square Tip) and SK59868-12R (Round Tip), Walls Down, Performance at Different Tip Mach Numbers

a. C_T/C_P vs C_P plot

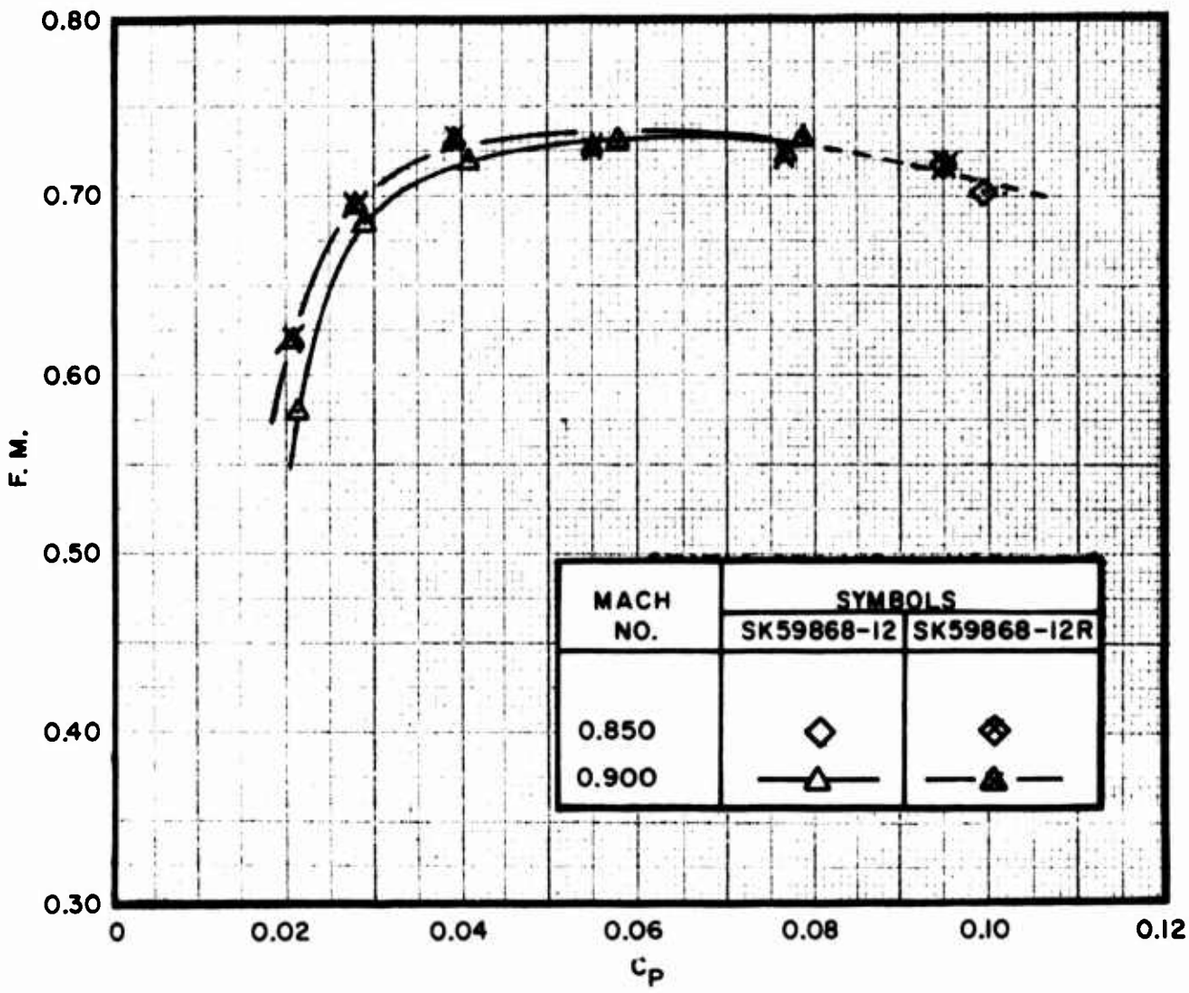

Figure 39. Continued

b. F. M. vs C_P plot

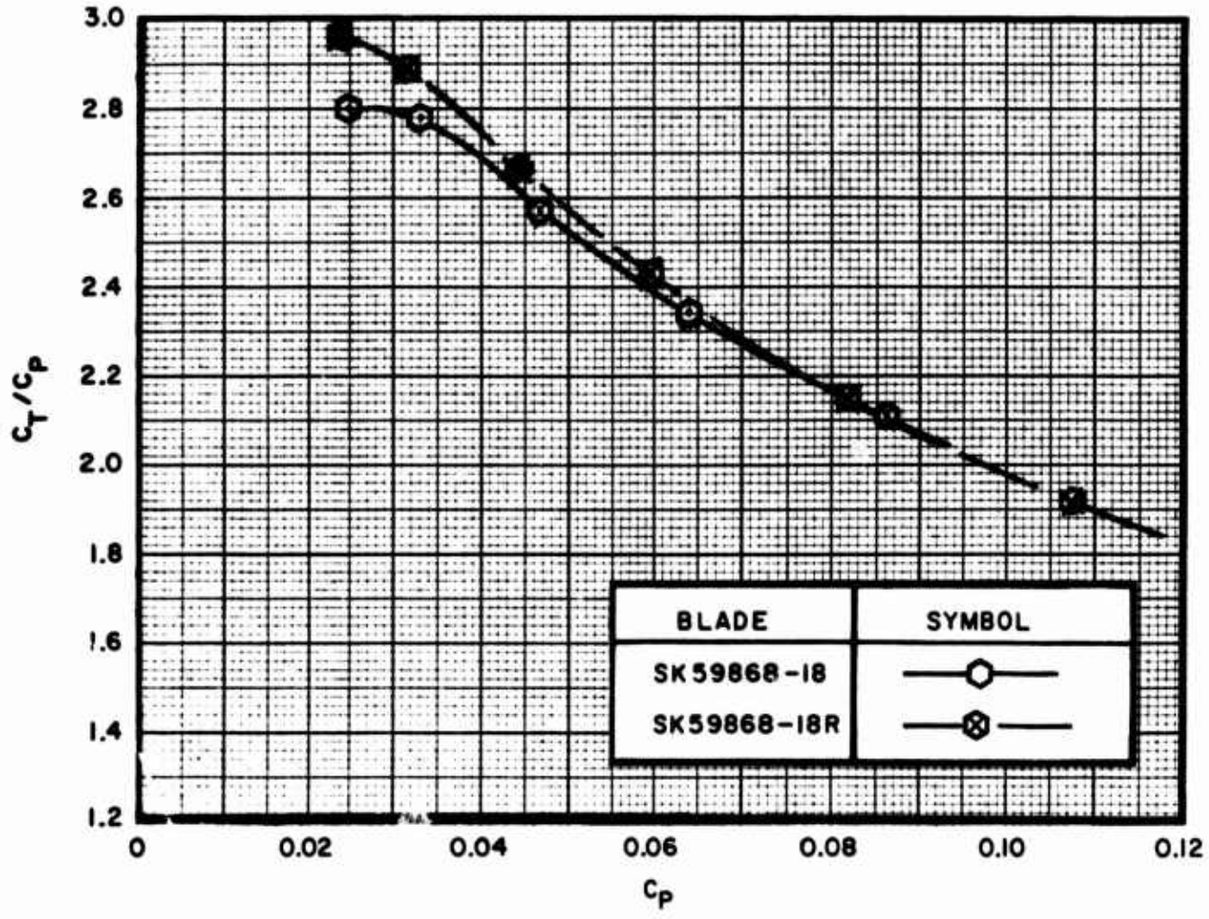

Figure 40. Comparison of SK59868-18 (Square Tip) and SK59868-18R (Round Tip), Walls Down, Performance at Different Tip Mach Numbers

a. C_T/C_P vs C_P plot

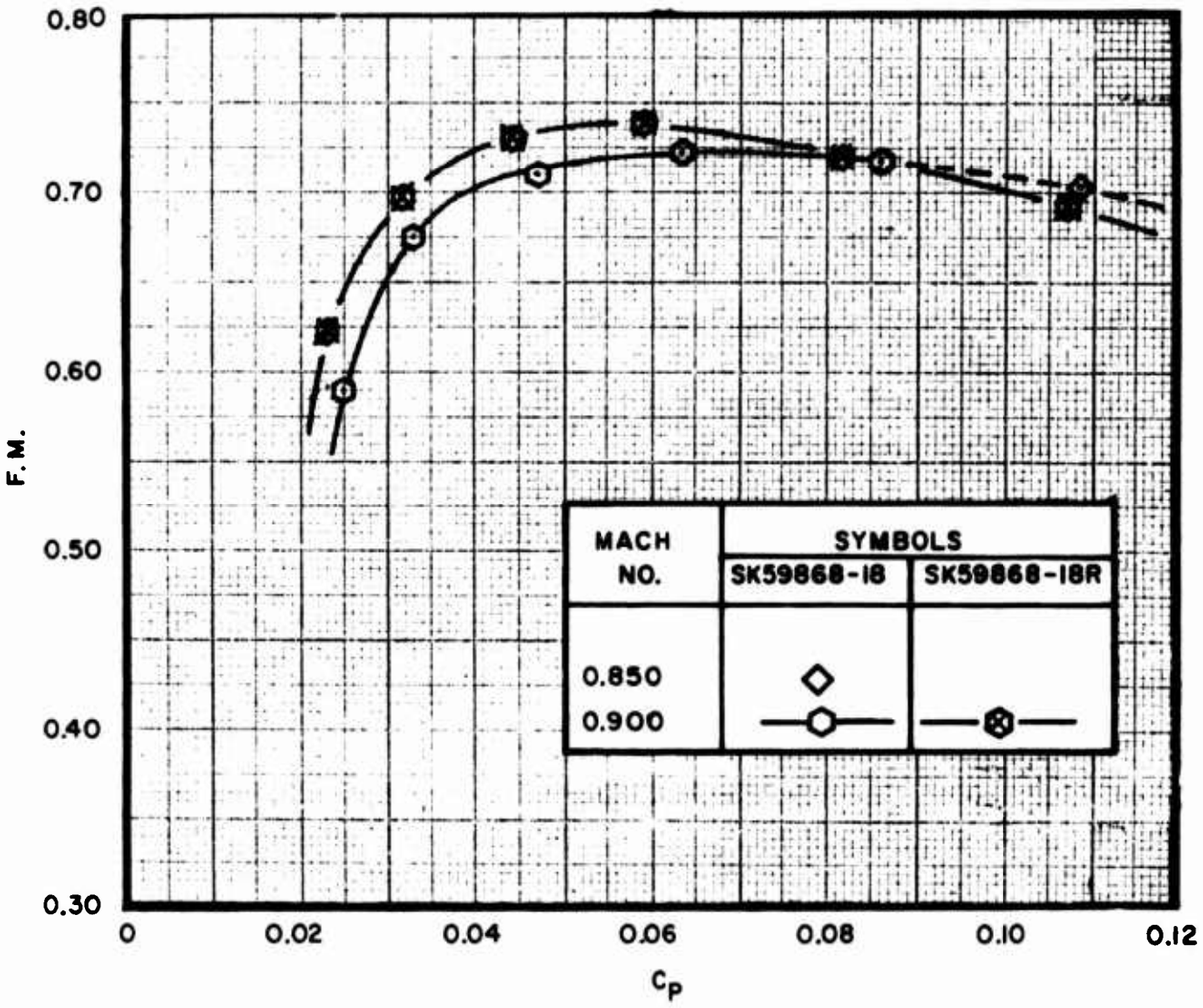

Figure 40. Continued

b. F. M. vs C_P plot

4. EFFECT OF TWIST

The following propellers were tested to determine the effects of blade twist. All other parameters were held constant. Each propeller was first tested with its designed twist and then retwisted the indicated number of degrees.

Twist was measured from 25% blade radius to the tip. (Twist = $\beta_r - \beta_R$.) All data presented is for increased twist as indicated for the propellers below (for exact radial twist distribution of each blade, see Propeller Blade Characteristic Data Sheets Nos. 3, 4, 6, and 8 in Appendix I).

**1. 47 x 91 to 47 x 95 = 3.0° (with cuffs)
**2. 47 x 92 to 47 x 96 = 3.0° (without cuffs)
*3. 6903A-0 to 6903A-0T = 4.8°
**4. 47 x 138 to 47 x 92 = 5.2°
*5. 47 x 75 to SK59868-0 = 6.6°

Figure 41 presents the trend of increased performance (F.M.) of these ten blades with increased twist for three power coefficients of C_P = 0.06, 0.08, and 0.10.

Figures 42 a/b show the difference in performance due to 4.8° $\Delta\beta$ for the 6903A-0 to 6903A-0T blades.

Figures 43 a/b show the differerence in performance due to 6.6° $\Delta\beta$ for the 47 x 75 to the SK59868-0 blades. It should be noted that the 6.6° twist difference between these blades was only in the 85% radius to the tip region of the SK59868-0 blade. Otherwise, the blades are identical in twist over the remainder of the radius. The increase in peak F.M. of 2 points shown in Fibure 43b is a significant quantity considering that the twist occurs only in the tip 15% of the blade. This implies a strong influence of the tip region on the peak performance.

Figure 44 a/b present results of the 47 x 138, 47 x 92, and 47 x 96 blades with a $\Delta\beta$ of 5.2° and 3.0°. These three designations represent the same blade with increased twist increments. The performance increase appears to be somewhat proportional to the amount of twist increase.

*Walls down
**Walls relocated

Figures 45 a/b show the difference in performance due to the 3.0° $\Delta\beta$ for the 47 x 91 to 47 x 95 blades which are the same as the 47 x 92 and 47 x 96 blades but which incorporate cuffs.

Figure 41 illustrates the trend due to operation, both with and without blade cuffs. The general trend is the same for both versions and the quantitative difference is attributed to the previous conclusion that operation with cuffs results in a general reduction in performance (see Paragraph 2 - Effect of Blade Cuff).

The trend, illustrated by Figure 41, is that an increase in twist will result in an increase in static performance. The upper limit of twist was not determined from these tests, however, performance was still increasing at β = 38.5°, which was the highest twist of any blade tested. The average performance increase observed from the slopes of the curves is approximately 1/2 point of F.M. per degree of twist. This trend appears to become greater at higher power coefficients in the range of C_P = 0.08 and 0.10

In all cases, the blade with increased twist indicated a higher C_T and F.M. for a given C_P above approximately C_P = 0.06.

5. EFFECT OF ACTIVITY FACTOR

a. Blade Activity Factor

Blade activity factor (AF) is defined as a nondimensional function of propeller planform designed to express the integrated capacity of a respective blade planform for absorbing horsepower.

Two basic sets of propellers were tested for this series, the first being the 47 x 91 with a blade activity factor of 105 and the 47 x 93 with a blade activity factor of 117. After these two propellers were tested, the cuffs were removed from the blades of each propeller, resulting in the 47 x 92 and the 47 x 94 blades with respective activity factors of 103 and 115.

Figures 46 a/b compare the 47 x 91 and 47 x 93 blades with respective activity factors of 105 and 117, and Figures 47 a/b compare the 47 x 92 and 47 x 94 blades with slightly reduced activity factors of 103 and 115.

The second set of propellers tested was the 2FE16A3-4A with a blade activity factor of 86 and the SK59868-12.22 with a blade activity factor of 109. The only difference between these two blades other than activity factor is a slight 2.5° tip twist from 0.95% R

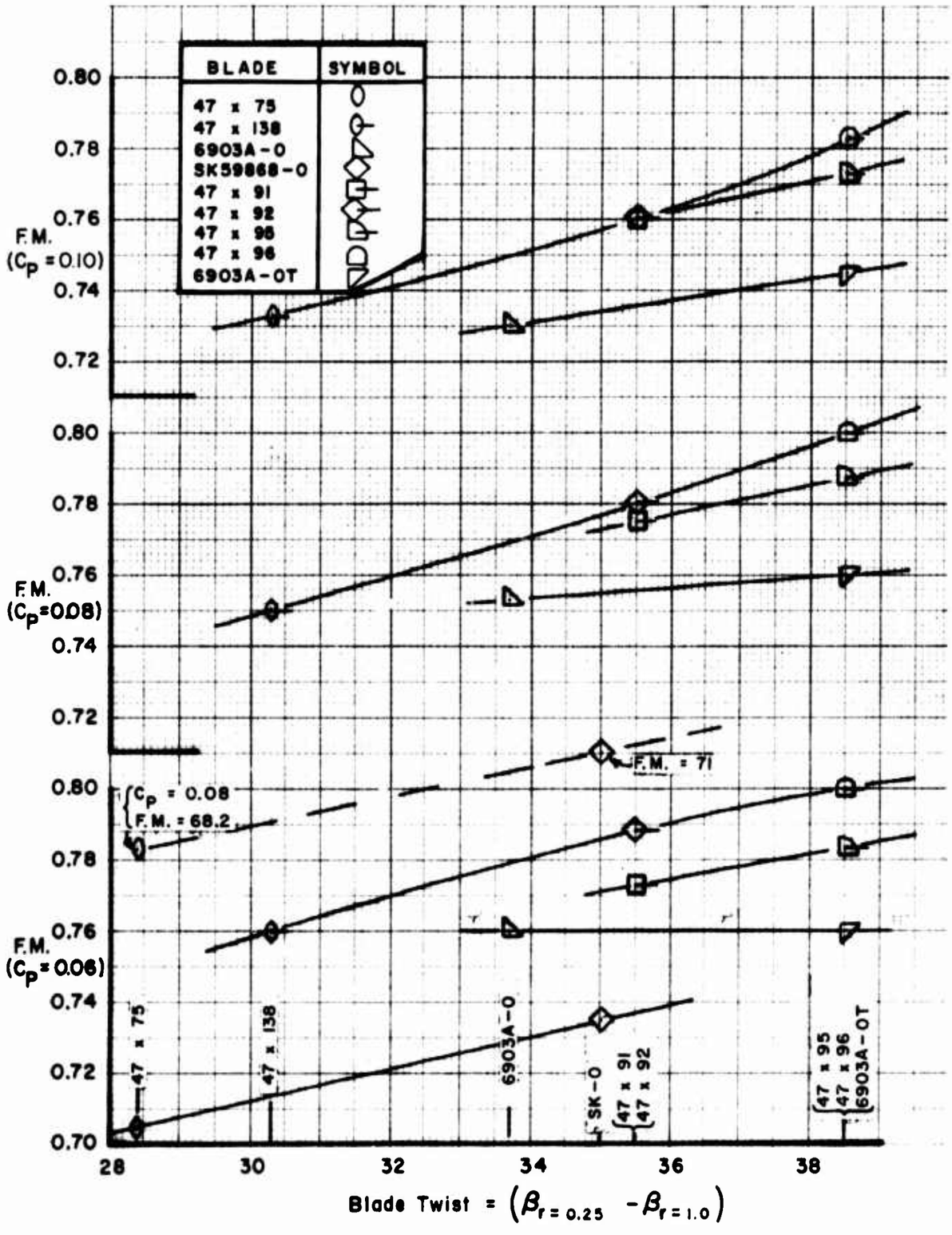

Figure 41. Figure of Merit vs Blade Twist at Tip Mach Number = 0.900 for Power Coefficients = 0.06, 0.08, and 0.10

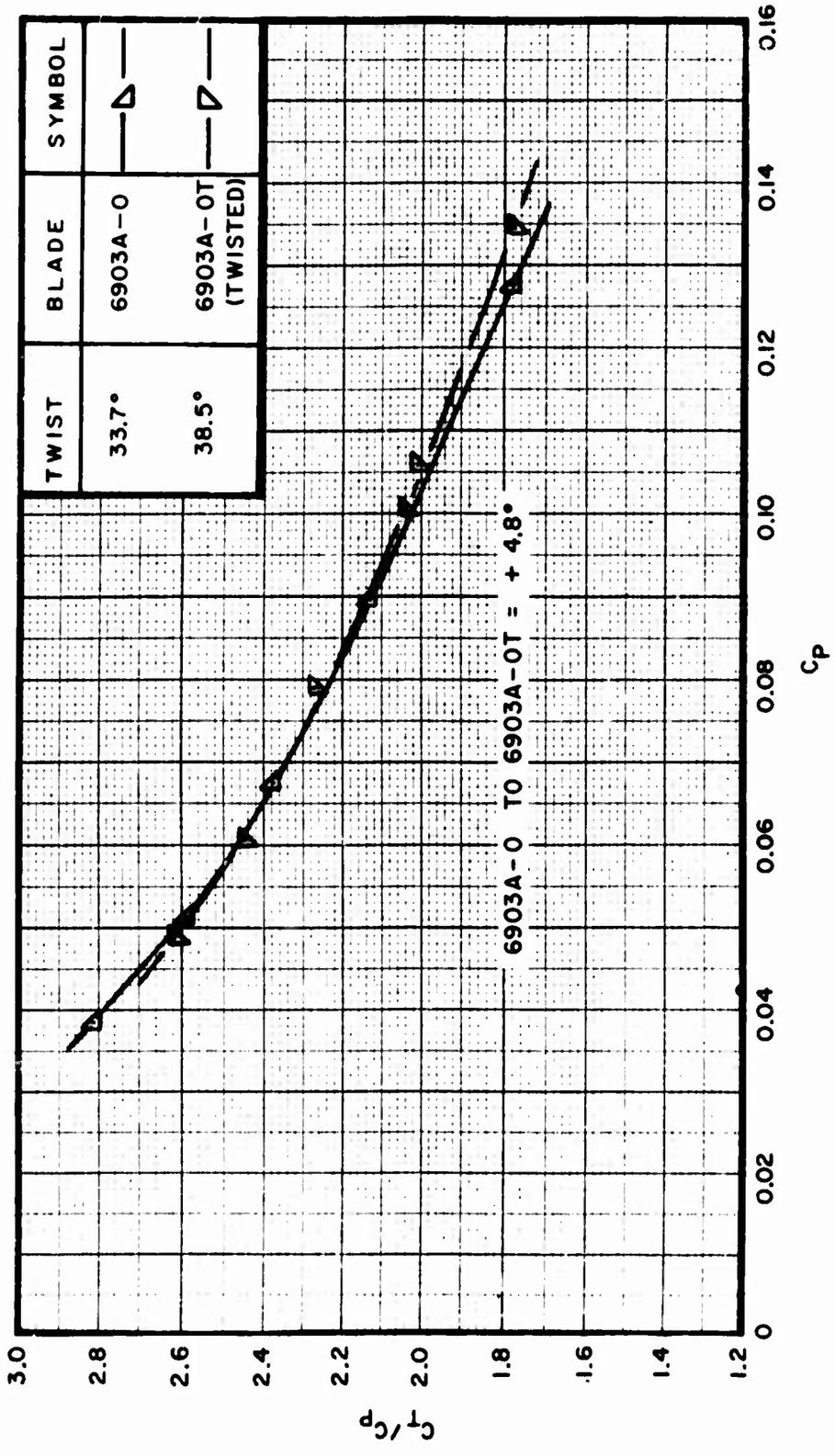

Figure 42. Comparison of 6903A-O and 6903A-OT ($\Delta\beta$ = 4.8°), Walls Down Performance, at Tip Mach Number = 0.800

a. C_T/C_P vs C_P plot

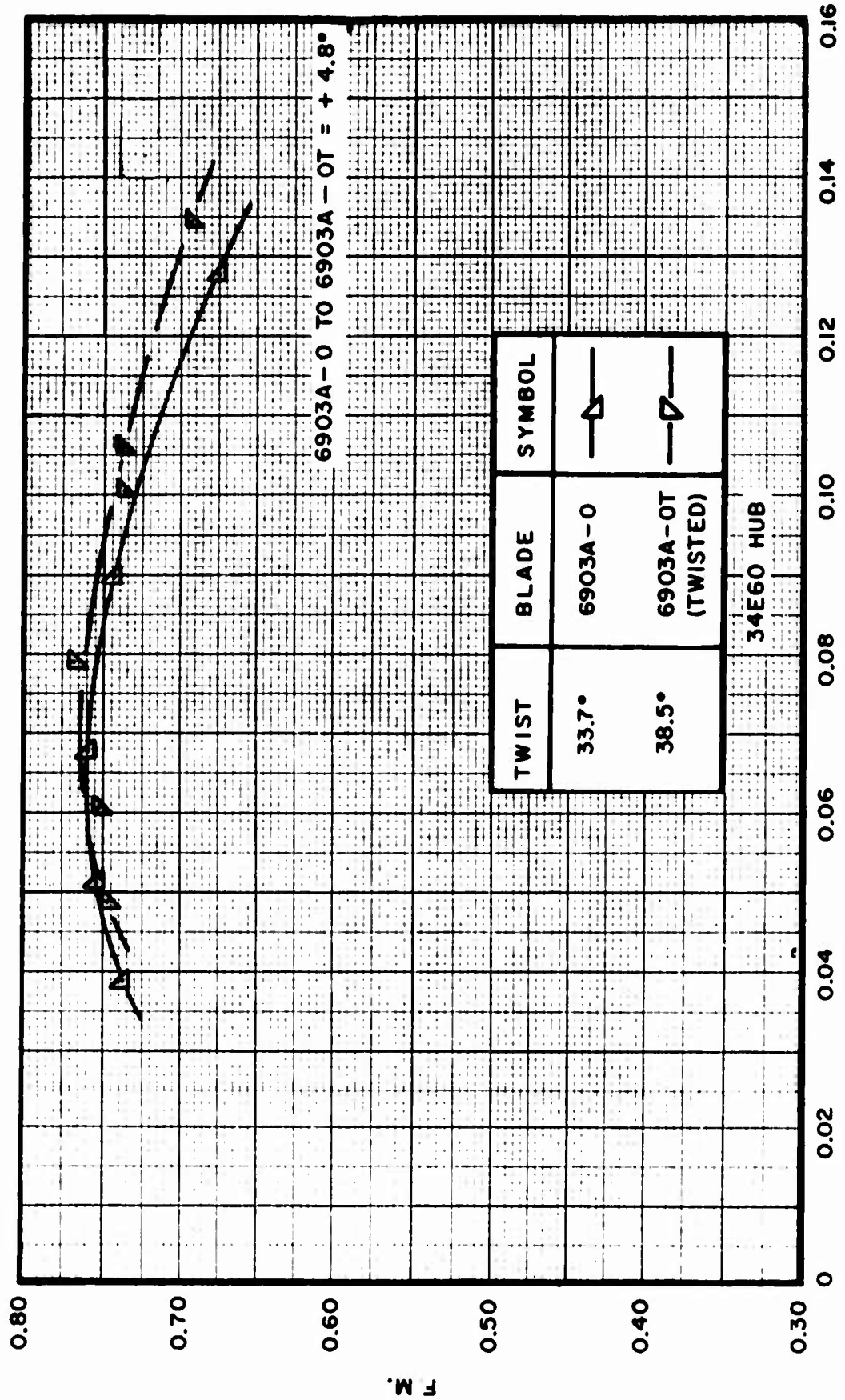

Figure 42. Continued

b. F.M. vs C_P plot

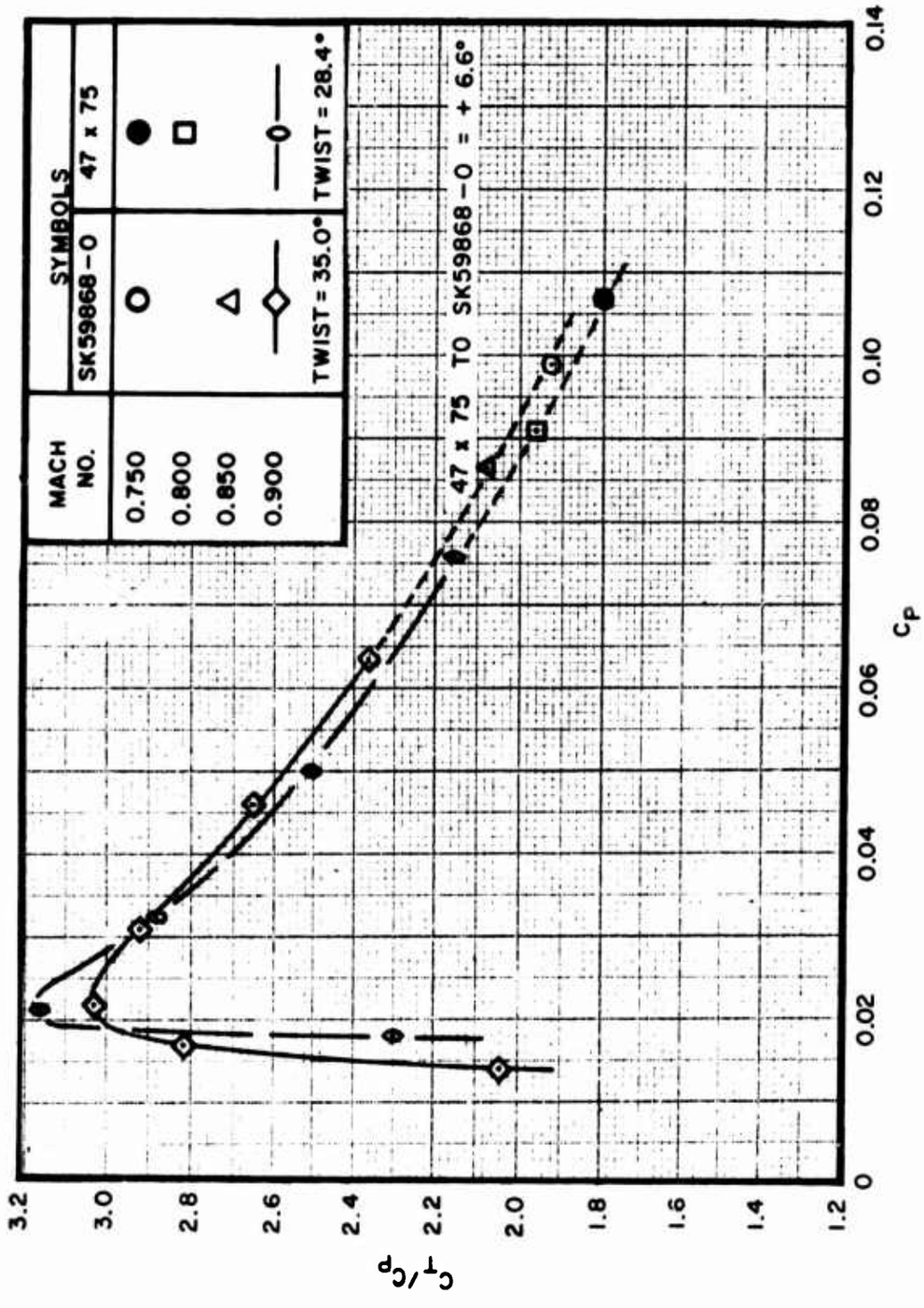

Figure 43. Comparison of SK59868-0 and 47 x 75 ($\Delta\beta$ = 6.6°), Walls Down Performance at Different Tip Mach Numbers

a. C_T/C_P vs C_P plot

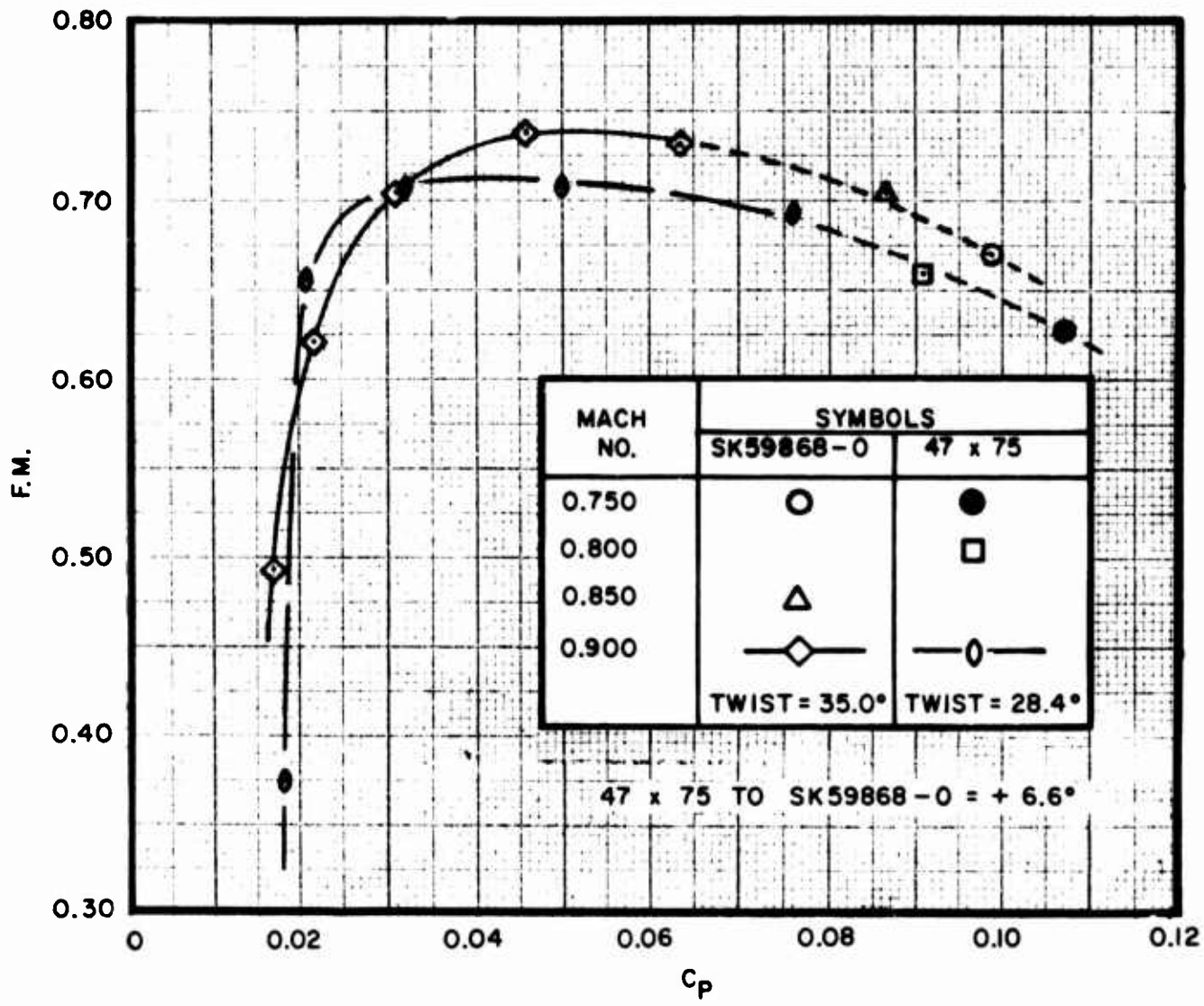

Figure 43. Continued

b. F. M. vs C_P plot

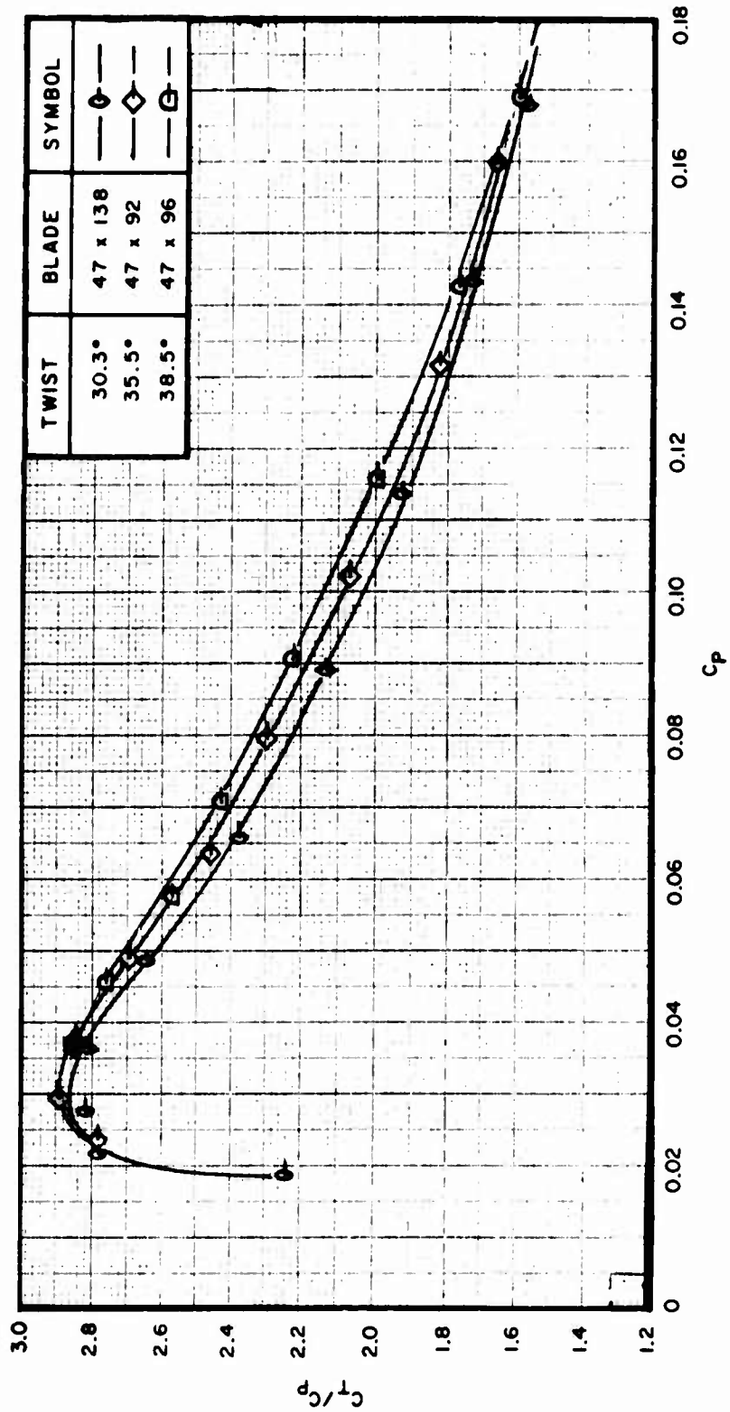

Figure 44. Comparison of 47 x 138, 47 x 92, and 47 x 96 ($\Delta\beta$ = 5.2° and 3.0°), Walls Relocated, Performance at Tip Mach Number = 0.900

a. C_T/C_P vs C_P plot

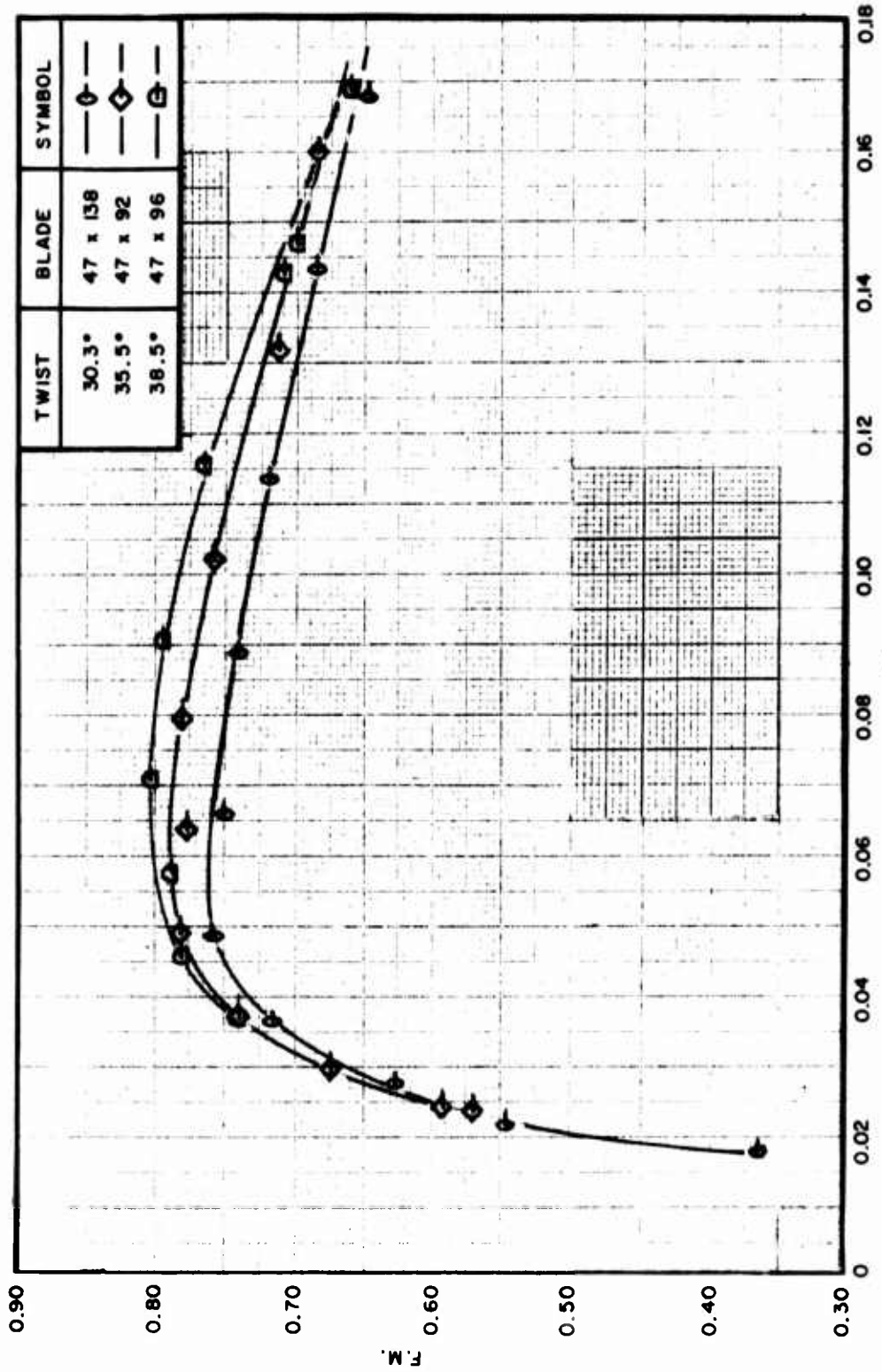

Figure 44. Continued
b. F.M. vs C_P plot

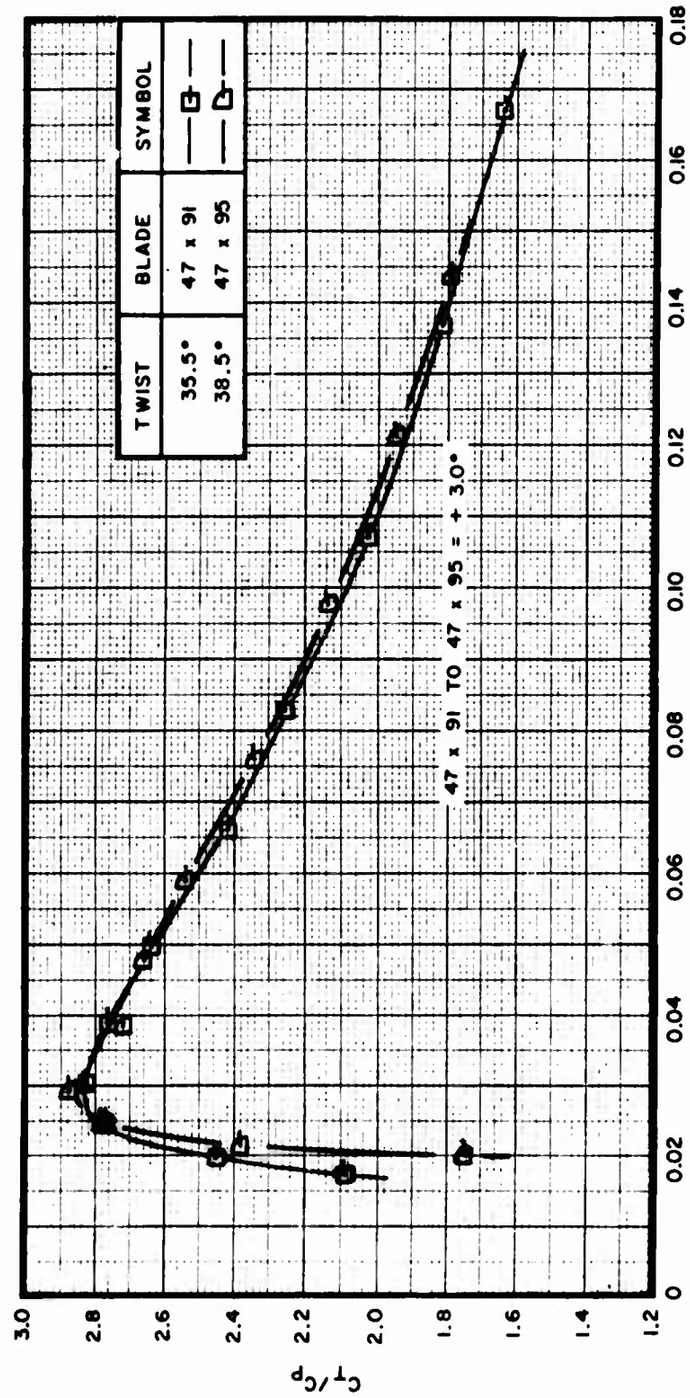

Figure 45. Comparison of 47 x 91 and 47 x 95 (With Cuffs, $\Delta\beta$ = 3.0°), Walls Relocated, Performance at Tip Mach Numbers = 0.900

a. C_T/C_P vs C_P plot

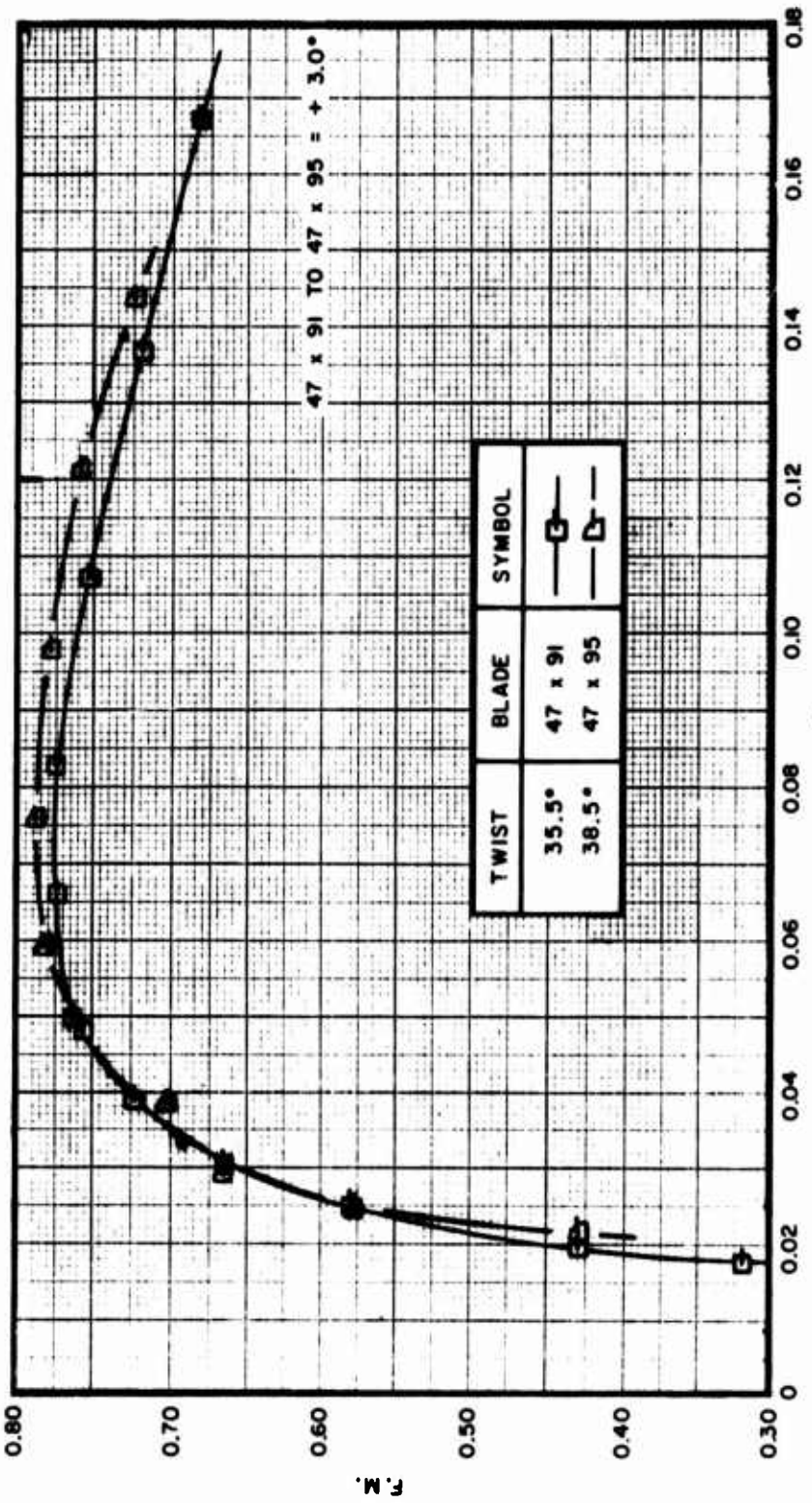

Figure 45. Continued
b. F. M. vs C_P plot

to the tip for the SK59868-12.22. It is believed that the significant shift in peak F.M. to a higher power coefficient for the SK12.22 blade is predominantly due to the increase in activity factor and not to the twist effect. Performance of these two blades is illustrated in Figures 48 a/b.

The above data show that increasing blade activity factor shifts the peak F.M. to a higher power coefficient without substantially increasing the peak F.M. value. This normally would be expected due to the capability of the blade to absorb more power.

b. Total Activity Factor

Total activity factor (TAF) is the sum of the activity factors of all the blades in the propeller (B x AF/blade).

A full-scale three-blade (3-way) and a four-blade (4-way) propeller using a 6903A-0 dural blade were tested during Phase II with the walls down. The production 3-way configuration as used on the C-121 Constellation was tested first. The test was then repeated with the 4-way configuration.

Total activity factor of the 3-way propeller was 297 (3 x 99) and that of the 4-way propeller was 396 (4 x 99). Figures 49 a/b illustrate that increasing the total activity factor of the propeller produced significantly greater thrust for any given power within the range tested and shifted the F.M. peak to a substantially higher power coefficient.

6. EFFECT OF CAMBER

Two different methods were used to investigate camber effect. The first method consisted of comparative testing of two solid aluminum blades each designed with different camber, and identified as 47 x 94 (C_{L_i} = 0.500) and 47 x 97 (C_{L_i} = 0.558). All parameters except camber were the same for each blade. Exact camber distribution for each blade is shown by Blade Characteristic Sheet No. 5 in Appendix I. The effect of this change in camber is very small, as shown in Figures 50 a/b. Because of the scatter in the 47 x 94 data, it was difficult to conclude if there is a significant difference between the two propellers. However, it was concluded that these two blades were too close in integrated C_{L_i} to survive the test scatter with a recognizable difference in performance.

The 2FE16A3-4A propeller was modified to provide the basis for the second method of investigating camber effect. The modification was accomplished by bonding a balsa wood tab to the face side trailing edge of the basic blade, as shown in Figure 51. The tab extended

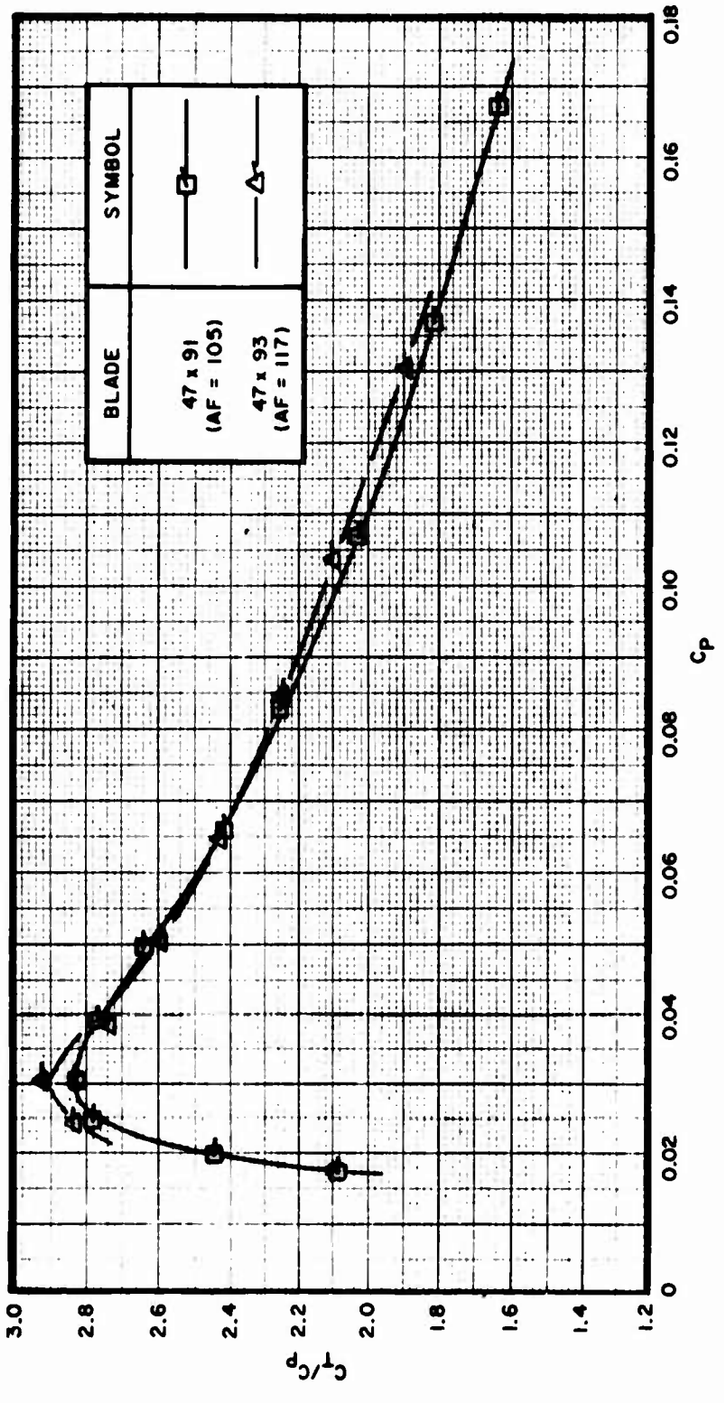

Figure 46. Comparison of 47 x 91 (AF = 105) and 47 x 93 (AF = 117), Walls Relocated, Performance at Tip Mach Number = 0.900

a. C_T/C_P vs C_P plot

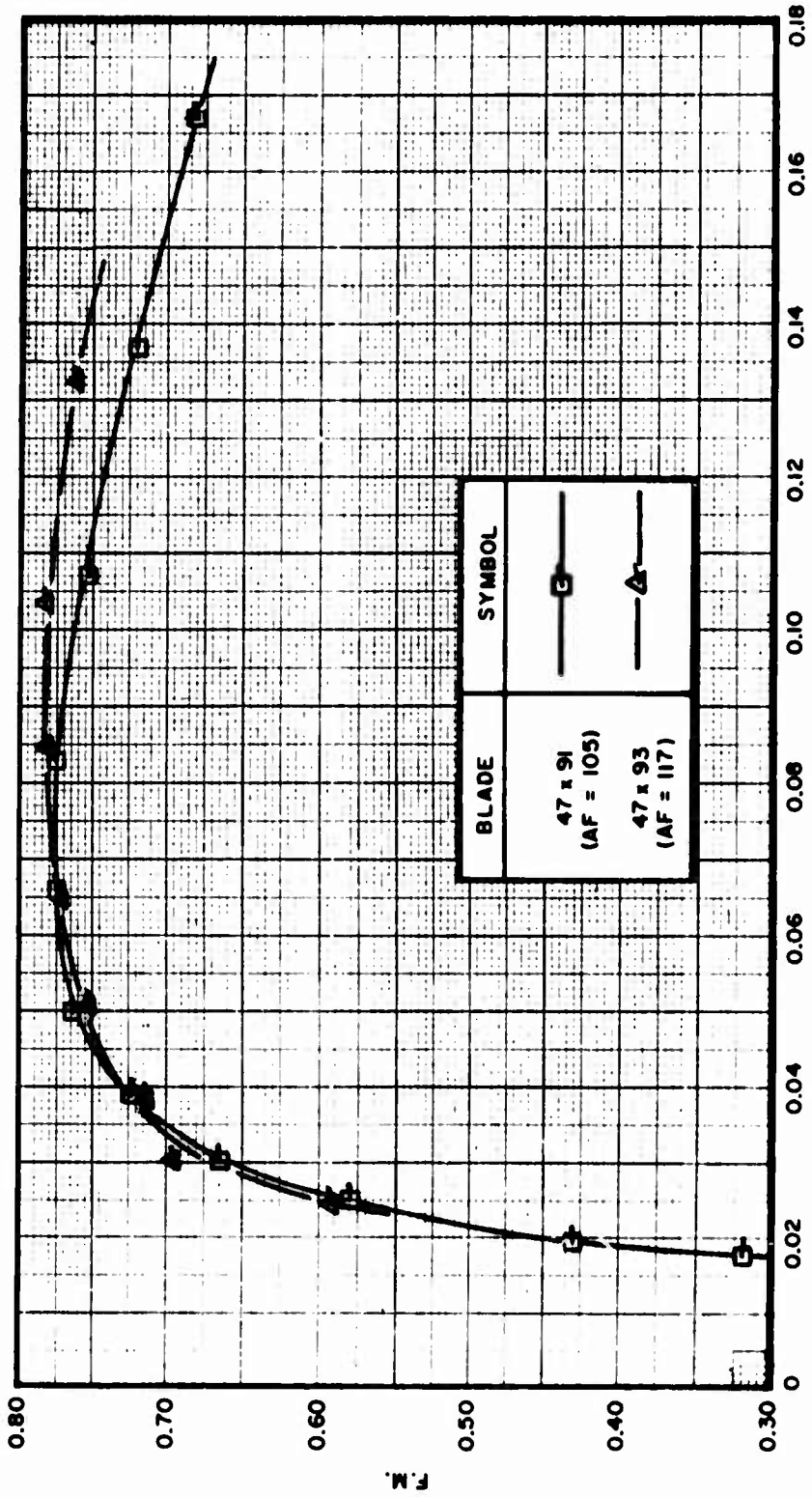

Figure 46. Continued

b. F.M. vs C_P plot

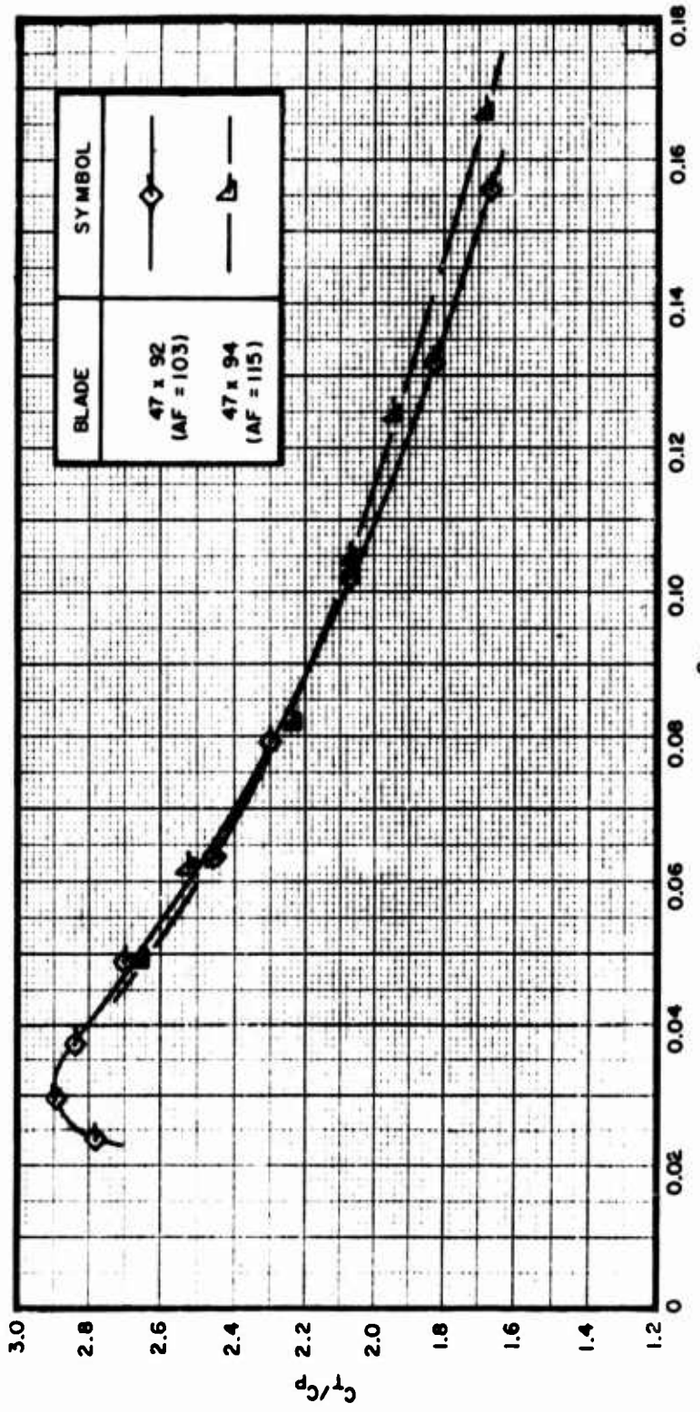

Figure 47. Comparison of 47 x 92 (AF = 103) and 47 x 94 (AF = 115), Walls Relocated, Performance at Tip Mach Number = 0.900

a. C_T/C_P vs C_P plot

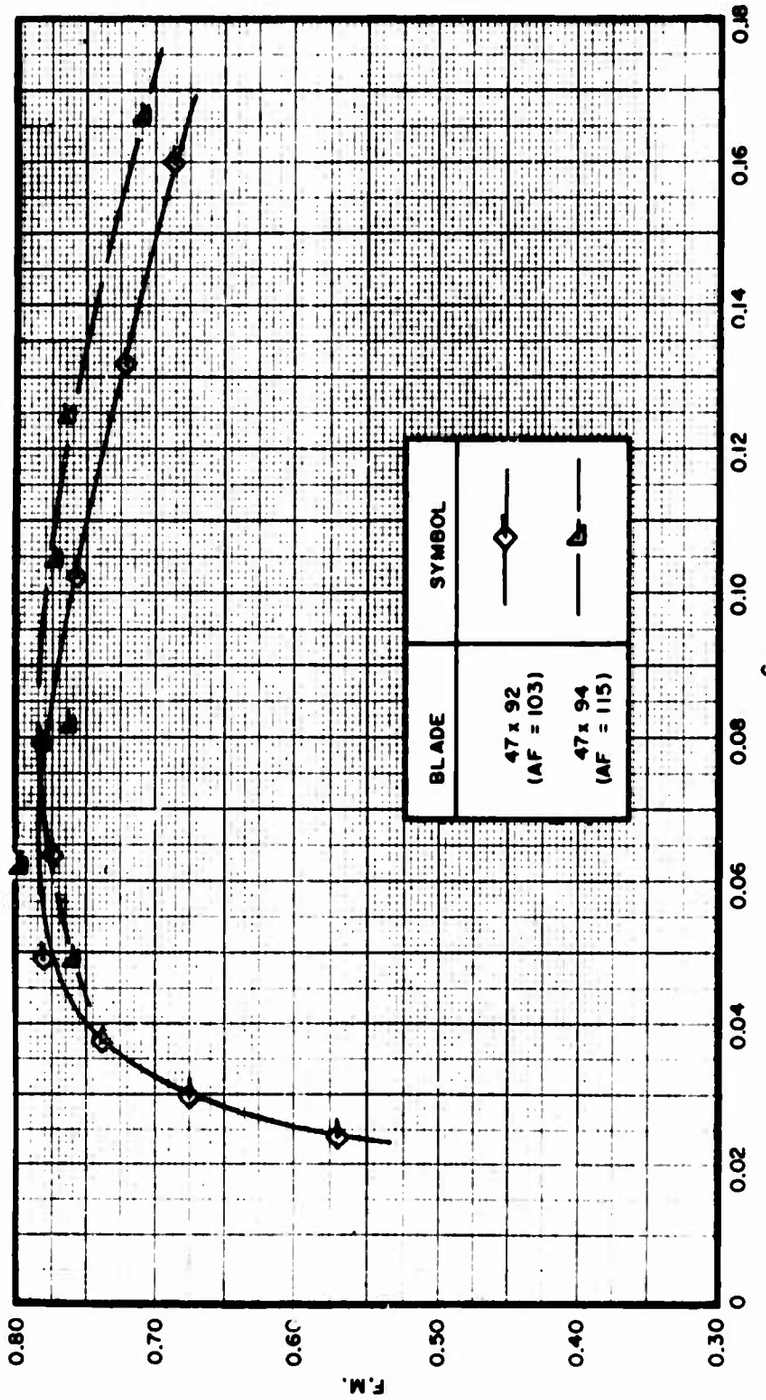

Figure 47. Continued
b. F.M. vs C_P plot

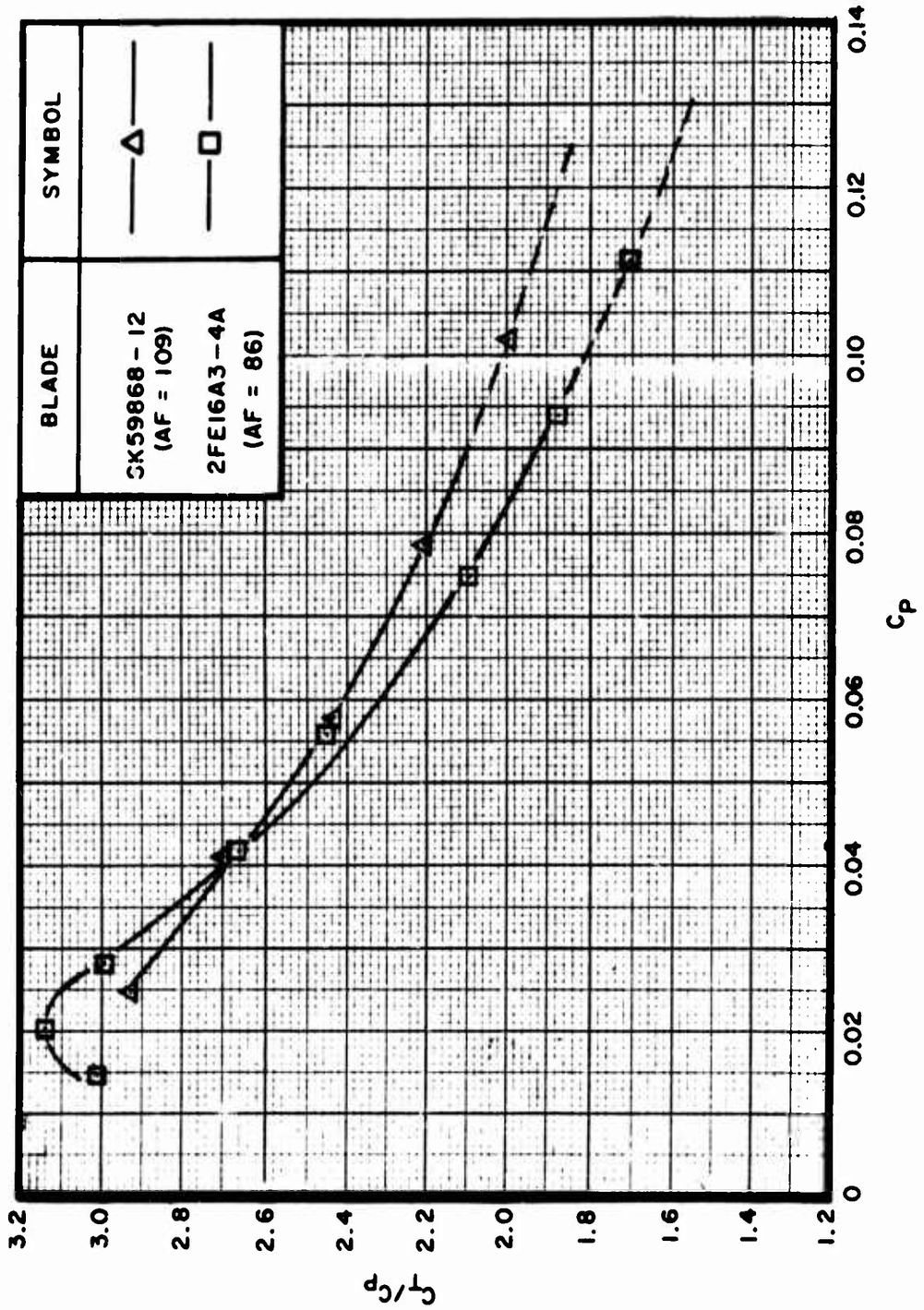

Figure 48. Comparison of SK59868-12 (AF = 109) and 2FE16A3-4A (AF = 86); Walls Down, Performance at Tip Mach Number = 0.900

a. C_T/C_P vs C_P plot

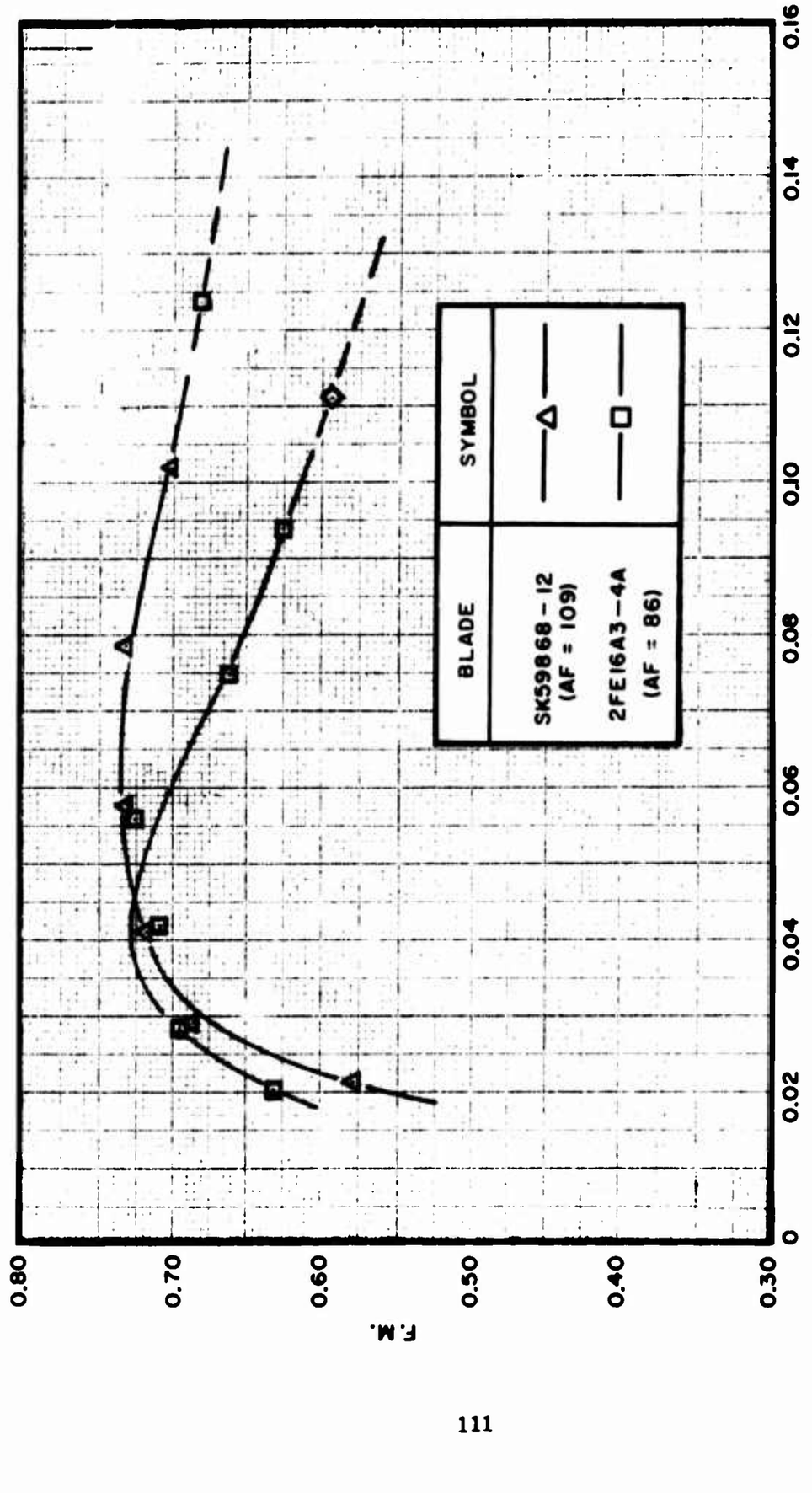

Figure 48. Continued
b. F.M. vs C_P plot

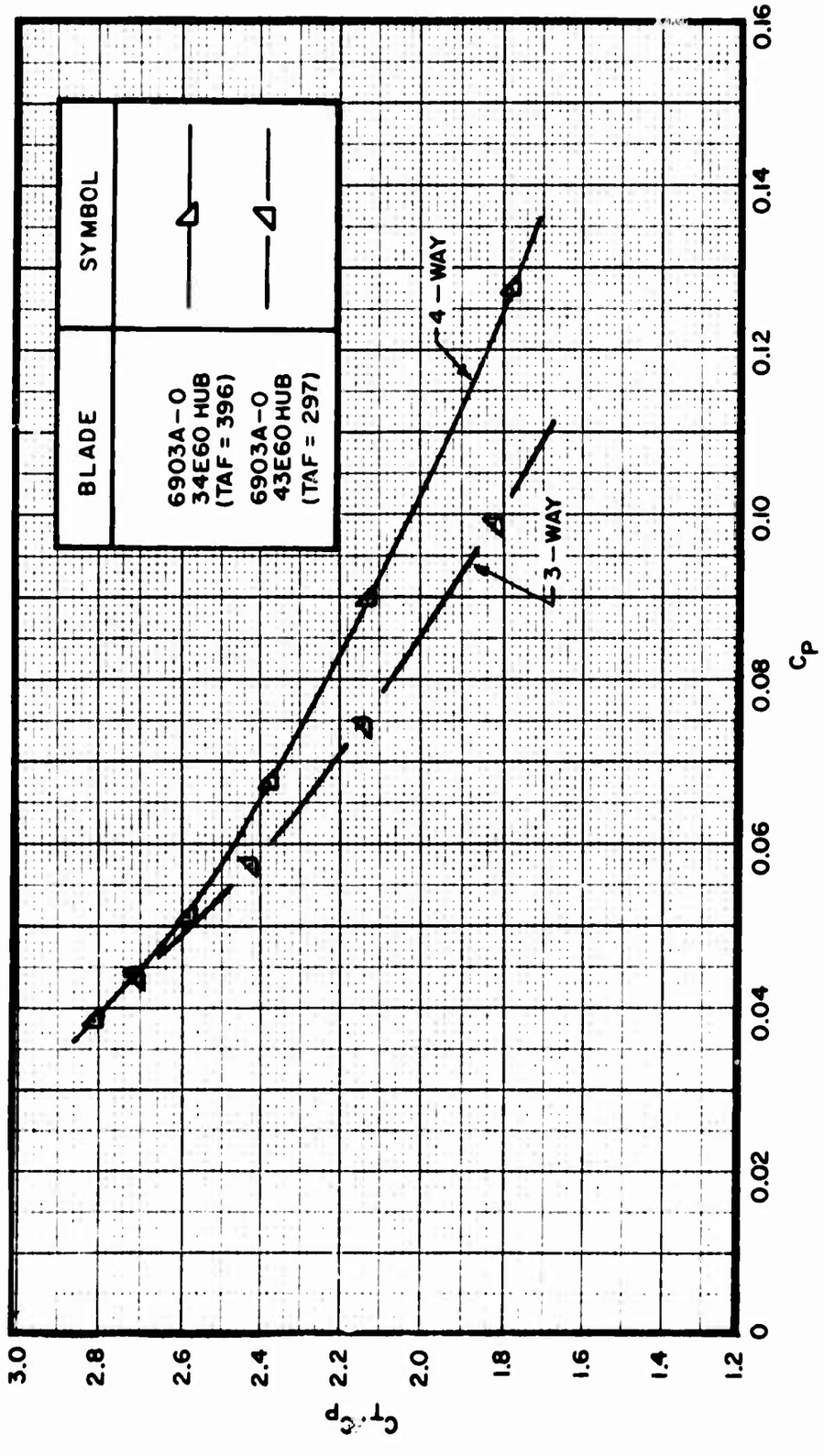

Figure 49. Comparison of 6903A-0 3-Way (TAF = 297) and 4-Way (TAF = 396), Walls Down, Performance at Tip Mach Number = 0.800

a. C_T/C_P vs C_P plot

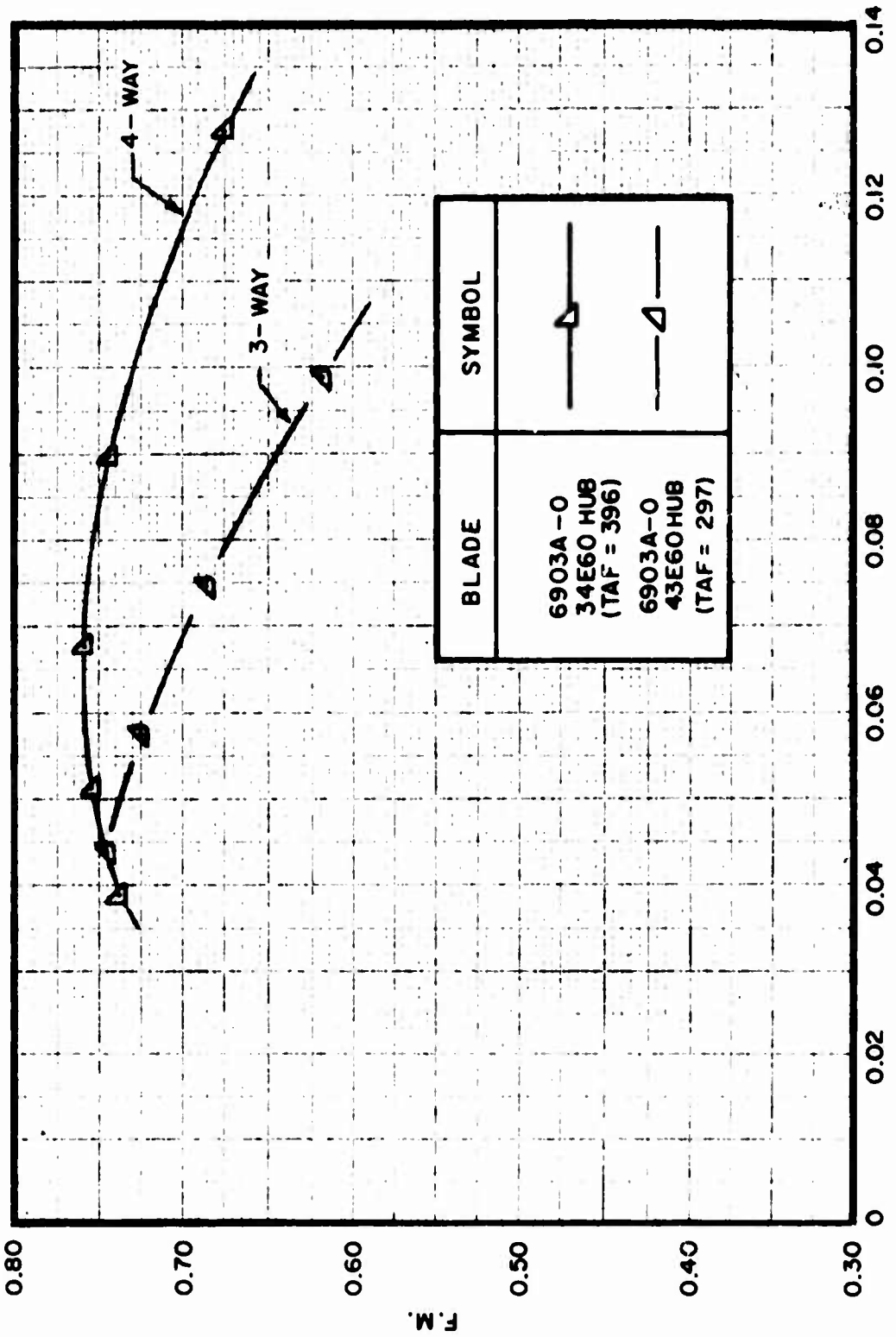

Figure 49. Continued

b. F.M. vs C_p plot

from the tip in-board to the 78-inch station. The wedge angle of the tab varied from 12° at the tip to 12.5° inboard, and the bonded width varied from 0.815 inch at the tip to 1.540 inches inboard. This modification resulted essentially in a NACA series 16 airfoil with a flap which provided an increase in local camber somewhat above that of the original section, and a blade integrated camber somewhat greater than the original 0.475.

Performance of the 2FE16A3-4A blade with the flap is shown in Figures 52 a/b, and a comparison with and without the flap is shown in Figures 53 a/b. These data indicate that, with the flap, a higher C_T/C_P is attained for a given C_P above $C_P = 0.05$. In addition, while the maximum value of F.M. did not appear to increase, the flap had the effect of shifting the F.M. curve into the higher C_P range, as illustrated by Figure 53b.

The author's opinion is that the 2FE16A3-4A blade with the modified wedge (or tab) would have shown a greater difference in performance if the modification had been built into the blade. The camber change effect achieved by the wedge is misleading in that the boat tail drag of the device is high. In turn then, the peak C_T/C_P is not substantially increased, since the C_T increase due to camber is partially offset by the C_P rise created by the increased drag. Consequently, the F.M. peak does not go up, but the F.M. curve is shifted across to a higher C_P level. It should be noted that Figures 52 and 53 are based on 0.85 tip Mach number data. The performance at the XC-142A take-off tip speed of 0.90 tip Mach was substantially reduced and less benefit would have been realized from the camber.

7. EFFECT OF AIRFOIL SECTION

The two blades compared during these tests were the 47 x 93 and the 47 x121 which were identical in all respects except for the airfoil section. The 47 x 93 incorporated a NACA Series 16 airfoil in the outer 40% of the radius and a NACA Series 64 airfoil in the inner 30% of the radius, with transition airfoils between the two regions. The 47 x 121 incorporated a NACA Series 65 airfoils along its entire radius.

Figures 54 a/b shown that the use of the NACA 16/64 series raises the peak F.M. very slightly, but more important, tends to flatten the curve somewhat and its peak is the higher power coefficient range. Use of the NACA 16/64 series, therefore would, result in the ability to maintain essentially the same F.M. over a wider power coefficient range.

In the opinion of the author, the shifting and flattening of the 47 x 93 (series 16/64) in the higher C_P range can be attributed to the use of the 16 series in the outer radius. This is due to the slight advantage in the critical Mach number of the 16 series over the 65 series.

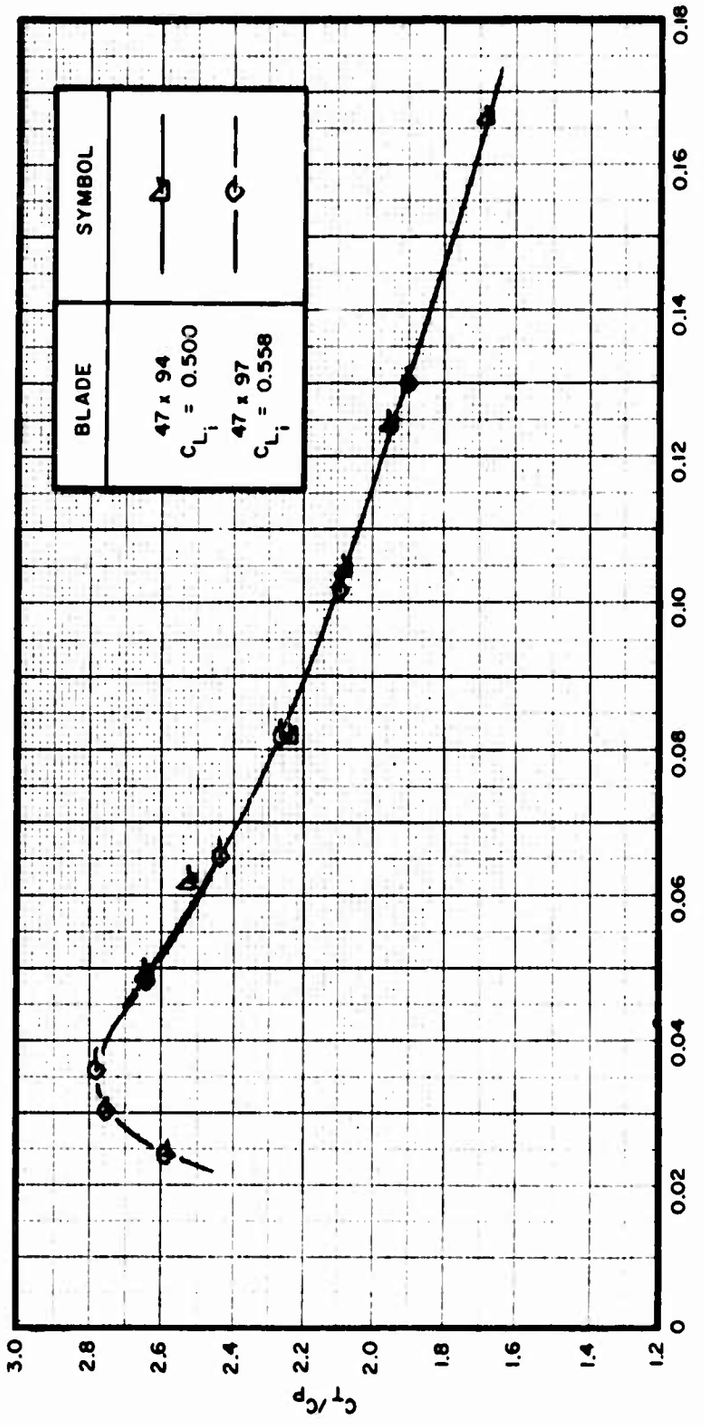

Figure 50. Comparison of 47 x 94 (C_{L_i} = 0.500) and 47 x 97 (C_{L_i} = 0.558); Walls Relocated, Performance at Tip Mach Number = 0.900

a. C_T/C_P vs C_P plot

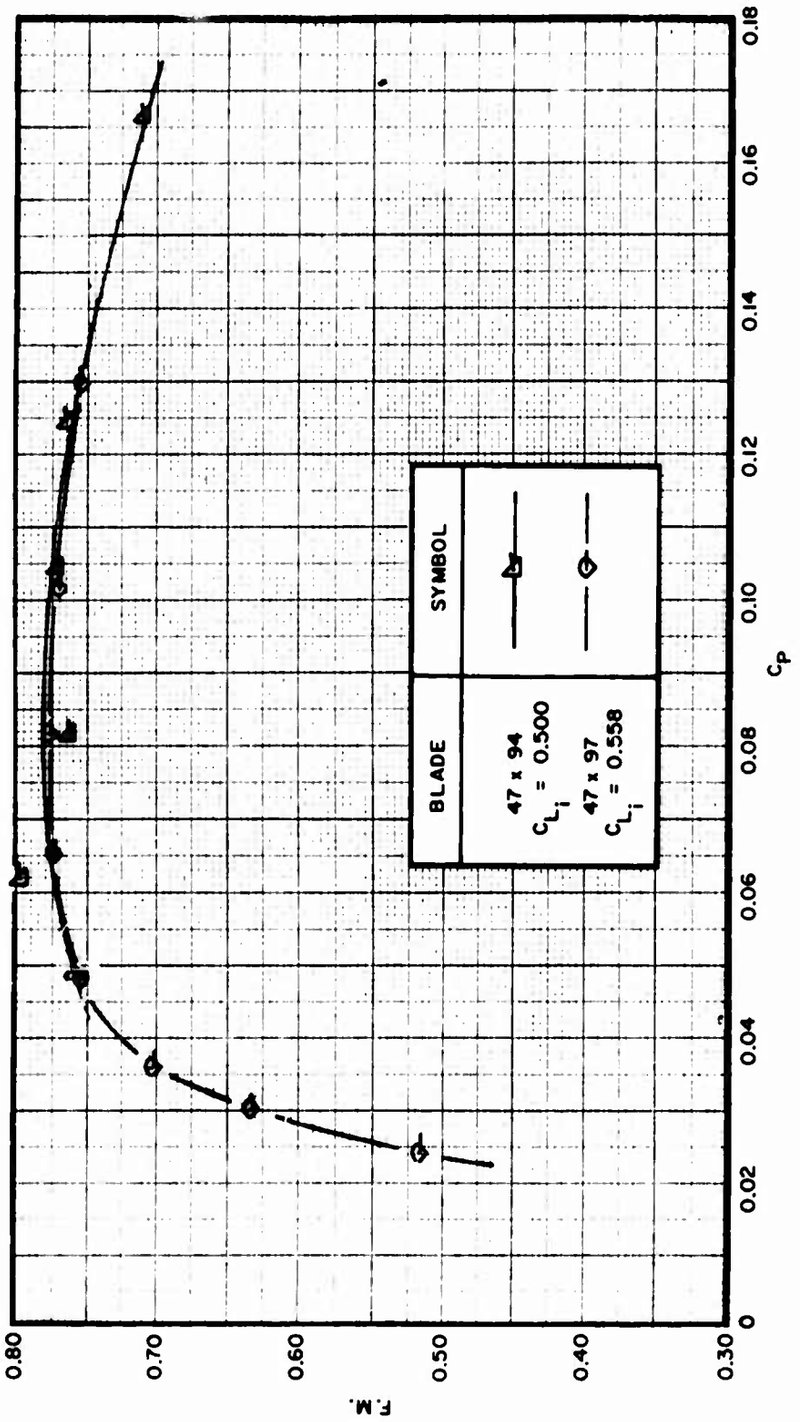

Figure 50. Continued
b. F.M. vs C_P plot

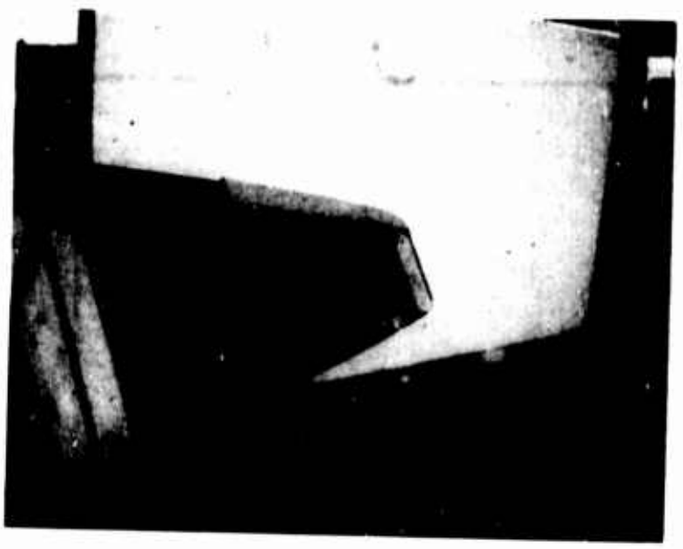

Figure 51. 2FE16A3-4A Blade With Balsa Wood Wedge (Tab) Bonded to Lower Side Trailing Edge

a. Bottom quarter view of blade

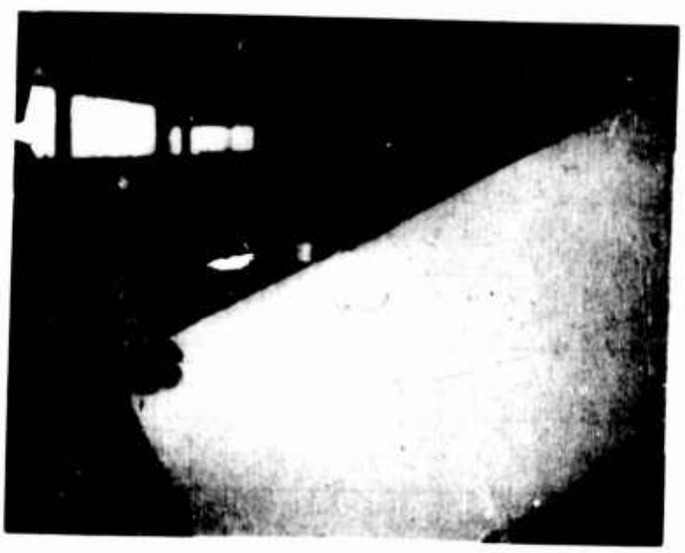

Figure 51. Continued

b. End view of blade

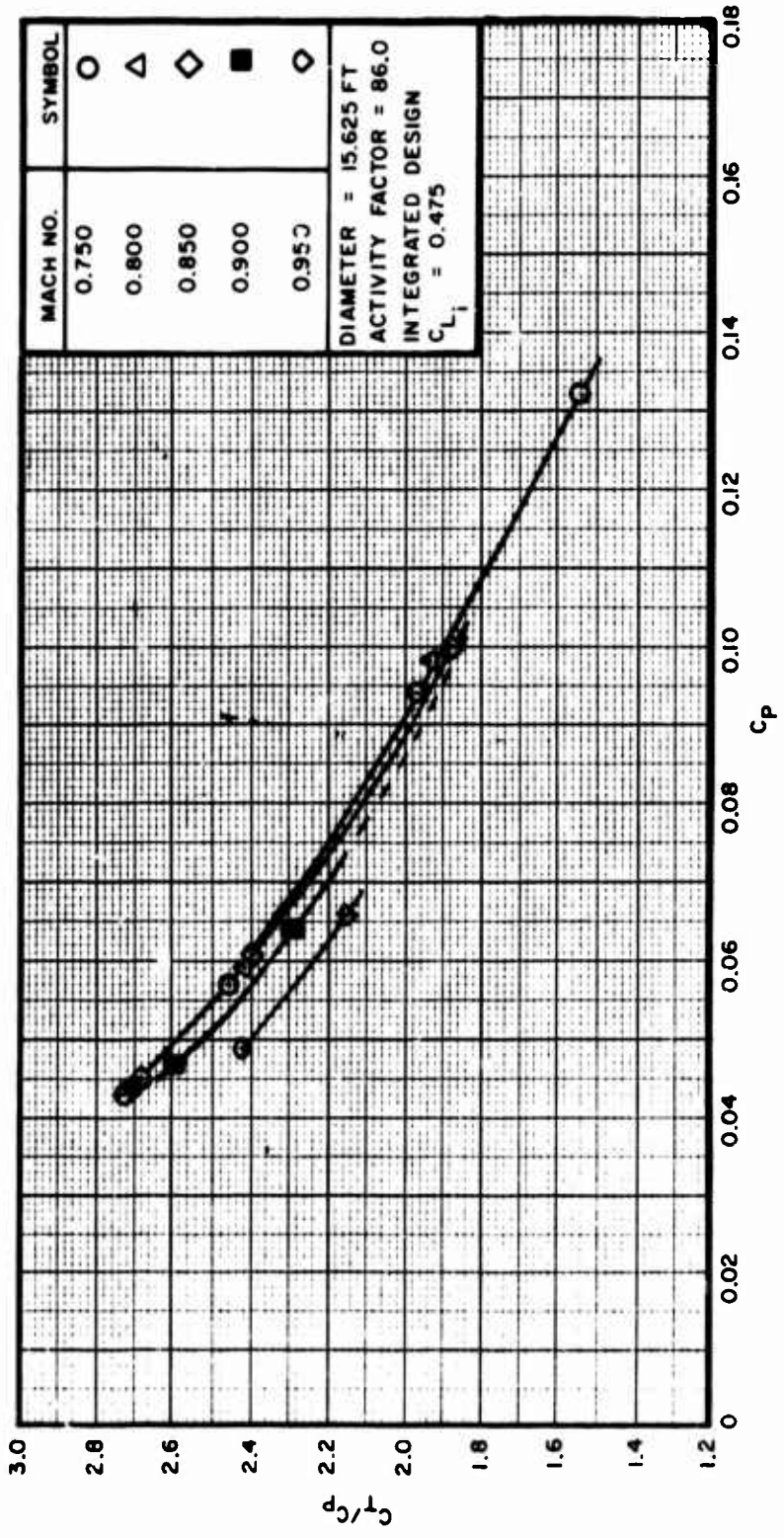

Figure 52. 2FE16A3-4A With Wedges (Tabs), Walls Down, Performance at Different Tip Mach Numbers

a. C_T/C_D vs C_P plot

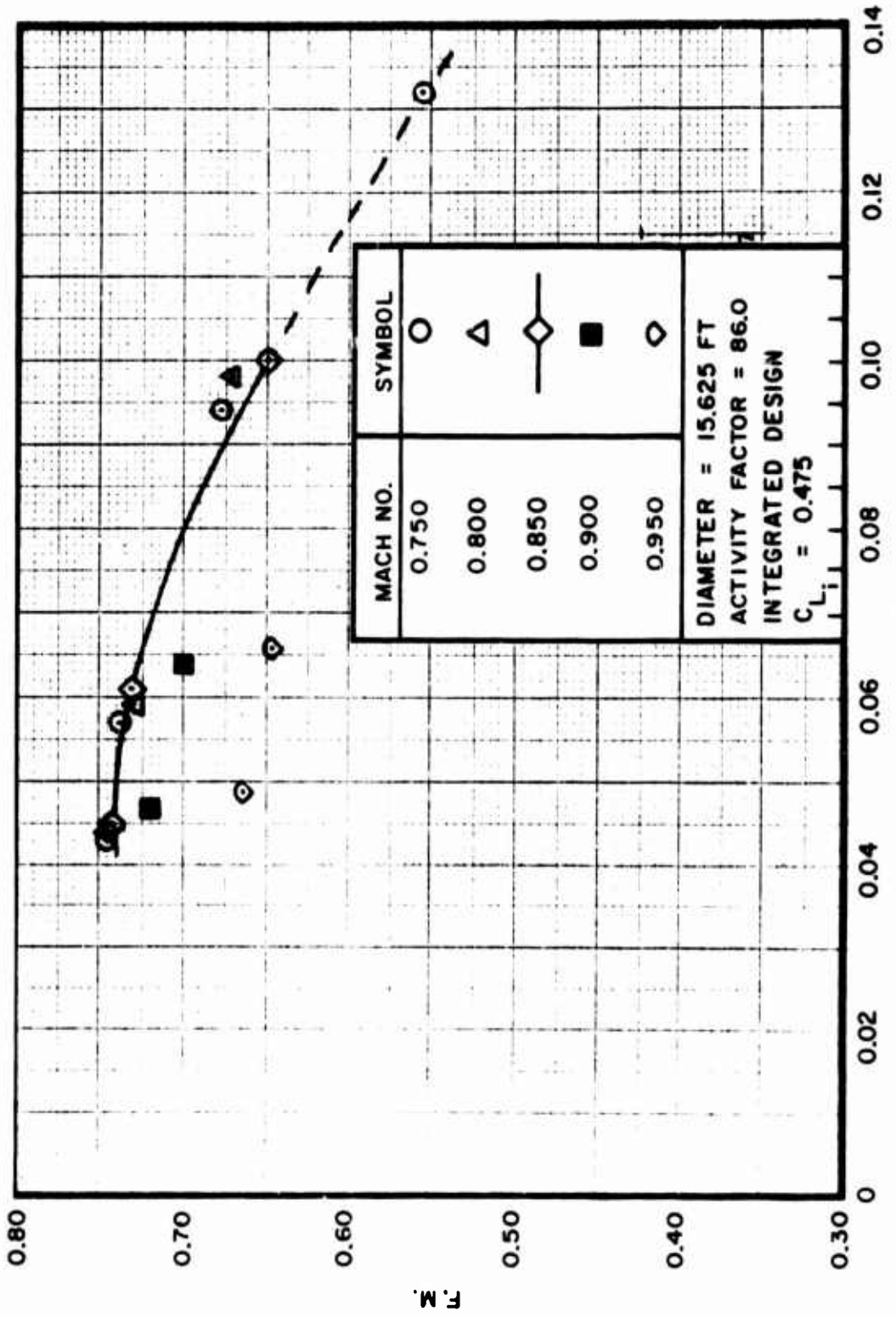

Figure 52. Continued

b. F.M. vs C_P plot

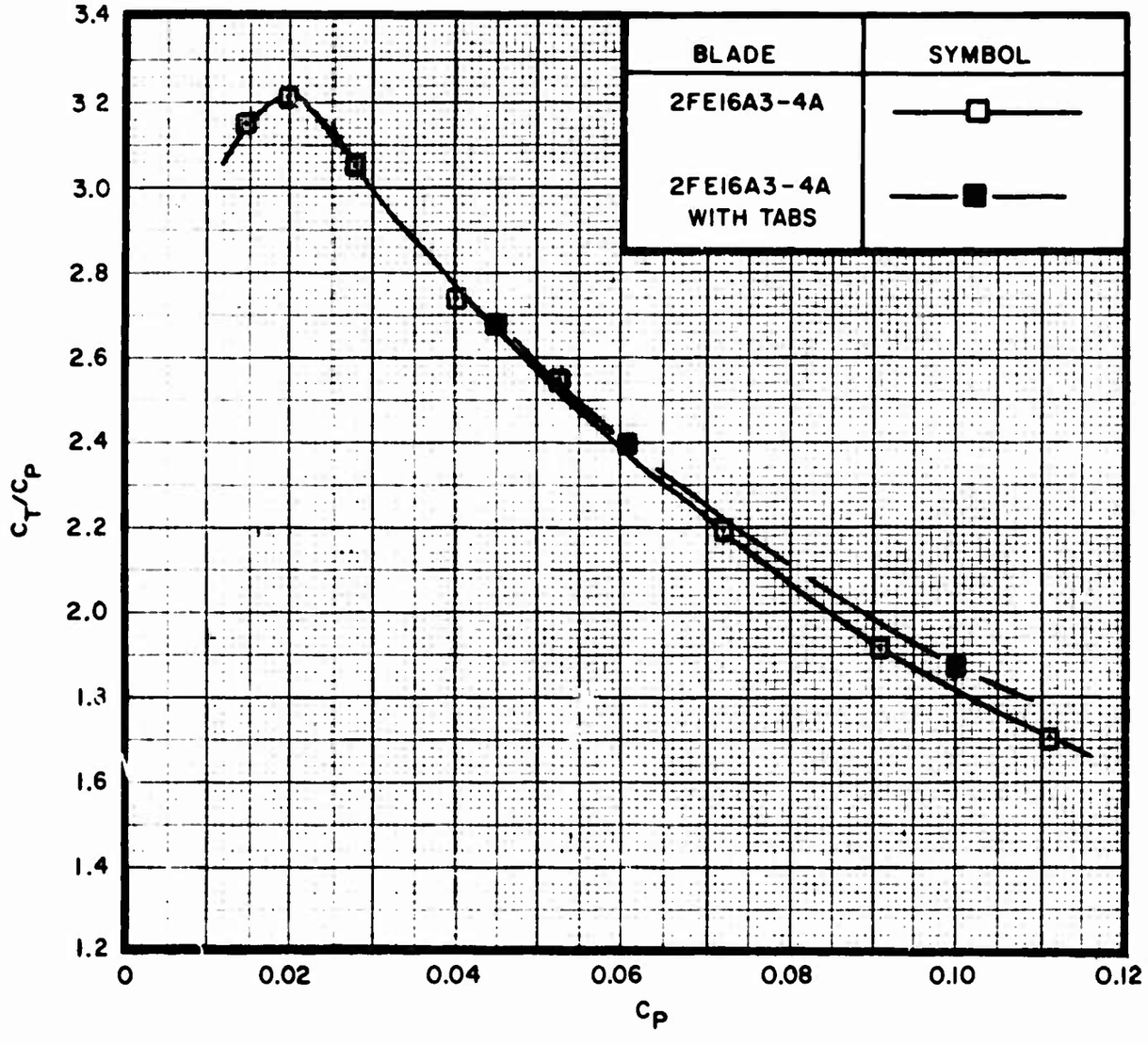

Figure 53. Comparison of 2FE16A3-4A With and Without Wedges (Tabs); Walls Down, Performance at Tip Mach Number = 0.850

a. C_T/C_P vs C_P plot

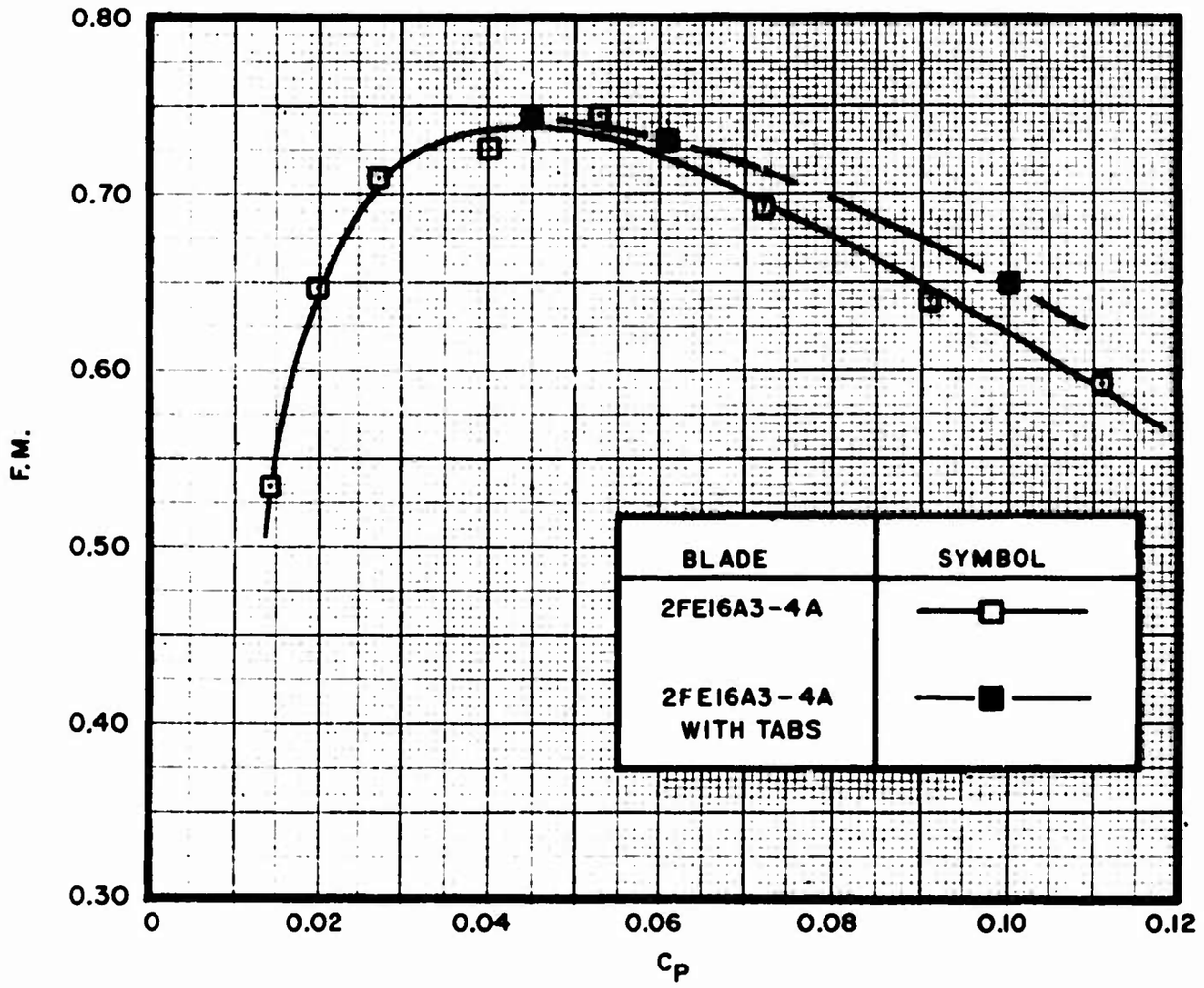

Figure 53. Continued

b. F.M. vs C_P plot

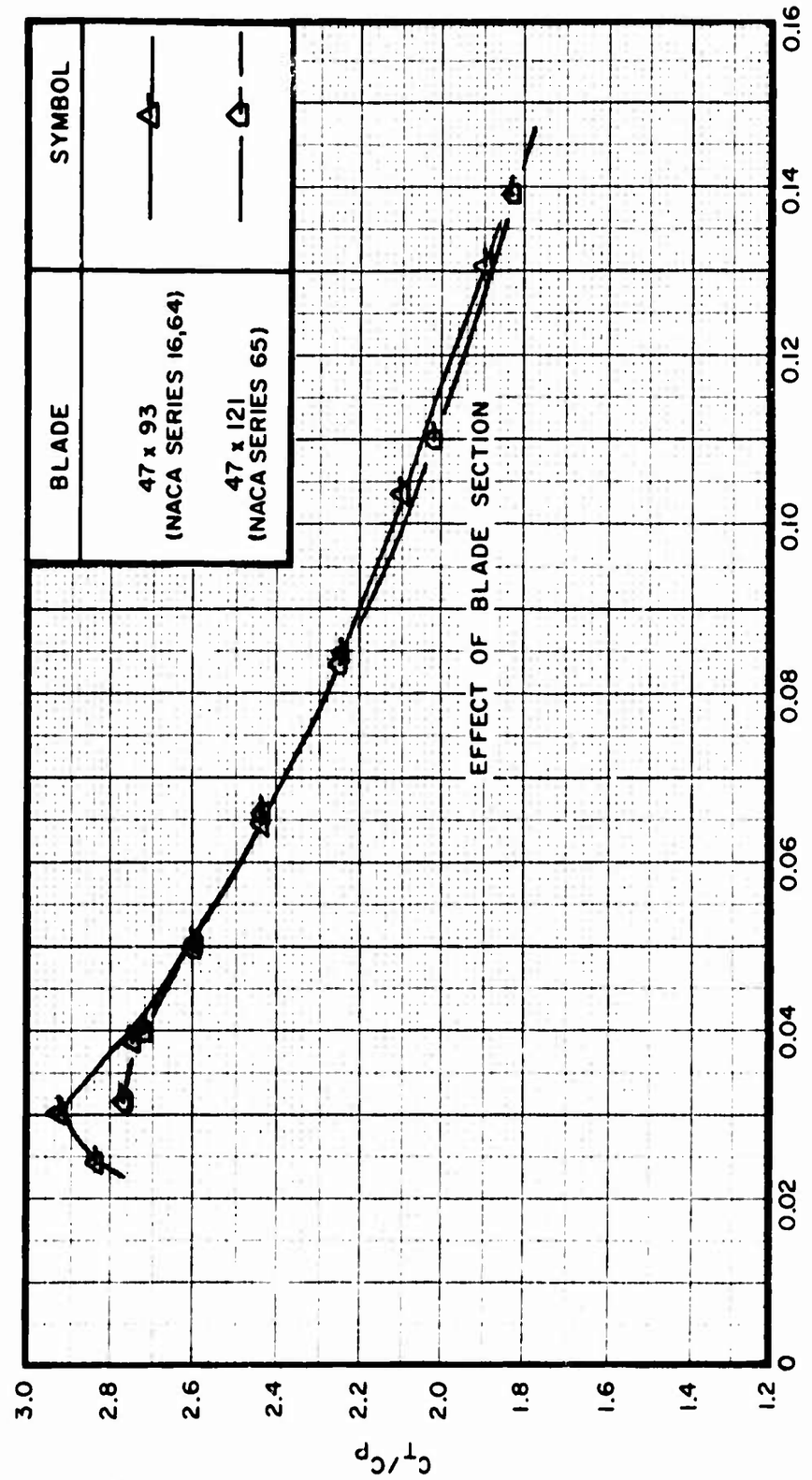

Figure 54. Comparison of 47 x 93 (NACA Series 16, 64) and 47 x 121 (NACA series 65), Walls Relocated, Performance at Tip Mach Number = 0.900

a. C_T/C_P vs C_P plot

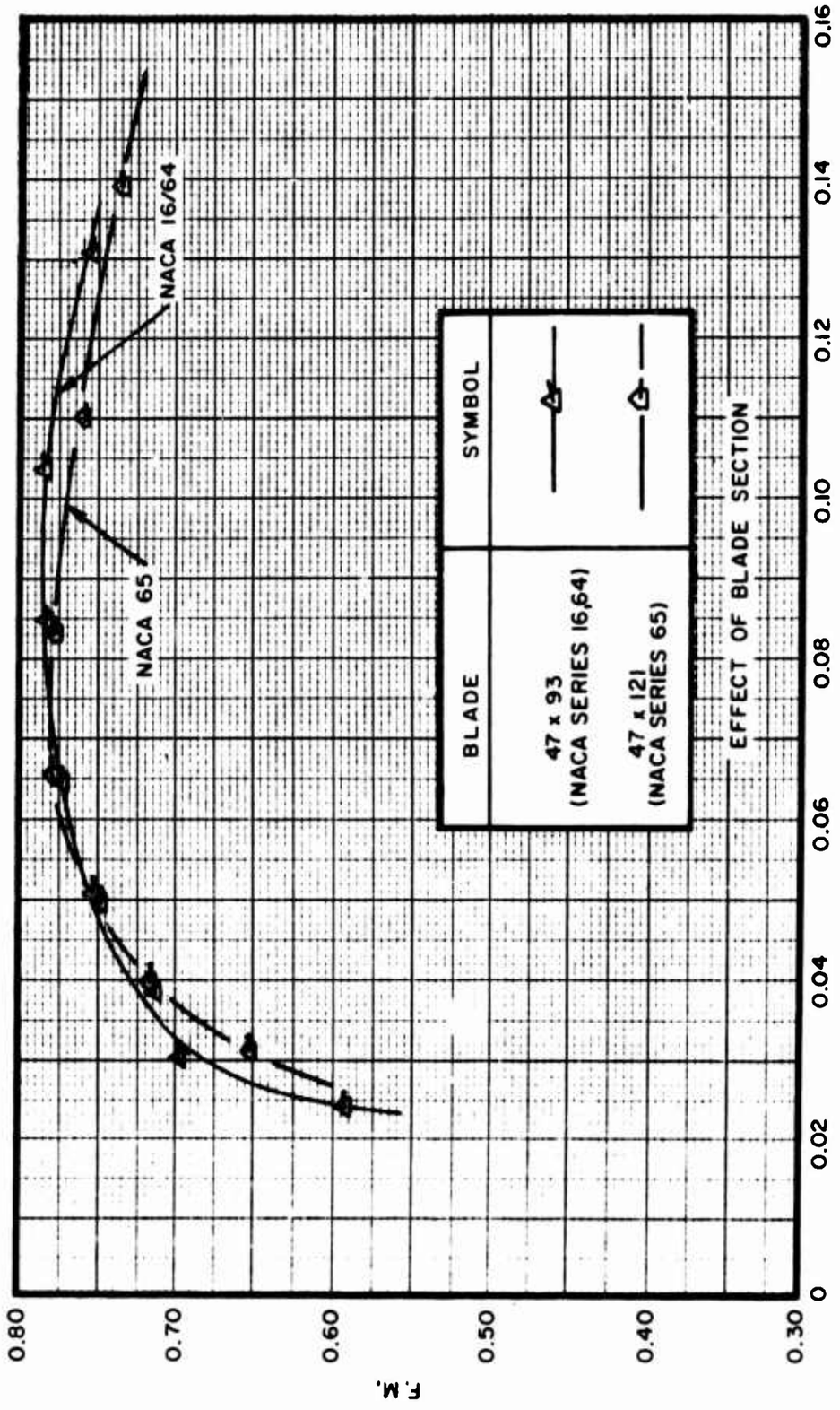

Figure 54. Continued

b. F. M. vs C_p plot

8. MISCELLANEOUS PROPELLERS

Paragraph 8 gives the performance of several miscellaneous propellers which were designed for or demonstrated high static thrust.

Figures 55 a/b compare the performance of the 2FE16A3-4A and the 156109A2P3 propellers tested on Rig No. 4. Both of these propellers are essentially the same diameter (15.625 ft and 15.500 ft) and were designed specifically for the operating conditions of the XC-142A. Each propeller featured lightweight blade construction, foam and fiberglass materials being used. As can be seen from the Blade Characteristics Sheet No. 14, the 156109A2P3 blade has a higher activity factor than the 2FE16A3-4A, and the peak camber distribution is at a greater spanwise location. The variation in tip camber and overall twist no doubt contributes to some performance difference, however the shift of the peak F.M. to a higher power coefficient is believed due primarily to the increase in activity factor. This peak F.M. shift to a higher C_p was also evident when comparing the SK59868-12.22 and 2FE16A3-4A blades discussed in paragraph E — Effect of Activity Factor — and illustrated in Figures 48 a/b.

Figures 56 a/b provide performance data on the 13166A10P3 blades built for the X-19 aircraft and tested on Rig No. 1. The X-19 is a small twin engine tandem wing VTOL aircraft with four tilting propellers. This data is provided for information purposes only and is not directly comparable to that of other blades tested on Rig 4. This is due to the difference between Rigs 1 and 4 and the fact that the X-19 blade was designed to optimize use of the "Radial Lift Force."

Figures 57 a/b give performance data on the 1490A2P3 blades used on the CL-84 aircraft. The CL-84 is a small twin engine tilt wing VTOL aircraft utilizing two fiberglass-foam propellers. The data obtained on Rig 4, although limited and scattered, indicates that a significant F.M performance level was achieved. The primary contribution of the CL-84 data is the Blade Characteristic Sheet which is included in Appendix I. It should also be noted that the performance data is presented at a low Mach No. = 0.700.

Figures 58 a/b show data obtained from an experimental propeller designated X-65SEJDR which was tested on Rig 1 and demonstrated relatively good static performance. This blade was the most highly twisted (45.5°) of any blade tested and had a relatively low integrated lift coefficient. It was also the smallest-diameter propeller covered in this report.

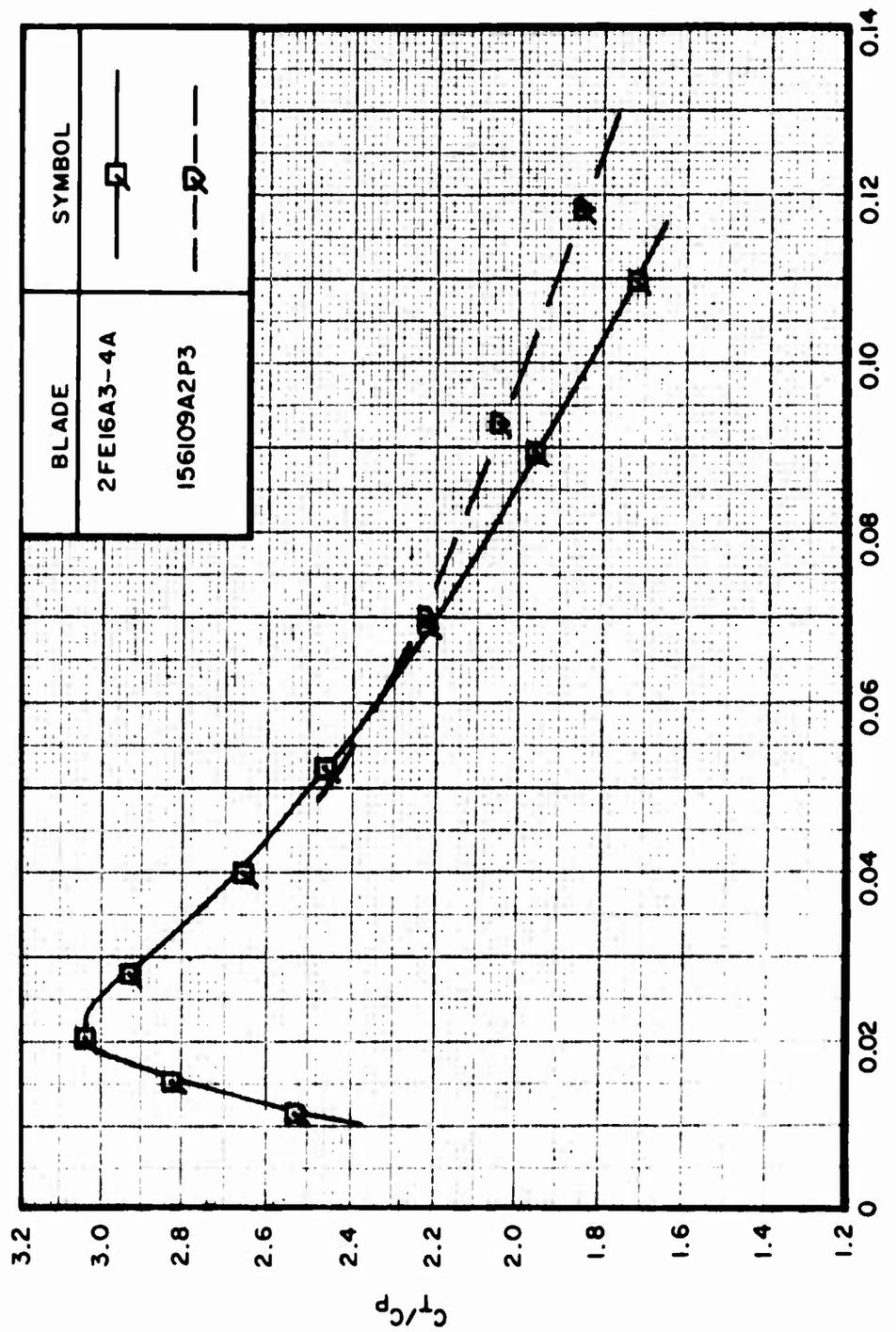

Figure 55. Comparison of 2FE16A3-4A and 156109A2P3, Walls Up, Performance on Rig No. 4 at Tip Mach Number = 0.850

a. C_T/C_P vs C_P plot

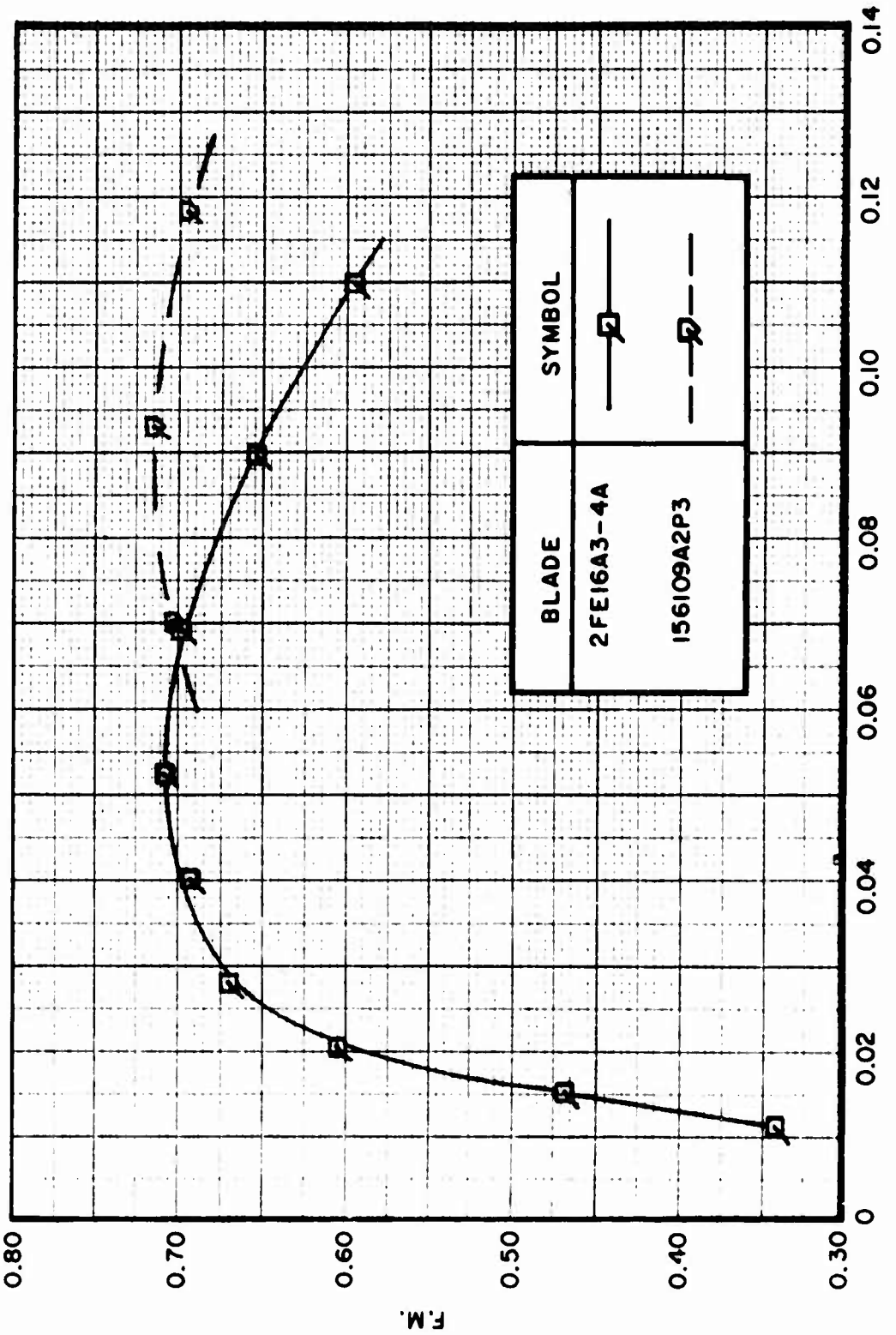

Figure 55. Continued
b. F.M. vs C_P plot

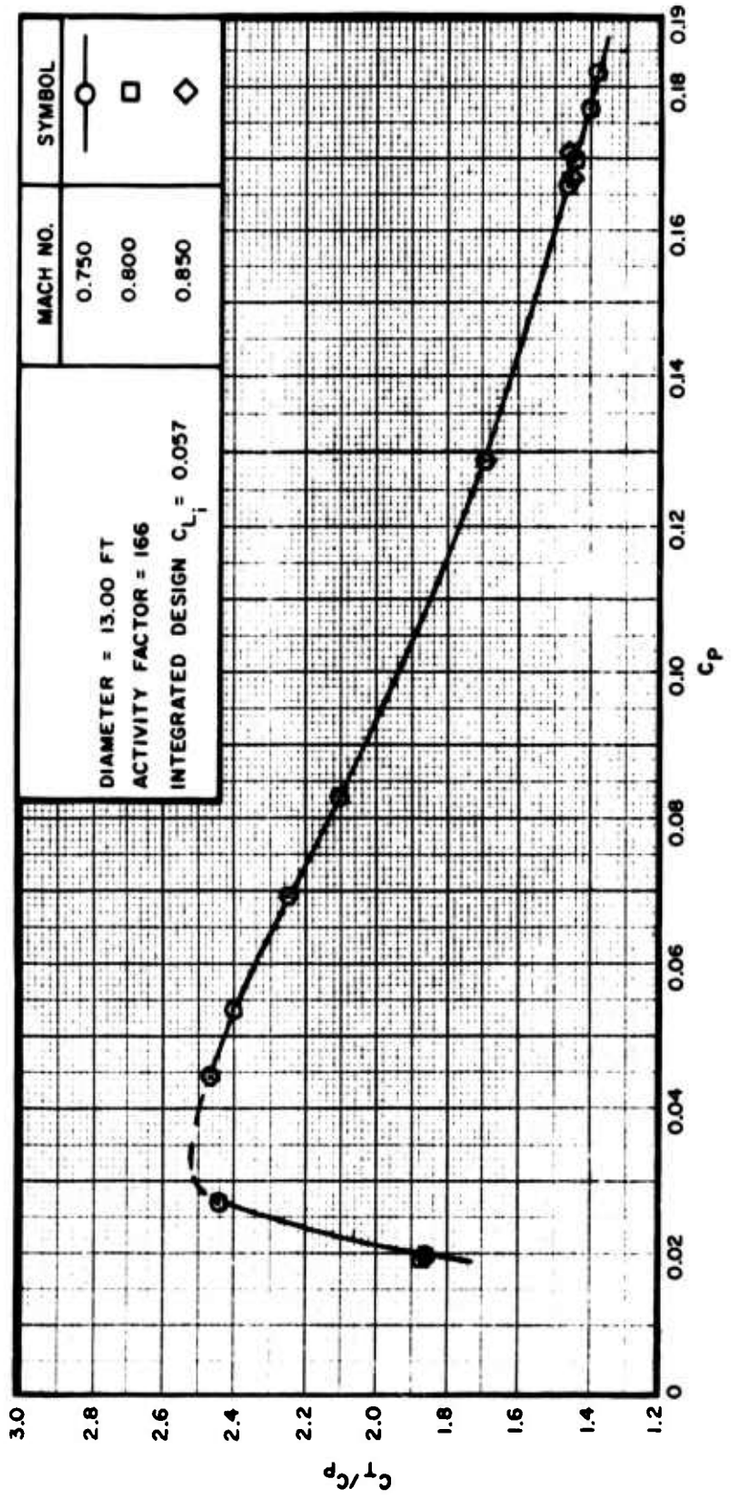

Figure 56. 13166A10P3 (X-19 Aircraft) Performance on Rig No. 1 at Different Tip Mach Numbers

a. C_T/C_P vs C_P plot

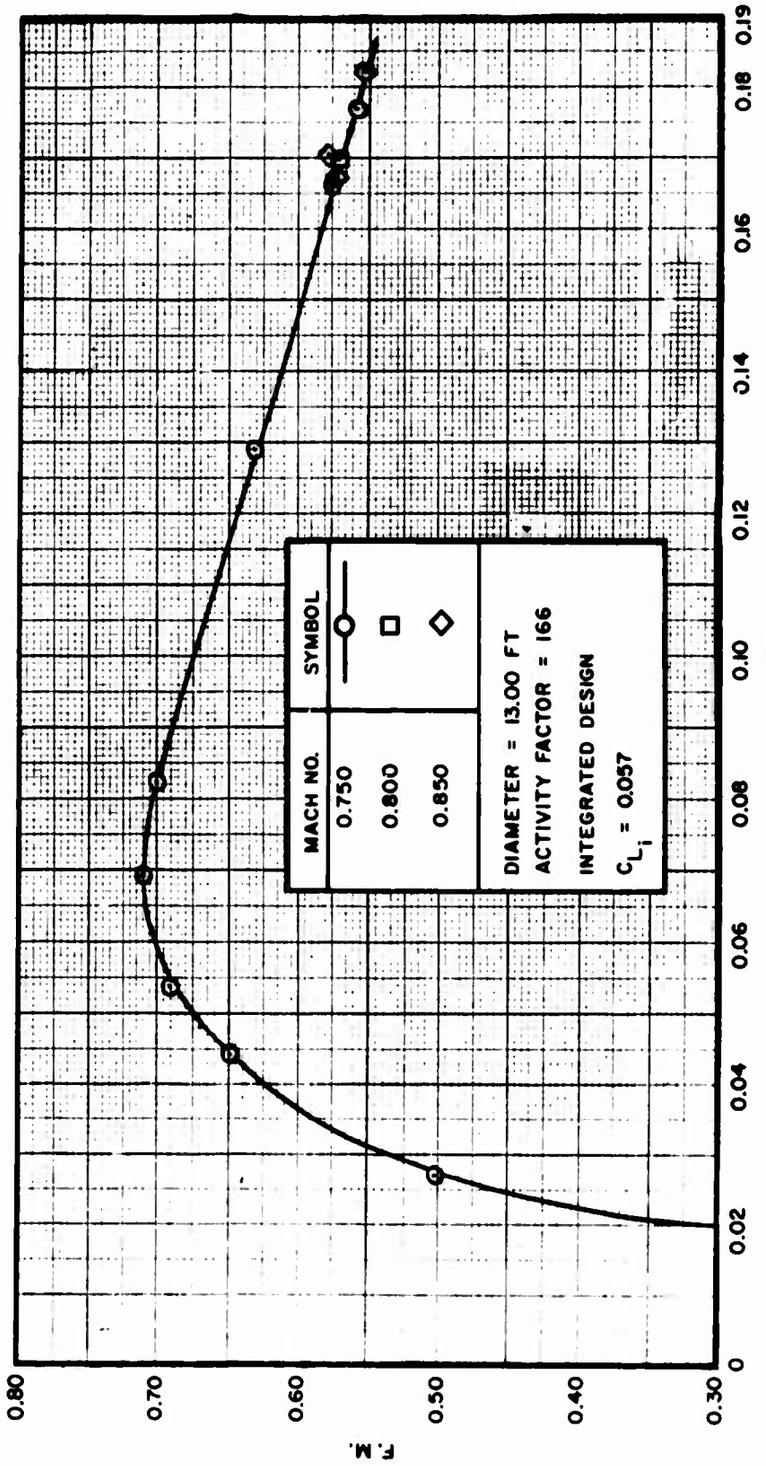

Figure 56. Continued
b. F. M. vs C_p plot

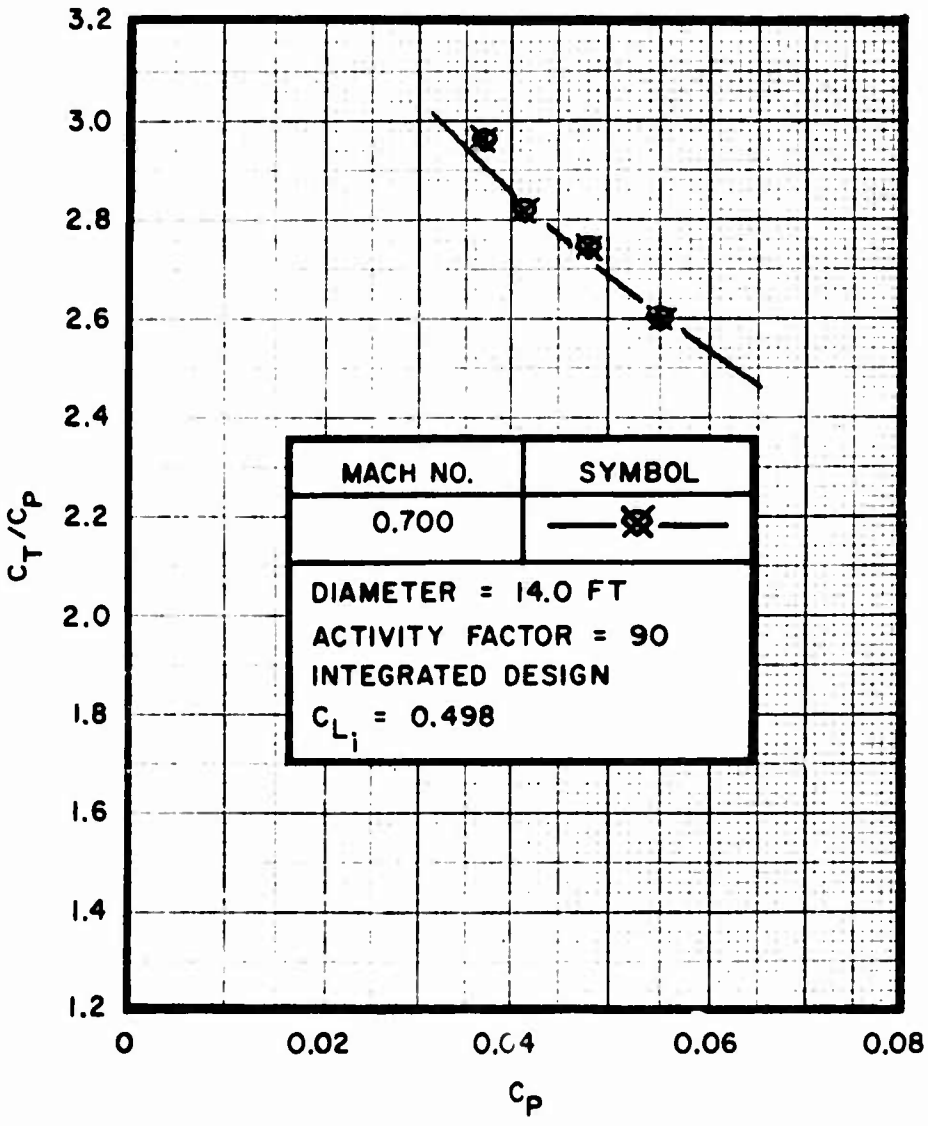

Figure 57. 1490A2P3 (CL-84 Aircraft) Walls Down, Performance on Rig No. 4 at Tip Mach Number = 0.700

a. C_T/C_P vs C_P plot

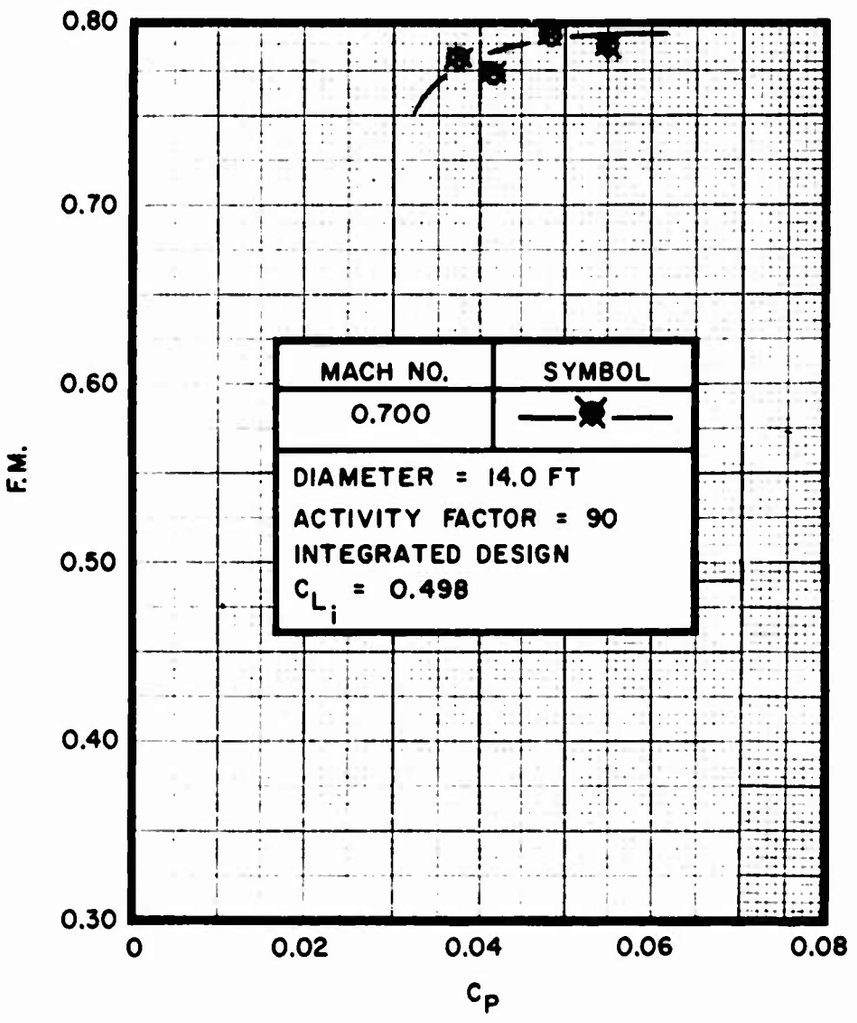

Figure 57. Continued

b. F. M. vs C_P plot

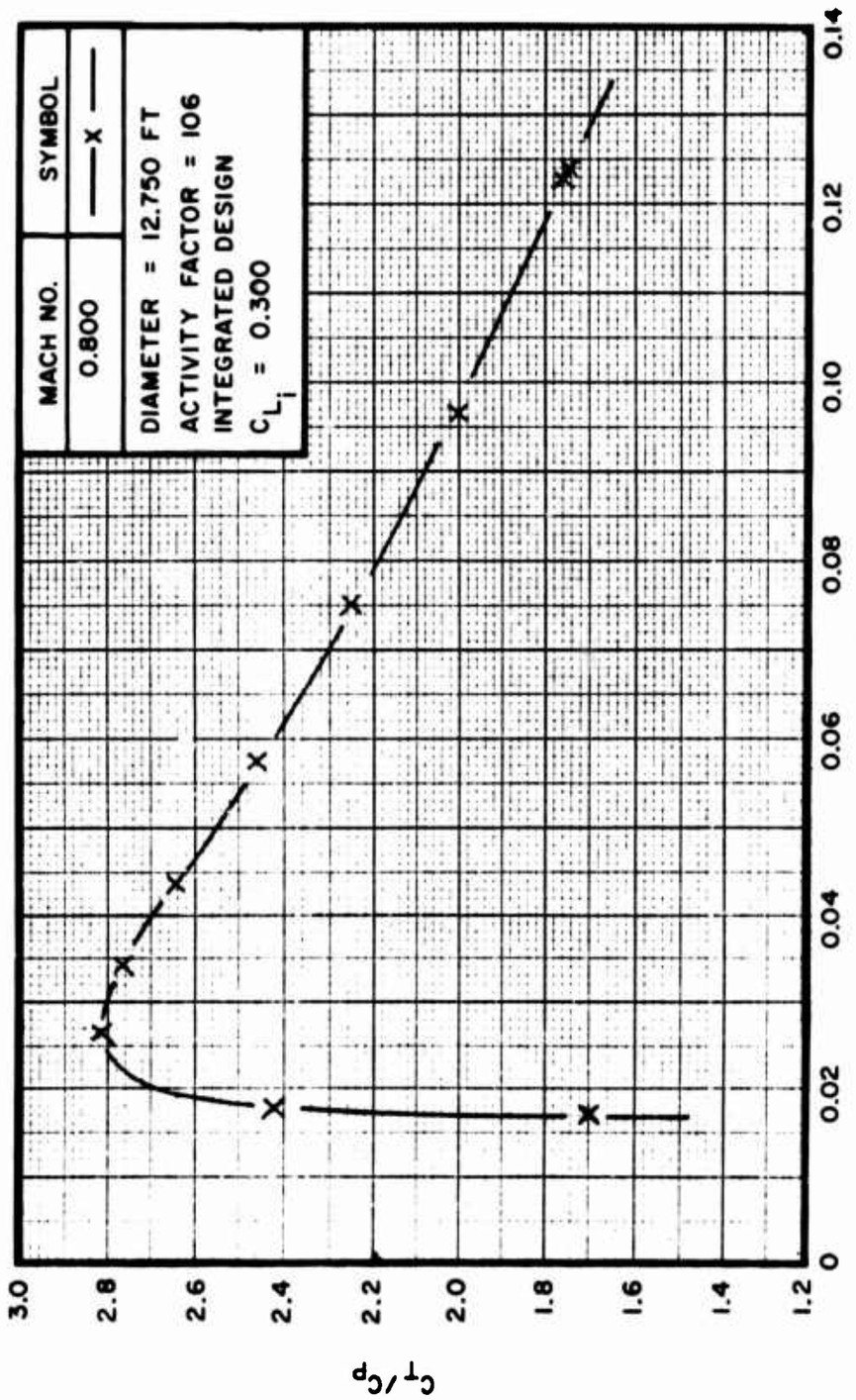

Figure 58. X65SEJDR Performance on Rig No. 1 at Tip Mach Number = 0.800

a. C_T/C_P vs C_P plot

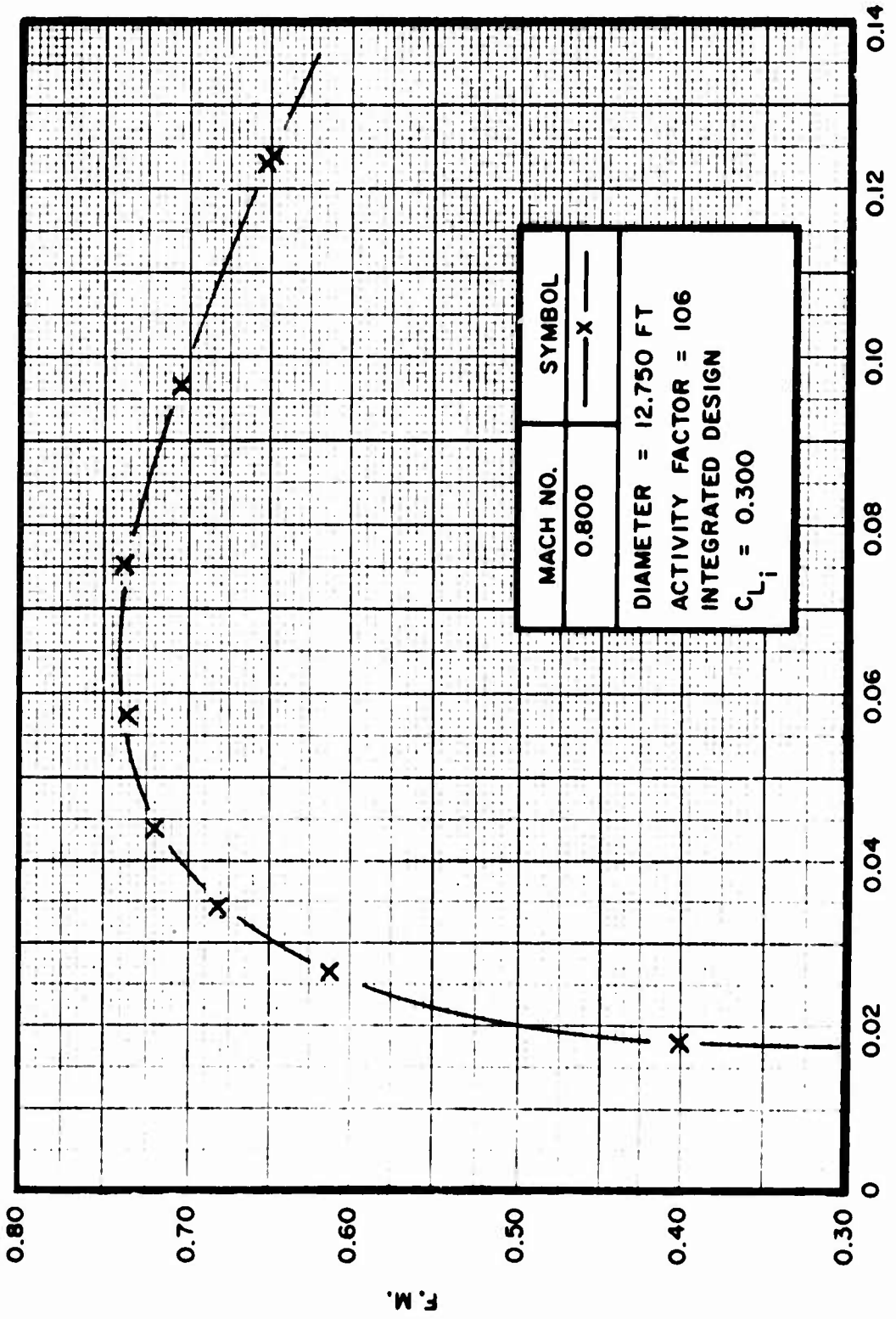

Figure 58. Continued
b. F.M. vs C_P plot

SECTION VI

CONCLUSIONS AND RECOMMENDATIONS

1. CONCLUSIONS

Conclusions reached, based upon the information obtained from these tests are as follows:

a. The original XC-142A propeller (2FE16A3-4A) indicated a static thrust deficiency of approximately 10 percent from the predicted value. (F. M. = 0.64 at C_p = 0.085 and M = 0.90 test conditions).

b. The redesigned XC-142A propeller (2FF16A1-4A) provided a significant increase in static thrust over the original propeller (2FE16A3-4A). Approximately 90 percent of the original thrust deficiency was eliminated. (F. M. = 0.745 at C_p = 0.085 and M = 0.90 test conditions).

c. The "induced inflow velocity" effect due to the proximity of the protective walls surrounding the test rig was dismissed as a contributing factor for the low performance of the original XC-142A propeller (2FE16A3-4A).

d. In general, removing the blade cuff improved propeller performance at power coefficients below approximately 0.09. Above 0.09, either no change was noted or a slight performance reduction was evident.

e. A round tip blade produced more thrust than a square tip blade for any given power coefficient up to approximately 0.08.

f. If identical blades are used, a 4-way propeller produces significantly greater thrust for a given power than a 3-way propeller of the same diameter, within the power range tested. The peak F. M. is shifted to a higher power coefficient because of the greater total activity factor of the 4- way propeller.

g. Increasing blade twist increased F. M. in the power coefficient range of 0.06 to 0.10. One-degree twist resulted in approximately 1/2 point F. M. increase.

h. Increasing blade activity factor shifts the peak F. M. to a higher power coefficient without substantially increasing the peak F. M.

i. The performance of the full scale fiberglass 2FF16A1-4A blades and the solid dural 47 x 91 (0.832-scale 2FF16A1-4A) blades did not correlate on a coefficient basis.

It should be emphasized that the value of this report cannot be defined in terms of the above conclusions. These conclusions were drawn from a narrow study sharply limited by available time and directed toward a particular goal. The real importance of this report is that it contains a vast amount of test data involving the interrelationships of many propeller design parameters from which the researchers should be able to derive many significant aspects of propeller static thrust related specifically to V/STOL aircraft applications. Data of this type and magnitude were not available prior to the test program described herein.

2. RECOMMENDATIONS

a. It is recommended that an extensive static performance test program be conducted to further study the parameters discussed in this report. Particular emphasis should be placed upon

(1) The effects of radial twist distribution on performance

(2) The effects of radial camber distribution on performance

(3) The significance of total blade twist on F.M.

(4) Expanding the range of activity factor, integrated lift coefficient and power coefficient.

b. It is further recommended that an analytical propeller static performance prediction program be initiated. The resulting prediction theories should then be compared with the empirical test results to determine the accuracy of the prediction methods.

c. A test facility should be constructed that can accurately test the static performance of large-diameter propellers. Electric Whirl Rig No. 4 could be modified and optimized for this purpose. Specific improvements might consist of at least the following:

(1) Fair in the flat face of the test rig and the extension shaft to improve the air flow in this region thus reducing the blockage effect.

(2) Install automatic data recording equipment to simultaneously record at least rpm, horsepower, thrust, and test chamber atmospheric temperature and pressure

(3) Provide a direct link from the automatic data recording equipment to the digital computer facility, thus providing timely data reduction on a 24-hour basis.

APPENDIX I

BLADE CHARACTERISTIC SHEETS

LIST OF BLADE CHARACTERISTIC SHEETS

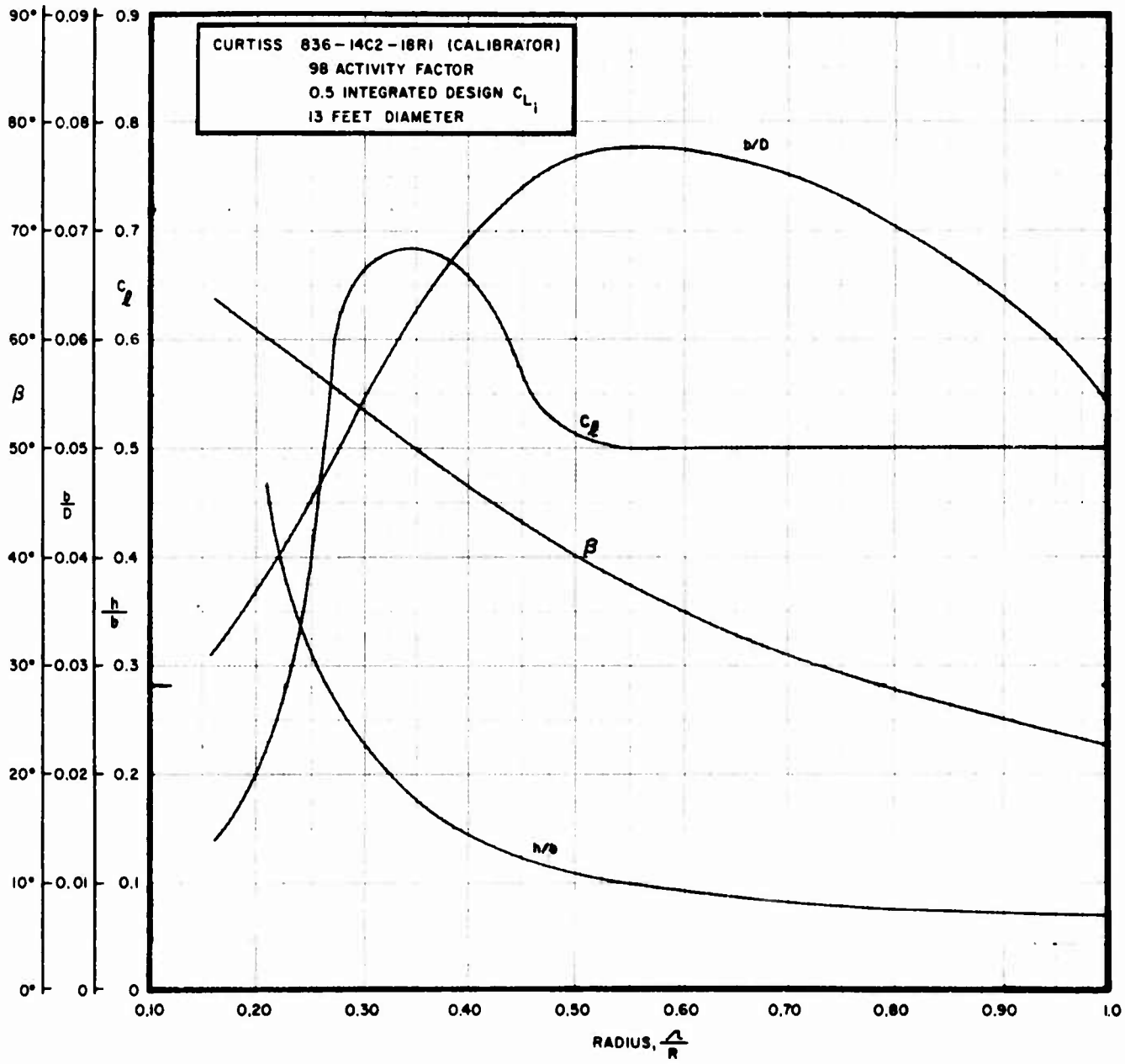

Blade Characteristic Sheet No. 1

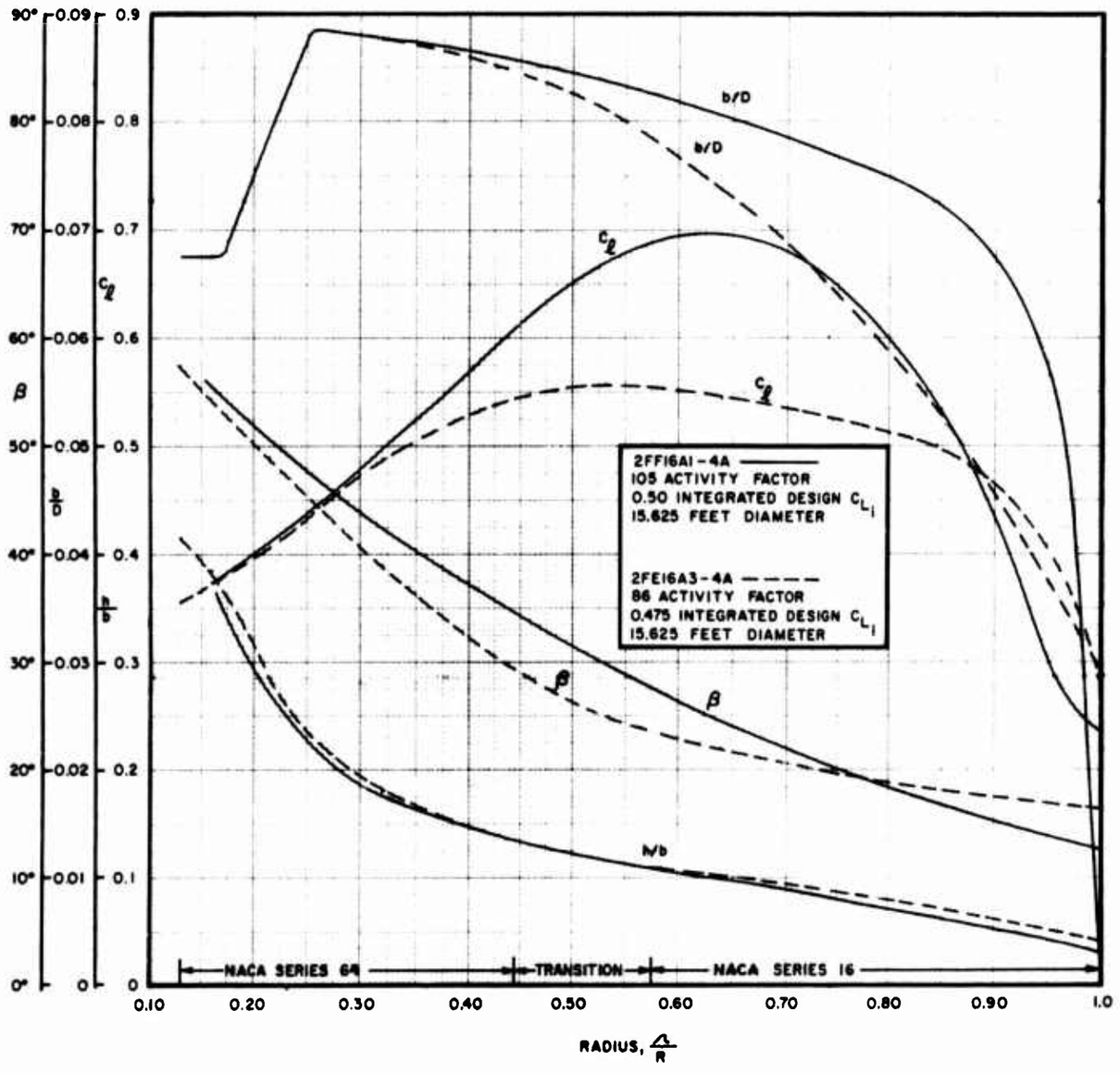

Blade Characteristic Sheet No. 2

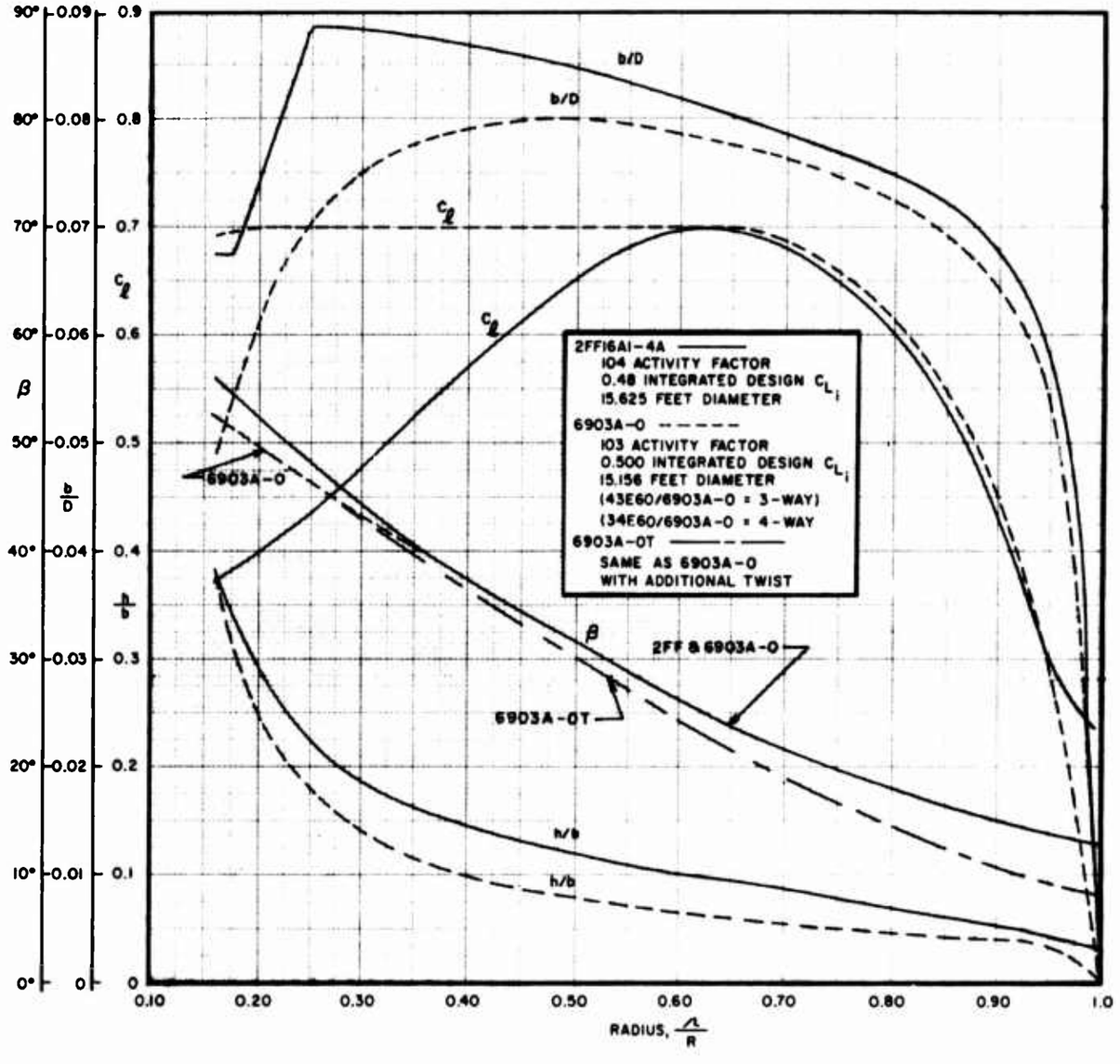

Blade Characteristic Sheet No. 3

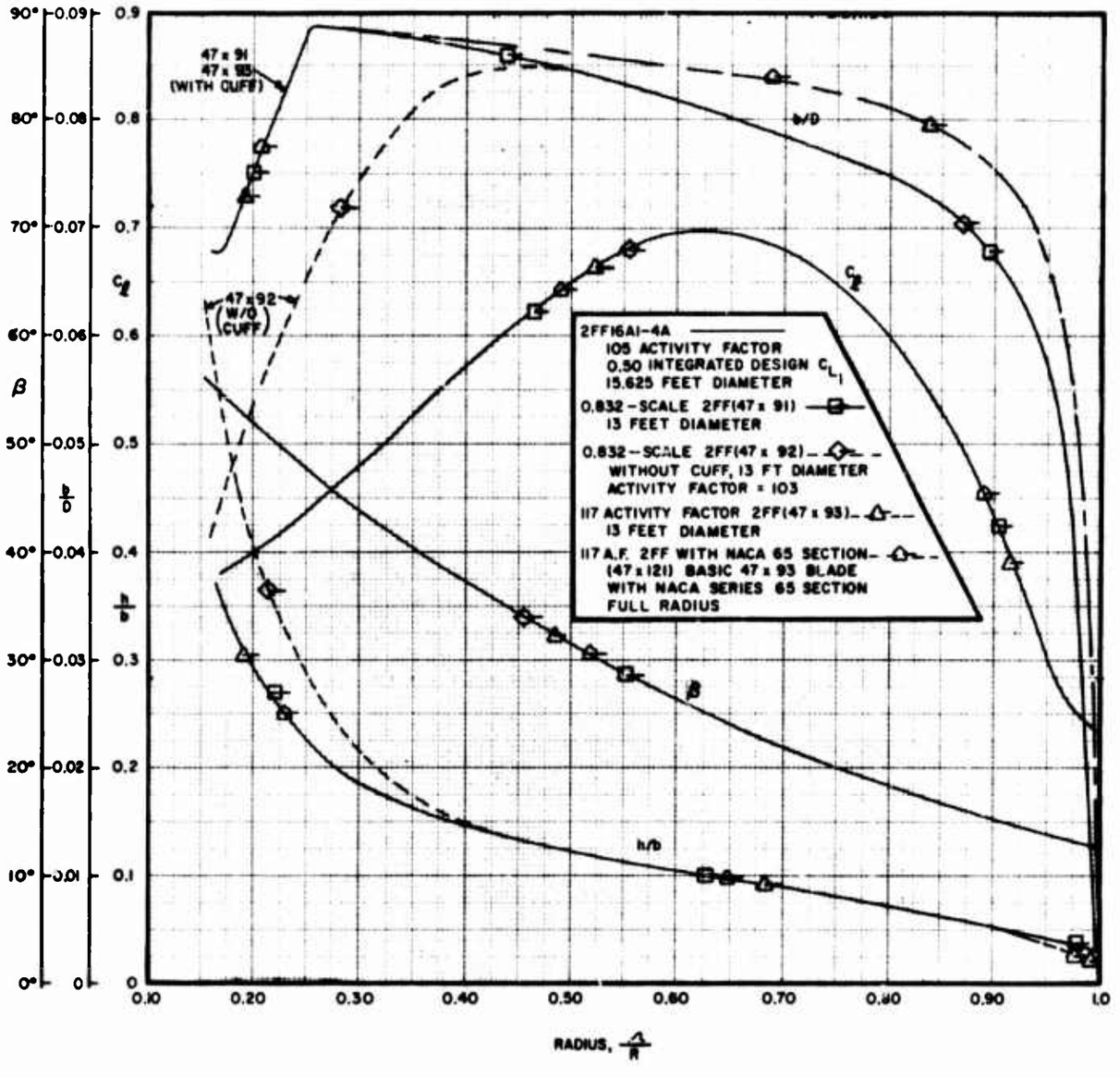

Blade Characteristic Sheet No. 4

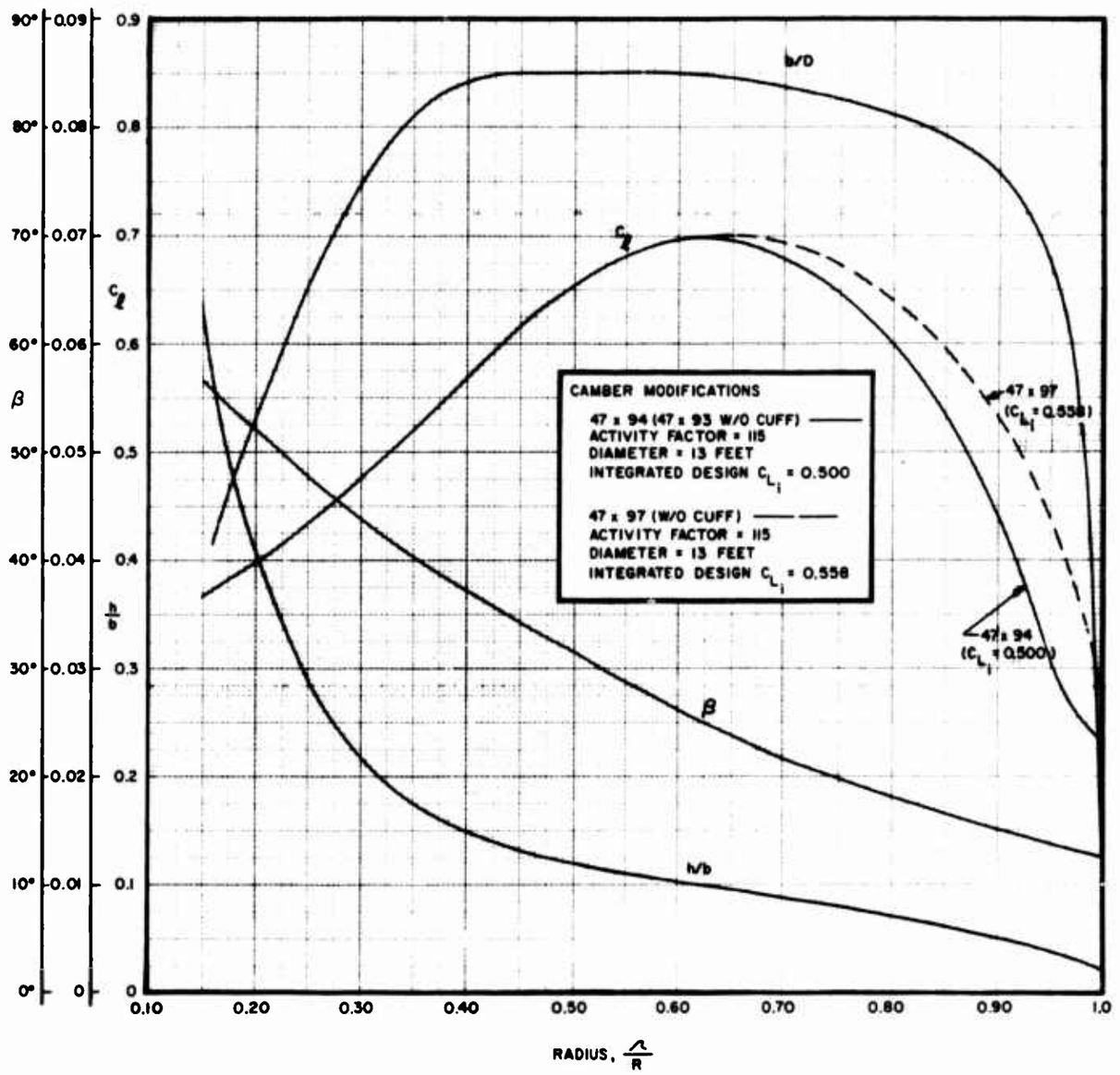

Blade Characteristic Sheet No. 5

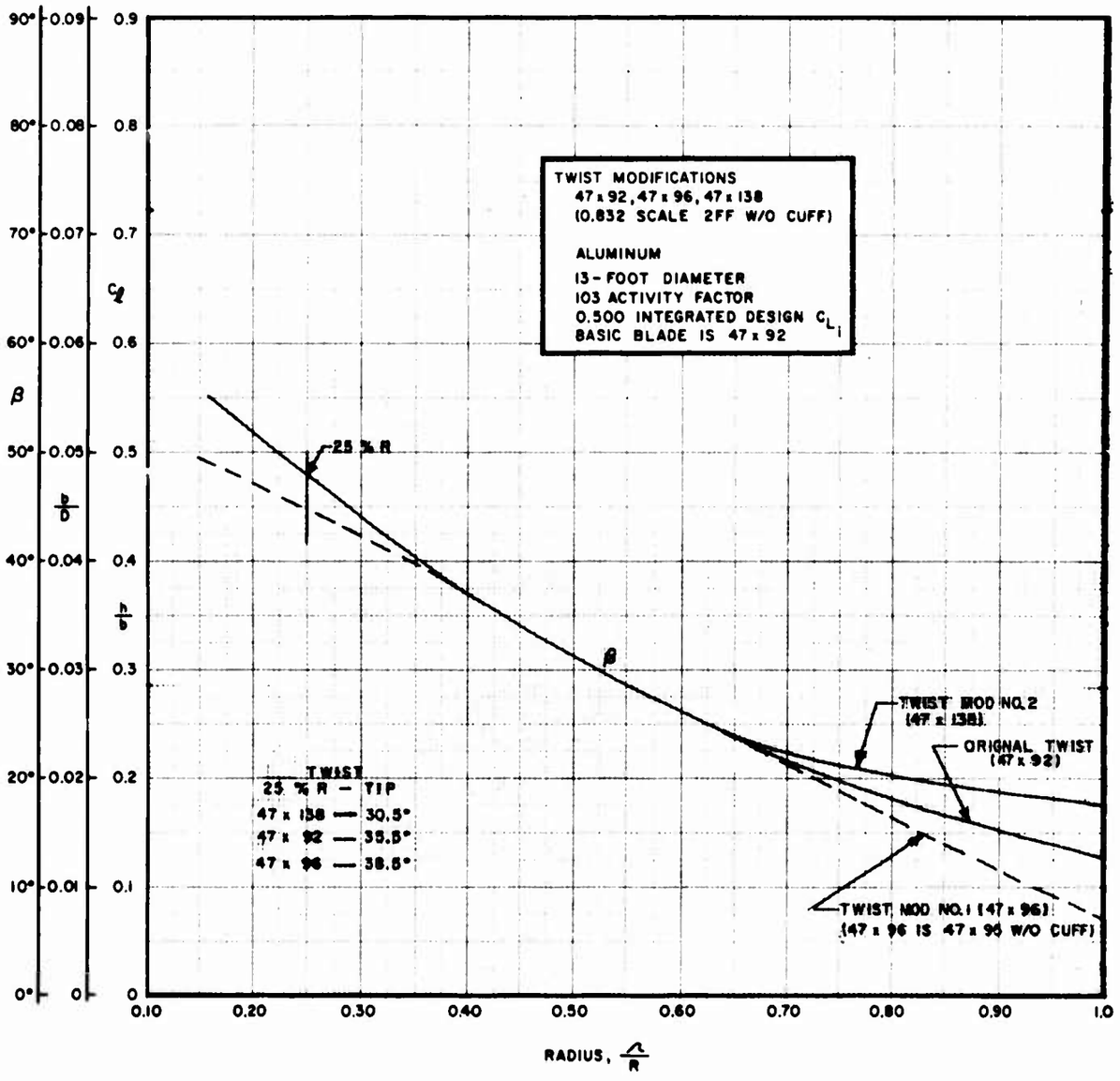

Blade Characteristic Sheet No. 6

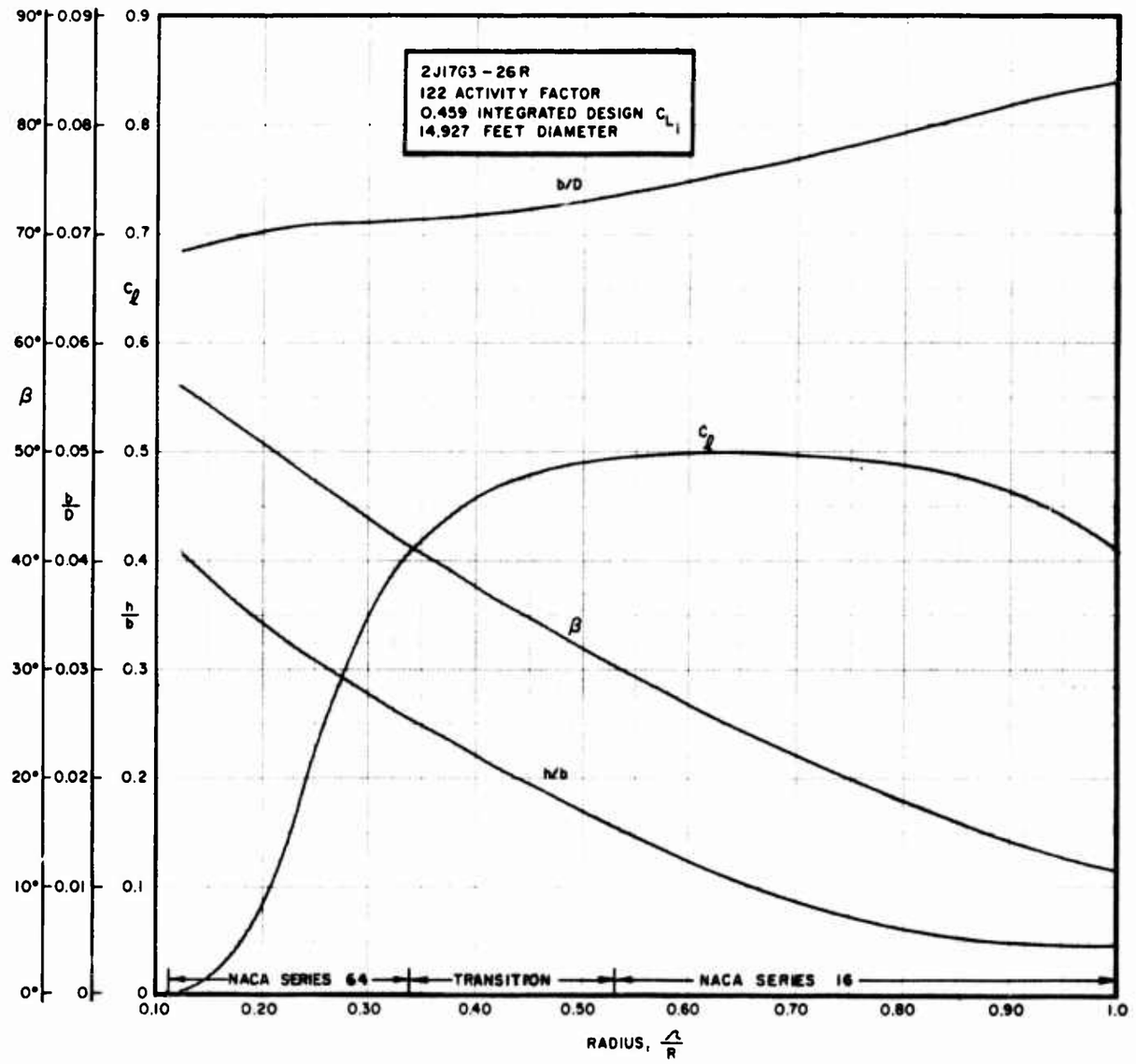

Blade Characteristic Sheet No. 7

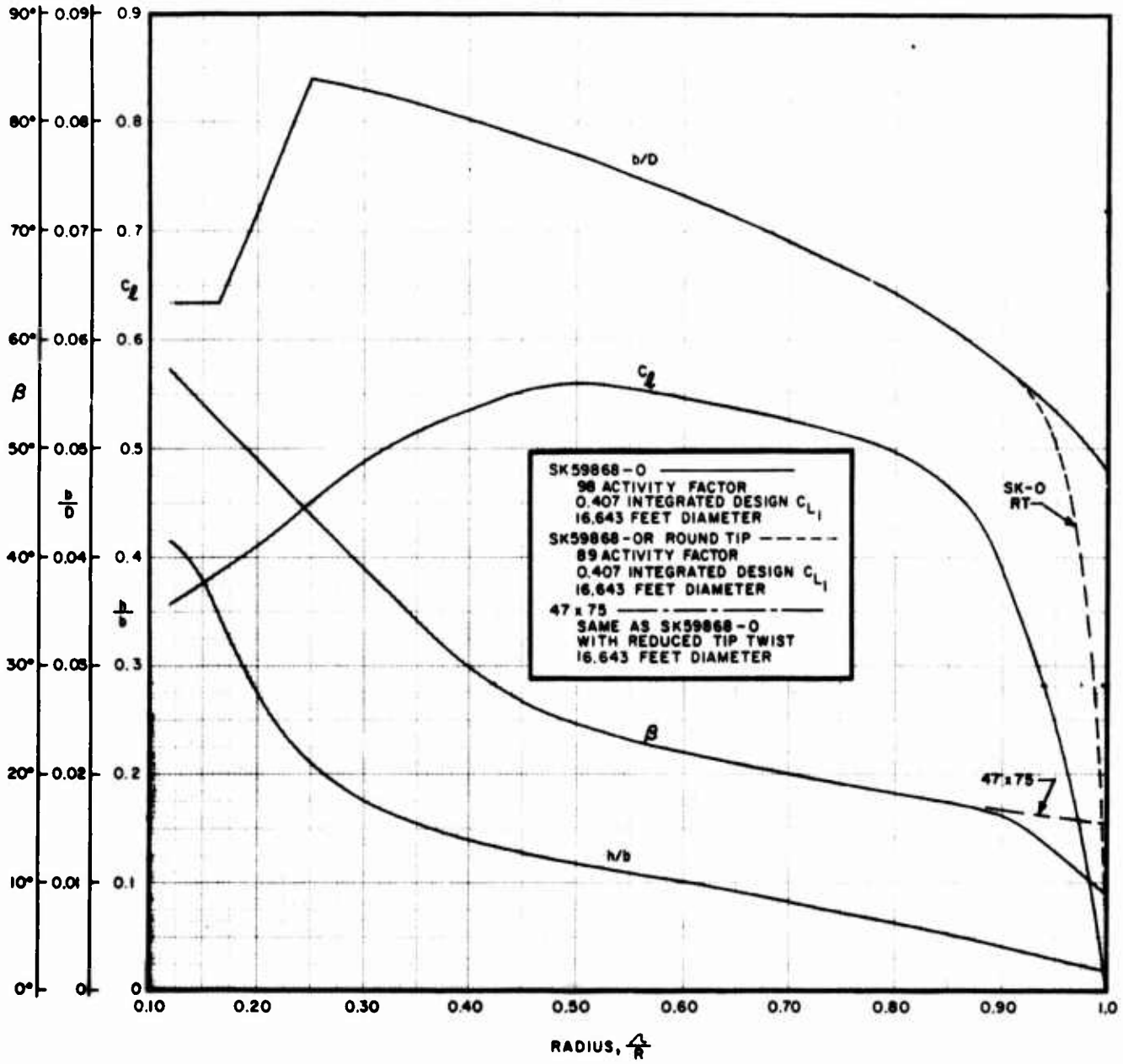

Blade Characteristic Sheet No. 8

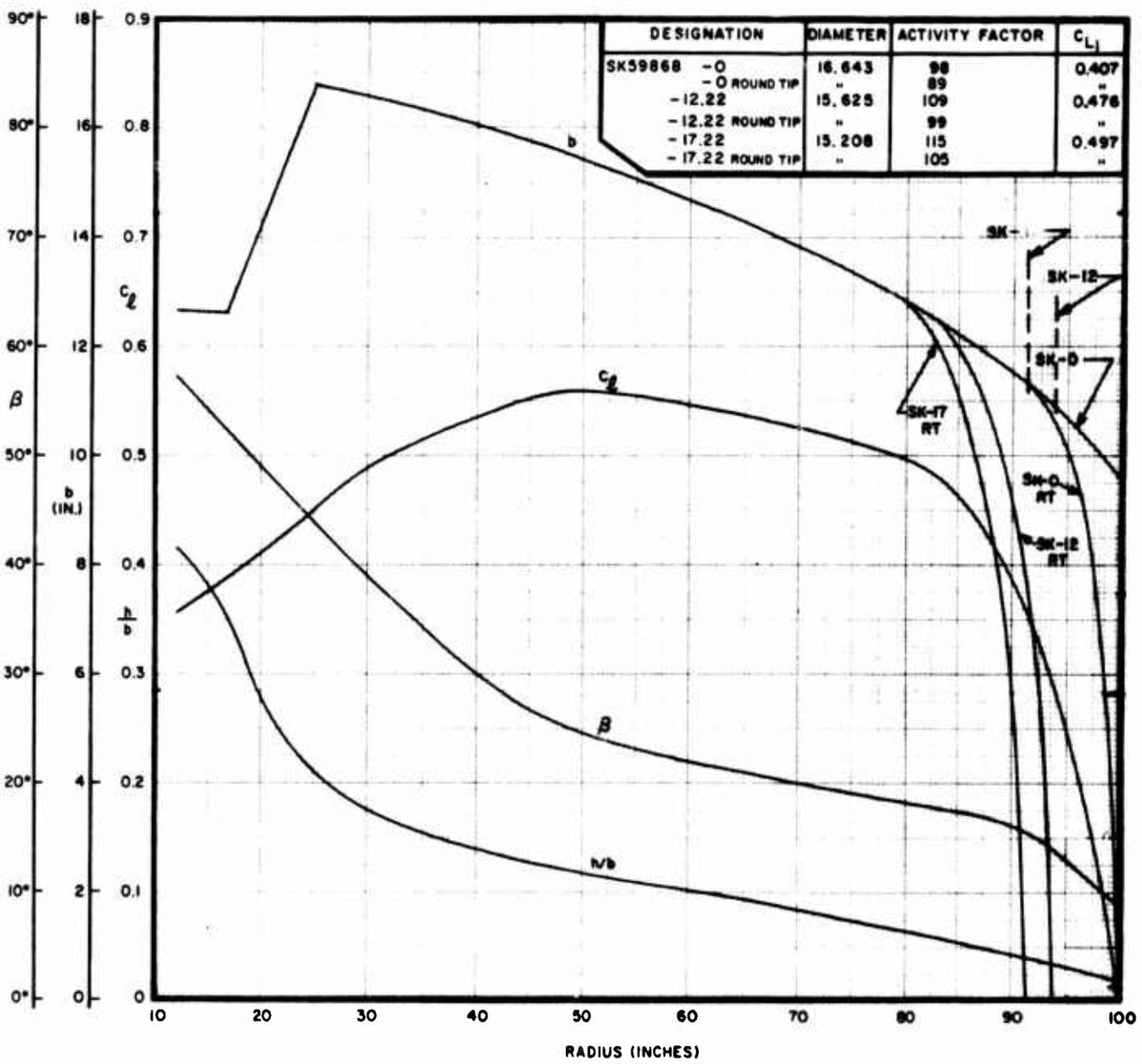

Blade Characteristic Sheet No. 9

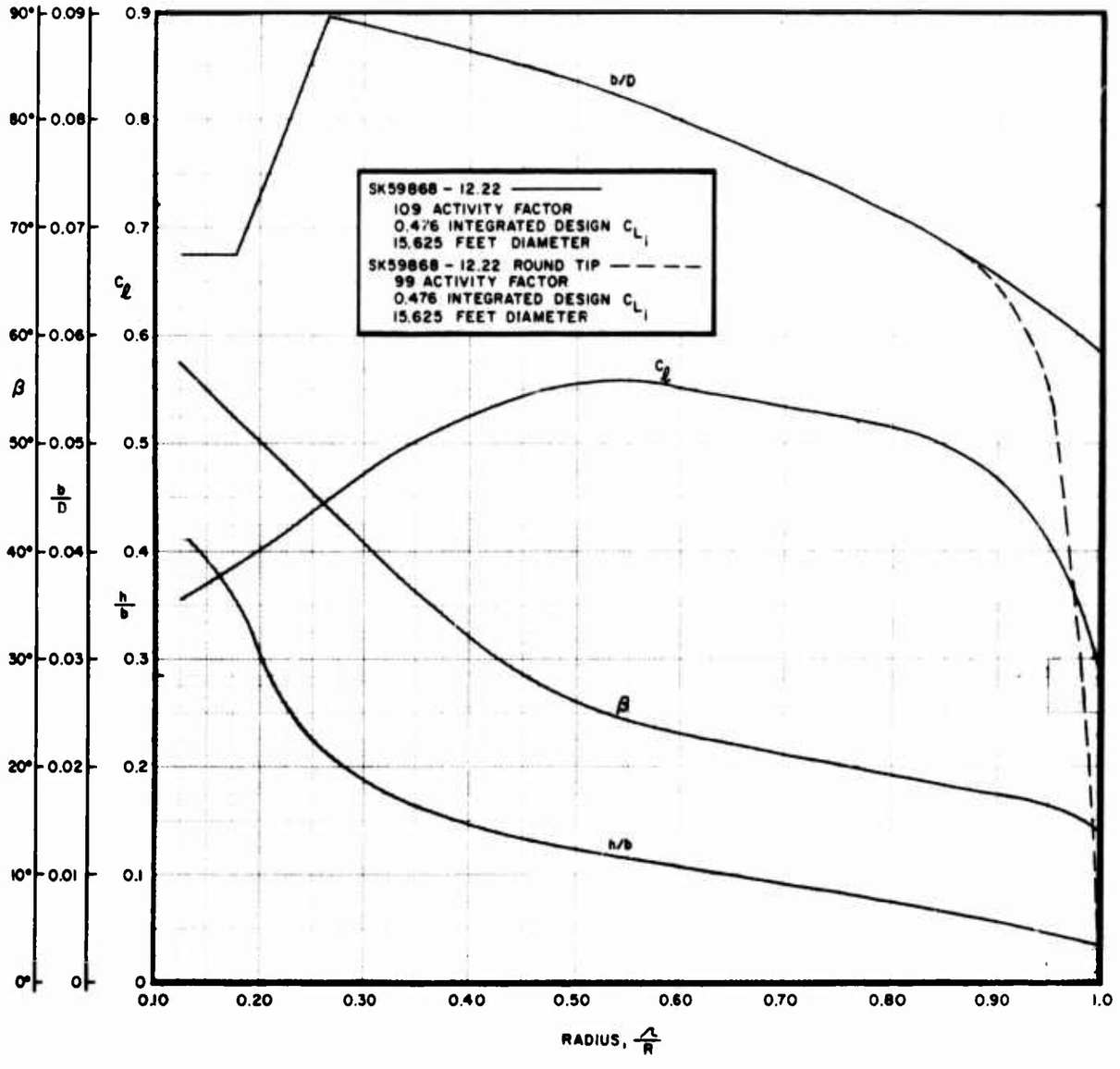

Blade Characteristic Sheet No. 10

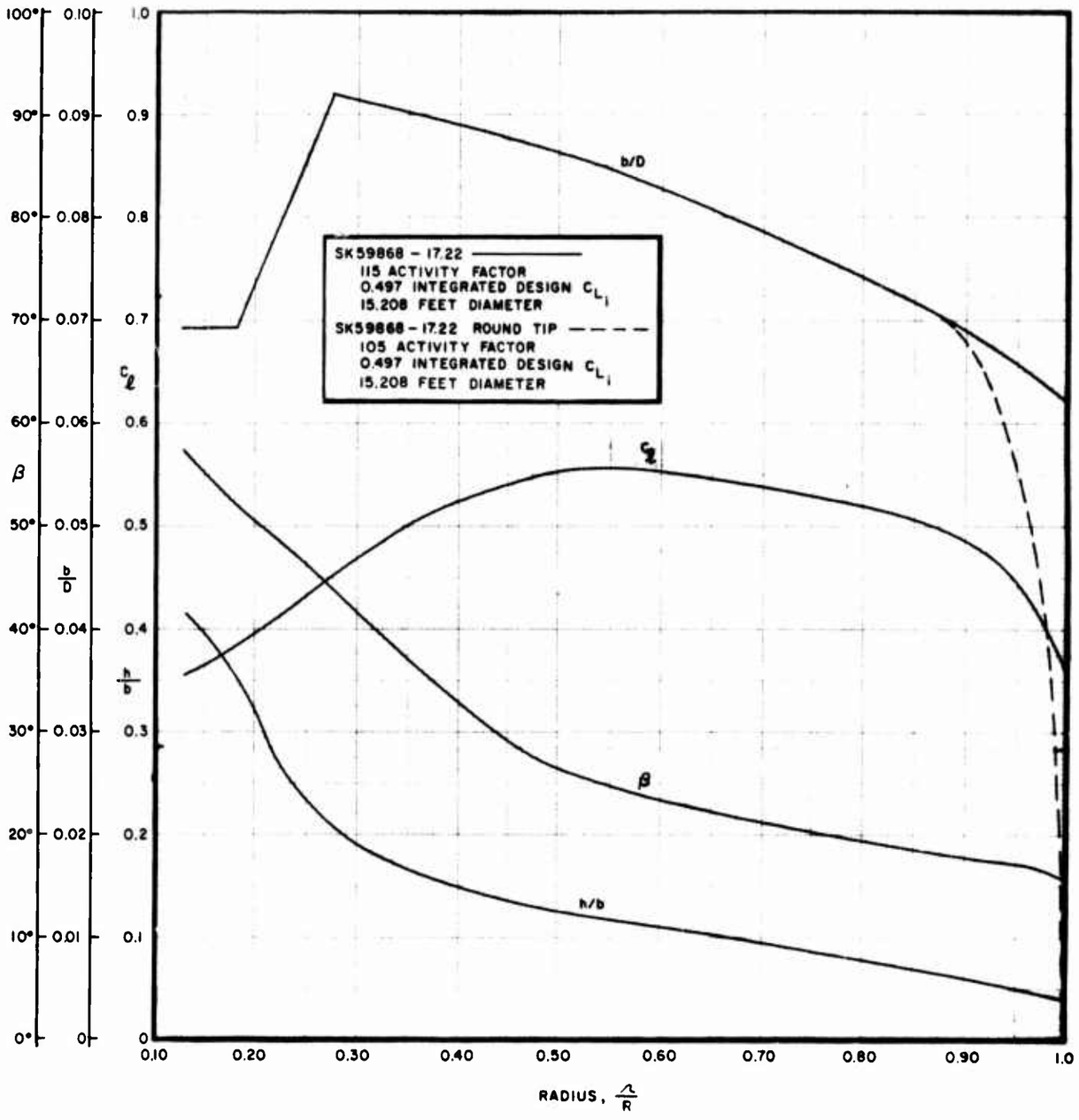

Blade Characteristic Sheet No. 11

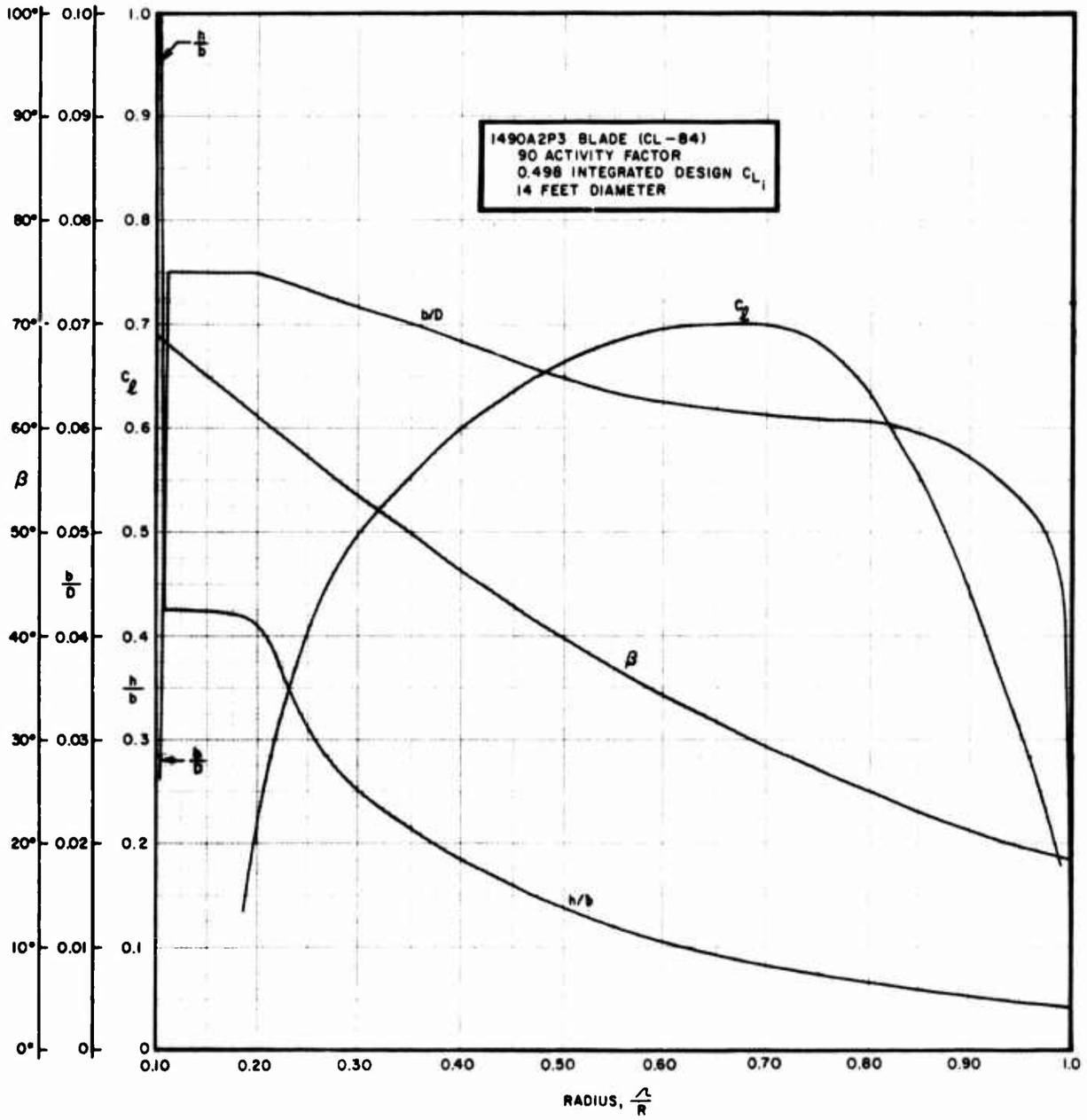

Blade Characteristic Sheet No. 12

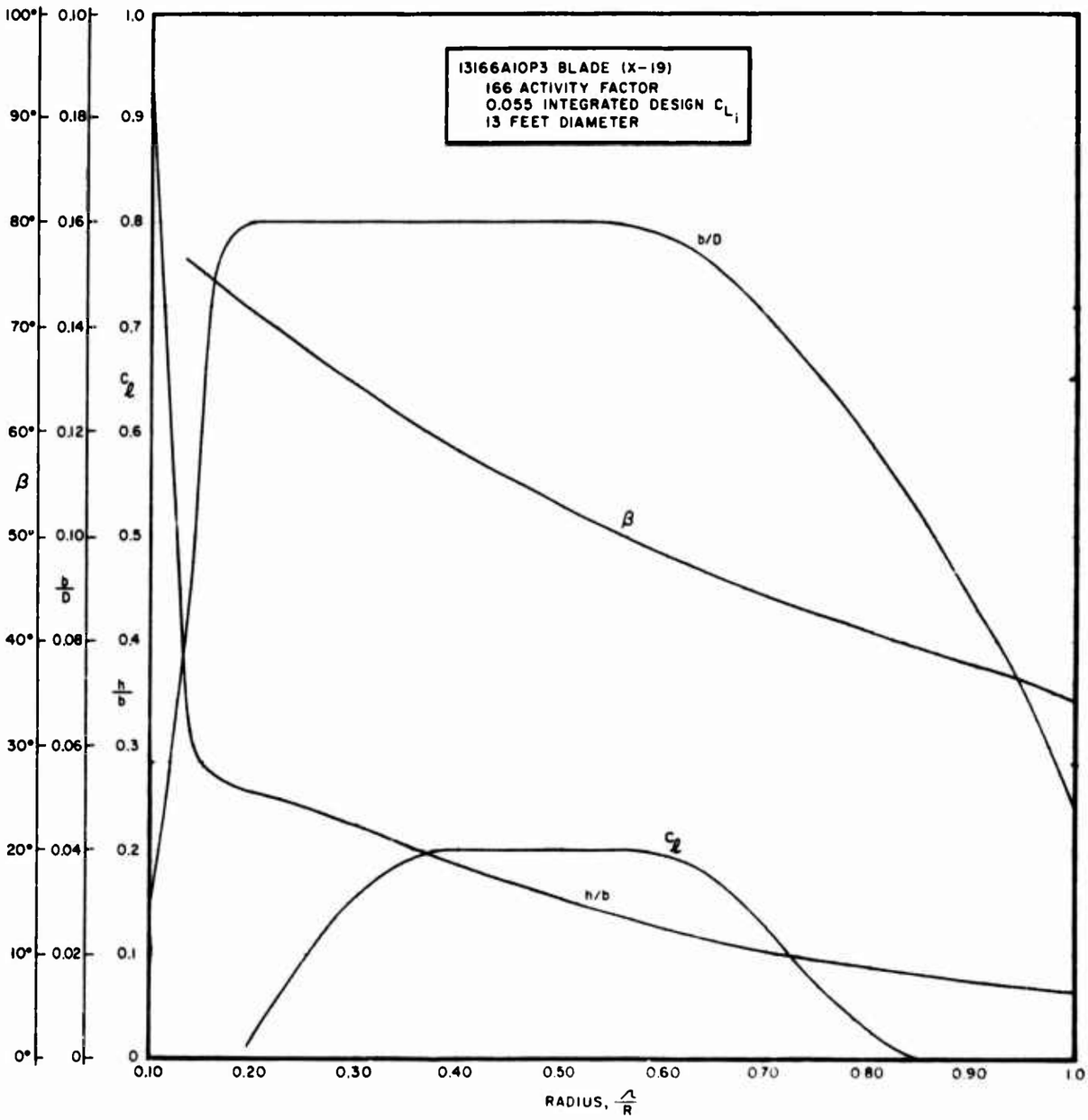

Blade Characteristic Sheet No. 13

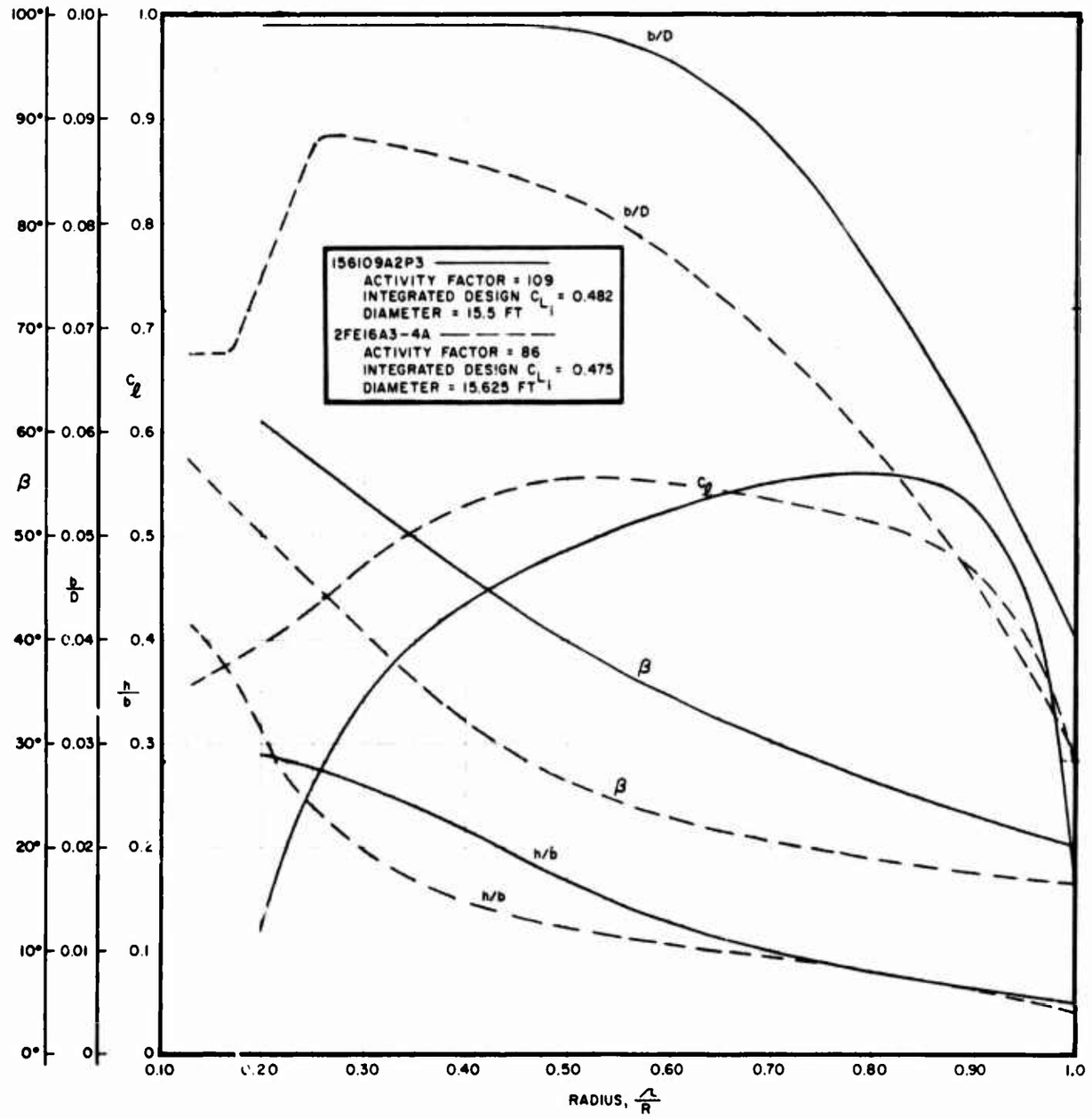

Blade Characteristic Sheet No. 14

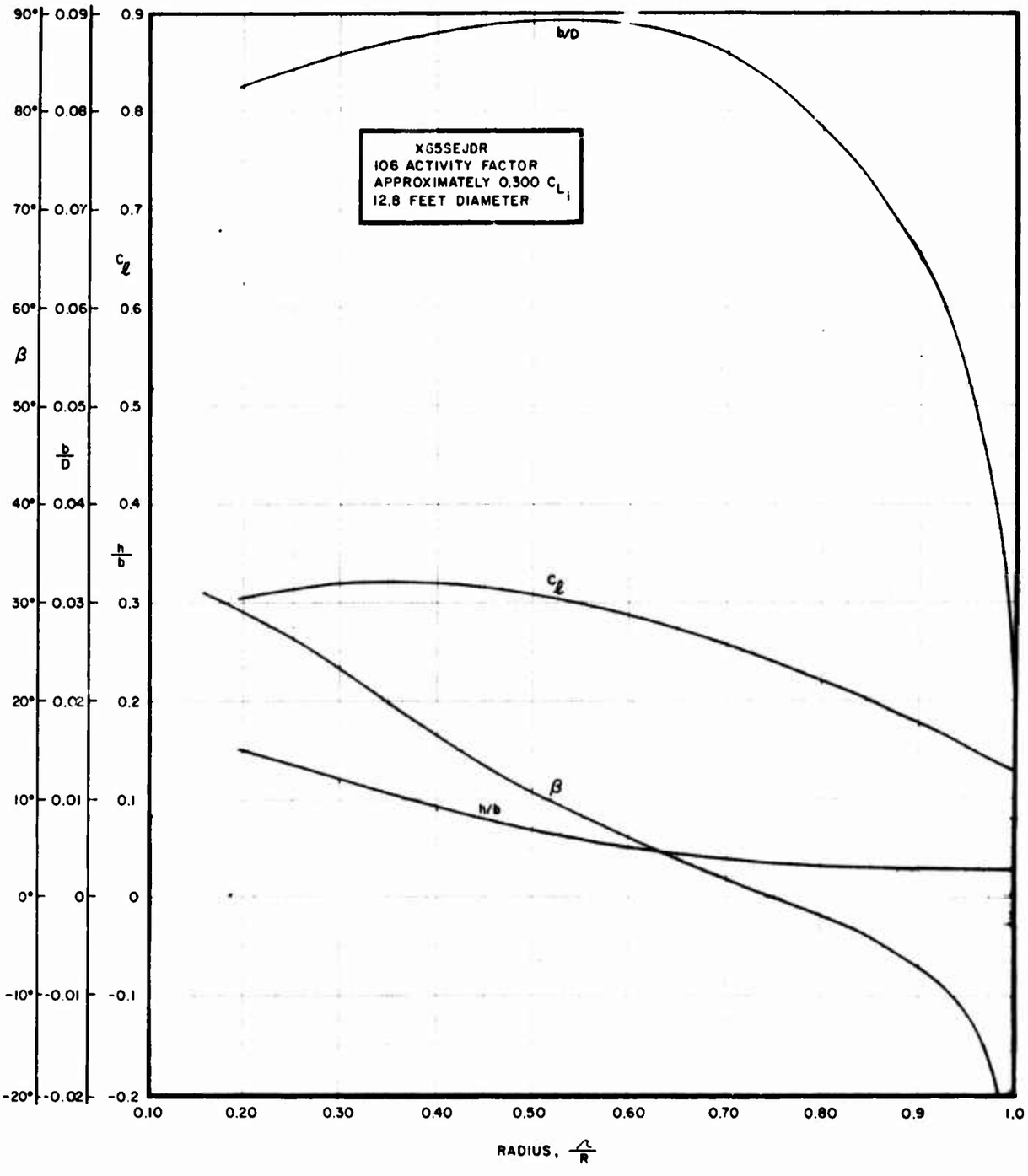

Blade Characteristic Sheet No. 15

APPENDIX II

ELECTRIC WHIRL RIG NO. 4

AND CALIBRATION DATA

FIGURES 59 THROUGH 64

Figure 59. Front View of Calibration Propeller on Whirl Rig No. 4, Showing Air Flow Rake Behind Propeller

RIG NO. 1 SHAFTS (12-B.C.)		
SHAFT SIZE	L_1	PART NO.
NO. 50	18⅛	E2317PL
NO. 60	18⅞	D1184PL
NO. 70	18⅞	D2508PL
NO. 80	18⅛	D2509PL
NO. 90	16⅛	H1433PL
NO. 100	15⅞	H1437PL

RIG NO. 2 SHAFTS (10-B.C.)		
SHAFT SIZE	L_1	PART NO.
NO. 40	18½	B2534PL
NO. 50	18⅛	F2518PL
NO. 60	17⅞	D1183PL
NO. 70	15⅞	H1433PL
NO. 80	13⅛	H1434PL

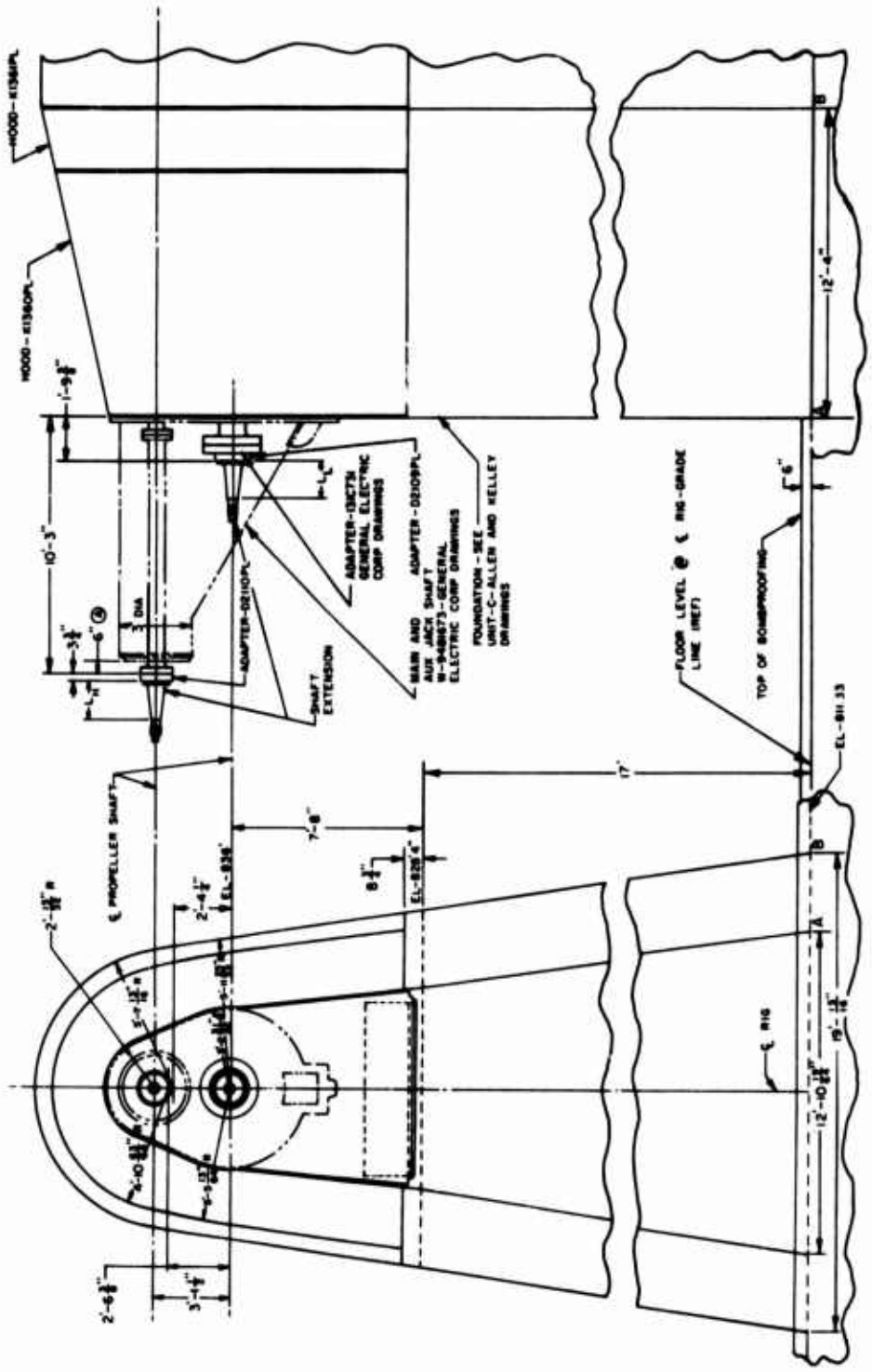

Figure 60. Propeller Mount, Configuration Rig No. 4 (Layout Drawing of Whirl Stand Providing Basic Dimensions)

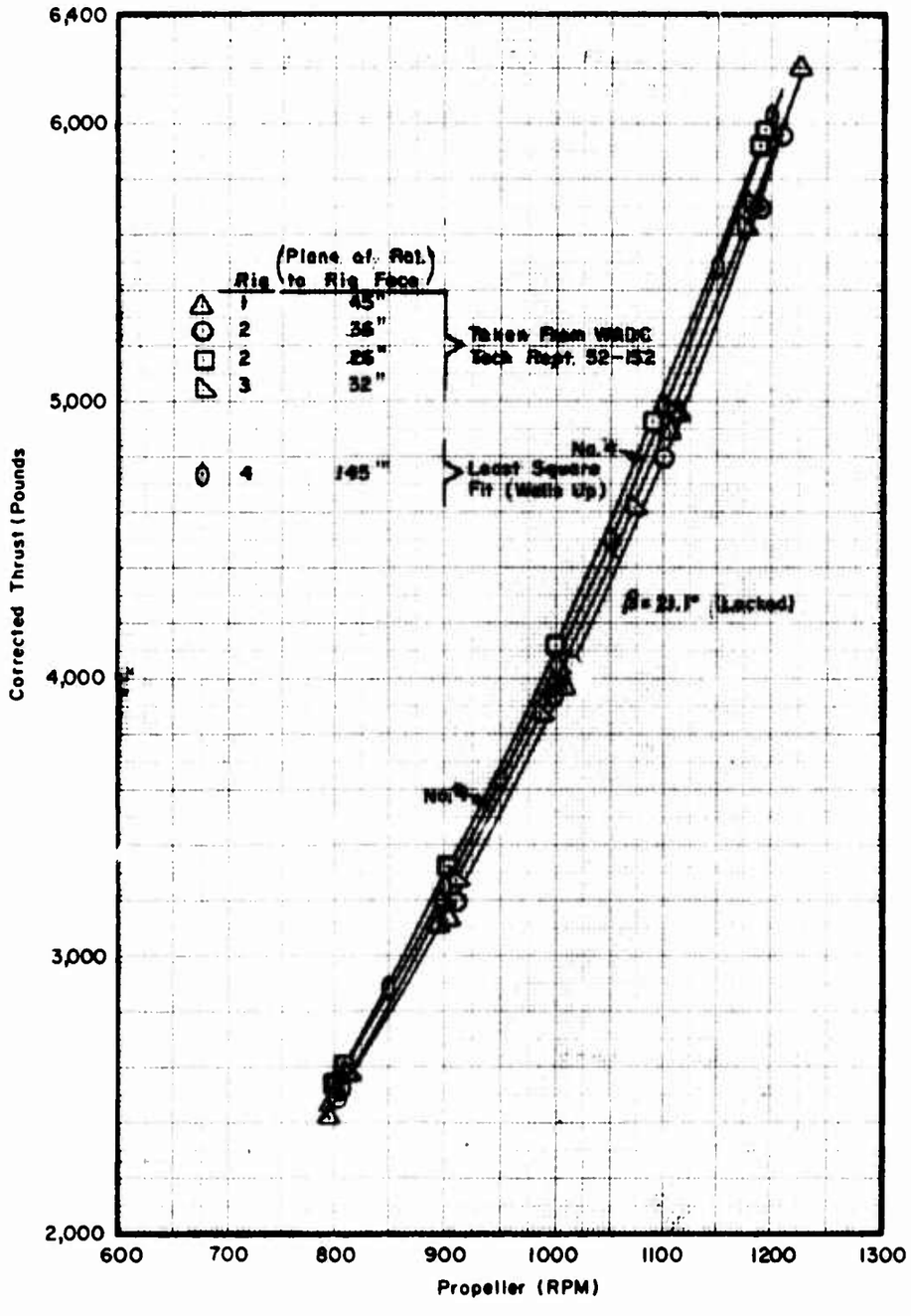

Figure 61. Effect of Distance from Plane of Rotation to Rig Faces on Calibrator Propeller; Thrust vs RPM

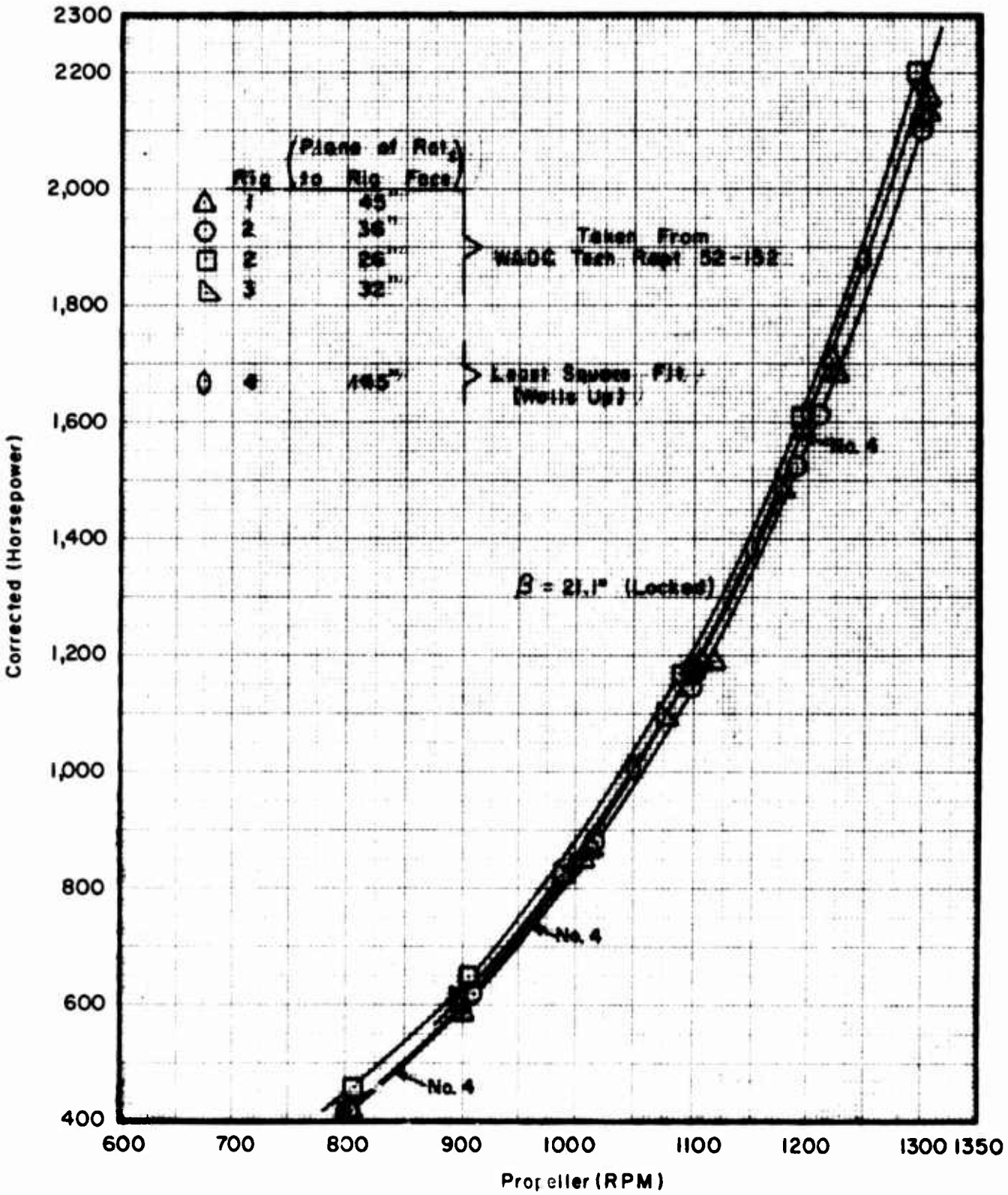

Figure 62. Effect of Distance from Plane of Rotation to Rig Faces on Calibrator Propeller; Horsepower vs RPM

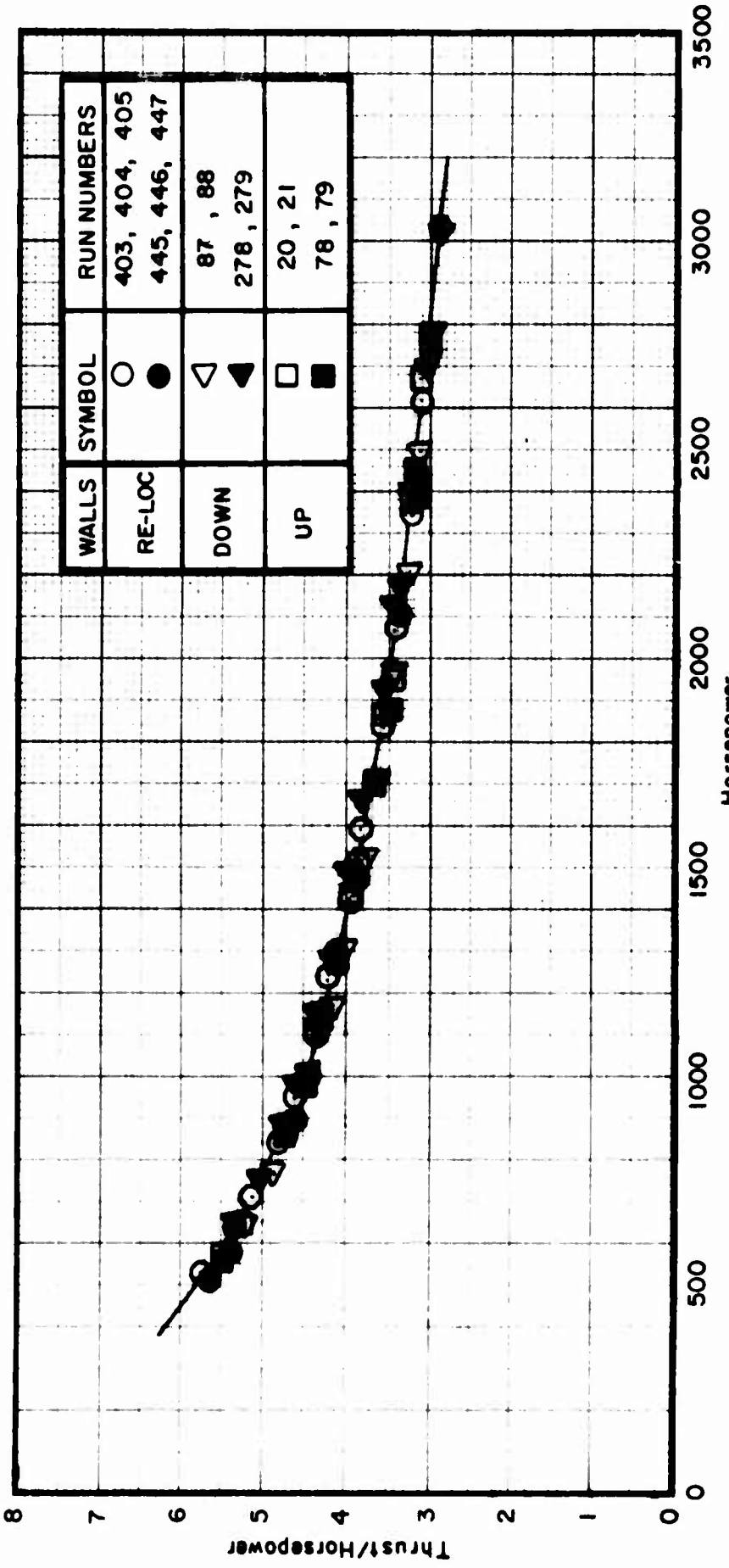

Figure 63. Calibrator Propeller, Rig No. 4, Typical Calibration Data; Thrust/Horsepower vs Horsepower

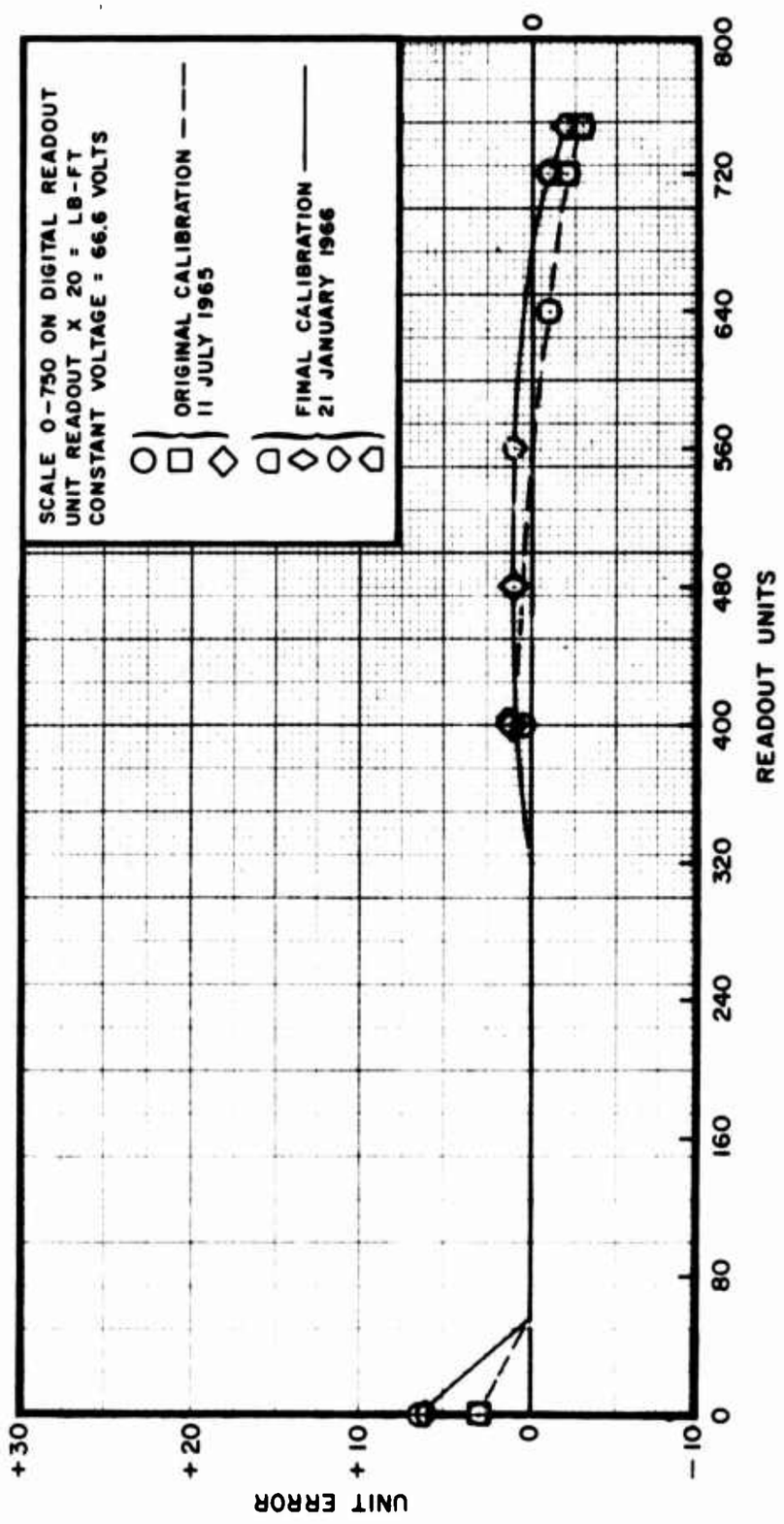

Figure 64. 15,000 Lb-Ft Torque Shaft Calibration Curves, Rig No. 4, Unit Error vs Readout Units

REFERENCES

1. Aircraft Propeller Handbook ANC-9 Bulletin, Issued Jointly by the Department of the Air Force, Navy, and Commerce, September 1956

2. Leland B. Salters, Jr. and Harry T. Norton, Jr. An Investigation of the Effect of The WADC 30,000 – Horsepower Whirl Rig Upon the Static Characteristics of a Propeller. NACA Research Memorandum RM SL52F20. July 1952.

3. Dana A. Webb and Jack E. Willer. Propeller Performance at Zero Forward Speed. WADC Technical Report 52-152. July 1952.

4. H. V. Borst, and R. M. Ladden. "Propeller Testing at Zero Velocity." CAL/USAALABS Symposium Proceedings, Vol I, Propeller and Rotor Aerodynamics. Buffalo, New York. 22-24 July 1966.

5. Gerald T. Cafarelli and Matthew H. Chopin. Computer Program for Reducing Static Propeller Test Data. ASD Technical Report 68-19. Aeronautical Systems Division, Wright-Patterson Air Force Base, Ohio.

6. Robin Ransone. XC-142A Category II Interim Letter Report; (AFFTC Report, Operational Suitability and V/STOL Performance, Stability and Control). October 1966.

7. LTV Preliminary XC-142A Flight Test Data, Flights Numbers 6 Through 29 on Aircraft Numbers 1, 2, and 3.

8. XC-142A, A Joint Static Thrust Investigation Program by LTV Corp., Hiller Co., and Ryan Co. Page 8.

UNCLASSIFIED

Security Classification

DOCUMENT CONTROL DATA - R & D

(Security classification of title, body of abstract and indexing annotation must be entered when the overall report is classified)

1. ORIGINATING ACTIVITY (Corporate author)	2a. REPORT SECURITY CLASSIFICATION
Deputy for Engineering Aeronautical Systems Division Wright-Patterson Air Force Base, Ohio	UNCLASSIFIED
	2b. GROUP

3. REPORT TITLE

PROPELLER STATIC PERFORMANCE TESTS FOR V/STOL AIRCRAFT: PART I SUMMARY

4. DESCRIPTIVE NOTES (Type of report and inclusive dates)

Work period from July 1965 to November 1967

5. AUTHOR(S) (First name, middle initial, last name)

Matthew H. Chopin

6. REPORT DATE	7a. TOTAL NO. OF PAGES	7b. NO. OF REFS
January 1969	178	8

8a. CONTRACT OR GRANT NO.	9a. ORIGINATOR'S REPORT NUMBER(S)
b. PROJECT NO.	ASD-TR-69-15, Part I
c. System 478A	9b. OTHER REPORT NO(S) (Any other numbers that may be assigned this report)
d.	

10. DISTRIBUTION STATEMENT

This document has been approved for public release and sale; its distribution is unlimited.

11. SUPPLEMENTARY NOTES	12. SPONSORING MILITARY ACTIVITY
	Deputy for Engineering Wright-Patterson Air Force Base, Ohio

13. ABSTRACT

Part I of ASD-TR-69-15 presents the test results obtained from an extensive series of propeller static performance tests conducted on Electric Whirl Rig No. 4, located at Wright-Patterson Air Force Base. The tests were made because of a static performance thrust deficiency encountered during flight tests of the XC-142A V/STOL Cargo Aircraft.

Twenty-eight versions of propellers were tested. Parameters studied during the tests included blade cuff (on or off), tip shape, twist, activity factor, camber, and airfoil section. Reduced data is presented in the form of performance coefficients and various tip Mach numbers for each configuration tested. Data on several other VTOL static thrust propellers is presented for additional information although they were not a part of this test series.

Complete blade characteristic charts describing the physical characteristics of each blade tested provide a means of comparing the distribution of twist, thickness, chord, and camber against blade redial location for any given blade.

A drawing of the 30,000-horsepower Propeller Mount Configuration (Rig No. 4) shows dimensions of the test stand. Its operation and effects of the protective walls on the measured static performance are discussed. Data reduction was performed in-house on the ASD IBM-7094 computer and details of a special program used for the reduction, originally published as ASD-TR-69-19, "Computer Program for Reducing Static Propeller Test Data," are included.

The performance of the original XC-142A propeller was verified to be approximately 10% from the predicted value. As a result of these tests, the "induced inflow velocity" effect, due to the proximity of the protective walls surrounding the test rig, was dismissed as a contributing

DD FORM 1 NOV 65 1473

UNCLASSIFIED

Security Classification

14. KEY WORDS	LINK A		LINK B		LINK C	
	ROLE	WT	ROLE	WT	ROLE	WT
Propellers for Aircraft						
V/STOL Aircraft						
Static Performance						
Testing						
Test Facilities						
Design Parameters						
Blade Characteristics						
Data Reduction						
Test Data						
Computer Program						
VTOL Aircraft						

DD FORM 1473 (CONTD)

factor to the low performance of the original XC-142A propeller. Approximately 90% of the thrust deficiency was eliminated by a redesigned propeller utilizing performance information obtained from these tests.

Perhaps the most significant finding was that for every degree of increased blade twist, the figure of merit was increased approximately one-half point.

The tests and their results represent the state-of-the-art and point the way for improving propeller static performance for V/STOL aircraft applications. The information obtained can be used to predict more accurately the static thrust for future propeller driven V/STOL aircraft. The vast amount of test data presented involves the inter-relationships of many propeller design parameters from which the researcher should be able to derive significant aspects of propeller static thrust related specifically to V/STOL applications.

Test results show that follow-on test programs should include investigations of the effects of radial twist and camber distribution on performance and the significance of total blade twist.